The 1st NIRS Symposium on
Reconstruction of Early Internal Dose
in the TEPCO Fukushima Daiichi Nuclear Power Station Accident

Chiba, Japan 2012

PROCEEDINGS

Editors:

O. KURIHARA

K. AKAHANE

S. FUKUDA

N. MIYAHARA

S. YONAI

NIRS

National Institute of Radiological Sciences

The 1st NIRS Symposium on

Reconstruction of Early Internal Dose

in the TEPCO Fukushima Daiichi Nuclear Power Station Accident

PROCEEDINGS

National Institute of Radiological Sciences

Editors:

Osamu KURIHARA, Ph. D
Internal Dosimeter Section
Department of Radiation Dosimeter
Research Center for Radiation Emergency Medicine
National Institute of Radiological Sciences

Keiichi AKAHANE, Ph. D
Team of Dose Assessment for Fukushima Residents
Project for Human Health
Fukushima Project Headquarters
National Institute of Radiological Sciences

Shigekazu FUKUDA, Ph. D
Technical Management Section
Department of Accelerator and Medical Physics
Research Center for Charged Particle Therapy
National Institute of Radiological Sciences

Nobuyuki MIYAHARA, Ph. D
Department of Technical Support and Development
Research, Development and Support Center
National Institute of Radiological Sciences

Shunsuke YONAI, Ph. D
Beam Delivery Section
Department of Accelerator and Medical Physics
Research Center for Charged Particle Therapy
National Institute of Radiological Sciences

Associate Editors:

Eunjoo KIM, Ph. D
Internal Dosimeter Section
Department of Radiation Dosimeter
Research Center for Radiation Emergency Medicine
National Institute of Radiological Sciences

Ms. Rei IMADA
Internal Dosimeter Section
Department of Radiation Dosimeter
Research Center for Radiation Emergency Medicine
National Institute of Radiological Sciences

Ms. Mie KAWADA
Internal Dosimeter Section
Department of Radiation Dosimeter
Research Center for Radiation Emergency Medicine
National Institute of Radiological Sciences

Contents

III

Preface

The 2011 earthquake off the Pacific coast of Tohoku district (northern Japan) and the massive tsunamis generated by the earthquake wreaked the most catastrophic damage Japan has experienced in recent centuries. About twenty thousand people were killed or went missing in this natural disaster. This disaster also caused an unprecedented accident at the Fukushima Daiichi Nuclear Power Station operated by Tokyo Electric Power Company. Three reactors in operation were automatically scrammed right after the earthquake; however, these reactors ultimately reached core melt-down by the loss of their cooling systems regardless of extensive efforts for recovery. An enormous amount of radioactive material was released into the environment due to vent operations and a series of explosive events at reactor buildings. The total amount of released radioactive material has been estimated to be about 900 PBq (in ^{131}I equivalents), which is around one-tenth of that in the Chernobyl accident.

Estimation of the dose to the public in affected areas is essential to assess the possible radiological risks in the accident. The National Institute of Radiological Sciences (NIRS) developed a system for estimating early external doses of residents in Fukushima mainly based on information on individual behavior in combination with ambient dose levels measured at various locations after the accident. NIRS has reported the external doses of about 100 thousand residents as of August 2012, revealing that a majority of the external doses are below a few mSv. However, it is difficult to estimate internal doses because of the limited data from individual monitoring or air sampling, especially in the early stage of the accident when radioiodine with a relatively short-half life would have existed as the largest contributor to the thyroid dose. Our current understanding is that there are only about 1,500 human thyroid data from the public and that the main route of intake in the accident was probably inhalation rather than ingestion, unlike the situation in the Chernobyl accident.

This year NIRS has launched a new project for estimating internal doses received by members of the public in affected areas. A symposium was organized by NIRS on July 10-11, 2012 as the first step of this project. The main purposes of this symposium were (1) to collect all information available for the above estimations, and (2) to discuss methods that could be used for the reconstruction of early internal doses. The symposium, attended by many participants from Japan and invitees from overseas, was a great success. It has been also my great pleasure to publish the Proceedings of the symposium, which contains the papers submitted by the presenters at the symposium. All the papers were carefully reviewed by international experts in related scientific fields. It is my hope that the publication of these Proceedings will be useful for future work on dose reconstruction related to Fukushima nuclear disaster. I would like to express my deep gratitude to all those who contributed to the symposium and to this publication.

Osamu KURIHARA, Ph. D.
Editor-in-Chief
Head of Internal Dosimetry Section
Department of Radiation Dosimetry
Research Center for Radiation Emergency Medicine
National Institute of Radiological Sciences (NIRS)

List of Contributors
(alphabetical order)

Akira OHTSURU	Fukushima Medical Univ.
André BOUVILLE	NCI, U.S.
Gayle A. SUGIYAMA	LLNL, U.S.
Gen SUZUKI	International Univ. of Health and Welfare Clinic
Haruyasu NAGAI	JAEA
Hiromi YAMAZAWA	Nagoya Univ.
John S. NASSTROM	LLNL, U.S.
Kathleen M. THIESSEN	SENES Oak Ridge, Inc., U.S.
Mikhail BALONOV	IRH, Russia
Mitsuhiro KAJIMOTO	JNESO
Nobuhiko BAN	Tokyo Healthcare Univ.
Nobuyuki SUGIURA	NIRS
Osamu KURIHARA	NIRS
Sergei Y. TOLMACHEV	WSU, U.S.
Stephen SOLOMON	ARPANSA, Australia
Takashi NAKAMURA	Tohoku Univ.
Takenori YAMAGUCHI	JAEA
Takumaro MOMOSE	JAEA
Tomoyuki TAKAHASHI	Kyoto Univ.
Toshimitsu HOMMA	JAEA
Yasuyuki MURAMATSU	Gakushuin Univ.
Yoshio HOSOI	Hiroshima Univ.

Session 1

Current Status of Internal Dose Estimation

Session 1-1   For Responders

Chair   :   T. MOMOSE
Co-chair   :   A. BOUVILLE
Rapporteur :   S. TOLMACHEV

Results of Whole Body Counting for JAEA Staff Members Engaged in the Emergency Radiological Monitoring for the Fukushima Nuclear Disaster

Chie TAKADA, Osamu KURIHARA[1], Katsuta KANAI, Takahiro NAKAGAWA, Norio TSUJIMURA, Takumaro MOMOSE

Nuclear Fuel Cycle Engineering Laboratories, Japan Atomic Energy Agency, 4-33 Muramatsu, Tokai-mura, IBARAKI, 319-1194, Japan

Abstract

A massive earthquake and tsunami on March 11, 2011, resulted in the release of an enormous amount of radioactive materials into the environment. On the day after the earthquake the Japan Atomic Energy Agency (JAEA) began emergency radiological monitoring. Measurements with a whole body counter (WBC) for the staff members who had returned from Fukushima began at the end of March because a power blackout for several days and lingering increased ambient radiation levels had rendered the WBCs inoperable. The measured activity level for ^{131}I due to inhalation for emergency staff varied from below detection limit to 7 kBq, which corresponds to an estimated initial intake range of <1 to 60 kBq when extrapolated back to the date the staff began the monitoring in Fukushima. The measured activity levels for ^{134}Cs and ^{137}Cs were both in the ranges from below detection limit to 3 kBq. When using the median values for each set of measurements, the ratio of the initial intake of ^{131}I to ^{137}Cs was 11. The maximum committed effective dose of 0.8 mSv was recorded for a member of the 4th monitoring team dispatched from March 15 to 20.

Keywords: internal dose; whole body counter; radioiodine; radiocesium

1. Introduction

The accident at the Fukushima Daiichi Nuclear Power Station, which was caused by a 9.0-magnitude earthquake and the subsequent massive tsunami on March 11, 2011, resulted in a series of substantial releases of radioactive materials into the atmosphere, the most serious of which occurred on March 15 ~ 16. Before the night of March 14, the prevailing winds carried the radioactive plumes over the Pacific Ocean; however in the next two days, the winds veered to the northwest and rainfall washed the radioactive materials from the plumes, creating serious inland contamination.

With the declaration of the nuclear disaster by the Prime Minister on the same date of the quake, the Japan Atomic Energy Agency (JAEA), one of the public institutions designated in the Basic Disaster Prevention Plan, activated a series of responsive actions to the disaster, one of which was the deployment of emergency radiological monitoring teams to Fukushima. The results of the environmental monitoring suggested that there was an increased potential for a large number of people to be exposed to both internal irradiation (due to the inhalation of the radioactive materials in the plumes) and external irradiation (from radioactive materials transported by the plumes and deposited on the ground).

Accordingly, the JAEA conducted internal contamination monitoring for the Tokyo Electric Power Co., Ltd. (TEPCO) workers and the residents of Fukushima in response to requests from TEPCO and the Fukushima government. Monitoring for the residents is on-going. The results of the internal contamination monitoring have already been partly reported elsewhere [1] and will be described in more detail in companion articles [2,3] in this issue. In addition, internal contamination

---

[1] *present affiliation: National Institute of Radiological Sciences*

measurements were made on 50 of the workers who were involved in the responsive actions to the disaster, including the abovementioned emergency radiological monitoring. The present report describes the results of the whole body counting conducted for the emergency personnel dispatched to Fukushima.

2. Subject workers

Fifty adult male workers out of 241 JAEA staff members who were dispatched to Fukushima during the initial month following the accident are the subjects in this report. All 50 workers were the staff members of the Nuclear Fuel Cycle Engineering Laboratories (NCL), one of the JAEA establishments, located in Tokai-mura, ~100 km south of the crippled plant and had been engaged in emergency radiological monitoring in Fukushima. After returning from the monitoring assignment, they were examined with whole body counters (WBCs) through the end of April. All of them had resided in and around Tokai-mura at the time the quake hit.

At the JAEA, right after the earthquake occurred, emergency radiological monitoring teams were assembled while inspections of the quake-hit facilities and utility recovery operations were undertaken by the skeleton crews. Initially, on March 12, two teams, a 1st three-man team and a 2nd eight-man team, were sent out to the Off-site Center (OFC), which is located in Okuma town, ~5 km west of the plant. The rise of airborne activity and the ambient dose rate forced the OFC to be evacuated; therefore, the both teams left OFC at 9:00 p.m. on March 14, returning to Tokai-mura. Since March 16, 2011, the 3rd and later dispatches were directed to the Fukushima prefectural office, the new local command post for the nuclear disaster, which is 60 km west of the plant. From this command post, the dispatched monitoring teams were redeployed throughout a 20 ~ 50 km zone surrounding the plant. The final 15th team stayed in Fukushima during the period from April 7 to 11.

All of the personnel dispatched were equipped with a personal dosemeter in addition to their regular work clothes, but without an anti-contamination suit or a respirator. They also didn't take any tablet of stable iodine because the local nuclear emergency response headquarters issued no instruction about taking stable iodine for residents. After returning to Tokai-mura, whole body counting for each worker was conducted in order to check for any elevation of internal contamination.

Herein, the results of the whole body count analysis of the monitors are discussed in comparison to those obtained for three staff members (one expert and two operators) involved in operating and maintaining the WBCs of the NCL. All of the WBC staff were residents of Tokai-mura and were present during the passage of the main radioactive plume, which began at around 4:00 a.m. on March 15. The WBCs were reactivated using a temporary generator on the morning of March 14, and background count measurements were initiated to check the variation in the ambient radiation levels and its possible effects on the lower limit of detection. In addition, the three staff members also took measurements of themselves in order to judge the overall system performance. The two operators remained in Tokai-mura up to the time of the WBC measurement, while the expert left three days after the evening of March 15 to visit the Fukushima Medical University (FMU). This group also took no stable iodine tablets.

3. Measurements

3.1. Whole body counter

A FASTSCAN WBC manufactured by Canberra, Inc. was used in this study. Figure 1 shows external and internal views of the FASTSCAN system [4] at the NCL. The FASTSCAN uses two 12.7 ×

7.6 × 40.6 cm^3 NaI(Tl) detectors configured in a linear array on a common vertical axis inside a booth-shaped shadow shield, in which a subject stands facing the detectors. The altitudes of each detector unit from the booth floor are 113.0 ~ 153.6 cm for the upper unit and 63.7 ~ 104.3 cm for the lower unit, and cover the range from the thyroid gland to the lower gastrointestinal tract for likely subject sizes with nearly flat counting efficiency. The measurable energy range is 300 keV to 1.8 MeV and the minimum detectable activity (MDA) is ~200 Bq for ^{137}Cs, with a counting time of 120 s for at the background levels in the NCL prior to the quake.
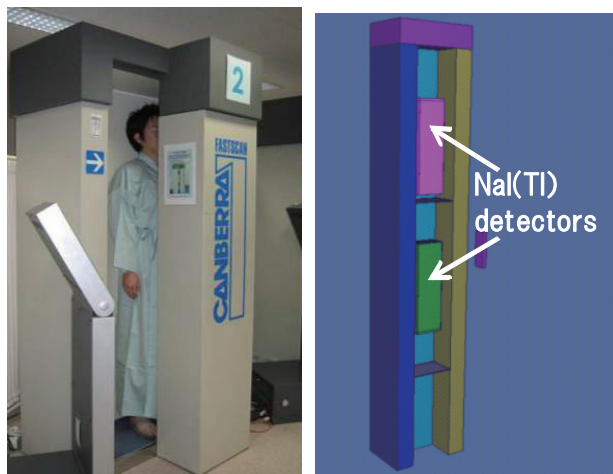
Figure 1. External and internal views of the FASTSCAN being used at the NCL

The PC-based software, ABACOS and GENIE, both provided by Canberra, were used for system operation and for data acquisition and spectrum analysis, respectively. Spectral data from the two detectors are acquired and displayed separately, and are then electronically summed to form the composite spectrum for peak analysis. The peak analysis method used in the GENIE system begins with a systematic erosion of the photo-peaks of an original spectrum in order to estimate the underlying continuum spectrum, and then creates a series of residual peaks by subtracting the estimated continuum spectrum from the original spectrum. The theoretical peaks of the user's library-specified radionuclides are fitted to the residual peaks using an iterative least-squares Gaussian fitting technique, and finally, the areas of the resolved peaks and thus their activities are determined.

Table 1 lists the radionuclides specified in the user's library, where some of the closely adjacent peaks were registered as single peaks with average energies and summed yields, in order to facilitate the peak analysis. A parent-progeny pair of ^{132}Te and ^{132}I was not included in this library because their activity was very low by the time the WBC examination was started at the end of March.

The calibration of counting efficiencies for the FASTSCAN was made using a Canberra Transfer Phantom (CTP), which consisted of the torso and neck sections, both of which are made of acrylic resin. The CTP in an upright position inside the booth can adequately simulate various counting geometries for the reference calibration phantom configurations by placing an appropriate calibration source into one of the several cavities. The appearance of the CTP and the calibration source can be seen in Figure 2. A 12 mL vial containing mixed gamma-emitting radionuclides (^{57}Co, ^{60}Co, ^{85}Sr, ^{88}Y, ^{109}Cd, ^{113}Sn, ^{137}Cs, ^{139}Ce, and ^{203}Hg) of known activities was placed into the middle cavity of the torso section, enabling the calibration of the system for the whole-body geometry, in which the radionuclides are uniformly distributed. The same vial was then placed into the cavity in the neck section, which was used for calibration in the thyroid counting geometry with no collimators. In fact, this source configuration gave accurate results for the thyroid content of iodine [3]. This was experimentally confirmed in direct measurements of TEPCO workers at authors' institute. However, in the early stage

of direct measurements after the nuclear disaster, the activity of ^{131}I in the body was determined as the whole-body content using the FASTSCAN, resulting in a large overestimation.

Table 1 Nuclide Library

Nuclide	Energy (keV)	Yield (%)
K-40	1461	10.7
I-131	364*	81.7
	637	7.2
Cs-134	<u>566</u>	<u>23.8</u>
	605	97.6
	<u>796.6*</u>	<u>94.2</u>
	<u>1167.94</u>	<u>1.8</u>
	1365	3.0
Cs-137	662	85.1

The underlined figures are corrected values and the photon energies lines marked with * are given the high priority in the activity calculation.

Figure 2. Canberra Transfer Phantom (CTP) and the calibration source

The calibration with the CTP was confirmed with a BOMAB phantom supplied by the Nuclear Science Research Institute of the JAEA as a part of the measurement quality assurance program. From this calibration, two counting efficiency curves as a function of photon energy were derived for the whole-body and thyroid counting.

3.2. Measurement conditions

The damage to utilities (electricity, water, gas, etc.) and roads, and the subsequent elevated level of the background radiation brought by the contaminated plume, delayed the resumption of the operation of the WBCs at the NCL. Monitoring stations at the site boundary of the NCL indicated a surge of the background gamma radiation around 7:00 a.m. on March 15 and a smaller surge around 5:00 a.m. on March 21, whose maximum momentary air kerma rates were 5 and 3 μGy/h, respectively. The background radiation measured with the FASTSCAN on March 15 formed a pulse height spectrum composed of discrete peaks for ^{132}Te, ^{131}I, and ^{133}Xe and broader, overlapped peaks around 600 ~ 670 keV and 770 ~ 800 keV for ^{131}I, ^{132}I, ^{134}Cs and ^{137}Cs (^{137m}Ba). The latter peaks were overwhelmed by ^{131}I and ^{132}I, preventing the peaks of ^{134}Cs and ^{137}Cs from being resolved. Figure 3 shows the measured spectrum around 10:00 a.m. on 15 March. Therefore, the precise quantitative evaluation of the activities of ^{134}Cs and ^{137}Cs became possible only around the end of March, by which time the peaks for ^{132}I and its parent, ^{132}Te, dissipated.
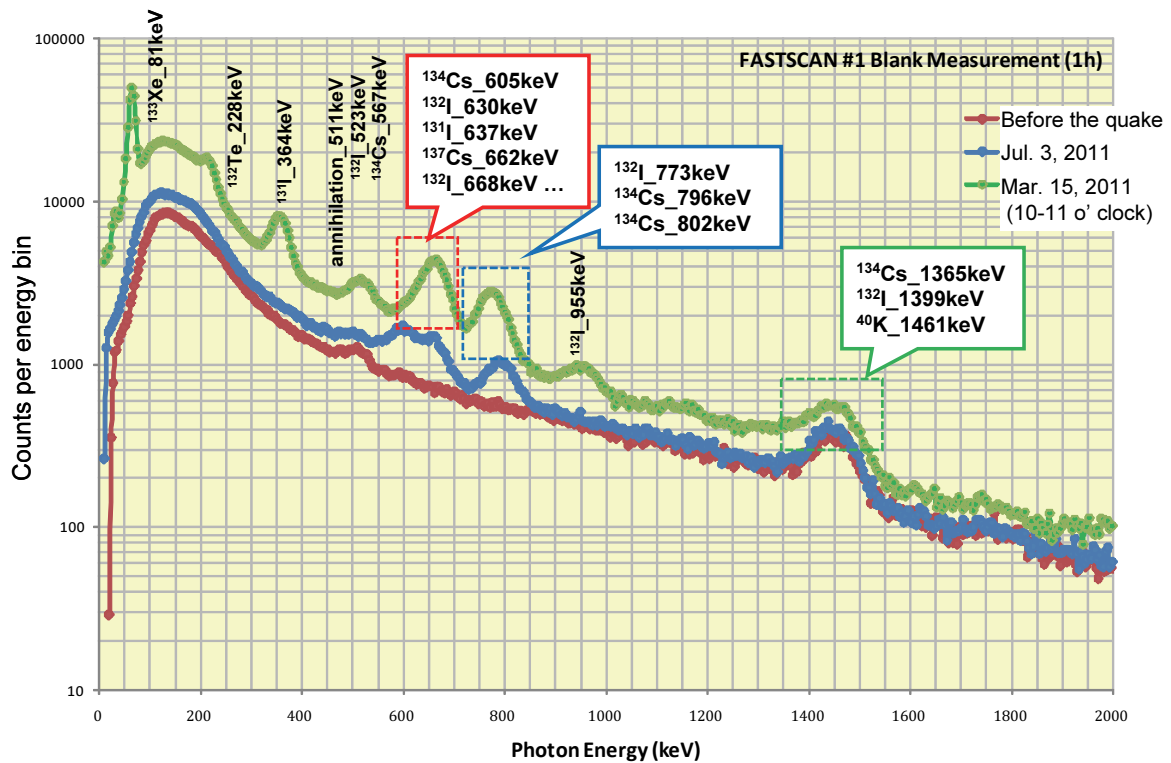
Figure 3. Background spectrum of the FASTSCAN at the NCL

For the 50 workers, whole body counting was conducted within a few days and then several weeks after their return; the earliest were completed on March 28 and the latest on April 28. The workers were counted in their regular work clothes, because they had a time to change into clean clothes and take normal bathing to wash any exposed skin surfaces and hair. However, as a precaution, they were requested to take off their work jackets in order to minimize of the possible effects from residual contamination materials. Reliable FASTSCAN data for the WBC operators was collected after March 28, although test measurements during the period of the high background radiation were conducted after March 15. While 30% of inhaled radioiodine concentrates in the thyroid gland and remains there for weeks, the other 70% is excreted in the urine within a few days; therefore, the contribution of ^{131}I gamma rays from other organs of the body must have been negligible at the time of the thyroid counting.

3.3. Dose estimation model

The exposure history of the emergency personnel was expected to be complex because of the potential for multiple inhalation. A percentage of the workers may have been affected by inhalation at both in Fukushima and Tokai-mura; for example, the members who worked at Fukushima and then returned to Tokai-mura before March 15 might have first inhaled radioactive materials at Fukushima and then inhaled additional radioactive materials at Tokai-mura after March 15. Therefore, it was assumed that a single inhalation took place either on March 15 or the first work day at the scene, i.e., the date that provided the longest elapsed time before measurement. This assumption would yield conservative dose estimation when the amount of intake during inhalation at Fukushima exceeded that at Tokai after March 15. In contrast, the two WBC operators who stayed at Tokai-mura during the month were expected to have inhaled after March 15.

The internal dose was evaluated in terms of the committed effective dose (CED), which was

calculated as a product of the dose coefficient and the estimated intake. The former was taken from ICRP Publ. 78 [5]; the latter was derived by dividing the measured body content using the retention function, or the fraction of the intake retained in the body at the time after intake. The retention function was calculated by the MONDAL3 code [6]. A type-F lung solubility class and a default activity median aerodynamic diameter (AMAD) of 5 μm for the particles were assumed.

4. Results and discussion

4.1. Results of whole body counting

The whole body measurements were completed by the end of April for a total of 50 persons, nearly all of which showed some activity other than that due to naturally-occurring ^{40}K. The radionuclides detected in their bodies were ^{131}I, ^{134}Cs and ^{137}Cs. Iodine-131 was detected for 47 persons, or 94% of the total. When no ^{131}I, ^{134}Cs or ^{137}Cs was detected, the MDA value was assigned to the body content value for a most conservative evaluation. The results of the measurements are described below.

Figure 4 shows the pulse height spectra measured for the worker with the highest detected ^{131}I burden. He joined the 2nd team dispatched to Fukushima during the first week following the accident. The figure compares three spectra, those acquired by the upper and lower detectors and the composite of the two detectors. Each spectrum identifies discrete peaks for ^{131}I (364 keV) and ^{134}Cs (796 keV, 802 keV) and a broad peak composed of ^{131}I (637 keV), ^{134}Cs (605 keV) and ^{137}Cs (662 keV), as well as a minor peak for ^{40}K (1461 keV). The relative counts from the two detectors provide an approximate measure of the distribution of the activity in the body. The observed count ratio of 6:4 in the ^{131}I peak region for the upper and lower detector was reasonably close to the ratio of 7:3 obtained for the calibration with the CTP. This result demonstrated that the thyroid counting was achieved with relatively little interference from the other contamination in the extrathyroidal organs or on the work clothes, even though no collimator for the thyroid gland was used.

Figure 5 depicts the whole body ^{134}Cs and ^{137}Cs content for the 50 emergency personnel and the 3 WBC workers. The level of ^{137}Cs at the time of the measurements ranged from below detection level to ~3 kBq. The ^{134}Cs activity was nearly the same range. When the maximum measured values were extrapolated back to the date of the initial intake, the initial intakes of 8 kBq for ^{137}Cs and 7 kBq for ^{134}Cs were calculated. In addition, an observed activity ratio of ^{134}Cs:^{137}Cs of 1:1 was found to be the same as that for the TEPCO workers as well as for all other samples taken in the environment. In addition, no variation in the radioactivity was detected throughout the period of the dispatch. Noticeably, the scatter of the plots around the 1:1 line is small.

A comparison of the initial intakes of ^{131}I and ^{137}Cs, both of which were also extrapolated back to the date of the initial intake, is presented in Figure 6. The initial intakes of ^{131}I were estimated to be in the range from below 1 kBq to around 60 kBq when extrapolated back to the date of the initial intake. The superimposed lines correspond to the ^{131}I/^{137}Cs ratios of 1, 10 and 100. In contrast to radiocesium, a poor correlation was found. The intake ratio of ^{131}I to ^{137}Cs for 50 emergency personnel ranged from 1 to the 50 with a median of 11, which is the same order as the ratio of 10–20 estimated by the Nuclear and Industrial Safety Agency (NISA) as a release source term.

The values of the ^{131}I/^{137}Cs ratio for the two WBC operators who stayed in Tokai-mura were both 1.4, and the average value of the initial intake of ^{131}I for the three WBC operators was estimated to be 2 kBq based on the basis of the FASTSCAN measurement.
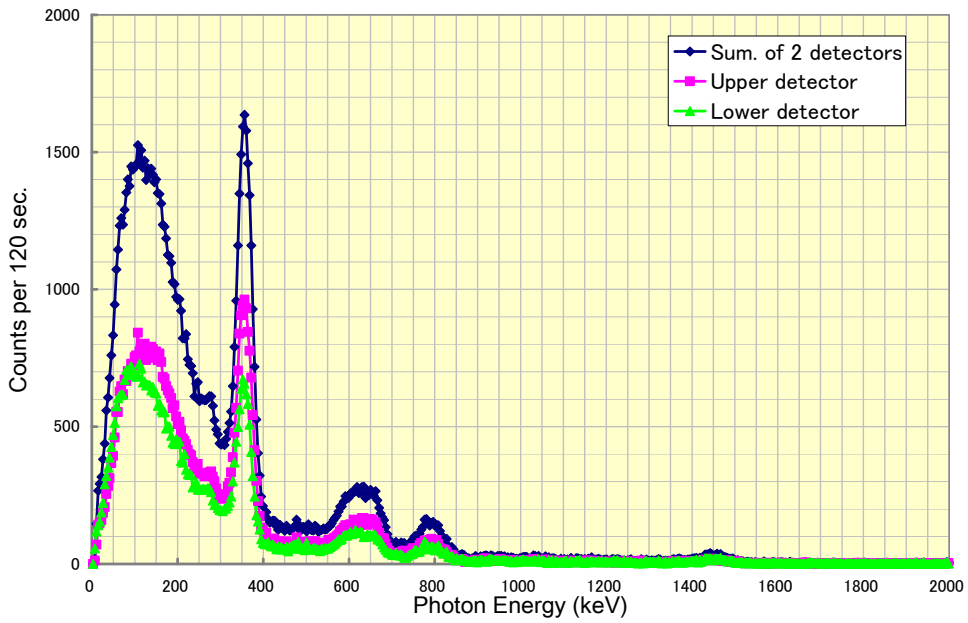
Figure 4. Energy spectra for the gamma rays from the worker found to have the highest levels of activity of the whole body content using the WBC
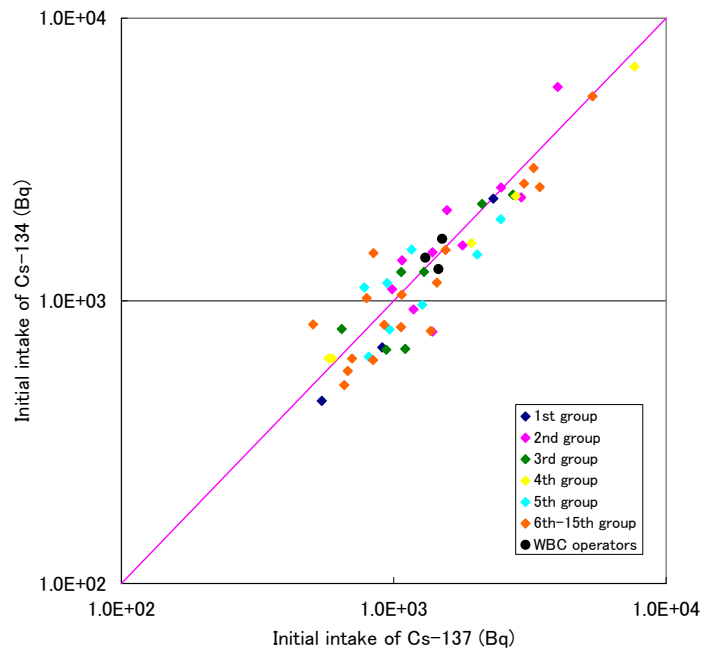
Figure 5. Correlation of the estimated initial intakes of ^{137}Cs and ^{134}Cs
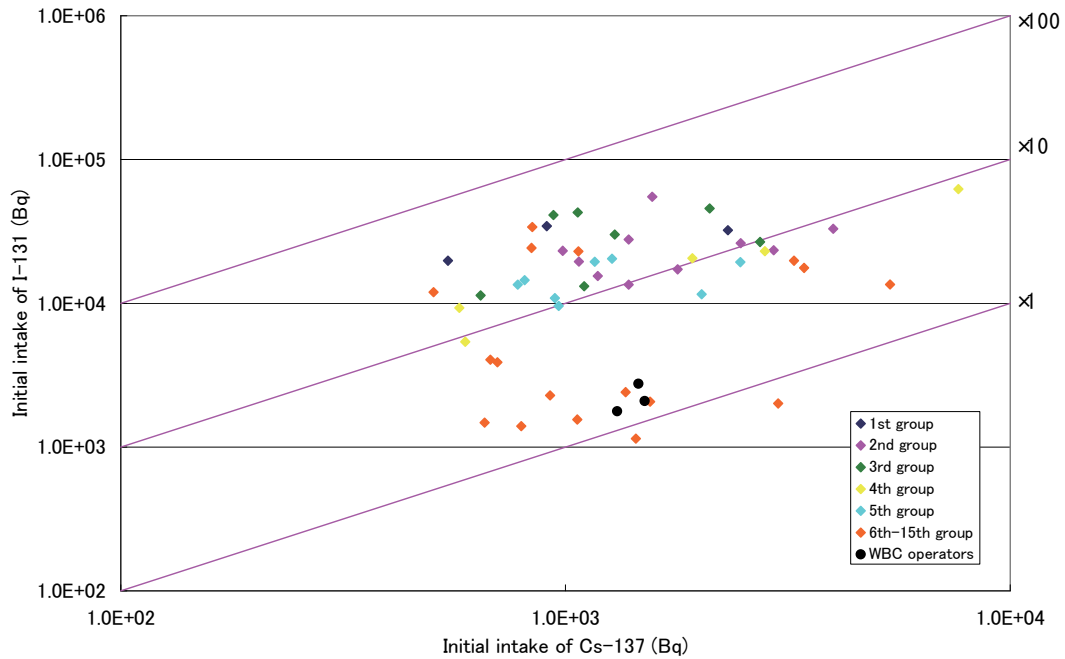
Figure 6. Correlation of the estimated initial intakes of ^{137}Cs and ^{131}I

4.2. Dose estimation results

Table 2 summarizes the ranges and averages of the CEDs due to ^{131}I and ^{134}Cs + ^{137}Cs, calculated from the measurements obtained using the FASTSCAN system. For the emergency personnel dispatched to Fukushima, the CEDs from inhalation were determined to be in the range of 0.03 ~ 0.8 mSv, with a median value of 0.24 mSv. Most of the values of the CEDs for the workers were due to ^{131}I. The CEDs of the three WBC operators, including the expert who had been to the FMU for three days in March were all calculated to be around 0.05 mSv, which is much smaller than that for the dispatched workers. Note that the measurements obtained for these three WBC operators established the expected range for the individual CEDs of the adult residents in Tokai-mura.

Table 2 Estimated CEDs

Group#	Locations and Period of Operation	Number of workers	MAX. CED (mSv)	MED. CED (mSv)
1st	Fukushima, Mar. 12–14	3	0.39	0.39
2nd	Fukushima, Mar. 13–14	10	0.64	0.29
3rd	Fukushima, Mar. 14–18	7	0.54	0.35
4th	Fukushima, Mar. 15–20	5	0.80	0.26
5th	Fukushima, Mar. 18–22	8	0.25	0.17
6th–15th	Fukushima, around 4 days during Mar. 20–Apr. 11	17	0.54	0.05
Sub Total		50	0.80	0.24
WBC operators	Tokai-mura, Mar. 15	3	0.05	0.05

4.3. Some Issues

Because the emergency monitoring in the initial few weeks after the earthquake was conducted with no systematic plan, there are no detailed records of the behavior of the staff members. More meaningful dose estimations could be obtained if the behavior records indicating the specific times and locations of monitoring activities were available.

In addition, in this study, the workers were not examined with a lead-collimated thyroid monitor because all the results for the whole body counting with the FASTSCAN system were relatively modest. In retrospect, however, we should have used both a WBC and a thyroid monitor should have been used to evaluate all subjects in order to obtain more accurate results for radioiodine.

Finally, the delayed start of the WBC examinations prevented the short-life nuclides such as ^{132}I, ^{133}I and ^{132}Te from being detected. The doses resulting from intakes of such nuclides should be estimated using information on the ratio data of radionuclides released relative to ^{131}I.

5. Conclusion

The nuclear disaster at the Fukushima Daiichi Nuclear Power Station in March 2011 resulted in the diffusion of various radioactive materials leading to potential for significant internal doses in large populations.

The whole body counting for 50 staff members engaged in the emergency monitoring activities was conducted approximately 3–8 weeks after the accident occurred. The results indicate that the maximum internal dose was 0.8 mSv of internal dose and the maximum total dose was 0.9 mSv, which confirms for the workers that there was no serious internal contamination. The median of the intake ratio of ^{131}I to ^{137}Cs for the 50 emergency personnel working in Fukushima was 11, and that for the WBC operators who stayed in Tokai-mura was 1.4.

These measurements serve as a further source of information that can be used to reconstruct the early internal doses experienced by the public.

References

1) C. Takada, O. Kurihara, N. Tsujimura, K. Kanai, T. Nakagawa, H. Miyauchi, T. Murayama, Y. Maruo, T. Momose and S. Furuta, Evaluation of Internal Exposure of the Workers and the Residents Caused by the Fukushima Nuclear Accident, Full papers of The 13th International Congress of the International Radiation Protection Association (IRPA13), Glasgow, UK, May 13-18, 2012. Available at http://www.irpa13glasgow.com/information/downloads/, (File P12.22.doc).
2) T. Momose, C. Takada, T. Nakagawa, K. Kanai, O. Kurihara, N. Tsujimura, Y. Ohi, T. Murayama, Result of whole body counting for Fukushima residents, The proceedings of NIRS symposium (this issue)
3) O. Kurihara, et al., Direct measurements of the employees involved in the Fukushima Daiichi Nuclear Power Station accident for internal dose estimates : JAEA's experiences, The proceedings of NIRS symposium (this issue)
4) Canberra Inc., FASTSCAN High-Throughput Whole Body Counter Model 2250, http://www.canberra.com/pdf/Products/FASTSCAN-SS-C9810.pdf
5) ICRP. Individual Monitoring for Internal Exposure of Workers, ICRP Publication 78. Ann. ICRP 27 (3-4), (1998)
6) N. Ishigure, M. Matsumoto, T. Nakano and H. Enomoto, Development of Software for Internal Dose Calculation from Bioassay Measurements. Radiat. Prot. Dosim. 109, 235-242 (2004).

Direct Measurements of Employees Involved in the Fukushima Daiichi Nuclear Power Station Accident for Internal Dose Estimates: JAEA's Experiences

Osamu KURIHARA[1], Katsuta KANAI, Takahiro NAKAGAWA, Chie TAKADA,
Takumaro MOMOSE, Sadaaki FURUTA

Nuclear Fuel Cycle Engineering Laboratories, Tokai Research and Development Center,
Japan Atomic Energy Agency, 4-33 Muramatsu, Tokai-mura, Naka-gun, IBARAKI, 319-1194, Japan

Abstract

Japan Atomic Energy Agency (JAEA) performed internal dose measurements of employees involved in the Fukushima Daiichi nuclear power station accident. Nuclear Fuel Cycle Engineering Laboratories (NFCEL), one of the JAEA's core centers, examined 560 of these employees by direct (*in vivo*) measurements during the period from April 20 to August 5 in 2011. These measurements consisted of whole-body counting for radiocesium and thyroid counting for radioiodine. The whole-body counting was conducted with two types of whole-body counters (WBCs): a standing-type WBC with two large NaI(Tl) detectors (Fastscan[TM], Canberra Inc.) and a chair-type WBC with HPGe detectors (GC5021, Canberra Inc.) installed in a shielded chamber made of 20-cm-thick steel. The thyroid counting was mainly performed using one of the two HPGe detectors equipped with the chair-type WBC. The subjects examined in this work were divided into two groups: Group 1 was the first 39 subjects who were measured up to June 17, 2011 and Group 2 was the remaining 521 subjects who were measured on and after June 18, 2011. The performance of our direct measurements was validated by comparing measurement results of the Group 1 subjects using two different methods (e.g., the standing-type WBC vs. the chair-type WBC). Tentative internal dose estimates of the subjects of Group 1 were also performed based on the assumption of a single intake scenario on either March 12, when the first hydrogen explosion occurred at the station or the first day of work after the accident. It was found that the contribution of ^{131}I to the total internal dose greatly exceeded those of ^{134}Cs and ^{137}Cs, the other major nuclides detected in the measurements. The maximum committed effective dose (CED) was found in a male subject whose thyroid content of ^{131}I was 9760 Bq on May 23, 2011; the CED of this subject was estimated to be 600 mSv including a small contribution of ^{134}Cs and ^{137}Cs. The typical minimum detectable activity for ^{131}I in the present thyroid counting was 10 Bq for a counting time of 10 min, making it difficult to identify a residual thyroid content corresponding to a CED of 20 mSv for the subjects of Group 2.

Keywords: internal dose estimates; Fukushima Daiichi nuclear power station; worker; radioiodine; radiocesium; direct measurement; whole-body counter

1. Introduction

The Great East Japan Earthquake Disaster of 2011 was precipitated when an earthquake with a magnitude of 9.0 occurred off of the Pacific coast of Tohoku at 14:46 JST on March 11. Subsequent tsunamis hit the Fukushima Daiichi Nuclear Power Station (FDNPS) run by Tokyo Electric Power Company (TEPCO), resulting in the loss of cooling functions for reactor cores due to station black-out[1]. This led to an unprecedented nuclear disaster with an enormous release of radioactive materials into the environment.

---

[1] *Present afflication: Research Center for Radiation Emergency Medicine, National Institute of Radiological Sciences, 4-9-1 Anagawa, Inage-ku, Chiba-shi, CHIBA, 263-8555, Japan*

Radiation protection instrumentation for employees involved in this accident failed to function. Most personal dosimeters were submerged by tsunamis and whole-body counter (WBC) systems were inoperable due to the elevated radiation background level at the station site. At the request of TEPCO, Japan Atomic Energy Agency (JAEA) sent a mobile WBC to Onahama, a town in Fukushima Prefecture (55 km south of the the FDNPS) where radiation levels were relatively low compared to surrounding areas, and then initiated direct measurements of emergency workers beginning March 22, 2011. However, the capability of this WBC was insufficient for the large number of emergency workers involved.

The measurements with the mobile WBC revealed that most of the examined subjects had internal contamination with radionuclides, and that ^{131}I was the predominant contributor to the internal dose. However, the thyroid content determined with the mobile WBC was expected to be overestimated because of the use of calibration coefficients for the activity distributed throughout the entire body; these coefficients were smaller than those obtained for the activity localized in the thyroid, resulting in overestimations of the thyroid content. External contamination that remained on the body surface also might have caused overestimations of the body content of radionuclides. Another problem that should be pointed out in the earliest dose estimates based on measured data of the mobile WBC was the assumption of a single intake scenario at the middle day of a working period [2] (a few months for most of the subjects presented in this work). This assumption was, however, not suitable for the subjects measured in April, 2011 or later because a large portion of the intake must have occurred during the first week after the accident. As a result, that assumption probably biased internal doses of the subjects toward underestimation, in particular for ^{131}I with a short half-life (8.02 days). The lack of air sampling in reactor workplaces made it difficult to model an actual scenario of the intake. It is also noted that the energy resolution of NaI(Tl) detectors equipped with the mobile WBC was not sufficient to identify various radionuclides existing in the early measurements.

Therefore, the demand for more reliable measurements was much increasing especially for workers with considerable internal contamination. After consulting with TEPCO, additional individual monitoring was proposed at Nuclear Fuel Cycle Engineering Laboratories of JAEA (JAEA-NFCEL). This laboratory is located in Tokai-mura, 110 km south of the FDNPS, in Ibaraki Prefecture. The main reason for this was that an HPGe detector installed in a low-background shielded chamber (as described later) was available for measurements of ^{131}I in the thyroid with sufficient sensitivity. Most of the initial intake amount of ^{131}I had already decayed out when the monitoring was initiated. The number of subjects examined at our laboratory during the period from April 20 to August 5, 2011 totaled 560. TEPCO performed internal dose estimates for most of these subjects based on measured data provided by us. The present paper describes methods and results of our direct measurements of these subjects, mainly the first 39 subjects who were examined with particular care. This paper also discusses the validity of these measurements for reliable internal dose estimates.

2. Materials and methods

2.1. Whole-body counting

Two types of WBCs for the whole-body counting were used; one was a chair-type WBC with two coaxial HPGe detectors (GC5021, Canberra Inc., US: relative efficiency of 50%) and another was a standing-type WBC with two large NaI(Tl) detectors (Fastscan^{TM}, Canberra Inc., US). The chair-type WBC is installed in a shielded chamber made of low background steel with a thickness of 20 cm. The two HPGe detectors view the chest and the abdomen of the subject from above, respectively. One of the two HPGe detectors equipped with this WBC was also used for the

thyroid counting as described later. The standing-type WBC is the same instrument as that used in the mobile WBC described in the introduction of this paper. The exteriors of the two WBCs are shown in Figure 1.

These WBCs were calibrated with different phantoms; the chair-type WBC was calibrated with a BOMAB phantom [3] (with a height of 175 cm and a weight of 66 kg) and the standing-type WBC was calibrated with a Transfer phantom supplied from the manufacturer [4].

When measuring subjects, the counting geometry had the same setting as that used in the calibration. In the measurements with the chair-type WBC, the subject and detector distance (SDD) was normally set at 15 cm for the upper detector and 20 cm for the lower detector. However, this arrangement was sometimes difficult especially for large-sized subjects. In that case, there were some differences from the above SDD values. For the standing-type WBC, the subject was asked to stand against the rear wall of the enclosure (see Figure 1). The counting time was set at 10 min for the chair-type WBC and at 2 min (or 5 min, in some cases) for the standing-type WBC.
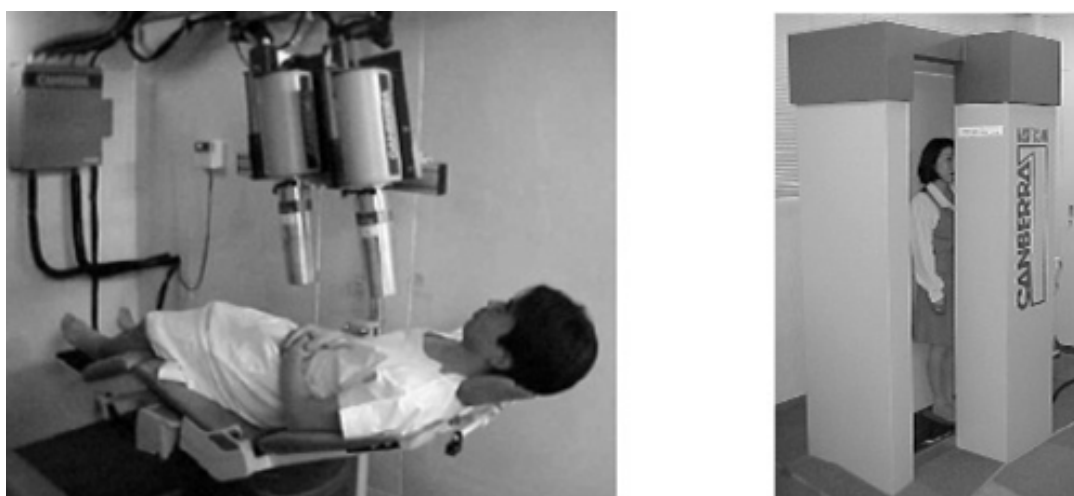
Figure 1. Exterior of the chair-type WBC (left) and the standing-type WBC (right)

2.2. Thyroid counting

Two types of detectors for the thyroid counting were used; one was the HPGe detector used in the chair-type WBC (as described above) and the other was a NaI(Tl) detector (type:51B51/2, Scionix, Netherlands) coupled with a spectrometer operated by a laptop. A collimator for shielding photons which come from ^{131}I existing in the rest of the body apart from the thyroid was not used in measurement with either detector. According to MONDAL3 [5], a software package for internal dose calculations, the residual activity ratio of the thyroid to the whole-body reached at a maximum (~95%) in the few days after the intake and then gradually decreases to a constant level (~85%) in the subsequent few months. It is considered that a relatively-large fraction of iodine still remain in the rest of the body other than thyroid. However, in this occasion, such a fraction would be small. Note that the first measurement of the subjects at our laboratory was conducted on April 20, 39 days after the first explosive incident at the FDNPS on March 12. In light of the counting geometry, it was expected that the fraction of ^{131}I in the rest of the body did not influence the thyroid counting significantly although this issue should be clarified in future studies.

Figure 2. Thyroid counting with a HPGe detector (left) and a NaI(Tl) detector (right)

The counting geometry for each detector was described as follows. The HPGe detector was placed over the neck and the neck-surface-to-detector distance (NDD) was adjusted to either 5 cm or 10 cm. Twenty-three of Group 1 (described later) were measured once with each of the two NDDs. On the other hand, the NaI(Tl) detector was placed directly on the neck by the subject. Both the detectors were placed to view the lower part of the anterior neck (see Figure 2). No ultrasound measurements to determine the actual location of the thyroid were performed. The counting time was set at 10 min for both detectors.

Both of the two detectors were calibrated with the neck part of the Transfer phantom which was also used for calibrating the standing-type WBC. This part uses a single vial source and is configured based on the specifications of American National Standard Institute (ANSI) [6].

2.3. Subjects

The 560 subjects were chosen by TEPCO based on provisional dose estimate results or some other priority (e.g., female employees). One of the criteria that TEPCO asked us to perform the individual monitoring at our laboratory was 20 mSv, which is the statutory dose limit for the effective dose. The subjects were divided into two groups. The first group consisted of 39 subjects including 6 female subjects; a few of these female subjects were non-radiation workers who were evacuated shortly after the outbreak of the earthquake. This group (Group 1) was accepted at our laboratory from April 20 to June 17 in 2011. The second group (Group 2) consisted of the remaining 521 subjects who were accepted from June 18 to August 5 in 2011. Regarding Group 1, most of the subjects were measured with two instruments for the whole-body and thyroid counting. Hence, this paper presents measurement results mainly for the subjects of Group 1. Internal dose estimates for these subjects were also attempted because information on their work shifts was provided by TEPCO.

3. Results

3.1. Whole-body counting and thyroid counting of the subjects

Figure 3 displays two energy spectra from the two types of the WBCs. These spectra were obtained from the first subject (Group 1) who was measured on April 20, 2011. Through the whole-body counting, ^{131}I, ^{134}Cs and ^{137}Cs were found to be major nuclides in the body. Small peaks from other nuclides such as ^{136}Cs, ^{129m}Te and presumably ^{110m}Ag were occasionally identified in measured spectra of subjects with a relatively high body content of major nuclides. Short-lived

nuclides (e.g., ^{132}Te, ^{132}I) were not detected although these nuclides were identified in early measurements with the mobile WBC.

Figure 4 plots the whole-body content of ^{137}Cs for the 39 subjects of Group 1 as a function of the time after intake. These data were obtained from measurements with the chair-type WBC. The dashed line in the figure represents the predicted content corresponding to 20 mSv in the committed effective dose (CED) on the assumption of a single intake event via inhalation of aerosols with default physicochemical properties: a particle size of 5 μm in activity median aerodynamic diameter (AMAD) and an absorption category of Type F. The intake day was assumed to be either March 12 or the first day of the work shift; the former was applied to the subjects who were working at the FDNPS during the earthquake and the latter was applied to the other subjects who entered the FDNPS for emergency work after March 12. As shown in the figure, the internal dose due to the intake of ^{137}Cs is much smaller than 20 mSv for all the subjects of Group 1. The average internal dose values of ^{134}Cs and ^{137}Cs for these subjects were 0.89 mSv and 0.61 mSv, respectively. Radiocesium was significantly detected in all subjects of Group 1 and Group 2.
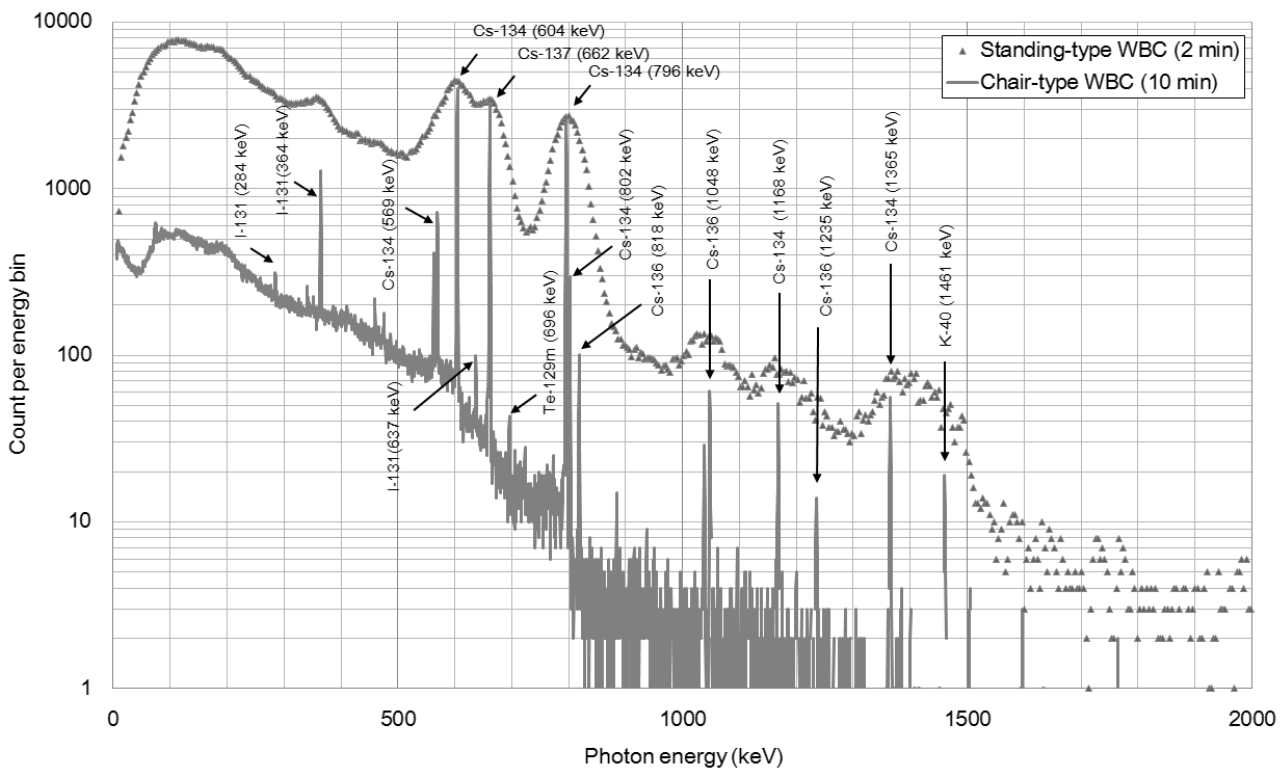
Figure 3. Energy spectra obtained from measurements of the first subject with two types of WBCs
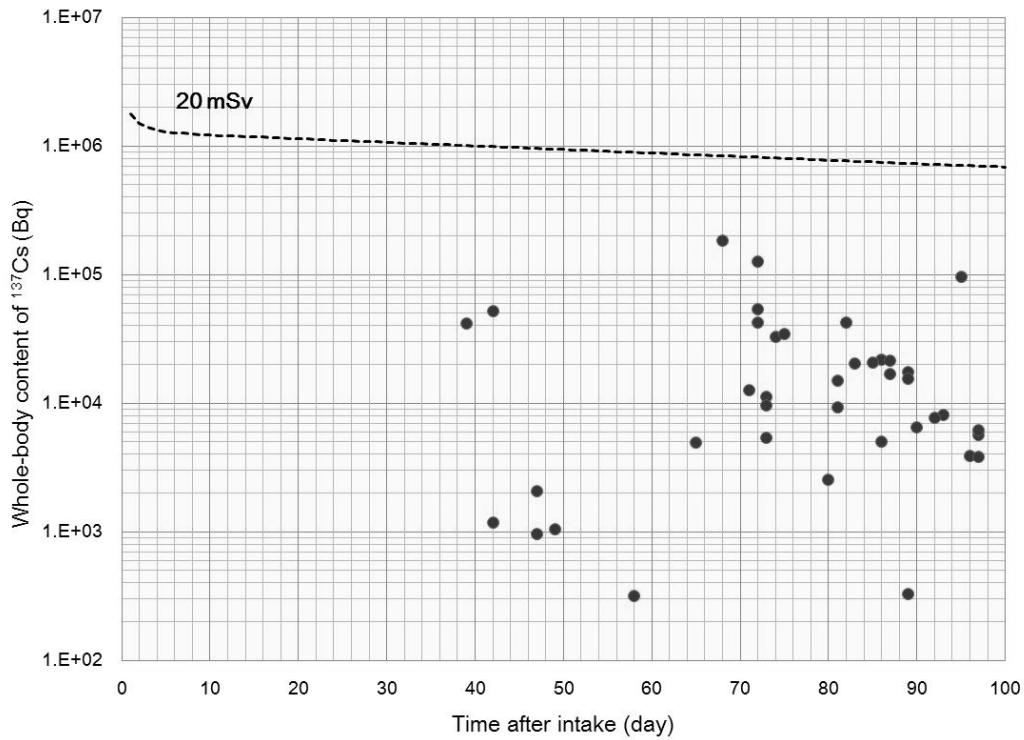
Figure 4. Whole-body content of ^{137}Cs as a function of the time after intake

Figure 5 compares the whole-body contents between ^{134}Cs and ^{137}Cs, showing that they were almost equal. These data were obtained from the same measurements as described in the previous figure. No correction for the half-life of radiocesium considering the difference of measurement days was made in Figures 5. The equal ratio of ^{134}Cs to ^{137}Cs is corroborated by results from various environmental samples collected after the accident [7].
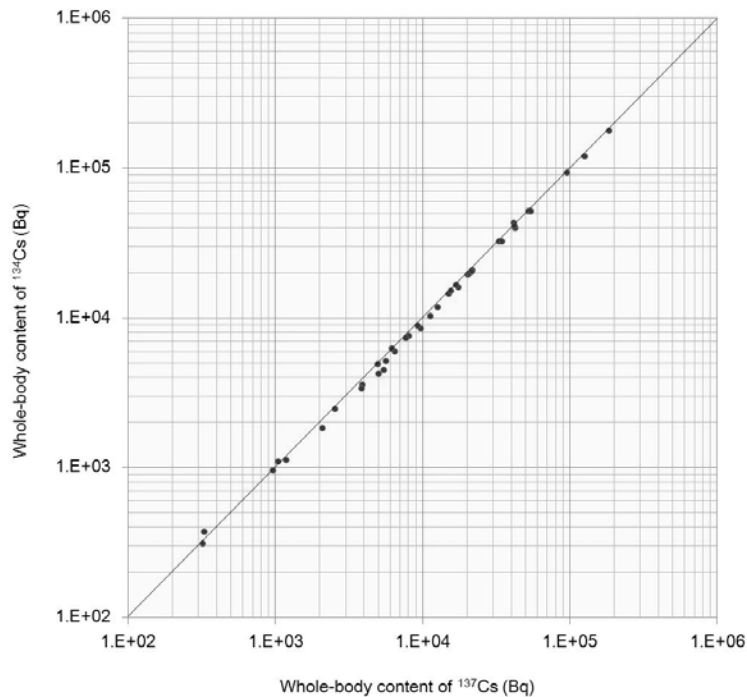
Figure 5. Comparison of the whole-body content of ^{134}Cs and ^{137}Cs

Figure 6 plots the thyroid content of ^{131}I for the 39 subjects of Group 1 as a function of the time after intake. Minimum detectable activity (MDA) values are displayed for three subjects with no detection of [131]I. These data were obtained from measurements with the HPGe detector. The intake day was assumed to be March 12. For the subjects who were measured twice with the two NDDs, measured values for the NDD of 10 cm are shown in Figure 6. The three lines in the figure represent predicted thyroid contents corresponding to 20 mSv, 100 mSv and 250 mSv in CED on the assumption of a single intake event via inhalation of iodine in a vapor form. The last value of 250 mSv was adopted as the temporary dose limit for workers who were engaged in preventing further worsening of the accident. According to our estimates, four subjects of Group 1 received internal exposure over 250 mSv by the intake of ^{131}I only. The first and second thyroid contents of 9760 Bq and 7690 Bq were determined in the two male subjects who were measured on May 23, 2011 (72nd day in the figure). Their received doses were calculated as 600 mSv and 470 mSv including [134]Cs and ^{137}Cs; these doses were almost all due to [131]I (~99%). It should be noted that the dose estimate values are not exactly the same as those reported by TEPCO [8]. This is because TEPCO implemented internal dose estimates for the two subjects based on measurement data obtained at the other institute.

Figure 7 compares the estimated intake amounts of ^{131}I and ^{137}Cs for 36 subjects of Group 1 (excluding three subjects with no detection of ^{131}I). The intake amounts of ^{131}I and ^{137}Cs were calculated by MONDAL3 based on the assumptions described before. Three lines in the figure represent the ratios of intake amounts of ^{131}I to ^{137}Cs corresponding to 1, 10 and 100. As shown in the figure, the observed ratios are widely scattered. The geometrical mean (GM) and geometrical standard deviation (σ_g) of these ratios were calculated as 41.7 and 5.9, respectively. The ratio was larger than 100 for 11 subjects of Group 1.
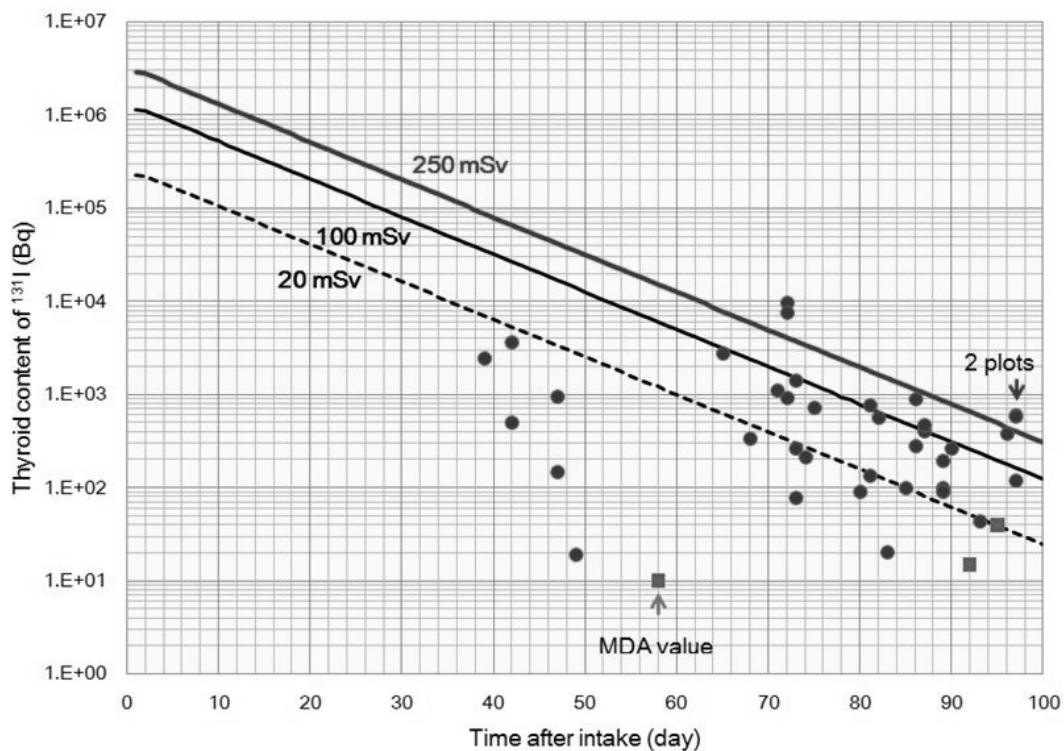
Figure 6. Thyroid content of ^{131}I as a function of the time after intake
(circle plots: measured values, square plots: minimum detectable activity values of 3 different subjects)
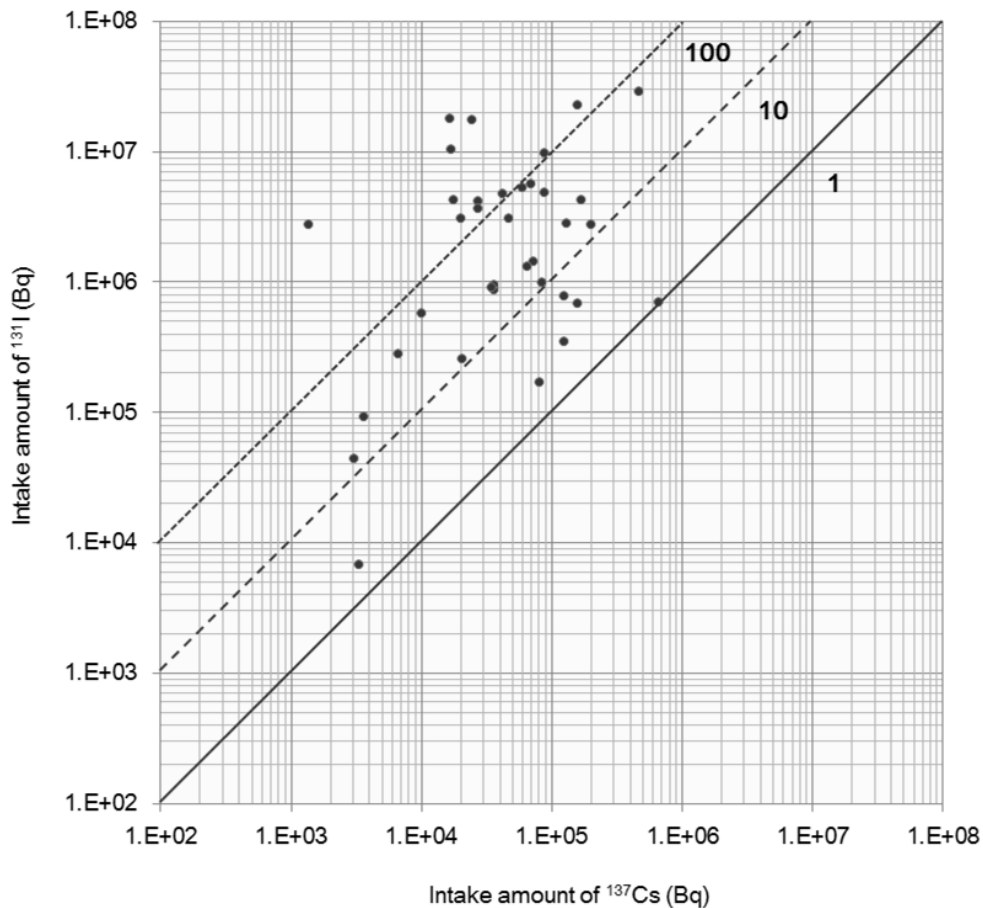
Figure 7. Comparison of the estimated intake amounts of ^{137}Cs and ^{131}I

3.2. Comparison of measured values between different methods

Regarding the whole-body counting and the thyroid counting for the subjects of Group 1, several comparisons of these measured values between different methods were made.

Figure 8 compares the whole-body content of ^{137}Cs between the chair-type WBC and the standing-type WBC, showing that the latter systematically yielded measured values that were larger by 20% than the former.

Figure 9 compares the thyroid content of ^{131}I determined by the HPGe detector using the two NDDs (5 cm and 10 cm), showing that measured values with the two NDDs agree well with each other. The data in the figure are from 23 subjects.

Figure 10 compares the thyroid content of ^{131}I using the HPGe detector (for the NDD of 10 cm) and the NaI(Tl) detector, showing that the latter systematically obtained measured values that were smaller by 20% than the those of the former. The data in the figure are from 21 subjects.

Figure 11 compares the thyroid content of ^{131}I between the HPGe detector (for the NDD of 10 cm) and the standing-type WBC. Note that the standing-type WBC was calibrated for the activity distributed throughout the entire body. Therefore, the measured data of ^{131}I from the standing-type WBC were treated as the whole-body content even though iodine is localized to the thyroid. The figure shows that the latter systematically obtained about three times larger measured values than the former. The data in the figure were obtained from 24 subjects.
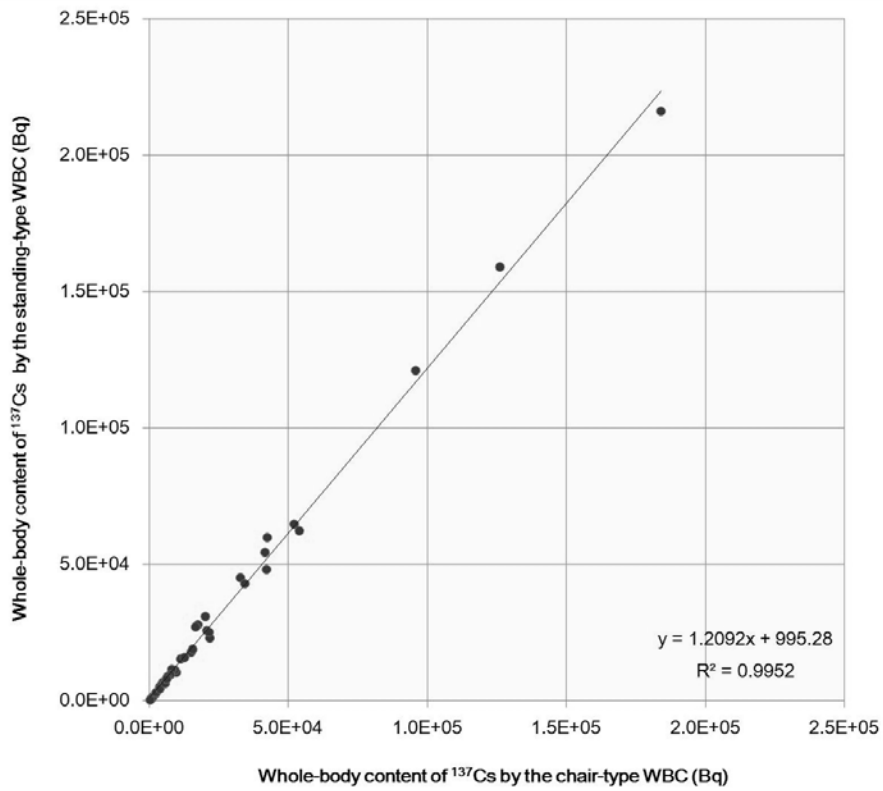
Figure 8. Comparison of the whole-body content of ^{137}Cs between two types of WBCs
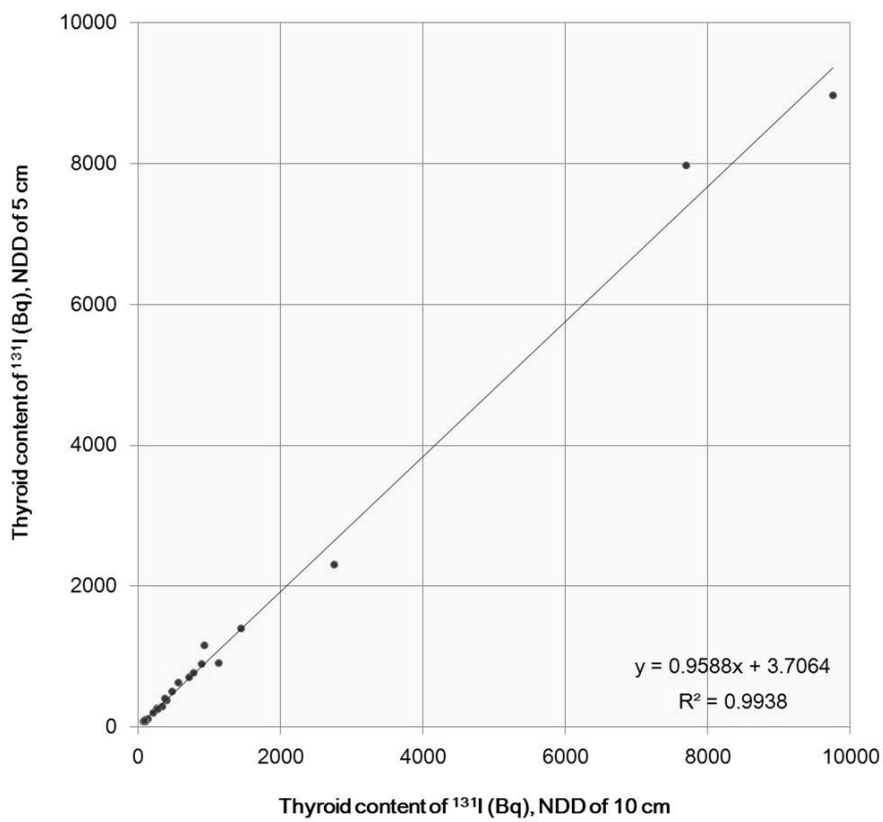
Figure 9. Comparison of the thyroid content of ^{131}I measured with the HPGe detectorusing two different NDDs
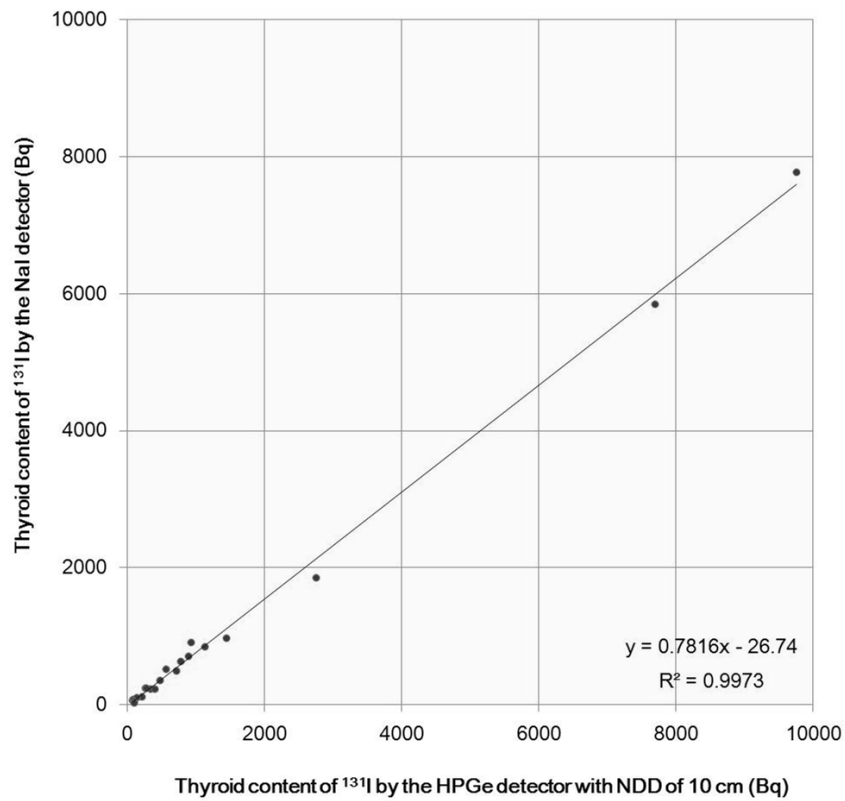
Figure 10. Comparison of the thyroid content of ^{131}I measured using two different types of detectors
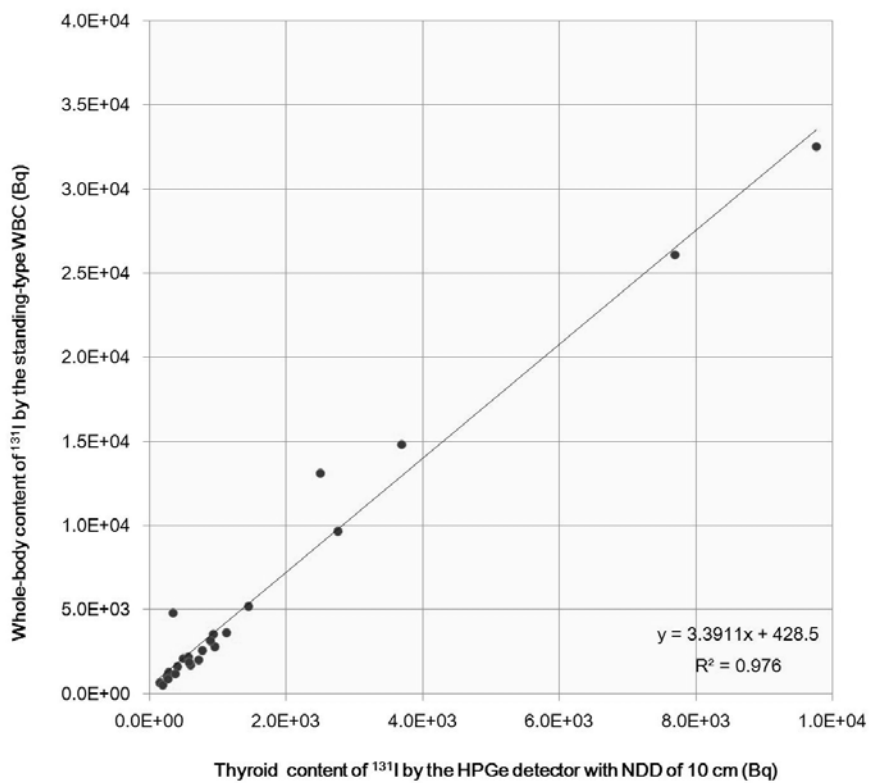
Figure 11. Comparison between the thyroid content measured using the HPGe detector and the whole-body content measured using the standing-type WBC (total-body calibration) for ^{131}I

4. Discussion

Our tentative dose estimates for the workers showed that the contribution of ^{131}I to the total internal dose was extremely high compared to the other major nuclides of [134]Cs and [137]Cs. Regarding the subjects of Group 1, the internal dose ratio of ^{131}I to all three nuclides was 93.5% on average. For the male subject with the highest internal dose, his dose was estimated to be 600 mSv consisting of 590 mSv from [131]I. This value is not exactly the same as the dose estimate value (590 mSv including contributions from other nuclides) officially reported by the TEPCO[8] although both the values are very similar to each other.

The detection sensitivity in the thyroid counting was crucial because of the rapid decay-out of [131]I. A typical MDA value for ^{131}I in the present thyroid measurements was 10 Bq for a counting time of 10 min although this value varied with the whole-body content of radiocesium. Such a level of detection sensitivity was, however, not sufficient for most of the subjects of Group 2 who were measured after June 18, 2011 (98 days after the presumed intake on March 12). A predicted thyroid content corresponding to 20 mSv in CED was calculated as 25 Bq on the 100th day (see Figure 6), suggesting that internal doses below 20 mSv could be ensured for most of the subjects of Group 2. In fact, for about 70% of these subjects, no ^{131}I was detected in the thyroid.

The ratio of intake amounts of ^{131}I to ^{137}Cs was widely scattered among the individual subjects (Figure 7). The GM value of these ratio, 41.7, was larger than the ratio of the discharged amounts of these nuclides evaluated from atmospheric dispersion simulations[9]. A wide scattering of the intake ratio indicates that the composition of radionuclides varied considerably with time and location. It is thus important to characterize these ratios depending on the subject's behavior. That ratio would be an important factor in internal dose estimates for the public whom sufficient thyroid monitoring was not available.

In this study, several comparisons of measured data between different methods were made for both the whole-body counting and thyroid counting. Reasons for discrepancies found in the measured data are described as follows.

- The discrepancy in the whole-body content of ^{137}Cs between the two WBCs (Figure 8) is partially due to the difference in the calibration phantoms. An additional experiment confirmed that the BOMAB phantom gave 10% lower counting efficiency values compared to the Transfer phantom in the standing-type WBC. The other reason for that discrepancy was presumably due to the difference in the counting geometry between the two WBCs.

- The agreement in the thyroid content between the two NDDs (Figure 9) indicates that the detection positioning relative to the thyroid was reasonable. Based on this result, all the subjects of Group 2 (except one) were thus measured once with the NDD of 5 cm.

- On the other hand, a systematic discrepancy was found in the thyroid content between the HPGe detector and the NaI(Tl) detector (Figure 10) although both detectors were calibrated with the same phantom (the neck part of the Transfer phantom). However, this phantom may not be suitable for thyroid measurements with a close counting geometry. From the detection point of view, the problem is to have a realistic counting geometry for thyroid measurements using an appropriate calibration neck phantom and a calibration source that simulate the active thyroid gland inside the neck of a person.

- There was a large discrepancy between the thyroid content from the HPGe detector and the whole-body content from standing-type WBC (Figure 11). This was caused by the fact that the standing-type WBC used an inappropriate counting efficiency for the thyroid content. In fact, the Transfer phantom can imitate four distributions of activity in the body: the thyroid, the GI, the lungs and the entire body. It was revealed that the counting efficiency value for the thyroid was three times as large as that for the entire body (at 364 keV for the primary peak of ^{131}I). This difference reasonably explains the above discrepancy. Additionally, the result suggests that the thyroid content can be satisfactorily quantified by the standing-type WBC and the Transfer

phantom well simulates the activity distribution both in the thyroid and in the entire body. However, this conclusion could not be drawn until the above result was obtained from the present measurements of the real subjects even though some overestimations were expected in the measurements with the standing-type WBC in Onahama.

The considerations listed above would validate our direct measurements of the subjects. All the measured data were reported to TEPCO and recommended the use of data obtained from the chair-type WBC (for ^{134}Cs and ^{137}Cs) and the HPGe detector (for ^{131}I) in the internal dose estimates.

5. Summary

This paper presents our direct measurements for employees involved in the accident at the Fukushima Daiichi nuclear power station operated by Tokyo Electric Power Company. The number of employees examined from April 20 to August 5 in 2011 totaled 560. Major nuclides detected were ^{131}I, ^{134}Cs and ^{137}Cs and ^{131}I was the predominant contributor to the internal dose. According to our tentative dose estimates, the highest committed effective dose (CED) was 600 mSv, which was found in a male subject measured on May 23, 2011; the thyroid content of ^{131}I for this subject was 9760 Bq at the time of the measurement. However, the assumption of the intake scenario for these dose estimates was made in a conservative manner. Several systems were used in the present measurements and compared the measured data among each instrument for the first 39 subjects in order to validate the measurement methods. Further investigations are still needed to improve internal dose estimations, especially for subjects who were suspected to have extremely high internal exposure, taking into account a more realistic intake scenario regarding the intake pattern and the physicochemical form of radionuclides and also the contribution of other short-life radionuclides (e.g., ^{132}I, ^{133}I and ^{132}Te).

Acknowledgements

References

1) Prime Minister of Japan and his cabinet, Report of Japanese Government to the IAEA Ministerial Conference on Nuclear Safety -The accident at TEPCO's Fukushima Nuclear Power Station-, http://www.kantei.go.jp/foreign/kan/topics/201106/iaea_houkokusho_e.html (Last accessed on 13 Mar 2012).
2) TEPCO, http://www.tepco.co.jp/en/press/corp-com/release/betu11_e/images/110812e14.pdf (Last accessed on 20 Aug 2012).
3) American National Standard, Specifications for the bottle manikin absorption phantom, ANSI/HPS N13.35-1999, (1999)
4) Canberra, The Canberra RMC-II (Model 2257) Transfer phantom.
5) N. Ishigure, M. Matsumoto, T. Nakano, H. Enomoto, Development of software for internal dose calculation from bioassay measurements. Radiat. Prot. Dosim, 109, 235-242 (2004).

6) American National Standard Institute, Thyroid radioiodine uptake and measurements using a neck phantom, ANSI N44.3-1973 (1973).

7) Japan Atomic Energy Agency, Results of the environmental radiation monitoring following the accident at the Fukushima Daiichi nuclear power plant –Interim report (ambient radiation dose rate, radioactivity concentration in the air and radioactivity concentration in the fallout)-, JAEA-Review 2011-035 (2011) [in Japanese].

8) TEPCO, http://www.tepco.co.jp/en/press/corp-com/release/betu11_e/images/110617e23.pdf (Last accessed on 20 Aug 2012).

9) M. Chino, H. Nakayama, H. Nagai, H. Terada, G. Katata, H. Yamazawa, Preliminary estimation of release amounts of ^{131}I and ^{137}Cs accidentally discharged from the Fukushima Daiichi nuclear power plant into the atmosphere. J. Nucl. Sci. Technol. 48, 1129-1134 (2011).

Direct Measurements for Highly-exposed TEPCO Workers and NIRS First Responders Involved in the Fukushima NPS Accident

Takashi NAKANO, Eunjoo KIM, Keiichi AKAHANE, Takako TOMINAGA,
Hideo TATSUZAKI, Osamu KURIHARA, Nobuyuki SUGIURA

National Institute of Radiological Sciences
4-9-1 Anagawa, Inage-ku, Chiba, CHIBA, 263-8555, Japan

Abstract

Direct measurements for internal dose estimates were performed at National Institute of Radiological Sciences (NIRS) on seven highly exposed workers of Tokyo Electric Power Company (TEPCO) and eight NIRS staff members who were first responders to the accident at the TEPCO Fukushima Daiichi Nuclear Power Station. For the TEPCO workers, the measurements were performed by both the whole-body counting and thyroid counting. The average effective half-life values of ^{131}I in the thyroid and of ^{134}Cs and ^{137}Cs in the body were 7.8 days, 92.0 days and 104.3 days, respectively. These values were consistent with biokinetic models proposed by the International Commission on Radiological Protection (ICRP). For the NIRS staff members, the thyroid counting was made on the day when they had returned. The amount of ^{131}I that was detected in the thyroid of all the eight subjects was small (~100 Bq) even though they went to places near the site of the accident in its early stage. This level was found to be comparable to those of other NIRS staff members who stayed in the Chiba area (about 200 km south of the reactor) during the early stage of the accident.

Keywords: *direct measurement; whole-body counting; thyroid counting; ^{131}I; ^{134}Cs; ^{137}Cs; effective half-life*

1. Introduction

National Institute of Radiological Sciences (NIRS), which has been designated a national center for radiation emergency medical preparedness in the nuclear disaster prevention system of Japan, was requested by Tokyo Electric Power Company (TEPCO) to perform internal dose estimates for seven heavily exposed workers who were suspected to have received effective doses over 250 mSv. These workers were engaged in emergency operations at the Fukushima Daiichi Nuclear Power Station (FDNPS) to prevent further worsening of the accident triggered by the Great East Japan Earthquake Disaster on March 11, 2011. This paper describes the results of direct (*in vivo*) measurements performed on these workers and also on eight NIRS staff members who were dispatched to places near the FDNPS in the early stage of the accident to support radiation-related responses. This report only presents results of the measurements. Issues regarding the internal dose estimates will be addressed in a future publication.

2. Instrumentation and calibration used for the direct measurements

2.2. Instrumentation

One system for thyroid counting and two systems for whole-body counting were used at NIRS to take direct measurements of subjects. The thyroid counting was performed by a system consisting of

a low energy-type HPGe detector (LX-70450/30P, ORTEC, US; 70 mm diameter and 30 mm thickness), a lead collimator with a thickness of 5 cm, and also a supporting device used to adjust the height of the detector (Figure 1). This HPGe detector was cooled by an electric cooling system (Xcooler II, ORTEC, US). On the other hand, the two systems used for whole-body counting consisted of a screening-type and a precision-type whole-body counters (WBCs). The two WBCs had a bed counting geometry. The screening-type WBC (Figure 2) has four NaI(Tl) detectors, each of which are 20.3 cm in diameter and 10.2 cm in height. These detectors are surrounded on the sides with an annular lead shield with a thickness of 5 cm. These detectors are arranged in a linear straight array under the bed that supports the subject. The precision-type WBC is installed in a large shielded chamber made of 20 cm-thick-steel. This WBC has six HPGe detectors, each of which has nominally 100% relative efficiency; four detectors are placed over (Figure 3 (a)) and two detectors are placed under the bed for the subject (Figure 3 (b)). Detailed specifications of this WBC have been presented elsewhere [1].

Thyroid counting was performed for all the subjects (seven TEPCO workers and eight NIRS staff members) described above, whereas the whole-body counting was partially cancelled for the NIRS staff members. Unfortunately, the March 11 earthquake made the precision-type WBC inoperative for a few weeks, and could not be used for the NIRS staff members responding to the initial phase of the accident. Consequently, they were measured only with the screening-type WBC. Meanwhile, we could measure all the TEPCO emergency workers with the precision-type WBC because these measurements were initiated on May 30, 2011 (and have continued to date).

Figure 1. System for thyroid counting

Figure 2. Screening-type WBC
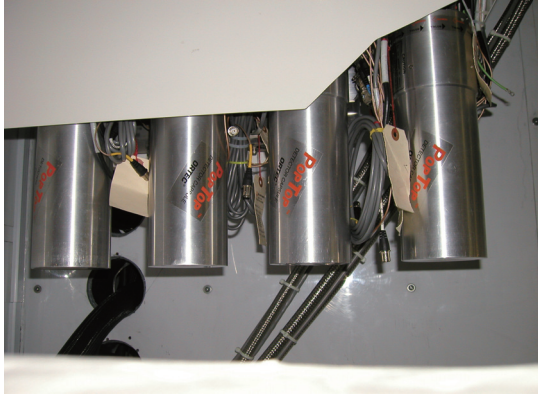
(a) Four detectors over the bed

(b) Two detectors under the bed

Figure 3. Detector arrangement for the precision-type WBC

2.2. Calibration

Calibration to obtain counting efficiency values of the above systems was performed using physical phantoms. For the thyroid counting, we used a neck phantom (Figure 4) developed by Nishizawa and Maekoshi [2]. This phantom is composed of an acrylic cylinder containing a thyroid gland-shaped container and other structures imitating the cervical vertebrae and the airway. To use the phantom, the thyroid container is filled with a radioactive solution of ^{133}Ba. For calibration of the two WBCs, a set of three BOttle MAnikin ABsorption (BOMAB) phantoms [3] with heights of 177 cm and weights of 70 kg were used (Figure 5). Each of these BOMAB phantoms separately contained ^{133}Ba, ^{137}Cs and ^{60}Co. Structural materials of the phantoms (the shell and the filler) are based on specifications by the American National Standard Institute (ANSI N13.35). Both the phantoms for the thyroid counting and the whole-body counting imitate an adult male.

The counting time for thyroid counting was 5 min (or 10 min in the case of subjects with less thyroid radioactivity). That for whole-body counting with the precision-type WBC was 30 min, while that with the screening-type WBC was variable. The body content of each radionuclide was calculated from the net peak count rates in the energy spectra from the direct measurements and the corresponding counting efficiency values.
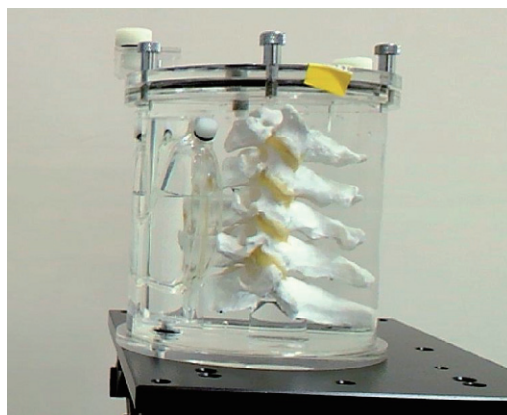
Figure 4. Exterior of the neck phantom used for the calibration [2]

Figure 5. Exterior of the BOMAB phantom used for the calibration [3]

3. Results and discussion

3.1. Results of TEPCO workers

The measurements showed that ^{131}I, ^{134}Cs and ^{137}Cs were the major radionuclides; other radionuclides (e.g., ^{136}Cs, ^{129m}Te) were occasionally detected at small amounts in several subjects. Our institute has performed repeated measurements for the TEPCO workers together with a medical checkup to the present (as of Oct. 2012).

Figure 6 displays the relative thyroid contents (normalized to the first measurement) of ^{131}I for the seven TEPCO workers as a function of time after the first measurement day. The measured values of ^{131}I are also provided in Table 1. Our measurements of the seven TEPCO workers showed that effective half-life values of ^{131}I in the thyroid ranged from 6.7 to 9.6 days. These values were obtained from three different measurements. The average value of the effective half-life of ^{131}I among the subjects was 7.8 days, which is in good agreement with the corresponding value predicted by a biokinetic model of iodine [4]. The latter value was calculated as 7.4 days for the case of inhalation, and during the first 10 days after the first uptake to the thyroid is terminated. Note that all the seven TEPCO workers were measured two months after the accident.

Figure 7 displays relative whole body contents of ^{134}Cs for the seven TEPCO workers. Table 2 shows the actual values and the dates of the measurements. The effective half-live for ^{134}Cs ranged from 84.7 to 101.1 days, with an average of 92.1 days. Figure 8 and Table 3 present the corresponding values for ^{137}Cs, showing that the effective half-life values ranged from 92.8 to 115.7 days, with an average of 104.2 days. The predicted effective half-life values of ^{134}Cs and ^{137}Cs based on the ICRP's biokinetic model for cesium were calculated as 95.6 days and 108.5 days, respectively. Note that these values were obtained from retention functions without a rapid excretion component in the first 10 days after the intake via inhalation. Our results thus support the ICRP's biokinetic model for cesium as well as that for iodine. This good agreement would be partially explained by the fact that all seven TEPCO workers were adult male subjects. Regarding Subject B, the whole-body contents of ^{134}Cs and ^{137}Cs were similar in the first three measurements while the corresponding values clearly decreased for the other subjects even with the small time span between measurements. The reason for this anomaly is unknown,
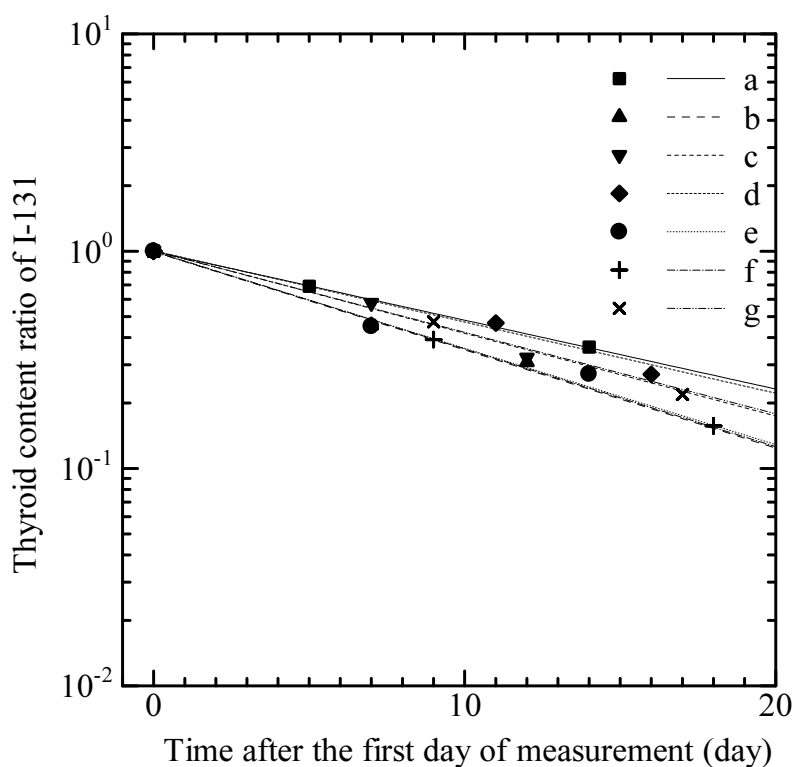
Figure 6. Relative thyroid contents of ^{131}I as a function of time after the first day of measurement

Table 1 Measured values of ^{131}I in the thyroid

Subject	Measured value (Bq)*			T_{eff} (d)
	RUN1	RUN2	RUN3	
A	58 Bq (2011.7.1)	40 Bq (2011.7.6)	21 Bq (2011.7.15)	9.6
B	366 Bq (2011.6.24)	167 Bq (2011.7.1)	113 Bq (2011.7.6)	7.0
C	279 Bq (2011.6.24)	161 Bq (2011.7.1)	90 Bq (2011.7.6)	7.4
D	306 Bq (2011.6.20)	143 Bq (2011.7.1)	83 Bq (2011.7.6)	8.7
E	754 Bq (2011.6.10)	340 Bq (2011.6.17)	205 Bq (2011.6.24)	7.5
F	4,670 Bq (2011.5.30)	1,830 Bq (2011.6.8)	734 Bq (2011.6.17)	6.7
G	4,710 Bq (2011.5.30)	2,230 Bq (2011.6.8)	1,030 Bq (2011.6.16)	7.8

* Measurement date (in parentheses)
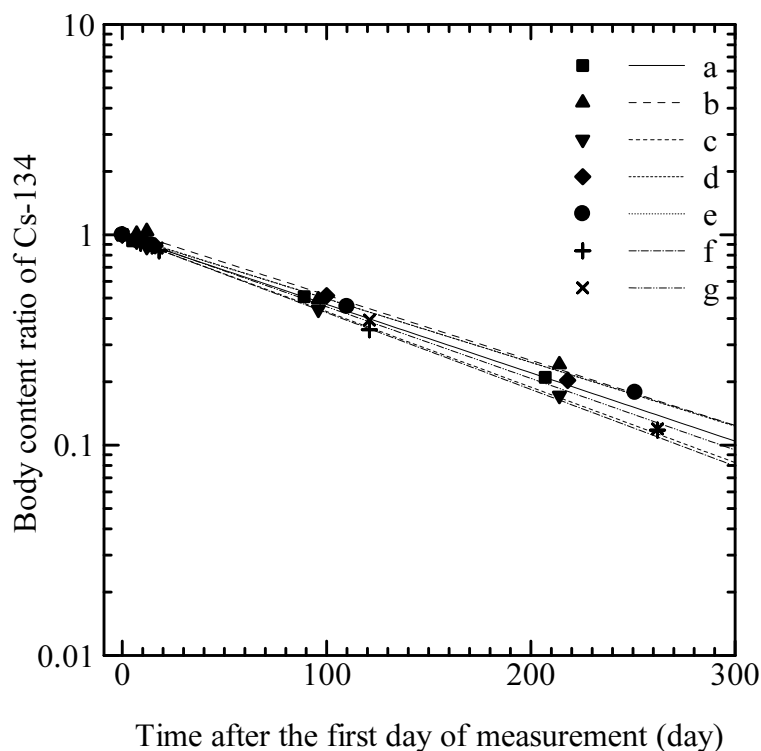
Figure 7. Relative body content of ^{134}Cs as a function of time after the first day of measurement

Table 2 Measured values of ^{134}Cs in the body

| Subject | Measured value (Bq)* | | | | | T_{eff} (d) |
	RUN1	RUN2	RUN3	RUN4	RUN5	
A	3,920 Bq (2011.7.1)	3,670 Bq (2011.7.6)	3,480 Bq (2011.7.15)	1,990 Bq (2011.9.28)	825 Bq (2012.1.24)	92.9
B	3,710 Bq (2011.6.24)	3,740 Bq (2011.7.1)	3,860 Bq (2011.7.6)	1,830 Bq (2011.9.28)	898 Bq (2012.1.24)	99.3
C	5,090 Bq (2011.6.24)	4,740 Bq (2011.7.1)	4,460 Bq (2011.7.6)	2,250 Bq (2011.9.28)	875 Bq (2012.1.24)	84.7
D	6,950 Bq (2011.6.20)	6,440 Bq (2011.7.1)	6,160 Bq (2011.7.6)	3,570 Bq (2011.9.28)	1,410 Bq (2012.1.24)	95.6
E	20,100 Bq (2011.6.10)	18,900 Bq (2011.6.17)	18,000 Bq (2011.6.24)	9,170 Bq (2011.9.28)	3,580 Bq (2012.2.16)	101.1
F	44,200 Bq (2011.5.30)	40,300 Bq (2011.6.8)	37,100 Bq (2011.6.17)	15,600 Bq (2011.9.28)	5,210 Bq (2012.2.16)	85.2
G	118,000 Bq (2011.5.30)	110,000 Bq (2011.6.8)	102,000 Bq (2011.6.16)	46,400 Bq (2011.9.28)	14,100 Bq (2012.2.16)	85.9

* Measurement date (in parentheses)
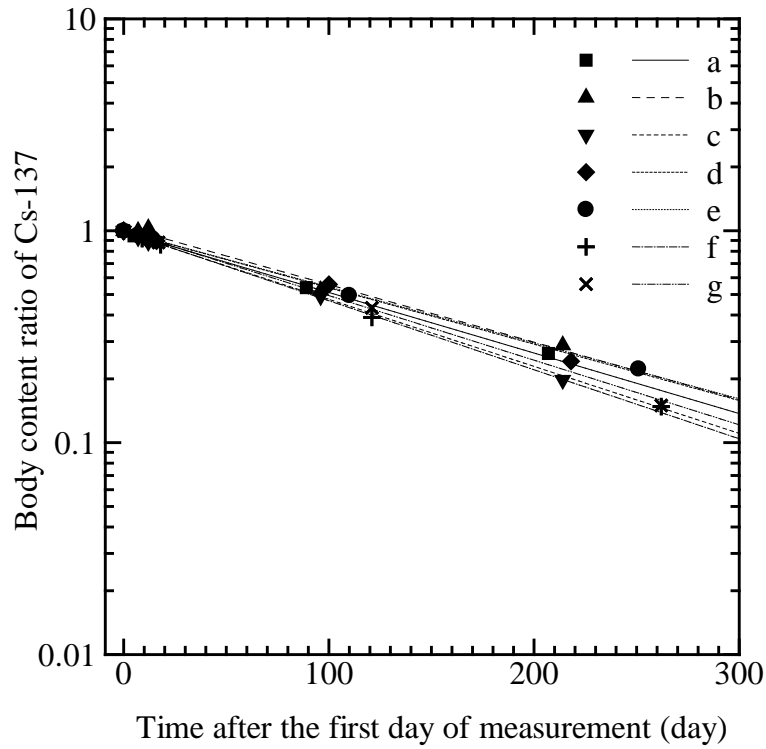
Figure 8. Relative body content of ^{137}Cs as a function of time after the first day of measurement

Table 3 Measured values of ^{137}Cs in the body

| Subject | Measured value (Bq)* | | | | | T_{eff} (d) |
	RUN1	RUN2	RUN3	RUN4	RUN5	
A	4,330 Bq (2011.7.1)	4,100 Bq (2011.7.6)	3,900 Bq (2011.7.15)	2,330 Bq (2011.9.28)	1,140 Bq (2012.1.24)	108.2
B	4,300 Bq (2011.6.24)	4,310 Bq (2011.7.1)	4,430 Bq (2011.7.6)	2,260 Bq (2011.9.28)	1,240 Bq (2012.1.24)	113.2
C	5,780 Bq (2011.6.24)	5,390 Bq (2011.7.1)	5,140 Bq (2011.7.6)	2,840 Bq (2011.9.28)	1,150 Bq (2012.1.24)	92.8
D	7,570 Bq (2011.6.20)	6,970 Bq (2011.7.1)	6,790 Bq (2011.7.6)	4,230 Bq (2011.9.28)	1,840 Bq (2012.1.24)	108.1
E	21,400 Bq (2011.6.10)	20,400 Bq (2011.6.17)	19,600 Bq (2011.6.24)	10,600 Bq (2011.9.28)	4,780 Bq (2012.2.16)	115.7
F	47,600 Bq (2011.5.30)	43,800 Bq (2011.6.8)	41,000 Bq (2011.6.17)	18,600 Bq (2011.9.28)	7,060 Bq (2012.2.16)	95.2
G	127,000 Bq (2011.5.30)	119,000 Bq (2011.6.8)	112,000 Bq (2011.6.16)	55,000 Bq (2011.9.28)	19,100 Bq (2012.2.16)	96.2

 * Measurement date (in parentheses)

3.2. Results of NIRS first responders

Eight NIRS staff members who were dispatched to areas closed to the FDNPS as first responders were measured in March, 2011. Four of the eight subjects were measured with both the system for thyroid counting and the screening-type WBC, and the other four subjects were measured with the thyroid monitor only. The whole-body content of ^{134}Cs and ^{137}Cs ranged from 670 Bq to 1200 Bq. However, these values might also include external contamination on the subjects or their clothing. Surface contamination tests were performed on the subjects using Geiger-Mueller-type survey meters, which showed slightly elevated counts compared to those in normal background counts. The thyroid content of ^{131}I ranged from 33 Bq to 124 Bq. These levels were comparable to results (62 Bq and 166 Bq) from two NIRS employees who had remained at Chiba (around 200 km south of the FDNPS).

Although our data are very limited, the results obtained from our subjects probably suggest that internal doses of public evacuees from areas within a 20 km-radius of the FDNPS (designated as the evacuation zone by the Japanese central government) were very low in the early stage of the accident[5]. Most of these evacuees moved outside of the zone before the largest release of radioactive materials into the environment on March 15, 2011. However, further investigations are needed on the individual behaviors of the NIRS first responders.

4. Summary and Future work

This paper presents results of our direct measurements of seven TEPCO workers involved in the accident at the FDNPS and eight first responders of NIRS who were dispatched to areas near the FDNPS at the early stage of the accident. The TEPCO workers were selected since they were suspected of receiving internal doses of over 250 mSv. The average effective half-life values of ^{131}I, ^{134}Cs and ^{137}Cs for the seven workers were 7.8 days, 92.1 and 104.2 days, respectively. These values were consistent with those predicted by the ICRP's biokinetic models for iodine and cesium. Several issues remain for future work. These include development of the best internal dose estimates for the TEPCO workers, how to determine the most appropriate intake scenario, how to evaluate the effectiveness of KI tablets administered to these workers and how to evaluate additional dose due to the intake of short-lived nuclides (e.g., ^{132}Te, ^{132}I, ^{133}I), etc. The internal doses of first responders from NIRS were found to be around 0.1 mSv in effective dose even at the maximum. However, in their cases as well as those of workers, the intake scenarios for the responders should be refined according to their behaviors during the response for more reliable internal dose estimates.

References

1) T. Suzuki, T. Nakano and E. Kim, Development of Integrated Whole Body Counter, Radiat. Prot. Dosim. 127(2007), 297-302

2) K. Nishizawa, H. Maekoshi, Thyroid ^{125}I Monitoring System Using a NaI(Tl) Survey Meter, Health Phys. 58(1990), 165-169.

3) Health Physics Society (1999) American National Standard-Specifications for the Bottle Manikin Absorption Phantom, ANSI/HPS N13.35-1999.

4) ICRP(1993) Age-dependent Doses to Members of the Public from Intake of Radionuclides: Part 2 Ingestion Dose Coefficients, ICRP Publication 67. Pergamon Press, Oxford.

5) Report of Japanese Government to the IAEA Ministerial Conference on Nuclear Safety –The Accident at TEPCO's Fukushima Nuclear Power Station, http://www.kantei.go.jp/foreign/kan/topics/201106/iaea_houkokusho_e.html (available on Oct. 19, 2012).

Retrospective Assessment of Internal Doses for Short-term Visitors to Fukushima within One Month after the Nuclear Power Plant Accident

Naoki MATSUDA[1,2], Atsushi KUMAGAI[3], Akira OHTSURU[3], Naoko MORITA[2], Miwa MIURA[2], Masahiro YOSHIDA[2], Takashi KUDO[2], Noboru TAKAMURA[2], Shunichi YAMASHITA[2,3]

[1]*Center for Frontier Life Sciences, Nagasaki University, 1-12-4 Sakamoto, Nagasaki, NAGASAKI, 852-8523, Japan*
[2]*Graduate School of Biomedical Sciences, Nagasaki University, 1-12-4 Sakamoto, Nagasaki, NAGASAKI, 852-8523, Japan*
[3]*Fukushima Medical University, 1 Hikarigaoka, Fukushima, FUKUSHIMA, 960-1295, Japan*

Abstract

Short-term visitors to Fukushima have been monitored for internal exposure by using the whole body counter of the Nagasaki University Medical School. The total number of subjects exceeds 900 at the end of July, 2012. The highest committed effective dose and thyroid equivalent dose in 173 people who stayed in Fukushima during March 11th to April 10th, 2011 were assessed around 1 mSv and 20 mSv, respectively.

***Keywords:** internal dose; whole body counter; short-term visitors*

1. Introduction

The horizontal bed-type scanning whole body counter (WBC) has been operated in Nagasaki University Medical School since 1968 in order to investigate internal exposure of various subjects including atomic-bomb survivors, residents around the Chernobyl nuclear power plant and patients who received treatment with radiopharmaceuticals. After the radiation accident at the Tokyo Electric Power Company (TEPCO) Fukushima-Daiichi nuclear power plant, short-term visitors to Fukushima have been monitored for internal exposure. Their internal radioactivity could provide us with a rough idea of how much Fukushima residents were internally exposed by the intake of radioactive materials.

2. Method

The WBC in Nagasaki University is configured with two NaI(Tl) scintillation detectors (8 inches diameter and 4 inches thickness) connected to four photomultipliers each, in both the upper and the lower position of a subject. The whole detection unit is protected from naturally occurring external radiation in a shielding room consisted of 20cm-thickness steel and 3mm-thickness lead (Figure 1). Two detectors scanned whole body of a patient longitudinally for 20 minutes at a constant speed. The results were shown as a gamma-ray energy spectrum through a multi channel analyzer. Then a spectrum analyzing software identified and quantified nuclides in term of activity on the body, including thyroid. To avoid any false-positive or false-negative detection, the results provided by the software were reconfirmed by a visual judgment of spectrum by two independent examiners who set the common criteria for identification of peaks for Cs-134 at 605keV and for Cs-137 at 662keV on spectra obtained from more than ten patients with very low radioactivity. The calibration of counting efficiency and energy resolution was performed in December 2009 and December 2012, using the bottle manikin absorption (BOMAB) phantom that satisfies specifications of American National Standard N13.35 (ANSI N13.35) [1]. The authors understood that thyroid counting geometry was the

best method for determination of radioiodine. However, we used whole body scan counting, not thyroid counting, because the purpose of the examination was to measure all detectable radionuclides that were present in a whole body of each patient at once in a limited time. For this reason, the calibration was done in a manner of whole body scan counting using a BOMAB phantom even though this method was for the assessment of activity distributed homogenously in a body. The overall system was configured and assembled by Fuji Electric, Tokyo, Japan.

More than 900 people were monitored for internal survey. The subjects in the earlier days comprised evacuees from the coastal area of Fukushima, so called Hama-dori, including residents and business visitors, while medical and governmental assistance team to aid quake, tsunami, and radiation victims from Nagasaki were mainly involved in the later days. Among them, 173 people had stayed for a period of 4 to 5 days around the Fukushima site during March 11th to April 10th, 2011. The number of men and women was 156 and 17, respectively, and their averaged age was 42.2 years old. The internal radioactivity obtained on the day of measurement was converted to the initial intake of each radionuclide according to the scenario of acute inhalation of particular aerosol (AMAD=1µm) with absorption type F on the first or on the last day of the period of residence in Fukushima district because the exact conditions of exposure for each individual was not available. Furthermore, the results from the scenario of ingestion as a route of intake are not shown in this report because the immediate shutdown of public water supply and transportation of food after the earthquake and tsunami made the local residents and visitors ingest foods only in-store or in a refrigerator which were not contaminated. The committed effective dose and thyroid equivalent dose were then estimated. All calculations were executed by using software named MONDAL3 developed and distributed by the National Institute of Radiological Sciences.
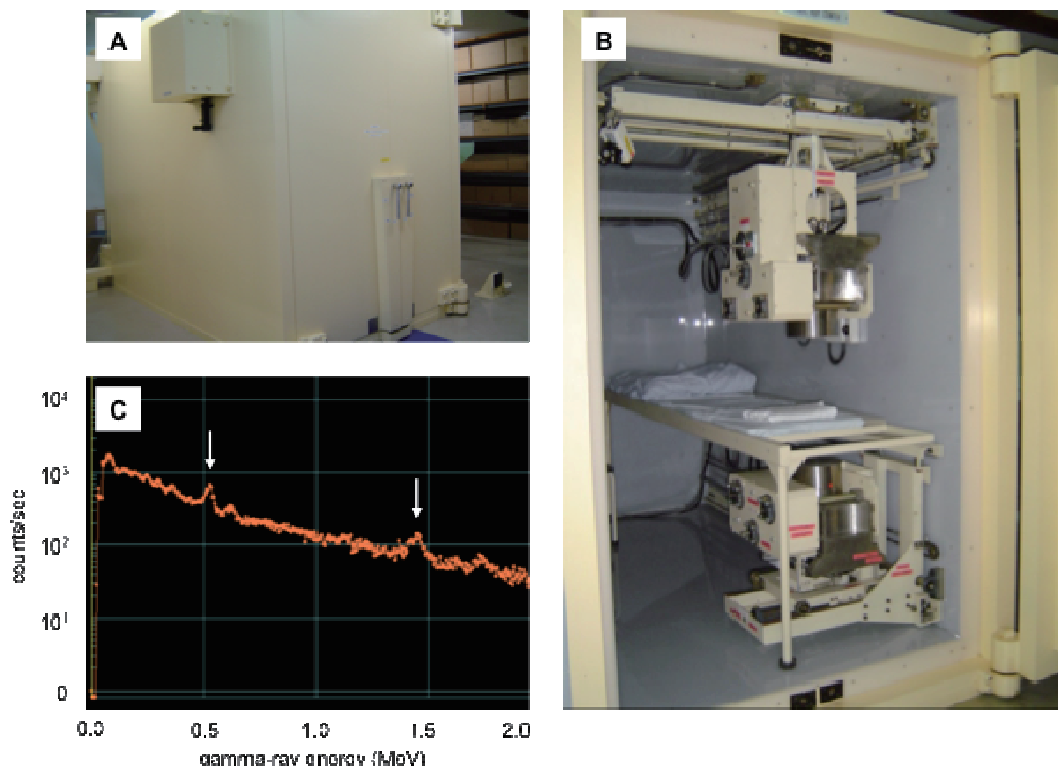
Figure 1. The whole body counting system in Nagasaki University Medical School. In the shielding room (A), two NaI detectors are set at the upper and lower position of a bed (B). The background energy spectrum demonstrates annihilation radiation and a gamma ray emitted from K-40 (left and right arrows, respectively).

3. Results

Figure 2(A) demonstrates the number of subjects who exhibited internal radioactivity in 173 people who had stayed in Fukushima during March 11th to April 10th, 2011. The number of subject positive for I-131, Cs-134 and Cs-137 was 55, 67, and 56, respectively. The difference in the numbers of subjects with Cs-134 and Cs-137 is due to the poor resolution between the low-energy Cs-134 and Cs-137 peaks. The ratio of positive subjects to the total population was higher than 30% in either nuclide (Figure 2(B)). The multiple intakes of three nuclides were found in forty-five subjects, corresponding to 26.0% of total population. I-131 was detected in 48 out of 67 (71.6%) in Cs-134 positive subjects and in 45 out of 56 (80.4%) in Cs-137 positive subjects (Table 1). However, I-131 was undetected or hardly observed in later period of exposure. For example, Figure 3 illustrates the whole-body energy spectrum of gamma-ray emitted from I-131 in the same subject who visited Fukushima twice in March and April. The significant peak for I-131 was observed after the first stay in March 13 to 18, whereas no peak was found in the second stay in April 12 to 21.
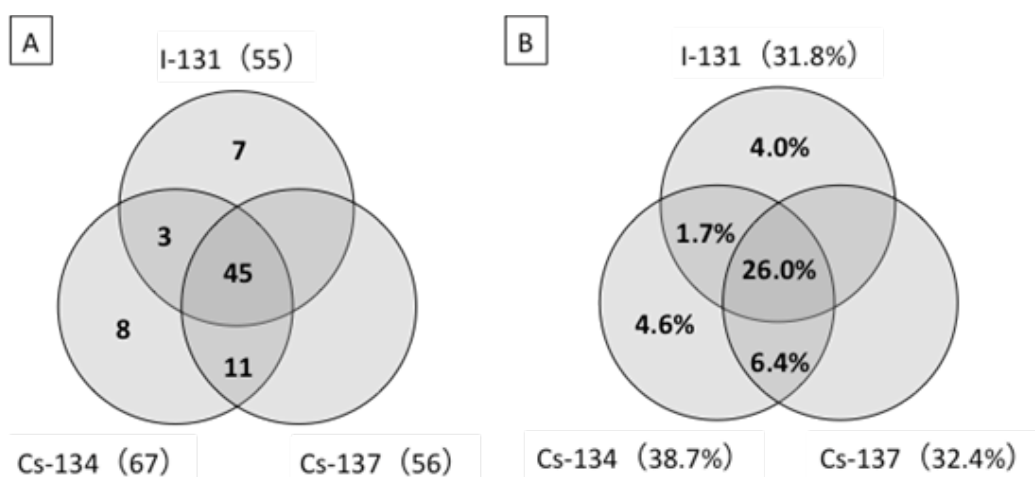
Figure 2. The number of subjects positive to I-131, Cs-134, Cs-137, and their combinations in 173 total population (A). The detection ratio to the total subjects (B).

Table 1 Internal I-131 found in Cs-134 or Cs-137 positive subjects.

	Total	I-131 positive	%
Cs-134 positive	67	48	**71.6**
Cs-137 positive	56	45	**80.4**
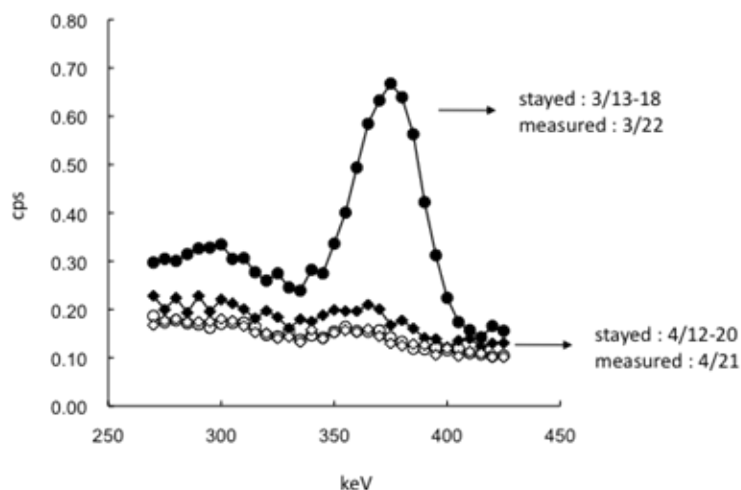
Figure 3. The differential gamma energy spectrum emitted from I-131 for the same visitor to Fukushima site at different periods of exposure

The estimated intake was 140kBq for I-131 and 16kBq for Cs-134 and Cs-137 in the highest case although the results varied widely among individuals. The highest committed effective dose as a sum of I-131, Cs-134 and Cs-137 was 1mSv, which was mainly contributed by I-131. The thyroid dose for the same subject was 20mSv. In other subjects, no case higher than 0.1mSv of effective dose and 2mSv of thyroid dose was observed.

4. Discussion

The accurate and reliable reconstruction of early internal doses after the Fukushima-Daiichi nuclear power plant accident is desired for all inhabitants, residents, and workers in Fukushima. However, lack of initial data on internal radioactivity, airborne concentration of radionuclides, and the radiation level of food contamination make it difficult to estimate doses both directly and indirectly. Although the number of subjects is quite limited, our results on internal doses of short-term visitors in Fukushima hopefully give a clue, in addition to the accurate data on inhabitants by in-situ investigations[2-4], to the rough estimation of doses in a larger number of people because the individual dose may reflect the environmental radioactivity at a certain place in a certain time. Our data suggested that multiple intake of radionuclides, including I-131, Cs-134 and Cs-137 at least, occurred in the very early period after the accident mainly due to inhalation of airborne radioactivity. Although the highest committed effective dose was as low as 1mSv, the possible inhalation may increase, depending on the distance from the nuclear plant and wind directions. The practical reconstruction model of early internal doses for Fukushima residents should be established urgently by putting every available data together, including the results from direct measurement of internal radioactivity, the simulated geographical distribution of radionuclides by environmental radiation monitoring, and the accurate estimation of the radioactivity discharged from the reactors.

5. Conclusions

The internal dose for the short-term visitors to Fukushima has been evaluated in Nagasaki using a whole body counter. The results for visitors in the early period after the event, suggested that multiple intakes of I-131, Cs-134 and Cs-137 occurred even if the period of exposure is short. The medical equipment allows to follow both iodine and cesium isotopes.

Acknowledgement

References

1)American National Standards Institute. An American National Standard on specifications for the bottle manikin absorption phantom. Health Physics Society; ANSI/HPS N-13.35. (1999).
2) Nuclear Safety Commission of Japan. Thyroid dose estimation in children of Fukushima. http://www.nsc.go.jp/anzen/shidai/genan2011/genan031/siryo4-3.pdf#page=1. (2011).
3) Tokonami S, Hosoda M, Akiba S, Sorimachi A, Kashiwakura I, Balonov M. Thyroid doses for evacuees from the Fukushima nuclear accident. Sci Rep 2 (2012), 507.
4) National Institute of Radiological Sciences. Internal dose estimation by NIRS. http://www.pref.fukushima.jp/imu/kenkoukanri/230724shiryo

Lessons Learned from Early Direct Measurements at Fukushima Medical University after the Fukushima Nuclear Power Station Accident

Makoto MIYAZAKI, Takashi OHBA, Akira OHTSURU

Department of Radiation Health Management, Fukushima Medical University,
1 Hikarigaoka, Fukushima, FUKUSHIMA, 960-1295, Japan

Abstract

The Fukushima Daiichi Nuclear Power Station (FDNPS) accident resulted in a month-long discharge of radioactive materials into the environment. These radioactive materials were detected at Fukushima Medical University (FMU), which is 57 km northwest of the FDNPS. Significant levels of six nuclides (i.e., ^{131}I, ^{132}Te, ^{132}I, ^{133}Xe, ^{134}Cs, and ^{137}Cs) were detected by a whole body counter (WBC) on March 15, 2011 when the ambient dose rate was suddenly elevated for the first time. This WBC has a dual detector system consisting of two NaI(Tl) detectors and two Ge detectors. We conducted periodical measurements of 32 humans and the background using the WBC. Because the three nuclides ^{131}I, ^{134}Cs and ^{137}Cs were still detected in the background by the WBC a few months after the accident, accurate WBC measurements were difficult. Here we describe the limitations of our measurements conducted in the early stage of the FDNPS accident.

1. Introduction

In 1999, Fukushima Medical University (FMU) was officially designated as a secondary Radiation Emergency Medical Hospital by the Japanese government, following the criticality accident of JCO Co., a nuclear fuel processing company. To improve the country's response to radiation emergency situations, various radioactivity measurement systems were newly arranged at FMU in 2001. Before 2011, these systems were used only for radiological emergency drills in Fukushima Prefecture, since there were no significant emergencies during those years. A whole-body counter (WBC) was installed and maintained at FMU as one of the above systems. This WBC (Accuscan-II, Canberra Inc., Meriden, CT, USA) was placed in a room without special shielding and without radioactive material-filtrating ventilation.

In the early stage of the Fukushima Daiichi Nuclear Power Station (FDNPS) accident shortly after the March 11, 2011 Tohoku earthquake and tsunami, radioactive materials released from the FDNPS site were continuously detected at FMU, which is located 57 km northwest of the FDNPS. Elevated radiation levels made it difficult to perform appropriate radiological monitoring. This paper briefly introduces problems that were identified when measurements were taken of individuals who had possible internal contamination with radionuclides under high-background radiation conditions.

2. Experimental Design

The WBC used at FMU is a Canberra Accuscan-II, a bed-type whole-body counter with dual detector systems: one is two sets of NaI(Tl) detectors and the other is two sets of HPGe detectors. These detector systems are mounted over the scanning bed for a subject and are installed in steel shielding. Soon after the FDNPS accident, periodical measurements with a counting time of 5 min were continued using this WBC. The subjects were changed by cloth for WBC examination.

In the early stage of the FDNPS accident, we used the WBC to examine 32 staff members of a radiation medical team that was established at FMU. Periodical measurements with the WBC were conducted from March 17, 2011 to April 25, 2011. These 32 subjects are divided into the following two groups: Group 1 consists of subjects who were working and were examined before March 17, 2011 (n=10), and Group 2 consists of subjects who were examined during the period March 17 to April 25 (n=22).

3. Data analyses

The whole-body contents of the individuals were calculated by gamma-ray spectrometry of spectra only from the HPGe detectors; those from the NaI(Tl) detectors were not available due to a poor energy resolution of these detectors, making it difficult to distinguish various radionuclides existing in the early stage of the accident. The gamma-ray spectrometry was performed with a software package (GENIE 2000, Canberra Inc.). For conservative internal dose estimations, an acute intake scenario on March 15, 2011 - when the largest release of radioactive materials into the environment was expected - was applied to all of the subjects. These calculations were made by the MONDAL-3 code, an internal dose calculation software package developed by the National Institute of Radiological Sciences, Japan [1].

4. Results and discussion

Figure 1 displays two background (blank) spectra from the NaI(Tl) detectors and the HPGe detectors. Six radionuclides (i.e., ^{131}I, ^{132}Te, ^{132}I, ^{133}Xe, ^{134}Cs, and ^{137}Cs) were clearly identified in the spectra from the HPGe detectors (the lower part of Figure 1), whereas they were not identified in the spectra from NaI(Tl) detectors (the upper part of Figure 1).
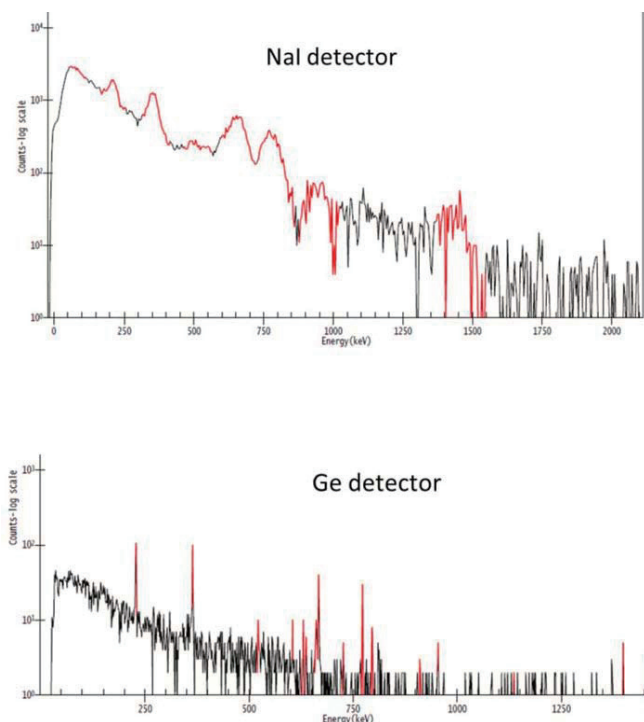
Figure 1. Background spectra of NaI(Tl) and HPGe detectors on March 15, 2011

Figure 2 displays the time trend of the activity for the above six radionuclides from March 15, 2011 to April 5, 2011. The activity was calculated using a counting efficiency for a whole-body configuration, and thus it is inappropriate to directly compare the activity among the radionuclides. However, Figure 2 provides information about the behavior of radioactive materials transported by plumes from the FDNPS site. Elevated levels of the activity were found on March 15–16 and March 20–21.

Figure 3 displays the time trend of minimum detectable activity (MDA) values [2] calculated from continuum counts under peaks to be analyzed. These MDA values were important to the evaluation of a lower limit of internal dose estimate by the WBC under elevated radiation levels. The highest MDA value was obtained on March 17–18, when the ambient dose rate reached approx. 14µSv h^{-1}. The MDA values for the various nuclides fluctuated after that day.
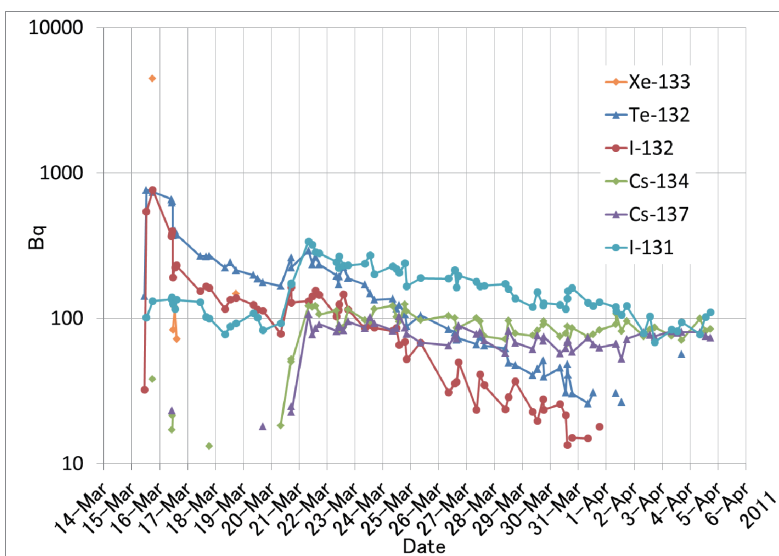
Figure 2. Time trend of activity for various radionuclides identified by HPGe detectors of the WBC
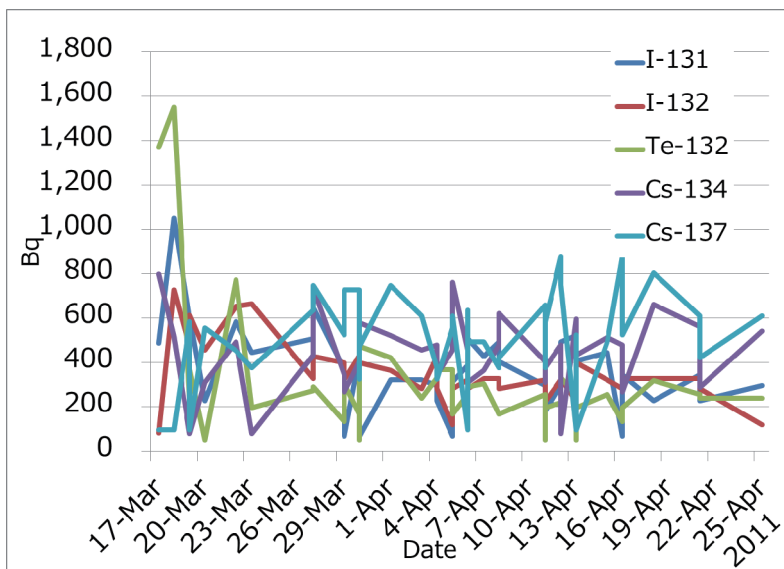
Figure 3. Time course of minimum detectable activity (MDA)

Table1 shows the MDA values of various nuclides obtained from the periodical measurements with the WBC. The data in the table were obtained under a counting time of 8 min and a whole-body scanning measurement. For ^{134}Cs and ^{137}Cs, the corresponding MDA values at the early stage of the accident were almost doubled compared to those taken before the accident.

Table 1 Distribution of MDA values from the WBC

MDA	^{131}I	^{132}I	^{132}Te	^{134}Cs	^{137}Cs
Average (n=32)	374	347	309	442	498
SD	182	141	287	171	215
50%Tile	369	327	257	480	526
95%Tile	602	650	742	727	800
before the accident				296	348

MDA: minimum detectable activity; WBC: whole body counter; Unit: Bq per body

Significant internal contamination with the radionuclides was found in three of the 10 subjects of Group 1; in contrast, there was no significant detection of contamination among the 22 subjects of Group 2 (Table 2). The detailed measurement data of the three subjects with significant detection are provided in Table 3. Regarding Group 1, we could not clarify a large discrepancy in behavior after the accident among the 10 subjects. We thought that it would be difficult to perform accurate quantifications of these subjects' body content of radionuclides with whole-body measurements under the elevated background levels and to remove the influence of possible surface contamination on the whole-body measurements.

Table 2 Number of subjects with significant detection of radionuclides

No. of detection	^{131}I	^{132}I	^{132}Te	^{134}Cs	^{137}Cs
Group 1 (n=10)	3	2	3	2	3
Group 2 (n=22)	0	0	0	0	0

Table 3 Whole-body content of three subjects with significant detection

Subject (date of measurement)	^{131}I	^{132}I	^{132}Te	^{134}Cs	^{137}Cs
A (Mar 17)	7070	2690	4200	ND	1180
B (Mar 18)	8110	4110	5190	1040	1340
C (Mar 22)	3970	ND	1740	1390	1590

Unit: Bq per body; ND: not detected

Subject C, one of the Group 1 subjects with significant internal contamination, was reexamined on April 2, 2011 (11 days after his first examination) using a different WBC at a different hospital at a non-contaminated location very far from the FDNPS. His data are provided in Table 4. The large decrease in subject C's whole-body content of radiocesium indicates the possibility of surface contamination, in light of radiocesium's relatively long biological half-life (approx. 100 days for adults). This possibility also agreed with ^{131}I. Table 5 provides the predicted intake amounts of ^{131}I, ^{134}Cs and ^{137}Cs based on an assumption of an acute intake scenario on March 15 via inhalation.

Table 4 Comparison of measurement data between two hospitals (Unit: Bq per body)

Subject C (date of measurement)	^{131}I	^{132}I	^{132}Te	^{134}Cs	^{137}Cs
FMU Hospital (Mar 22)	3970	ND	1740	1390	1590
Other hospital (Apr 2)	346	ND	ND	64.8	64.8

Unit: Bq per body; ND: not detected

Table 5 Predicted intake amounts of ^{131}I, ^{134}Cs and ^{137}Cs
based on an acute intake scenario on March 15 via inhalation

	^{131}I	^{134}Cs	^{137}Cs
FMU	77000	4600	5200
Other University	16000	240	230

Unit: Bq per body

5. Lessons learned

Our whole-body measurements posed a problem in that it was difficult to perform appropriate internal dose estimates under the high background radiation levels caused by a large-scale nuclear disaster, even though the whole-body facility is located far from the site of the disaster. It is also difficult to control surface contamination with radionuclides inside the facility. Based on this experience, we contend that the WBC should have been placed in a building that has adequate shielding and the ability to shut down the air ventilation from outside. Frequent surface contamination surveys of the people entering and exiting the building were also crucial in the response to this disaster.

Acknowledgement

References

1) N. Ishigure, Development of software for internal dose calculation from bioassay measurements. Radiation Protection Dosimetry 109(3), 2004, 235-242.
2) Health Physics Society (HPS). Performance Criteria for Radiobioassay. An American National Standard. HPS N13.30-1996. New York, American National Standards Institute, 1996.

Summary of Session 1-1

S. TOLMACHEV

Dr. Momose pointed aims of the session: 1.1 for responders; 1.2 for residents and visitors
Five talks were given to cover each of the aims.

Talk 1 by Chie TAKADA
Presented activities and efforts performed by Nuclear Fuel Cycle Engineering Laboratory (NCL) of JAEA for monitoring of JAEA staff members engaged in the accident.
Two teams of experts were sent to the Fukushima site on March 12 and 13, 2011 both teams left FDNPP site and returned to Tokai-mura on March 14th.

Talk 2 by Osamu KURIHARA
This talk continued topic started by Dr. Takada on JAEA activities for monitoring of employees involved the FDNPP accident and estimation of doses from internally deposited radionuclides – ^{131}I and ^{134,137}Cs.
Highest contribution to the internal dose was due to ^{131}I. Dose calculation where performed based on 'single acute intake' scenario.
In total, measurements on 560 employees involved in FDNPP accident were performed using JAEA whole body counting systems. Only 6 subjects received equivalent dose greater than 250 mSv.

Questions:
Dr. Tolmachev – did you consider to use 'multiple intakes' vs 'single intake' scenario for a better fit of ^{131}I intake estimation?

Answer - No

Talk 3 by Takashi NAKANO
Dr. Nakano presented protocols of direct measurements for highly exposed TEPCO workers performed at NIRS using WBC (for ^{134,137}Cs) and thyroid (for ^{131}I) monitor.
Based on the measurements, effective half-life for ^{134,137}Cs and ^{131}I were estimated.
Highest, estimated by NIRS, effective dose of ~ 600 mSv was in a good agreement with JAEA estimations.

Talk 4 by Naoki MATSUDA
Dr. Matuda covered the topic of retrospective dose assessment from internal radionuclide for short-term visitors to Fukushima area.
Measurements and estimations were made for 173 adults who visited Fukushima area within one month after the accident.

Using System for Prediction of Environment Emergency Dose Information (SPEEDI) data the intake of ^{131}I and ^{134,137}Cs were estimated for relocated individual.
Maximum committed effective dose was calculated to be 1.04 mSv, and maximum committed equivalent dose for thyroid was 20 mSv.

Question/Comment:
Q: Dr. Balonov: Why you are considering inhalation only, not combination with ingestion?
A: No food supply from local stores, so ingestion was excluded
Dr. Homma pointed on discrepancy on intake estimation due to people movement using SPEEDI data.
Dr. Suzuki interested in ^{132}Te/^{131}I activity ratio and dose contributions from ^{132}Te and other short-lived I isotopes.

Talk 5. Makoto MIYAZAKI

General Discussion (Chaired by A. BOUVILLE)
On behalf of invited experts Dr. Bouville thanked Organize Committee for the invitation.
General question 1:   What could be done in terms of instrument calibration for derivation of doses based on measurements using different instruments?
S. Salomon suggested to perform intercompariosn of the used measurement systems, and asked if there is any intent to perform such intercomparison.
Q2. In what form iodine presents in the environment after the release – particular or gas? Should we consider both physical forms for dose assessments?
Dr. Nagataki brought the question how to account (should we account?) iodine dietary intake.

Session 1

Current Status of Internal Dose Estimation

Session1-2　　For Residents and Visitors

Chair   :   N. BAN
Co-chair   :   S. SOLOMON
Rapporteur :   S. TOLMACHEV

Thyroid Equivalent Doses due to Radioiodine-131 Intake for Evacuees from Fukushima Daiichi Nuclear Power Plant Accident

Shinji TOKONAMI[1], Masahiro HOSODA[2], Suminori AKIBA[3], Atsuyuki SORIMACHI[1], Ikuo KASHIWAKURA[1, 2], Mikhail BALONOV[4]

[1]*Department of Radiation Physics, Institute of Radiation Emergency Medicine, Hirosaki University, 66-1, Hon-cho, Hirosaki, AOMORI, 036-8564, Japan*
[2]*Departmentof Radiological Life Sciences, Graduate School of Health Sciences, Hirosaki University, 66-1, Hon-cho, Hirosaki, AOMORI, 036-8564, Japan*
[3]*Department of Epidemiology and Preventive Medicine, Graduate School of Medical and Dental Sciences, Kagoshima University, Kagoshima, KAGOSHIMA, 890-8544, Japan*
[4]*Protection Laboratory, Institute of Radiation Hygiene, Mira St 8, 197101 St., Petersburg, Russia*

Abstract

A primary health concern among residents and evacuees in affected areas immediately after a nuclear accident is the internal exposure of the thyroid to radioiodine, particularly I-131, and subsequent thyroid cancer risk. In Japan, the natural disasters of the earthquake and tsunami in March 2011 destroyed an important function of the Fukushima Daiichi Nuclear Power Plant (F1-NPP) and a large amount of radioactive material was released to the environment. Here we report for the first time extensive measurements of the exposure to I-131 revealing I-131 activity in the thyroid of 46 out of the 62 residents and evacuees measured. The median thyroid equivalent dose was estimated to be 4.2 mSv and 3.5 mSv for children and adults, respectively, much smaller than the mean thyroid dose in the Chernobyl accident (490 mSv in evacuees). Maximum thyroid doses for children and adults were 23 mSv and 33 mSv, respectively.

1. Introduction

On 11th March 2011, a 9.0 magnitude earthquake and subsequent tsunami led to major problems in the stabilization of nuclear power reactors in F1-NPP[1-3]. Following plural hydrogen explosions and fire damage to the facilities, a large amount of radioactive material was released to the environment [4, 5]. Radiation monitoring data [6] in Iitate near Tsushima District and mathematical simulations based on dosimetry data [7, 8] indicate that a highly radioactive plume arrived at around 1 p.m. on March 15th. Note also that it started to rain at around 5 p.m. on March 15th. Namie Town and Iitate Village, located to the northwest of F1-NPP, are among the municipalities heavily contaminated by radioactive plumes from the crippled plant [9]. Concern over exposure to radioactive materials prompted the local health authorities to conduct a preliminary screening test for activity in the thyroid of children in Iwaki City, Kawamata Town and Iitate Village. However further investigations were needed to fully understand the situation.

When considering the release of radioactive materials to the air, special attention must be paid to volatile elements including iodine (I-131, I-132, I-133), cesium (Cs-134, Cs-136, Cs-137) and tellurium (Te-132), as well as inert gases such as xenon (Xe-133) [10, 11]. A primary concern among residents and evacuees, staying in heavily contaminated areas in the early days after the accident, is the internal thyroid exposure of children to radioiodine and consequent thyroid cancer risk. Once taken into the human body, 10-30% of radioiodine accumulates in the thyroid [12]. After the Chernobyl accident, thyroid cancer increased among children who had internal exposure to radioiodine through milk intake [13]. The thyroid weight of an infant is much smaller and milk consumption per unit mass is much larger

compared with an adult. However, in Fukushima, internal exposure through ingestion is considered negligible since local products including milk were not given to children [14]. Therefore, inhalation is considered to be the most probable pathway of intake in this F1-NPP accident.

According to the survey by Japan Broadcasting Corporation (NHK), more than 6,000 residents including infants evacuated from coastal areas and stayed in Namie Town, Tsushima District, for several days from March 12th to 15th. The system for Prediction of Environmental Emergency Dose Information (SPEEDI) estimated that the thyroid dose for 1-year-old infants spending time outdoors in various areas of Tsushima District during the period between 6:00 on March 12th to 0:00 on April 6th may range from 100 mSv to 500 mSv as shown in (Figure 1) [15]. On 23rd March, 2011, based on the estimated thyroid dose among 1-year-old infants obtained from SPEEDI, an advisory panel for the Nuclear Safety Commission (NSC) of Japan recommended evaluation of the internal thyroid exposure to I-131 for children in high-radiation dose areas. In response to the recommendation, local health authorities measured the activity in the thyroid of 1,149 children under the age of 15 in Iwaki City, Kawamata Town and Iitate Village from March 24th to 30th [14]. For this measurement a 1-inch × 1-inch NaI(Tl) scintillation survey meter was placed on the neck of examinees. In this examination, 1% of children exceeded 0.04 μSv h[-1]. The maximum dose rate was 0.07 μSv h[-1], which was considered to be equivalent to a thyroid dose of 35 mSv [14]. Since this examination could only be regarded as a screening test, more detailed measurements were needed. Although the NSC pointed out the need for further investigation, no further examinations were carried out by the local authorities at the time. It should be noted that I-131 has a half-life of 8 days and therefore it is necessary to make activity measurements of I-131 in the thyroid rapidly.

We report for the first time extensive measurements of the exposure to I-131 revealing I-131 activity in the thyroid of 46 out of the 62 residents and evacuees measured.
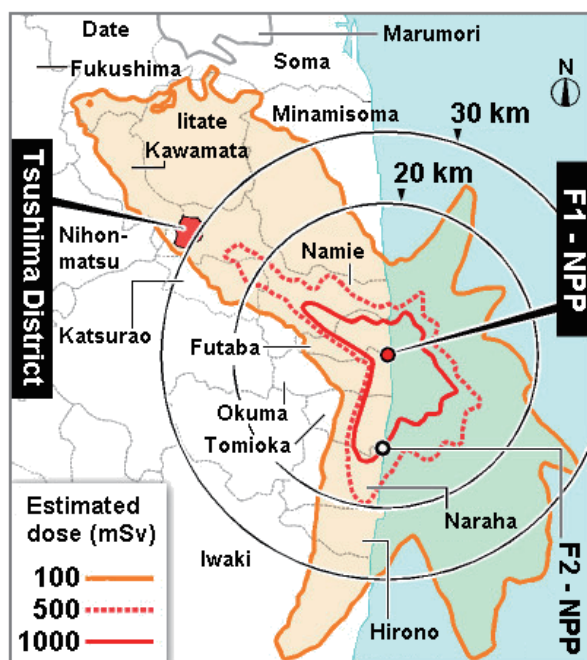
Figure 1. Thyroid dose contour map. The dose for one–year-old infants in the areas surrounding the reactor was estimated by SPEEDI (System for Prediction of Environmental Emergency Dose Information). Tsushima District of Namie Town is located within the 30-km-radius zone around the reactor. The figure was provided by the Asahi Shinbun and modified.

2. Methods

2.1. Evaluation of thyroid equivalent dose

We made I-131 activity measurements in the thyroid for examinees from two different areas. Seventeen were residents in Tsushima District of Namie Town, heavily contaminated with radioactive materials released from the crippled plant. Forty five were those evacuated from coastal areas including Minami-soma City located to the north of Fukushima Dai-ichi Nuclear Power Plant. We measured activity in the thyroid during the period from April 12th to 16th, 2011, using a 3-inch × 3-inch NaI(Tl) scintillation spectrometer (JSM-112, Hitachi Aloka Medical, Ltd., Tokyo). We wrapped the detection head with plastic foil and cleaned the neck with alcohol wipes so as to avoid radioactive contamination. We then placed the detection head on the cleaned part of the neck and started the measurement (Figure 2). After 300 sec, we obtained a gamma-ray pulse height spectrum. Using the I-131 counting data, we calculated the activity by the equation (1):

$$A_T = \frac{n_t - n_b}{\eta} \qquad (1)$$

Where A_T is the I-131 radioactivity in the thyroid (Bq); n_t is the net count rate in the identified region of the examinee (counts per second, cps), n_b is the background net count rate (cps), and η is counting efficiency of the equipment (cps/Bq). We calculated these two net count rates by the Covell method (Figure 3) [16]. We estimated a minimum detectable count rate (N) with the background net count rate calculated according to Covell and equation (2):

$$N = 3\sqrt{2n_b} \qquad (2)$$

Figure 2. I-131 activity in the thyroid measurements for evacuees

We used the counting efficiency obtained from experiments with a neck phantom and a thyroid phantom filled with I-131 solution [17]. The distance between the neck and thyroid phantoms was 1 cm. Ishikawa and Uchiyama prepared three thyroid phantoms with different volumes, i.e., 4, 12 and 16 ml. We used conservative counting efficiencies of 4 ml for young children (3.49×10^{-2} cps/Bq) and 12 ml for adults (3.96×10^{-2} cps/Bq) [17]. We calculated the thyroid equivalent dose from I-131 activity in the thyroid obtained by the measurement as follows:

$$D_{T,0} = \frac{A_T}{(0.5)^{t/T_{eff}}} \cdot f \cdot i^{-1} \qquad (3)$$

Where $D_{T,0}$ is the thyroid equivalent dose (mSv) assuming that they inhaled I-131 on March 15th, t is the elapsed time between March 15th and the measured date, T_{eff} is the effective half-life of I-131 [18], f is the equivalent thyroid dose coefficient [18, 19], and i is the thyroid uptake factor equal to 0.3. The effective half-lives of 3 months (from 0 to 1 year of age), 5 years (more than 2 to 7 years of age), 15 years (more than 12 to 17 years of age), and adult (more than 17 years of age) were calculated using each biological half-life given by ICRP Publication 67 [18], and they were estimated to be 4.67, 5.94, 7.15, and 7.27 days, respectively.
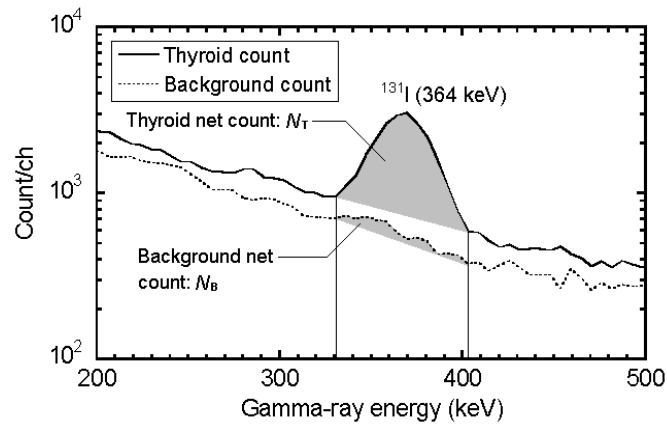
Figure 3. Energy spectrum of gamma radiation emitted from thyroid measured by 3 × 3-inch NaI(Tl) scintillation spectrometer

2.2. Retrospective thyroid equivalent dose by inhalation for young children

In order to estimate the retrospective thyroid dose by inhalation for young children with high risk, we used the maximum atmospheric I-131 concentration estimated from the thyroid activity of evacuees. We calculated the concentration (C_I: Bq m^{-3}) as the following equation:

$$C_I = \frac{A_T}{(0.5)^{t/T_{eff}}} \cdot (V \cdot i)^{-1} \qquad (4)$$

Where V is the breathing volume over 4 hours (m^3) and we used the typical value at each age given by ICRP Publication 71 [19]. The maximum concentration ($C_{I\text{-max}}$) among all the examinees was 23 ± 2 kBq m^{-3} and we estimated the retrospective thyroid dose (D: mSv) for young children by the following equation:

$$D = C_{I-max} \cdot V \cdot f \qquad (5)$$

3. Results and discussion

3.1. Results

We conducted I-131 activity measurements in the thyroid of residents and evacuees during the period from April 12th to 16th, placing a 3-inch × 3-inch NaI(Tl) scintillation spectrometer at the neck of examinees. The study was approved by the Committee of Medical Ethics of Hirosaki University Graduate School of Medicine (Hirosaki, Japan). In total, 62 people aged from 0 to 83 years old (of which accurate information on age was unavailable for eight people) underwent the measurement with informed consent. Net thyroid and background count rates were determined from the detected gamma spectra measured for the most conservative dose assessment, we used thyroid equivalent dose coefficients for iodine in elemental form, as given by ICRP Publication 71[19], and the thyroid uptake factor equal to 0.3. We found detectable I-131 activity in 39 of the 45 people evacuated from coastal areas, and in 7 of the 17 residents in Tsushima District. Figure 4 illustrates the distribution of thyroid equivalent dose in children and adults assessed using the equivalent dose coefficient by inhalation and by ingestion for their comparison[18, 19]. Table 1 summarizes the range of I-131 activities and thyroid doses according to age. Thyroid equivalent doses by inhalation ranged from none detected (*N.D.*) to 33 mSv. The median thyroid equivalent dose for children (under 20 years of age) and adults was 4.2 and 3.5 mSv, respectively.
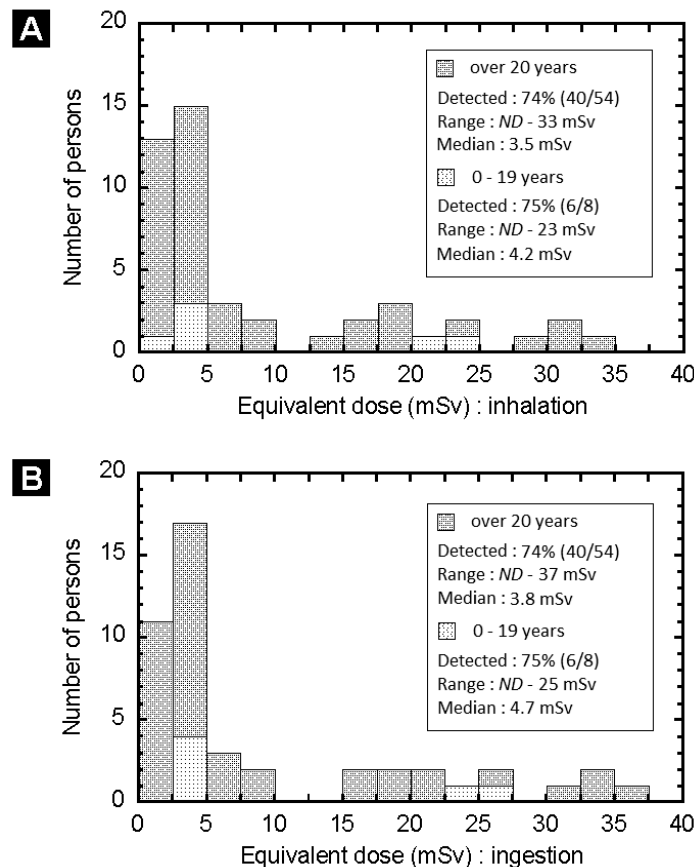
Figure 4. Distribution of measured persons by thyroid equivalent dose from inhalation (A) and ingestion (B) of I-131. Each dose was calculated according to I-131 activity in the thyroid and the age-dependent equivalent thyroid dose coefficient[18, 19].

Table 1 Number of persons by group, range of thyroid activity measured on April 12 to 16, 2011, and equivalent thyroid dose

Age group	Number of persons	I-131 thyroid activity range (kBq)	Thyroid dose range (mSv) : inhalation	Thyroid dose range (mSv) : ingestion
0–9	5	*N.D.*–0.017	*N.D.*–21	*N.D.*–24
10–19	3	0.090–0.54	3.8–23	4.2–25
20–29	9	*N.D.*–0.59	*N.D.*–16	*N.D.*–17
30–39	6	*N.D.*–0.17	*N.D.*–4.4	*N.D.*–4.9
40–49	4	*N.D.*–1.5	*N.D.*–33	*N.D.*–37
50–59	10	*N.D.*–1.1	*N.D.*–31	*N.D.*–34
60–69	12	*N.D.*–0.20	*N.D.*–5.3	*N.D.*–5.8
70–79	3	0.090–1.5	2.3–31	2.5–34
80+	2	*N.D.*–0.70	*N.D.*–19	*N.D.*–21
Unknown	8	*N.D.*–1.4	*N.D.*–28	*N.D.*–30

3.2. Discussion

The thyroid equivalent doses assessed in this study were much smaller than the mean thyroid dose in the Chernobyl accident (which was 490 mSv in evacuees) [13]. Thyroid equivalent doses assessed assuming an ingestion pathway was similar to those found for inhalation. Even when either of the two intake pathways or their combination was assumed, no dose exceeded 50 mSv.

Table 2 Estimation of possible thyroid equivalent dose for children using the assumed maximum atmospheric I-131 concentration

Age	Breathing volume per 4 h (m^3)	Total I-131 intake (kBq)	Thyroid dose coefficient[19] (mSv kBq^{-1})	Thyroid equivalent Dose (mSv)
3 months	0.48	10.9 ± 0.9	3.3	36 ± 3
1 year	0.86	19.7 ± 1.6	3.2	63 ± 5
5 years	1.45	33.4 ± 2.6	1.9	63 ± 5
10 years	2.55	58.5 ± 4.6	1.0	56 ± 4
15 years	3.35	76.9 ± 6.1	0.6	48 ± 4

Some children were known to have stayed in heavily contaminated areas from March 11th to 18th. As the most conservative scenario, we estimated the thyroid dose to children, using the atmospheric I-131 concentration assessed from the thyroid measurements of adults. As mentioned earlier, we considered that the rainfall on March 15th resulted in deposition of ambient radioactive materials on the ground and subsequent less possibilities to inhale them. The maximum I-131 activity detected in the thyroid of an adult was 1.5 kBq. Assuming the inhalation exposure took place for 4 hours on the afternoon of March 15th, we estimated that this person could inhale as much as 85 kBq of I-131. Using the thyroid activity and breathing rate [19], the maximum atmospheric I-131 concentration was estimated to be 23 kBq m^{-3}. In our data analysis, we did not consider I-132 exposure due to lack of information.

Using the maximum atmospheric concentration, the thyroid dose for different age groups from inhalation of I-131 was calculated for children as shown in Table 2. In this estimation the dose for 1-, 5- and 10-year-old children could exceed 50 mSv. If children in this age range remained in Tsushima District after the radioactive plume arrived in the afternoon of March 15th, they might have experienced further exposure to I-131. Since the maximum I-131 concentration was obtained from an adult's activity, inhaled activity by infants could be less because they usually stay indoors in cold winter weather.

4. Conclusion

We suggested that it is necessary to identify children who were outdoors during the period when the highly radioactive plume arrived, and to periodically examine them. From both radiological and risk-assessment aspects, it is important to conduct these investigations to better understand the initial exposure conditions following the accident.

References

1) Sato, M. et al. Displacement above the hypocenter of the 2011 Tohoku-oki earthquake. Science 322, 1395 (2011).
2) Kawagucci, S. et al. Disturbance of deep-sea environments induced by the M9.0 Tohoku earthquake. Sci. Rep. 2, 270; DOI:10.1038/srep00270 (2012).
3) Tanimoto, T., Uchida, N., Kodama, Y., Teshima, T., Taniguchi, S. Safety of workers at the Fukushima Daiichi nuclear power plant. Lancet 377, 1489-1490 (2011).
4) Endo, S., et al. Measurement of soil contamination by radionuclides due to the Fukushima Dai-ichi Nuclear Power Plant accident and associated estimated cumulative external dose estimation. J. Environ. Radioact. 111, 18-27 (2012).
5) Zheng, J., et al. Isotopic evidence of plutonium release into the environment from the Fukushima DNPP accident. Sci. Rep. 2, 304; DOI:10.1038/srep00304 (2012).
6) Fukushima Prefectural Government, http://www.pref.fukushima.jp/j/20-50km40.pdf (accessed 3 April 2012).
7) Chino, M. et al. Preliminary estimation of release amounts of ^{131}I and ^{137}Cs accidentally discharged from the Fukushima Daiichi Nuclear Power Plant into the atmosphere. J. Nucl. Sci.Technol. 48, 1129-1134 (2011).
8) Katata, G., Terada, H., Nagai, H., Chino, M. Numerical reconstruction of high dose rate zones due to the Fukushima Dai-ichi Nuclear Power Plant accident. J. Environ. Radioact. 111, 2-12 (2012).
9) Hosoda, M. et al. The time variation of dose rate artificially increased by the Fukushima nuclear crisis. Sci. Rep. 1, 87; DOI: 10.1038/srep00087 (2011).
10) Matsumura, H., Saito, K., Ishioka, J., Uwamino, Y. Behavior of radioactive materials from Fukushima Daiichi nuclear power station obtained by radiation on the expressways. J. At. Energy. Soc. Jpn.10, 152-162 (2011).
11) Monzen, S. et al. Individual radiation exposure dose due to support activities at safe shelters in Fukushima prefecture. PLoS ONE 6, e27761; DOI:10.1371/journal.pone.0027761 (2011).
12) Yoshizawa, Y., Kusama, T. Weight, iodine content and iodine uptake of the thyroid gland of normal Japanese. Jpn. J. Health Phys. 11, 123-128 (1976).
13) United Nations Scientific Committee on the Effects of Atomic Radiation. UNSCEAR 2008 report Vol. II. Effects of ionizing radiation. Annex D: Health effects due to radiation from the Chernobyl accident (United Nations, New York, 2011).

14) Akiba, S. Epidemiological studies of Fukushima residents exposed to ionising radiation from the Fukushima Daiichi Nuclear Power Plant prefecture-a preliminary review of current plans. J. Radiol. Prot. 32, 1-10 (2012).

15) Nuclear Safety Commission of Japan, http://www.nsc.go.jp/mext_speedi/0312-0406 _ex.pdf (accessed 3 April 2012).

16) Covell. D. F. Determination of gamma-ray abundance directly from total absorption peak. Anal. Chem. 31, 1785-1790 (1959).

17) Ishikawa, T., Uchiyama, M. Calibration of apparatus for measuring ^{131}I thyroid burden, using anthropometric phantoms of different sizes. Jpn. J. Health Phys. 32, 67-70 (1997).

18) International Commission on Radiological Protection, Age-dependent doses to members of the public from intake of radionuclides - Part 2 Ingestion dose coefficients (ICRP Publication 67. Ann. ICRP. 22, 1992).

19) International Commission on Radiological Protection, Age-dependent Doses to Members of the Public from Intake of Radionuclides -Part 4 Inhalation Dose Coefficients (ICRP Publication 71. Ann. ICRP. 25, 1995).

Screening Survey on Thyroid Exposure for Children after the Fukushima Daiichi Nuclear Power Station Accident

Eunjoo KIM, Osamu KURIHARA, Toshikazu SUZUKI, Masaki MATSUMOTO,
Kumiko FUKUTSU, Yuji YAMADA, Nobuyuki SUGIURA, Makoto AKASHI

Research Center for Radiation Emergency Medicine,
National Institute of Radiological Sciences,
4-9-1 Anagawa, Inage-ku, Chiba, CHIBA, 263-8555, Japan

Abstract

In response to a serious accident at the Fukushima Daiichi Nuclear Power Station, National Institute of Radiological Sciences (NIRS) established a protocol for a screening survey of thyroid exposure for children living in areas where thyroid doses were predicted to be high. The aim of the screening survey was to implement measurements for a large number of subjects with conventional NaI(Tl) scintillation survey meters. This protocol was applied to the screening survey of 1,149 children at five locations in three municipalities (Kawamata Town, Iitate Village and Iwaki City). Among 1,080 children (excluding 69 subjects from evaluation), there were no subjects who exceeded a screening level (0.2 μSv h^{-1}) corresponding to a thyroid equivalent dose of 100 mSv (for the age group of 1-y-old as of March 24). No significant signals were detected in 55.4% of these subjects and the maximum dose was found to be 43 mSv. This paper presents details on the protocol as well as results of the screening survey.

Keywords: screening survey; thyroid exposure; screening level; equivalent dose

1. Introduction

The 2011 Tohoku earthquake with a magnitude of 9.0 and subsequent massive tsunami disabled reactor core cooling systems of the Fukushima Daiichi Nuclear Power Station (FDNPS) run by Tokyo Electric Power Company. This led to critical damages at reactor buildings (Units 1, 2 and 3), resulting in an enormous release of radioactive materials into the environment [1]. The radiological contamination has had a serious impact on the livelihood of populations in Fukushima.

To avoid possible radiation risks, the Japanese government instructed the residents within 20 km of the site of the FDNPS to evacuate the area and those between 20 km and 30 km of the FDNPS to stay indoors. These instructions were issued on March 12 and March 15. On March 23, the Nuclear Safety Commission (NSC) of Japan performed preliminary calculations of thyroid equivalent doses for small children by the System for Prediction of Environmental Emergency Dose Information (SPEEDI) along with other monitoring data. The calculations revealed that areas where thyroid doses were relatively high exceeded the evacuation zone (within 20 km radius) in the northwest and south of the FDNPS (Figure 1) [2]. Although these calculations likely overestimated the thyroid doses for people staying indoors, a screening survey on thyroid exposure due to the intake of radioiodine (mainly ^{131}I) for children was requested by the NSC. This survey was implemented for 1,149 children in Kawamata Town, Iitate Village and Iwaki City from March 24 to March 30. The screening showed that there were no children who exceeded a screening level corresponding to a thyroid equivalent dose of 100 mSv for an age group of 1-y-old [1].

This screening survey was performed with conventional NaI(Tl) scintillation survey meters, which are widely used in Japan for measuring ambient dose rates. A main reason for this was to allow a limited number of staff members to perform thyroid measurements as soon as practicable. At the request of the NSC, the National Institute of Radiological Sciences (NIRS) immediately

established the protocol for the screening survey and the screening level. This paper presents these items as well as results of the screening survey.
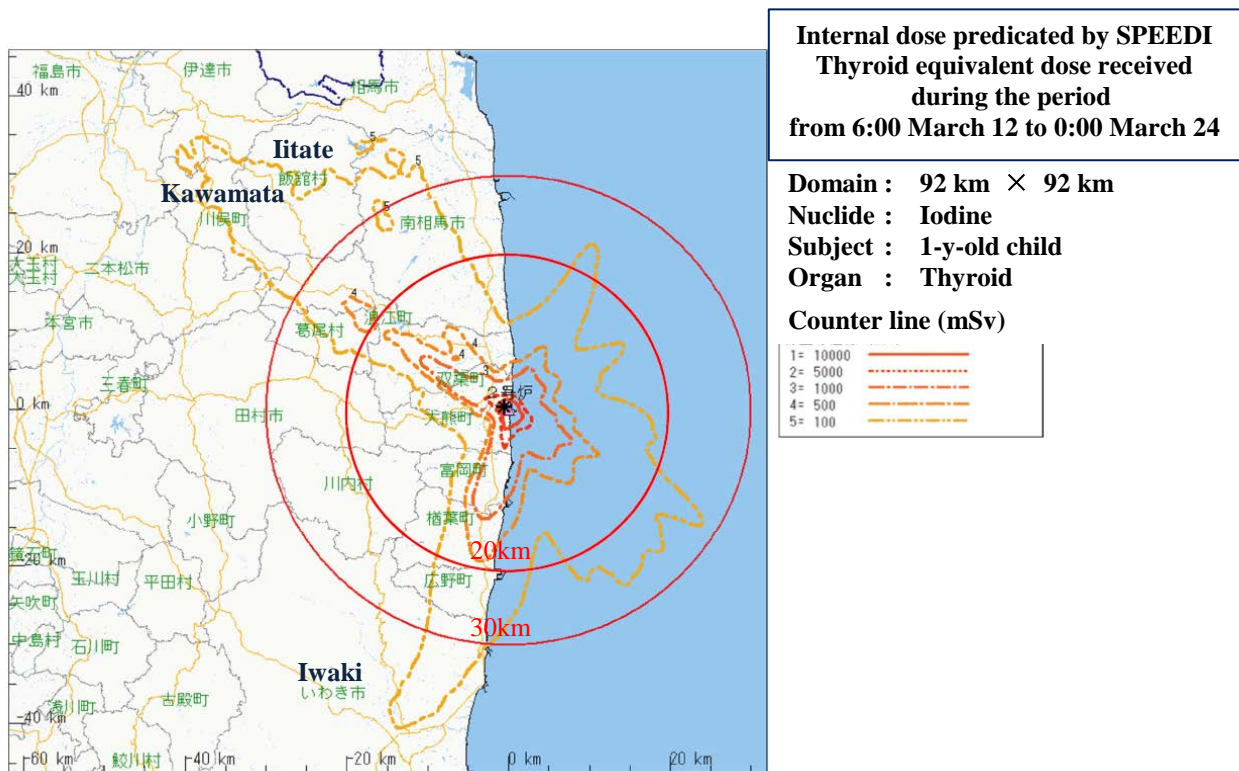
Figure 1. Predicted thyroid equivalent dose map by the SPEEDI (English translation) [2]

2. Protocol for the screening survey on thyroid exposure

NIRS proposed the use of NaI (Tl) scintillation survey meters (TCS-161, TCS-171 and TCS-172, Hitachi-Aloka Medical, Ltd., Japan) for the screening survey on thyroid exposure for children. The survey meter with an NaI(Tl) crystal of 2.54-cm diameter and 2.54-cm height contains an energy compensation circuit which is to obtain the similar energy response for photons over the energy range from 50 keV to 3 MeV. A neck phantom (Kyoto Kagaku Co. Ltd., Japan) was used to determine a calibration factor of the screening level. This neck phantom is a 5-mm-thick methacrylate cylinder of 10-cm diameter and 10-cm height filled with water (Figure 2). It contains a simulated neck bone, windpipe and thyroid. The thyroid container has a volume of 20.5 ml corresponding to the thyroid of Reference Man of the International Commission on Radiological Protection (ICRP) [3]. Details on the phantom are described elsewhere [4]. On this occasion, the thyroid container was filled with an activity standard solution of ^{133}Ba. The average energy of photons from ^{133}Ba (276 keV) is different from that from ^{131}I (375 keV). However, it was expected that this difference was not significant with regard to response levels for the above devices (Figure 3). A calibration factor was then obtained based on the relationship between the activity loaded in the thyroid container and an ambient dose rate on the surface of the neck phantom. Different volumes of the solution equivalent to the thyroid weight of each age (a 1-y-old child, a 6-y-old child and a 15-y-old child) were loaded in the thyroid container to simulate the subject's age-dependency in the size of the thyroid. These ages can be classified to age groups described in ICRP Publication 72 [5]. In the case of a 1-y-old child with a thyroid mass of 2.5 g [6] the calibration

factor was 22 kBq/μSv h^{-1}. The screening level was then determined to be 0.2 μSv h^{-1} (as a net value) on March 25. This level corresponded to a thyroid equivalent dose of 100 mSv for the age group of 1-y-old as the most critical group. The dose of 100 mSv was obtained by an internal dose calculation code MONDAL-3 [7], based on the assumption of constant intake of elemental iodine via inhalation from March 12 to March 23 (12 days) at the same rate; measurements were performed on March 24. This intake scenario was the same as the prediction by the SPEEDI. A similar intake scenario was also used for individual dose calculations described below. Table 1 provides predicted thyroid doses for different age groups of subjects when the screening level of 0.2 μSv h^{-1} is detected. It should be noted that these doses vary by measurement date and intake scenario.

a:100 mm, b:100 mm, c: 55 mm, d:45 mm, e:20 mm
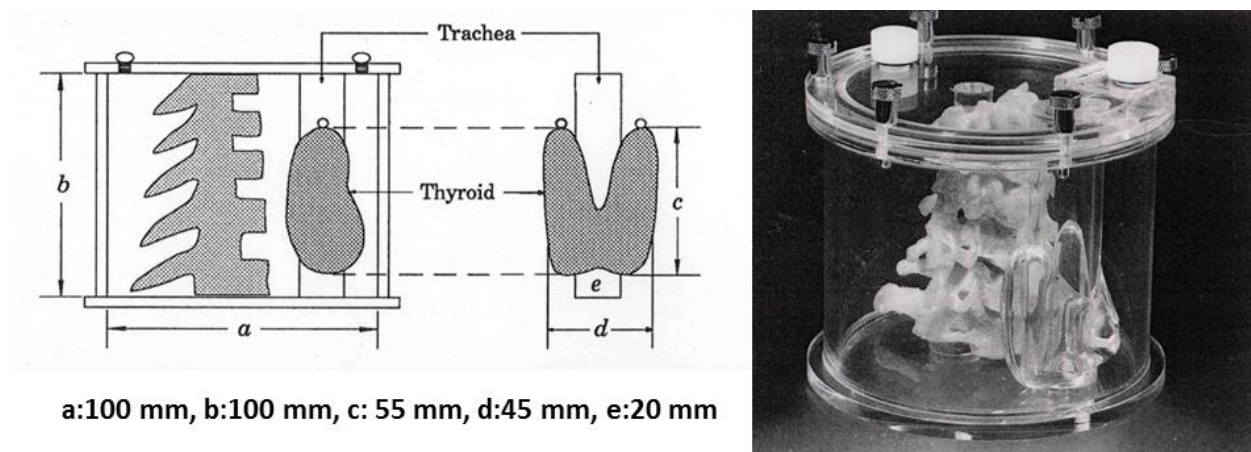
Figure 2. Neck phantom used in this study [3]
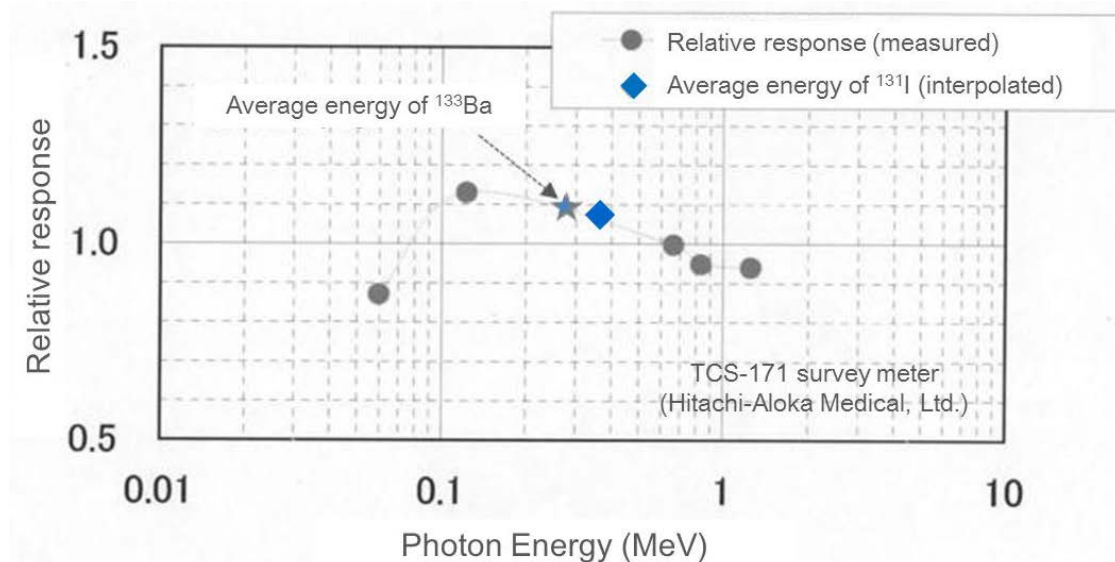
Figure 3. Relative response of an NaI(Tl) scintillation survey meter as a function of photon energy

Table 1 Predicted thyroid doses for different subject groups at the screening level of 0.2 μSv h⁻¹

Age-group	Thyroid mass (g)	Thyroid content of ^{131}I (Bq)	Thyroid equivalent dose* (mSv)
1-y-old (from 1 y to 2 y)	2.5	4,400	108
5-y-old (more than 2 y to 7 y)	6.1	4,690	64
15-y-old (more than 12 y to 17 y)	19	6,030	16

* Intake scenario: chronic intake for 12 days and measurement on 13th day.

The protocol for the screening survey was issued from NIRS on March 23 and March 25. An additional instruction on the measurement conditions (described below) was included in the revised version of the protocol issued on March 25. This was because the first survey at Kawamata Town (see Table 2) was not available for dose estimations due to high background levels.

1) Purpose: this protocol was applied to simple examinations of the activity in the thyroid.
2) Subjects to be measured: children from around 1 to 15-y-old
3) Devices: NaI(Tl) scintillation survey meters
   (types: TCS-161, TCS-171, TCS-172, Hitachi-Aloka Medical, Ltd., Japan)
4) Measurement conditions
   - No sound mode
   - Time constant: 10 seconds
   - Measurement unit: μSv h⁻¹
   - Record the average value of three readings. Each reading value is obtained after 30 seconds of measurement time.
   - Detector probe should be covered with plastic wrap or plastic bag to avoid contamination. Additionally, a piece of clean cotton paper is wrapped around the probe.
   - Perform the measurement under low background levels only (< 0.2 μSv h⁻¹).
5) Background measurement
   - Measure and record the background radiation level at the measurement location before performing the screening survey for subjects.
6) Subject measurements
   - Wipe the subject's neck with wet cotton before the measurement. Water to wet the cotton should be non-contaminated.
   - Place the detector probe on the cross-point between the body axis and clavicles and then take a measurement.
   - Record the reading value and then estimate the net value by subtracting the background value from the reading value.
   - Determine the residual activity level using the net value. The residual activity in the thyroid is approx. 22 kBq when a net value is 1.0 μSv h⁻¹. This is the case for a 1-y-old child. The residual activity decreases with increasing subject's age.
   - Record the net values as well as the subject's other information (address, evacuation route).
   - Report to NIRS in the case of the net values over 0.2 μSv h⁻¹.

The screening survey at each measurement location was performed by local staff members organized by other institutes. Exact information is not available on whether the protocol was strictly applied or not. According to interviews with persons related with the screening survey, it was reported that the background was measured for each subject and the probe was placed near the subject because the background level fluctuated during the measurements.

3. Results

The screening survey on thyroid exposure for children was conducted for 1,149 subjects at five locations in three municipalities (Kawamata Town, Iitate Village and Iwaki City) (Table 2) [8]. Sixty-nine of the 1,149 subjects were excluded from evaluations due to high background levels during measurements on March 24 and three subjects of uncertainty age. Figure 4 displays the age distribution of the subjects. Figure 5 displays the distribution of net values (μSv h^{-1}) for 1,080 subjects. No significant signals were detected for 55.4% of these subjects. Figure 5 displays the distribution of resulting thyroid equivalent doses. A chronic intake scenario from March 12 to the day before measurements (e.g., March 12-26 in the case of the measurements on March 27 in Iwaki City) was used in these dose calculations. The maximum dose of 43 mSv was found for a subject belonging to the age group of 1-y-old (Table 1).

Table 2 Number of subjects for each measurement location (Reproduced [8])

Date	Measurement location	Number of subjects	Subjects from 1-y- to 15-y-old
March 24	Heath care center (Kawamata)	18	(18)[*1]
	Yamakiya branch (Kawamata)	48	(48)[*1]
March 26-27	Health care center (Iwaki City)	137	134[*2]
March 28-30	Central community center (Kawamata)	631	631
March 29-30	Local government office (Iitate)	315	315
Total		1,149	1,080

*1 Excluded from evaluations due to high background levels of radiation.
*2 Excluded from evaluations due to age uncertainty.
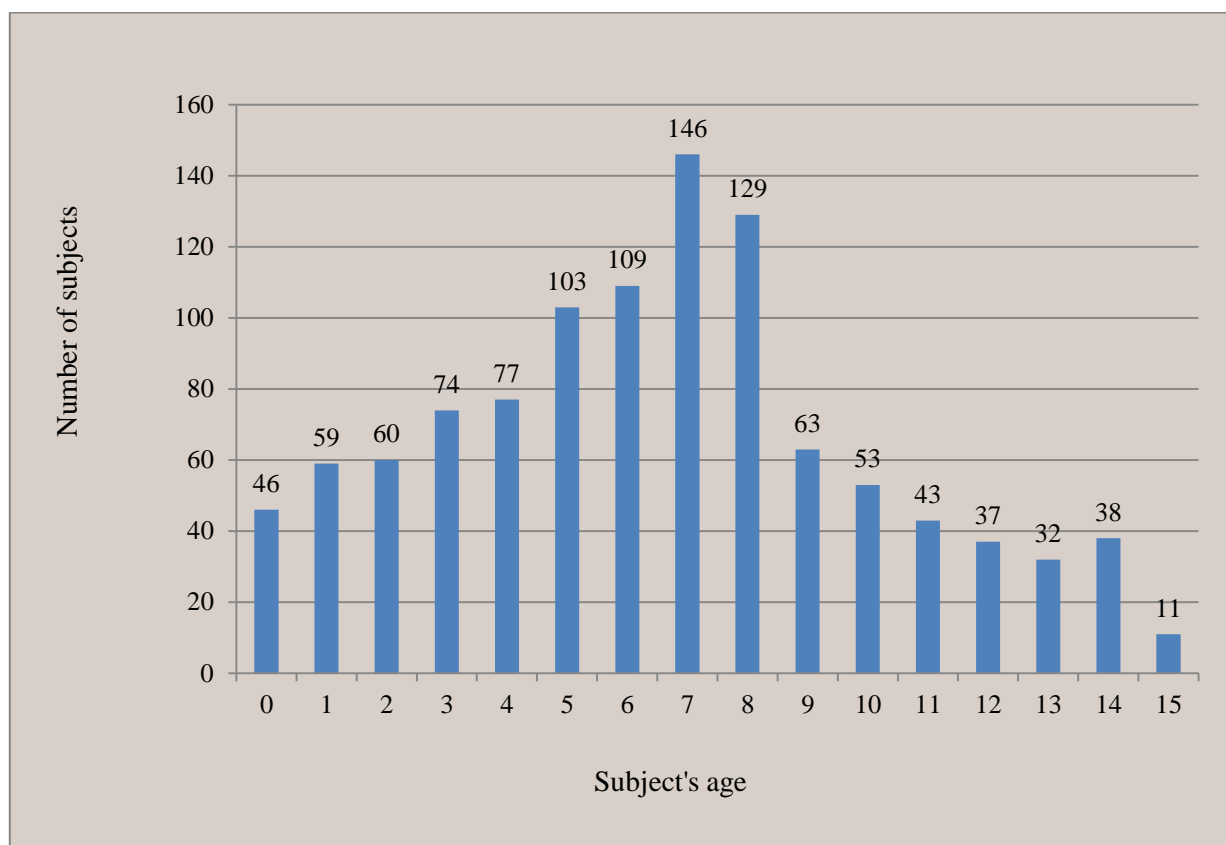
Figure 4. Age distribution of the subjects
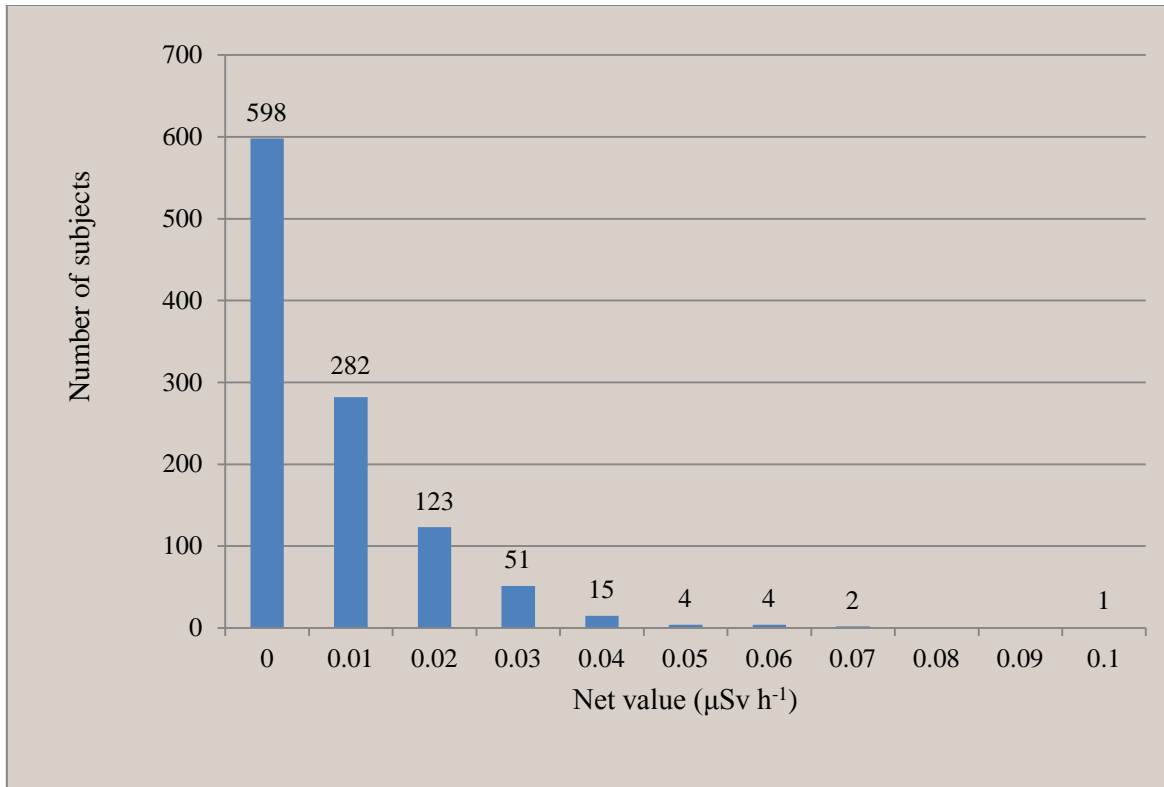
Figure 5. Result of the screening survey on thyroid exposure of the subjects (Reproduced [8])
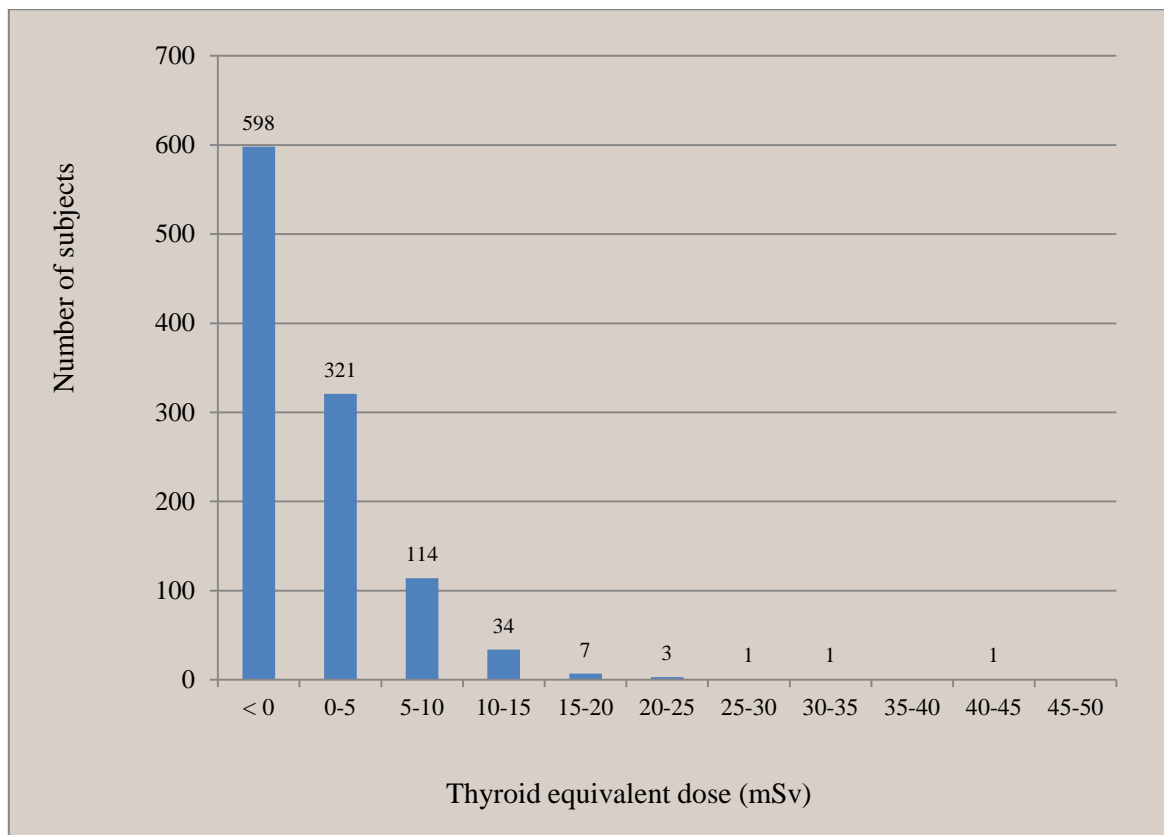
Figure 6. Distribution of thyroid equivalent doses estimated by the results of the screening survey and the intake scenario from March 12 to the day before measurements

4. Discussion and future tasks

The result of the screening survey suggested that thyroid exposure of the screened children was much lower than that predicted by the SPEEDI. The thyroid equivalent dose was expected to be lower than 10 mSv for most of the children examined, even allowing for possible uncertainties such as unknowns in intake scenario or measurement errors. However, an appropriate detection limit for this type of screening survey should be established in future studies. This will require a deep understanding of detection properties of the devices used to measure actual radiation fields at the measurement sites. Average background ambient dose rates of Iwaki City, Kawamata Town (except for the measurements on March 24) and Iitate Mura were 0.17 μSv h^{-1}, 0.09 μSv h^{-1} and 0.12 μSv h^{-1}, respectively, being much higher than the net values (Figure 5).

Regarding the screening level, it is necessary to refine the intake scenario and the calibration factor from the neck phantom. The intake scenario used in this work was not realistic, because radioactive plumes arrived at the selected areas several times and with different magnitudes. However, the lack of air-sampling data made it difficult to create a realistic intake scenario for each area. Thus, updated atmospheric dispersion simulations are currently planned to use for this purpose. The present calibration was not an ideal way to estimate an appropriate calibration factor for small children because of the unavailability for suitable phantoms. The calibration factor of 22 kBq/μSv h^{-1} was somewhat larger than that reported elsewhere [9]. A possible reason for this is that the neck phantom imitates an adult neck and the wall thickness in front of the thyroid container of this phantom was kept constant in the calibration because of just changing the volume of the solution in the thyroid container in the neck phantom. This wall thickness was 11.2 mm in water-equivalent [4].

The screening survey presented in this paper is the most comprehensive dataset available for the Fukushima Daiichi Nuclear Power Station accident in terms of thyroid measurements of the public. It is thus important to examine results of the screening survey carefully and extract information for the reconstruction of early internal doses as much as possible.

References

1) Prime Minister of Japan and his cabinet, Report of Japanese Government to the IAEA Ministerial Conference on Nuclear Safety -The accident at TEPCO's Fukushima Nuclear Power Station-, http://www.kantei.go.jp/foreign/kan/topics/201106/iaea_houkokusho_e.html (Last accessed on 30 Oct 2012).

2) Nuclear Regulation Authority of Japan, http://www.nsr.go.jp/archive/nsc/mext_speedi/0312-0324_in.pdf

3) International Commission of Radiological Protection, Report of Reference Man: Anatomical, physiological and metabolic characteristics, ICRP Publication 23, Pergamon Press (1975).

4) K. Nishizawa and H. Maekoshi, Thyroidal ^{125}I monitoring system using an NaI(Tl) survey meter, Health Phys., 58, 165-169, (1990).

5) International Commission of Radiological Protection, Age-dependent dose to members of the public from intake of radionuclides: Part 5, ICRP Publication 72, Ann. ICRP 26(1), Pergamon Press (1995).

6) Fred H. Mettler, David V. Becker, Bruce W. Wachholz, Andre C. Bouville, Chernobyl: 10 Years Later, J. Nucl. Med., 37, 24N-27N (1996).

7) N. Ishigure, M. Matsumoto, T. Nakano, H. Enomoto, Development of software for internal dose calculation from bioassay measurements. Radiat. Prot. Dosim., 109, 235-242 (2004).

8) Y. Fukushima, Results of simplified survey for thyroid internal exposure of children in Fukushima and other surveys, Jpn J. Health Phys., 47, 17-19 (2012) [*Japanese*].

9) Nuclear Safety Research Association (NSRA), REMnet.
http://www.remnet.jp/english/lecture/b03_01/e_04-03-03.html (Last accessed on 30 Oct 2012)

Whole-body Counting of Fukushima Residents after the TEPCO Fukushima Daiichi Nuclear Power Station Accident

Takumaro MOMOSE[1], Chie TAKADA[1], Takahiro NAKAGAWA[1], Katsuta KANAI[1],
Osamu KURIHARA[1,4], Norio TSUJIMURA[1], Yoshihiro OHI[2], Takashi MURAYAMA[2],
Takashi SUZUKI[2], Yasuhiro UEZU[3], Sadaaki FURUTA[1]

[1]*Nuclear Fuel Cycle Engineering Laboratories, Japan Atomic Energy Agency, 4-33 Muramatsu, Tokai-mura, IBARAKI, 319-1194, Japan*
[2]*Nuclear Science Research Institute, Japan Atomic Energy Agency, 2-4 Shirakata-shirane, Tokai-mura, IBARAKI, 319-1195, Japan*
[3]*Fukushima Environmental Safety Center, Japan Atomic Energy Agency, 6-6 Sakae-chou, Fukusima, FUKUSHIMA, 960-8034, Japan*
[4]*Research Center for Radiation Emergency Medicine, National Institute of Radiological Sciences, 4-9-1 Anagawa, Inage-ku, Chiba,CHIBA, 263-8555, Japan (present affiliation)*

Abstract

At the request of the Fukushima government, the Japan Atomic Energy Agency (JAEA) started whole-body counting of residents on July 11, 2011, to assess radiation exposure after the TEPCO Fukushima Daiichi Nuclear Power Station accident. JAEA has examined residents in Iitate, Kawamata, Namie, and eight other local communities. The measurement capacity of the whole-body counting device is approximately 100 persons per day, and the total number of people to measure reached 9,927 by the end of January 2012. Two types of whole-body counter (WBC), each of which has two large-sized NaI(Tl) detectors, were used to perform the measurements. Physical phantoms (a Canberra RMC-II transfer phantom or a water-filled block phantom developed by JAEA) were used to perform the efficiency calibration of the WBCs, and results of this calibration were verified by comparing them with different-sized BOttle Mannequin ABsorber (BOMAB) phantoms imitating an adult male, a 10-year-old child, and a 4-year-old child. Short half-life radionuclides (e.g., ^{131}I) originating from the accident were not detected in the present work, because the measurements were made starting four months after the accident. These measurements showed that about 80% of the residents were below a minimum detectable amount (MDA) of the measured radionuclides in the whole-body content. No artificial nuclides other than ^{134}Cs and ^{137}Cs were detected in the present whole-body counting. The maximum whole-body content of radiocesium (^{134}Cs and ^{137}Cs in total) was 2.7 kBq for children (< 8 years old) and 14 kBq for adults. The radioactivity ratio (^{137}Cs/^{134}Cs) was estimated to be from 1.12 to 1.26. An acute intake scenario via inhalation of radiocesium was assumed in the present dose estimation for all the residents who were measured by the end of January 2012. The committed effective dose (CED) to 99.8% of the residents was found to be below 1 mSv. There were only 25 subjects with a CED greater than 1 mSv, and the maximum CED recorded was 3 mSv. The extrapolated 50th percentile (median) values of the CED for two age groups of 13-17 years old and > 17 years old were 0.02 mSv and 0.025 mSv, respectively. These values provide useful information for the dose reconstruction of early internal exposure to all of the residents in affected areas.

Keywords: Fukushima accident; internal exposure; Fukushima residents; ^{134}Cs; ^{137}Cs; whole-body counting; committed effective dose

1. Introduction

A magnitude 9.0 earthquake and subsequent massive tsunami on March 11, 2011, deprived the Tokyo Electric Power Company's (TEPCO's) Fukushima Daiichi Nuclear Power Station (FDNPS) of the ability to cool the reactor cores [1]. The resultant loss of the reactor integrity led to a series of releases of radionuclides, such as radioiodine and radiocesium, into the environment. The expectation was that a swift evacuation before a major release of radionuclides would minimize the levels of internal exposure via inhalation.

From March 26 through March 30, the local headquarter for responses to this nuclear disaster carried out a screening survey on radioiodine in the thyroid for 1,080 children age 0 to 15 years old from the three municipalities of Iitate Village, Kawamata Town, and Iwaki City, where the thyroid doses of residents were predicted to be relatively high according to the System for the Prediction of Environmental Emergency Dose Information [2]. The screening survey was performed by placing a NaI(Tl) scintillation survey meter on the anterior surface of the neck. The methodology for this was proposed by the National Institute of Radiological Sciences (NIRS) at the request of the Nuclear Safety Committee (NSC) of Japan. Although slightly positive readings were found in the screening survey, there were no detections above the level of 0.2 μSv/h (corresponding to a thyroid equivalent dose of 100 mSv for a hypothetical 1-year-old child). It was thus considered at this time that significant intake of radioiodine (mainly ^{131}I) had not occurred in the examined children. Neither the central government nor the NSC announced further actions to estimate internal doses for residents in affected areas during the early stage of the accident.

The reactors involved in the accident were relatively stabilized within three months after the nuclear disaster. However, public concern about the possible health effects from the remaining contamination has increased greatly with time. In response to this concern, the Social Health and Welfare Department of the Fukushima government launched an examination program for residents in Fukushima Prefecture by whole-body counting in June 2011. As a pilot study of this program, individual monitoring for internal exposure by both *in vivo* and *in vitro* measurements was performed by NIRS from June 27 to mid-July. Subjects of the pilot study included 122 residents from the three municipalities of Iitate Village, Namie Town, and the Yamakiya District of Kawamata Town, all of which were designated as being in an established "deliberate evacuation zone" because of the relatively-high recorded ambient dose rates. These municipalities are located outside the restricted area (within the 20-km radius of the FDNPS). The residents in the municipalities were asked to evacuate in late April and were thought to have been exposed to high doses of radiation. The pilot study revealed that about 50% of the subjects have significant levels of radiocesium in the body, and the highest whole-body contents of ^{134}Cs and ^{137}Cs were 3,100 Bq and 3,800 Bq, respectively.

Following the pilot study, the Japan Atomic Energy Agency (JAEA) initiated whole-body counting for other residents on July 11, 2011, at the request of the Fukushima government. Three whole-body counters (WBCs) owned by the Tokai Research and Development Center of JAEA (in Ibaraki Prefecture and located about 100 km south of the FDNPS) were used for *in vivo* measurements. The monitoring capability of the three WBCs in total was around 100 subjects per day for an operational time of 3-4 hours. Additional measurements were also started in September 2011 using a mobile WBC system of JAEA. These measurements were performed at schools in Fukushima City and western areas in Fukushima Prefecture where evacuees have temporarily settled. The number of subjects examined by JAEA reached 9,927 at the end of January 2012 [3]. These subjects were residents from Iitate Village, Kawamata Town, Namie Town, Minamisoma City, Katsurao Village, Futaba Town, Okuma Town, Tomioka Town, Kawauchi Village, Naraha Town, and Hirono Town. Currently, the whole-body counting organized by the Fukushima government is being continued by JAEA and also other institutes.

Overall results of the whole-body counting program by the Fukushima government

(including JAEA's measurements) have been released on the website of Fukushima Prefecture [4]. According to this information, 15,408 residents had been measured as of the end of January 2012, and the internal dose estimates for 15,383 of them (99.8%) were below 1 mSv in committed effective dose (CED). However, these estimations did not take into account the contribution of radioiodine and other short-lived radionuclides to the dose.

The elucidation of the early internal dose related to the TEPCO FDNPS accident is crucial for assessing possible radiation effects on the public in affected areas. As described above, the individual monitoring of internal exposure was implemented in Fukushima Prefecture after the accident. However, insufficient data are available on the intake of short-lived radionuclides, such as ^{131}I, ^{132}I, and ^{132}Te, for estimating internal doses to the public from these radionuclides. At a symposium on the reconstruction of early internal dose in the FDNPS accident (organized by NIRS on July 10-11, 2012), it was recognized that the compilation of individual and environmental monitoring data taken by various organizations was important for the dose reconstruction. The purpose of this paper is to present the method and results of whole-body counting by JAEA for a future work on the reconstruction of early internal doses to the public.

2. Materials and Methods

2.2. Whole-body counters

Two types of WBC were used for the measurements at the Tokai Research and Development Center of JAEA; one has stand-up geometry, and the other has chair geometry. Detectors used for these WBCs are adapted to a shadow shield method. Figure 1 displays external views of these WBCs. The specifications of the WBCs are summarized in Table 1. The stand-up WBC is a FASTSCAN^{TM}, a product commercially available from Canberra Inc. (USA). It has two large rectangular NaI(Tl) scintillation detectors, which are vertically arrayed in a column in front of the subject. The chair WBC was manufactured by Aloka Co. (Japan) based on a design drawing by JAEA. This WBC has two cylindrical NaI(Tl) scintillation detectors placed in front of the subject's torso. Spectral analyses were performed by a commercial software package, GENIE2K (Canberra Inc., USA), for the FASTSCAN and by a fixed region of interest (ROI) method for the chair WBC. A suitable background subtraction method was also applied to the spectral analyses. Minimum detectable amount (MDA) values of ^{134}Cs and ^{137}Cs were calculated as 300 Bq and 300 Bq in two minutes of measurement for the FASTSCAN and 340 Bq and 370 Bq in three minutes of measurement for the chair WBC. These values were slightly increased compared to those before the accident (~ 200 Bq of ^{137}Cs for both the WBCs). Ambient dose rate levels at the Tokai Research and Development Center are currently around 0.1 μSv/h. JAEA used three stand-up WBCs (FASTSCANs) and one chair WBC for the measurements of the Fukushima residents. One of the stand-up WBCs was mounted on a vehicle for use as a mobile system.

Figure 1. Picture of the WBCs used in this work (left, stand-up geometry; right, chair geometry).

Table 1 Specifications of the WBCs used in this work

Location of installation	Units	Geometry	Manufacturer	Shadow shield	Detector	Counting operation system	Meas. time (min)	MDA (Bq)	Remarks
JAEA Tokai/ Nuclear Science Research Institute	1	Chair	Aloka	lead, 5-cm thickness	NaI (8" diameter $\times$ 4") 2 sets	SEIKO-EG &G, Spectrum-navigator ver.2.1.1	3	^{134}Cs: 340 ^{137}Cs: 370	MDA values as of July 2011
JAEA Tokai/ Nuclear Fuel Cycle Engineering Laboratories	2	Stand-up	Canberra, FASTSCAN	low background steel, 10-cm thickness	NaI (16" $\times$ 5" $\times$ 3") 2 sets	Canberra, Genie-2000	2	^{134}Cs: 300 ^{137}Cs: 300	MDA values as of July 2011
On the vehicle	1	Stand-up	Canberra, FASTSCAN	low background steel, 10-cm thickness	NaI (16" $\times$ 5" $\times$ 3") 2 sets	Canberra, Genie-2000	2	^{134}Cs:160~ 270* ^{137}Cs: 210~300*	*MDA values changed depending on the background radiation level at the measurement location.

2.2. Calibration of WBCs

An RMC-II Transfer phantom [5] and a water-filled block phantom have been used for routine calibration of the WBCs installed at the Tokai Research and Development Center of JAEA. The RMC-II Transfer phantom was used for the stand-up WBCs, and the block phantom was used for the chair WBC (Fig. 2). The former was designed by Canberra to perform calibration for WBC products from this manufacturer, and the latter was made by JAEA to imitate a Japanese male with an average body size (168 cm in height and 60.2 kg in weight) [6]. These two phantoms were compared to an adult male-sized BOttle MAnnequin ABsorption (BOMAB) phantom [7] (175 cm in height and 66 kg in weight). The BOMAB phantom has been used as a standard source in the USA and Canada. Figures 3 and 4 show a comparison of peak efficiency values for various energies between the phantoms, demonstrating that the two phantoms for routine calibration well simulate

the BOMAB phantom; the discrepancy was 10% at most in the case of a ^{137}Cs peak (662 keV) for the stand-up WBC (see Fig. 3). However, it was necessary to examine the body-size dependency in the sensitivity of the WBCs, because we would be making measurements in subjects of all ages. Thus, body-size dependency was investigated using three BOMAB phantoms, one of which imitated a 4-year-old child, one of which imitated a 10-year-old child, and one of which imitated an adult male (described above). We found that the peak efficiency value for ^{137}Cs decreased with decreasing the body size of the BOMAB phantoms for the stand-up WBC. This was considered to be due to the placement of the detectors, which is optimized for most adult subjects. Table 2 provides a list of relative counting efficiency values of a P4 phantom (4-year-old child) and a P10 phantom (10-year-old child) compared to those of the adult male-BOMAB phantom. To avoid even slight underestimations for children, we examined the sensitivity of the stand-up WBC when the P4/P10 phantom was stood on a stool with a height of 30 cm or 45 cm to improve the counting geometry. The relative counting efficiency values for the P4 phantom with no stool, with a 30-cm-high stool, and with a 45-cm-high stool were 0.91, 1.21, and 1.28, respectively. On the other hand, the relative counting efficiency value for the P10 phantom without the stool was 1.02, showing no significant difference from the adult male-BOMAB phantom. Based on these results, we decided that the 30-cm-high stool should be used in the measurement when the subject was a small child less than 130 cm tall. Although this probably gives some overestimations of the whole-body content of radiocesuim or ^{40}K for small children, we believe that our procedure is practical. The tendency of the determined ^{40}K activity as a function of the subject's weight roughly agrees with that reported by the United Nations Scientific Committee on the Effects of Atomic Radiation (UNSCEAR): 61 Bq kg^{-1} for children and 55 Bq kg^{-1} for adults [8]. In the case of the chair WBC, the results of similar experiments suggested that no corrections were necessary in measurements of small children. Based on the investigation of the sensitivity of the WBCs, we decided to keep the counting efficiency values from the phantoms for routine calibration in all measurements of Fukushima residents with ages above 4 year-old.

Standard phantom

Routinely used phantom
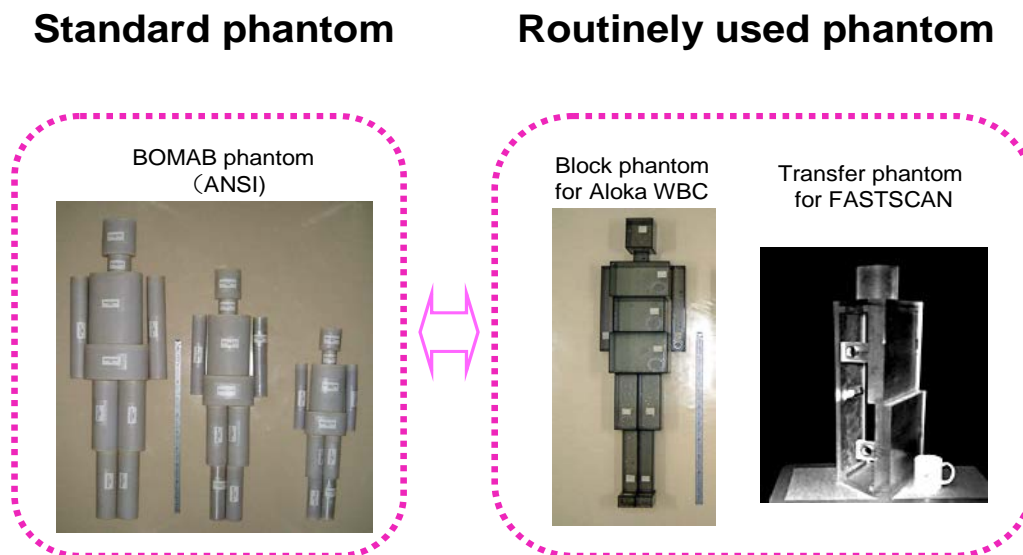
Figure 2. WBC calibration phantoms used in this work. The specifications of the bottle mannequin absorption (BOMAB) phantom were standardized following the American National Standard (ANSI N13.35.). The routinely used phantoms shown in this figure were employed for periodic verification of the counting efficiency of the JAEA WBCs. The peak efficiencies obtained using the standard and routinely used phantoms were compared.
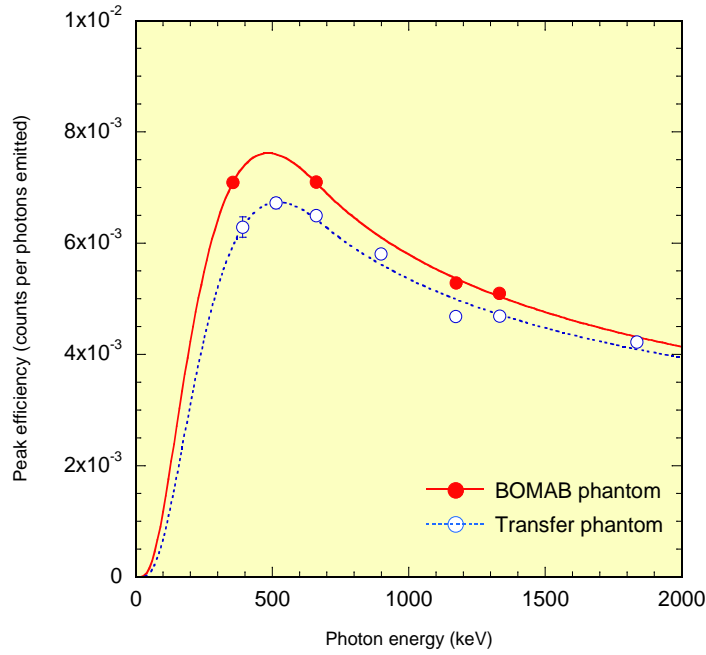
Figure 3. Peak efficiency of the FASTSCAN WBC used in this work for an adult BOMAB phantom and an RMC-II transfer phantom. The solid line and dotted line show peak efficiency curves derived by the least-squares method with log-log polynomial equations. The error bar indicates the estimated uncertainty (standard deviation: 1σ) of peak efficiency. An estimated uncertainty is only given for one point. The uncertainty for other peak efficiencies was too small to be described in this figure.
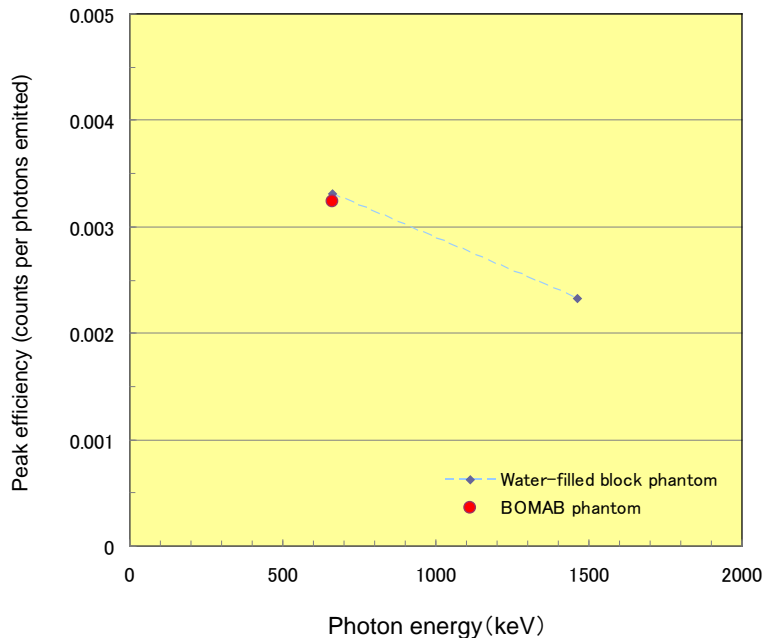
Figure 4. Peak efficiency of the Aloka WBC used in this work. As the water-filled block phantoms use only two kinds of standard radionuclides (^{137}Cs and ^{40}K), only 3 measurement results are shown in this figure. The ^{137}Cs peak efficiency for the adult BOMAB phantom and that for the water-filled phantom show good agreement.

72

Table 2 Phantom size dependence of the FASTSCAN WBC peak efficiencies. The peak efficiency values are normalized to those of an adult-size BOMAB phantom.

Nuclide	Energy (keV)	Size of BOMAB phantom			
		4 y (no stool)	4 y (30-cm stool)	4 y (45-cm stool)	10 y (no stool)
^{133}Ba	356	1.01	1.31	1.40	1.11
	356 + 384	0.89	1.15	1.22	0.97
^{137}Cs	662	0.91	1.21	1.28	1.02
^{60}Co	1173	0.87	1.14	1.22	0.98
	1333	0.83	1.12	1.18	0.97
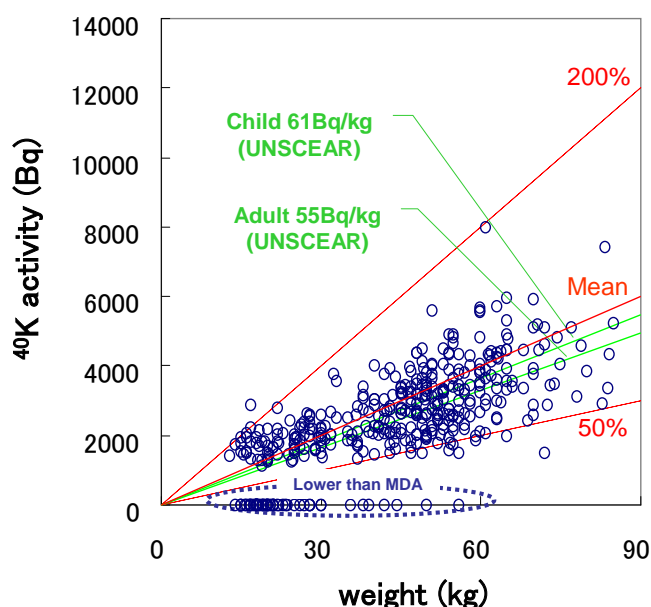
Figure 5. Body weight versus evaluated systemic potassium 40 measured in this work. These data were obtained from whole-body counting performed in February 2012. Good agreement is seen between the measured values and UNSCEAR standard values.

2.3. Overview of the whole-body counting for residents of Fukushima

The total number of residents measured at JAEA had reached 9,927 by the end of January 2012. These residents are originally from eleven towns in Fukushima Prefecture, and some of them have evacuated to other areas since the accident. Table 3 tabulates numbers of each age group and sex. The whole-body counting was initiated for residents who lived in Iitate Village, Namie Town, and Kawamata Town before the accident. These municipalities were designated as being in the "deliberate evacuation zone" located outside the 20-km radius of the FDNPS and in areas where the external annual dose was expected to be above 20 mSv. These measurements were conducted during the period from July 11, 2011, to the end of August 2011. The whole-body counting forresidents who lived in Futaba County, designated as being in the "evacuation zone," was started on September 1, 2011.

The priority order of subjects being examined was as follows: pregnant women (the first priority), mothers of children under 4 y old (as a surrogate for children), 4－12-y-old children, 13－17-y-old children, and adults (the last priority). Children under 4 y old were not measured due to the difficulty in taking accurate measurements. Instead of this, a mother of the child was measured as a surrogate for the child. The selection of the subjects was conducted by each municipality before they came to Tokai Research and Development Center for examinations. Figure 6 shows the sequence of these examinations. A surface contamination survey on cloth was performed by using a Geiger-Muller (GM) survey meter before the whole-body counting. This survey is employed by experts with experience in radiation control. After the whole-body counting, JAEA staff members explained results of the examinations to the residents and provided consultation to the residents if necessary. The results included the whole-body content of radiocesium (^{134}Cs and ^{137}Cs) and the resulting internal dose based on the assumption described above. The internal dose was given as a single-digit CED such as below 1 mSv, 1 mSv, 2 mSv, and so on. These figures are recorded in a prescribed format where fundamental information on radiation risk is described.

Table 3 Number of subjects examined from July 11, 2011, to January 31, 2012, by the JAEA

Age	Male	Female	Total
<8	1,239	1,150	2,389
8-12	1,451	1,394	2,845
13-17	772	793	1,565
>17	756	2,372	3,128
Total	4,218	5,709	9,927
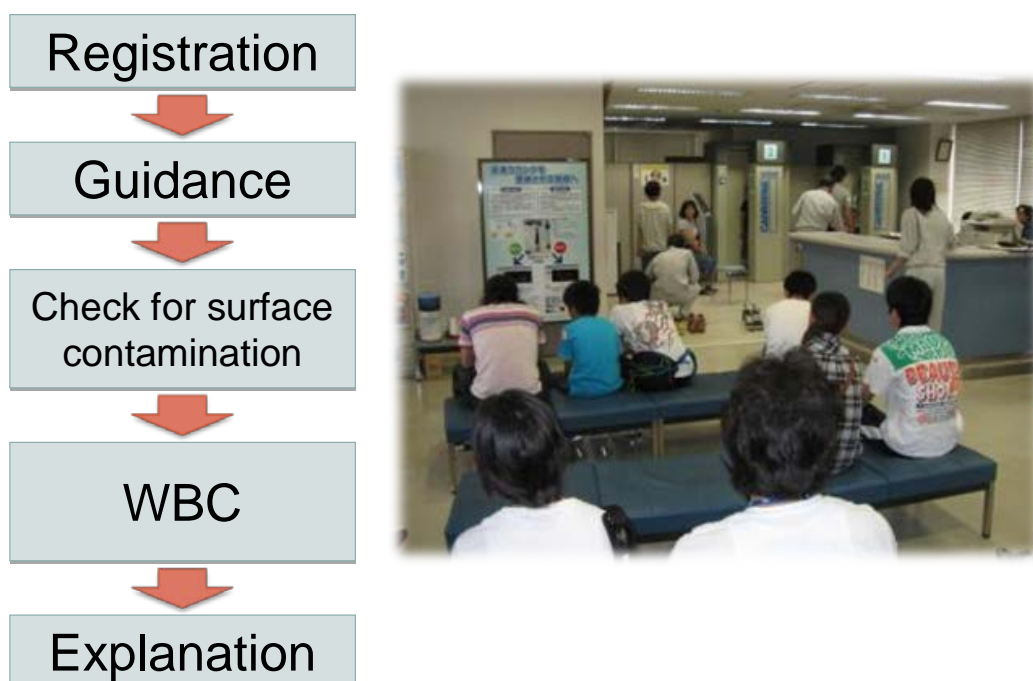
Figure 6. Flow chart and picture of the whole-body counting performed by JAEA. Beginning in January 2012, all residents who underwent whole-body counting changed into a contamination-free gown before measurement to avoid overestimation caused by any amount of contamination on their clothing.

2.4. Internal dose estimation

Internal dose estimation based on the assumption of a single intake scenario via inhalation was performed because of insufficient information on intake. The intake day was set at March 12, 2011, when the first explosive incident occurred at FDNPS. This scenario was applied until the end of January, 2012; a continuous intake scenario via ingestion has been applied since then, and up to the present. The internal dose based on the single intake scenario was calculated using the following equation:

$$I_i = M_i / m_i(t)$$

I_i is the intake activity of radionuclide i (units: Bq)
M_i is the total body content of radionuclide i measured by the WBC (units: Bq/total body)
$m_i(t)$ is the age-dependent retention function for systemic activity at time t after intake

$$D = \Sigma I_i \cdot e_i$$

D is the internal dose in CED up to the age of 70 (mSv)
e_i is the age-dependent dose coefficient (mSv per Bq)

where the radionuclides of concern are ^{134}Cs and ^{137}Cs, $m_i(t)$ is obtained from a software package for internal dose calculations, the MONDAL-3 code [9], and e_i is obtained from ICRP publication 72[10]. Radiocesium was assumed for aerosols with an activity mean aerodynamic diameter (AMAD) of 1 μm and an absorption type in the lungs of Type F. Table 4 summarizes the dose coefficients used in the present dose estimations.

Table 4 Dose coefficient for inhalation (mSv/Bq)

Age	^{134}Cs (type F)	^{137}Cs (type F)
4-7	5.2E-06	3.6E-06
8-12	5.3E-06	3.7E-06
13-17	6.3E-06	4.4E-06
>17	6.6E-06	4.6E-06

(taken from ICRP publication 72)

3. Results and Discussion

3.1. Body content

No artificial nuclides originating from the accident other than ^{134}Cs and ^{137}Cs were found in the present whole-body counting for Fukushima residents. Approximately 80% of the residents had levels below the MDA (see Table 1). Figure 7 shows the measured ^{134}Cs and ^{137}Cs activities retained in the whole bodies of the residents. As shown in the figure, the range of whole-body content becomes wider with increasing age. The maximum contents for children under 8 years of age and adults were 2.7 kBq and 14 kBq (of the total of ^{134}Cs and ^{137}Cs), respectively. The ^{137}Cs/^{134}Cs activity ratios were approximately 1.12-1.26. This ratio seems to be reasonable, because if the ^{137}Cs/^{134}Cs activity ratio in the source term of the accident is assumed to be 1.0 at the time of the early phase of the accident, it is corrected to 1.1-1.3 at the time of the implementation of whole-body counting using the physical half-life of radiocesium.
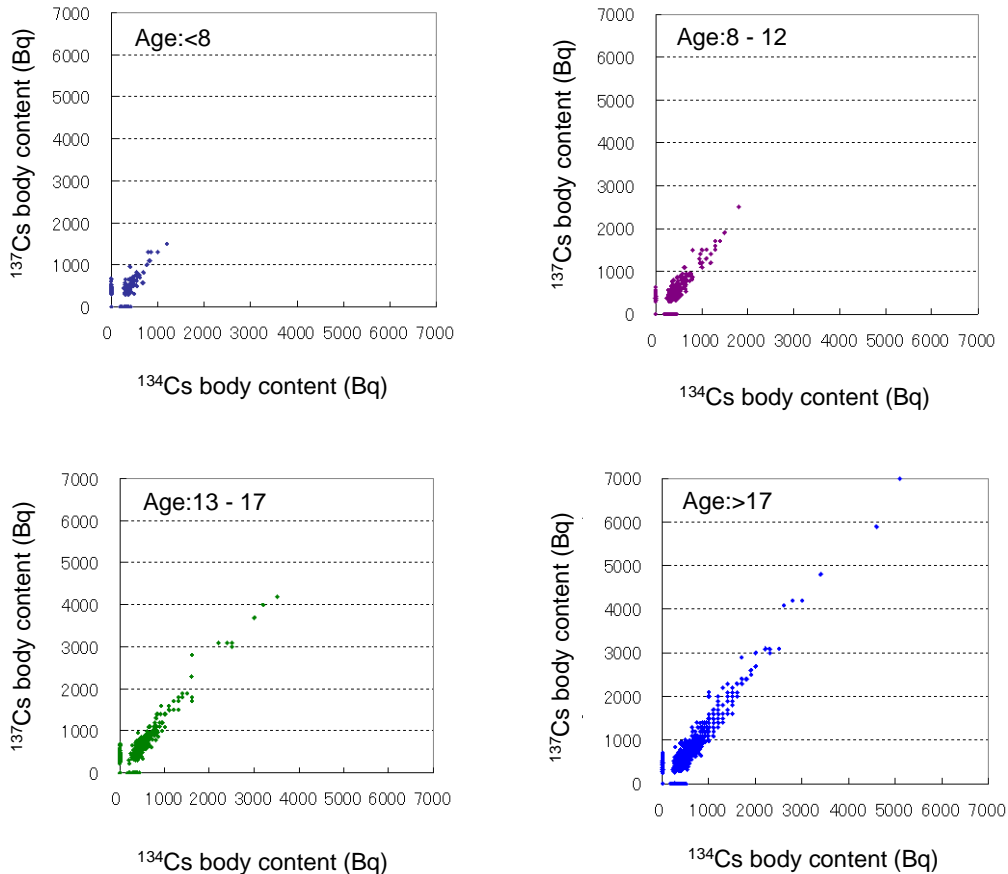
Figure 7. ^{134}Cs *and* ^{137}Cs *body content measured by whole-body counting. Only significant values over the MDA were plotted in this figure. Body content at the time of whole-body counting was plotted without correction of the half-life of radiocesium.*

3.2. Committed effective dose

Table 5 summarizes the effective dose distribution of the residents measured by JAEA from July 2011 to the end of January 2012. The CEDs of 99.8% of the residents were under 1 mSv; however, there were 22 individuals with CEDs that exceeded 1 mSv, with a maximum CED of 3 mSv. All were children or teenagers with the exception of one adult with a CED >1 mSv who had worked in the damaged plant.

Figure 8 shows the frequency distribution of the CED for each age group. The distribution of CEDs for children <8 years old was relatively broader than that for adults, and the estimated doses of the children were distributed in the higher dose region beyond the adults' doses. This result was inconsistent with the general relationship in doses expected from age-dependent differences in breathing rates and dose coefficients between children and adults.

If a significant body content >MDA was observed in a child <8 years of age, additional whole-body counting were performed on the child's parents or family who were evacuated in the same manner as the child to allow a better assessment of the child's result. Figure 9 shows a comparison of the effective doses of children and their parents, which revealed a large difference in the results.

76

Table 5. Committed effective dose distribution of Fukushima residents measured by JAEA from July 11, 2011, to January 31, 2012

Age	Number of individuals measured	Number of individuals falling in the committed effective dose interval			
		<1 mSv	1 mSv	2 mSv	3 mSv
<8	2,389	2,373 (99.3)	6 (0.3)	8 (0.3)	2 (0.1)
8-12	2,845	2,840 (99.8)	5 (0.2)	0 (0.0)	0 (0.0)
13-17	1,565	1,565 (100)	0 (0.0)	0 (0.0)	0 (0.0)
>17	3,128	3,127 (100)	1 (0.0)	0 (0.0)	0 (0.0)
Total	9,927	9,905 (99.8)	12 (0.1)	8 (0.1)	2 (0.0)

The values of CED $\geqq$ 1 mSv were rounded to one significant figure. The dose intervals of the three rightmost columns correspond to 1 - 1.4 mSv (1 mSv), 1.5 - 2.4 mSv (2 mSv), and 2.5 - 3.4 mSv (3 mSv), respectively. Values in parentheses indicate percentages.
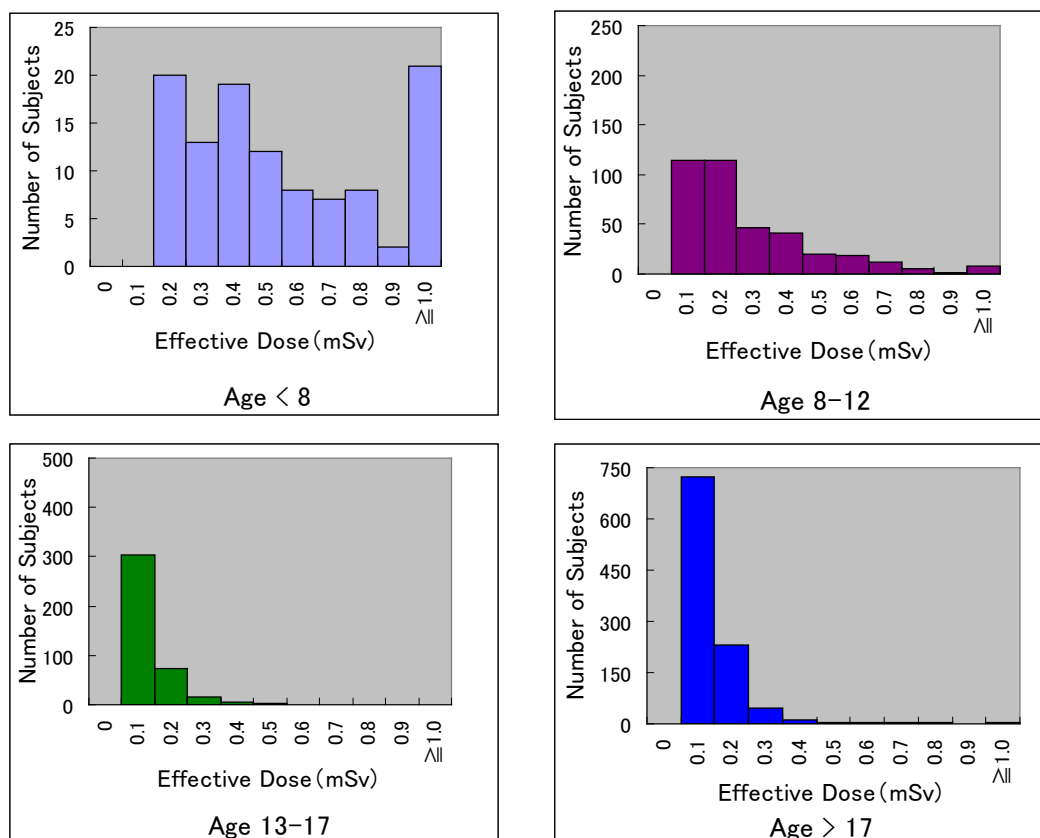
Figure 8. CED distribution derived from ^{134}Cs and ^{137}Cs body contents of residents who underwent WBC measurement by the JAEA
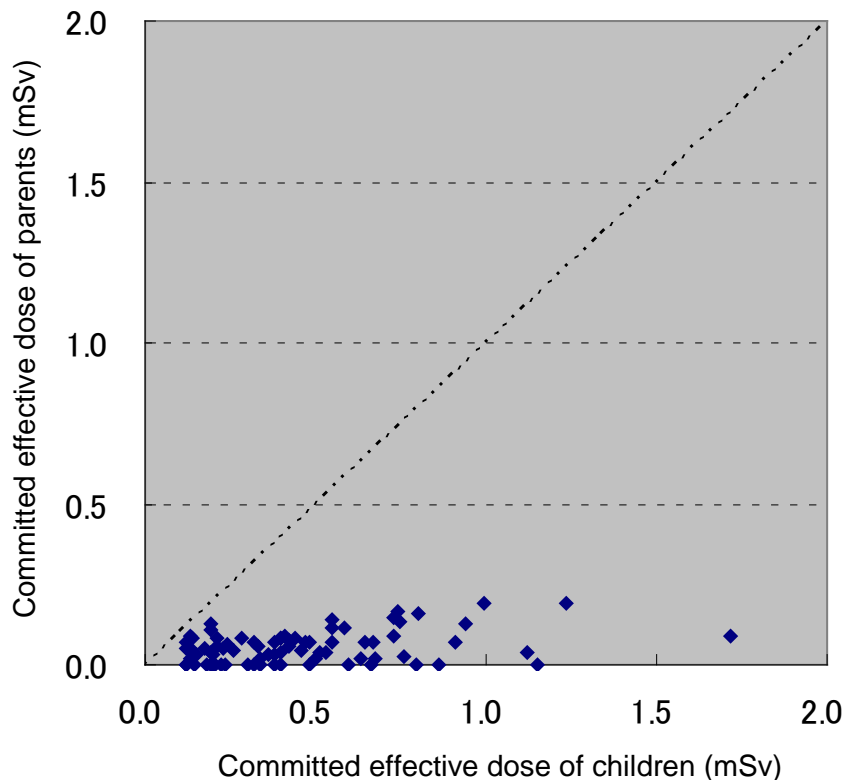
Figure 9. Comparison of CEDs of children and their accompanying parents. The parents of children under 8 years of age who showed a significant value in WBC measurement were selected for additional measurement. The parent or other family member who experienced the same evacuation pattern was measured at the same time. A large discrepancy was observed in the CEDs between children and their parents/other family members.

Despite checking for contamination on the subjects' street clothes before the measurements, small amounts of contamination were occasionally detected on clothing in the whole-body counting for some residents. Table 6 presents examples of a significant value detected on contaminated clothes in the measurements. Changing into contamination-free gowns by the subjects made the number of detection significantly reduced. It should be noted that a second period of temporary access into the restricted area started in September. Some residents returned to their hometown by car and brought back their property and clothing. It seems probable that a small amount of contamination on clothes may have affected the measurements results up to the end of December 2011. To avoid the false positive detection caused by contamination on closes, the subjects were asked to change into contamination-free gowns before measurement beginning in January 2012.

These results suggest that WBC the whole-body counting for children was affected by a small amount of radioactive contamination on their clothes or else that the assumption of a single uptake on March 12 was not always valid for children, who have a shorter radiocesium retention half-time than that of adults. Therefore, although the subjects whose dose was estimated to be >1 mSv were almost all children, their actual doses were highly likely to have been smaller than the estimated CEDs.

Table 6 Examples of significant detection caused by contaminated clothes in whole-body counting

Date of measurement	Detected activity in whole-body counting			
	Before changing clothes		After changing clothes	
	^{134}Cs (Bq)	^{137}Cs (Bq)	^{134}Cs (Bq)	^{137}Cs (Bq)
2011/10/19	5,800	8,200	ND	370
2011/11/11	980	1,300	ND	ND
2011/11/11	450	450	ND	ND
2011/11/15	330	330	ND	ND
2011/11/17	430	610	ND	ND
2011/11/17	1,800	2,500	ND	ND
2011/11/17	2,900	4,100	ND	ND
2011/11/17	1,200	1,800	300	470

ND: not detected

3.3. Dose distribution analysis

Figure 10 shows the cumulative frequency distribution of estimated CED values for the two subject groups ages 13-17 years old and >17 years old. Note that internal doses were assumed to be zero when the whole-body content of radiocesium was below the MDA values. The straight lines in the figure indicate that the CED values agree with a log-normal distribution in an upper dose range. However, a deviation of the dose distributions from the straight lines was found in the low dose range below 0.06 mSv. This suggests that the CED values corresponding to the whole-body content close to the MDAs are overestimated to some extent.

As shown in the figure, a small difference is found in the dose distribution between the above two subject groups. That difference can be explained by the fact that dose coefficients by inhalation of radiocesium are very close between these groups, as are their breathing volumes. The 95th percentile values of the estimated CEDs for the subjects 13-17 years old and those >17 years old were 0.10 mSv and 0.13 mSv, respectively. The extrapolated 50th percentile values were 0.02 mSv and 0.025 mSv, respectively.

Figure 11 shows the cumulative frequency distribution of the estimated CED values obtained from different municipalities. Here each subject's address was based on information prior to the accident. The dose distribution of the residents is slightly higher in Iitate Village and Futaba Town compared to the other municipalities. The 95th percentile value of the estimated CED values was 0.22 mSv for both Iitate Village and Futaba Town. However, the current internal dose estimates are associated with a large uncertainty regarding the intake scenario. It is difficult to identify when or how radionuclides were incorporated by individuals without information on those individuals' behavior during the evacuation. Thus, future work is necessary to establish a more appropriate intake scenario. The lack of information on air sampling will be covered by sophisticated simulations regarding atmospheric dispersion processes of radioactive materials.
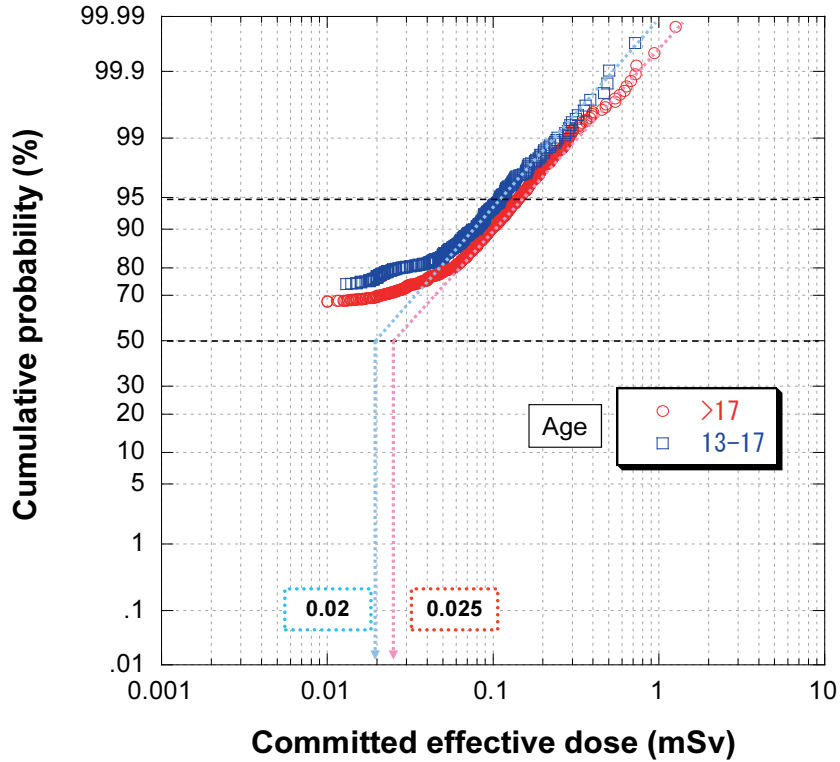
Figure 10. Cumulative frequency distribution of the CED of the measured persons. We did not use the number of individuals with detectable activity in the body but the number of measured individuals as the population parameter when we derived the cumulative probabilities in this work. When the body content of radiocesium was below the MDA, the CEDs was assumed to be zero.
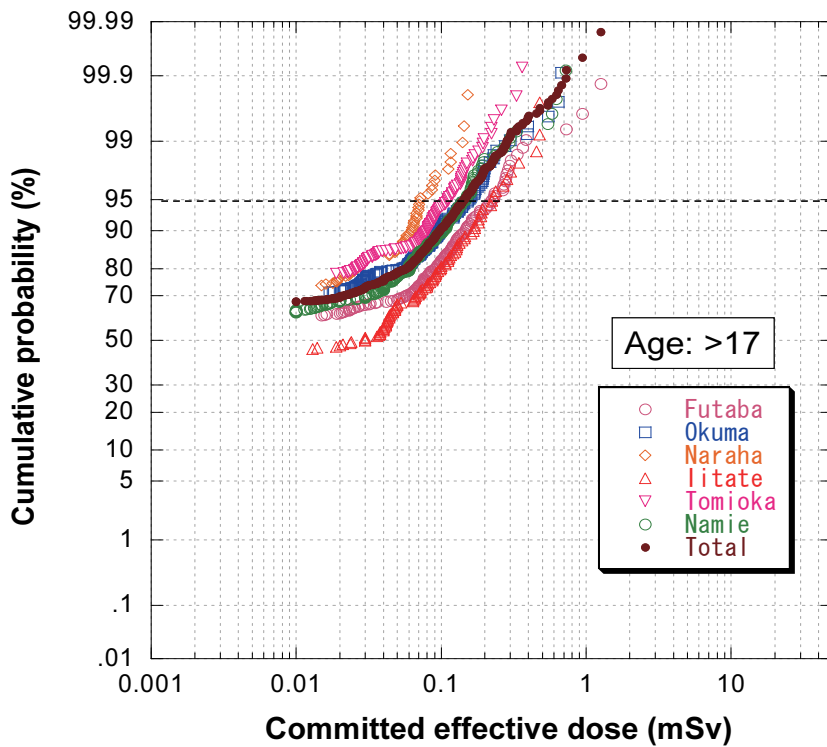
Figure 11. Cumulative frequency distribution of CEDs according to the municipality where residents lived before the accident

4. Conclusions

JAEA has performed whole-body counting for Fukushima residents since July 11, 2011, at the request of the Fukushima government to examine levels of the body-content of radiocesium (^{134}Cs and ^{137}Cs). The number of subjects had reached 9,927 by the end of January 2012. Estimated internal doses were less than a CED of 1 mSv for 99.8% of the subjects, even based on the most conservative assumption regarding the intake scenario. The maximum dose was found to be 3 mSv. Our analyses also revealed the following: (1) the 95th percentile value of internal doses to all subjects was on the order of 0.1 mSv, (2) this value is very similar among regional districts, and (3) the extrapolated 50th percentile values of the two age groups of 13-17 years old and >17 years old were 0.02 mSv and 0.025 mSv, respectively. The knowledge from this study will be useful for the reconstruction of the public's early internal radiation exposure from the FDNPS accident if an appropriate intake amount ratio of other nuclides, in particular, ^{131}I, to the radiocesium can be obtained. In addition, a detailed behavior survey of each individual during the period when internal exposure possibly occurred is needed to establish a more realistic intake scenario.

References

1) Nuclear Emergency Response Headquarters Government of Japan, Report of the Japanese Government to the IAEA Ministerial Conference on Nuclear Safety - the accident at TEPCO's Fukushima Nuclear Power Station,
http://www.kantei.go.jp/foreign/kan/topics/201106/iaea_houkokusho_e.html#top (last accessed on 25 August 2012).
2) Nuclear Emergency Response Headquarters Government of Japan, Additional Report of the Japanese Government to the IAEA - the accident at TEPCO's Fukushima Nuclear Power Stations - (Second Report),
http://www.meti.go.jp/english/earthquake/nuclear/iaea/iaea_110911.html (last accessed on 25 August 2012).
3) C. Takada, O. Kurihara, N. Tsujimura, K. Kanai, T. Nakagawa, H. Miyauchi, T. Murayama, Y. Maruo, T. Momose, and S. Furuta, Evaluation of internal exposure of the workers and the residents caused by the Fukushima nuclear accident, Full papers of The 13th International Congress of the International Radiation Protection Association (IRPA13),
http://www.irpa13glasgow.com/information/downloads/, File P12.22.doc.
4) Fukushima Prefecture, Results of the WBC examination for internal exposure (in Japanese),
http://www.pref.fukushima.jp/imu/wbc/20120223WBC_joukyou.pdf (last accessed on 25 August 2012).
5) O. R. Perry, Calibration of the Accuscan II in vivo system for I-131 thyroid counting, INL/EXT-11-22507, (2011).

6) S. Kinase, Study on advancement of in vivo counting using mathematical simulation, JAERI-Research 2003-011, (2003).

7) American National Standard, Specifications for the bottle manikin absorption phantom, ANSI/HPS N13.35-1999, (1999).

8) United Nations, Sources and effects of ionizing radiation, exposures of the public and workers from various sources of radiation, UNSCEAR 2008 Report, Volume I, Annex B, (2008).

9) N. Ishigure, M. Matsumoto, T. Nakano, and H. Enomoto, Development of software for internal dose calculation from bioassay measurements. Radiat. Prot. Dosim, 109, 235-242, (2004).

10) International Commission on Radiological Protection, Age-dependent doses to the members of the public from intake of radionuclides - Part 5. Compilation of ingestion and inhalation coefficients, ICRP Publication 72. Ann. ICRP 26 (1), (1995).

Estimation of Ingestion Dose due to I-131 in the Initial Month by using Food-monitoring Data after the Fukushima Nuclear Disaster in Japan

Ichiro YAMAGUCHI

Department of Environmental Health, National Institute of Public Health
2-3-6, Minami, Wako, SAITAMA, 351-0197, Japan

Abstract

The committed equivalent dose to the thyroid caused by I-131 and the effective dose caused by I-131, Cs-134 and Cs-137 due to ingestion immediately after the accidental releases following the Fukushima nuclear disaster in March 2011 were estimated retrospectively by using measured food data. A food monitoring dataset provided by the Ministry of Health, Labour and Welfare (MHLW) up to April 18, 2011 (N=1,752) was used for this study. Information on food consumption by 99 food categories was made available by using the original data of the Japanese National Food Consumption Survey, which was conducted in 2009 (N=9,942). Food concentration every 4 days and food consumption in each food category was randomly picked up (N=100,000). The levels of radioactive iodine and cesium were summed for one month and then converted to equivalent doses to the thyroid and effective doses. These doses in the first month after the Fukushima nuclear power plant accident were evaluated by using the food monitoring dataset provided by the MHLW. Assuming that food was randomly extracted from monitored food samples and food restrictions were fully immplmented, the 90%tile of the equivalent doses to the thyroid and the effective doses in 1- to 6-year-old children were estimated to be around 1 mSv and 0.07 mSv, respectively. Several diffrent methods should be considered to reduce limitations of this estimation.

Keywords: internal dose; ingestion; radioactive iodine; concentration of food

1. Introduction

The Great East Japan Earthquake and Tsunami that occurred on March 11, 2011 induced a severe accident at Fukushima Dai-ichi Nuclear Power Plant. The Japanese Ministry of Health, Labour and Welfare (MHLW) set derived intervention levels (DILs) for radioactive materials in food and tap water on March 17. The DILs are shown in Table 1. These levels are based on protective action guides (PAGs) of a 50 mSv/year thyroid-equivalent dose for radioactive iodine and a 5 mSv/year effective dose for radioactive cesium in emergency situations [1, 2]. The Nuclear Safety Commission (NSC) previously designated these levels in preparation for emergency situations.

The first results of the emergency monitoring surveys conducted in Fukushima Prefecture and Ibaraki Prefecture were announced on March 19. According to these results, instructions on restrictions of distribution and/or consumption of foods were given to the public based on the Act on Special Measures Concerning Nuclear Emergency Preparedness, for foods such as spinach, kakina (non-head type leafy vegetables) and raw milk in Fukushima Prefecture on March 21. Thereafter, the Nuclear Emergency Response Headquarters required Fukushima and its neighboring prefectures to restrict the distribution of certain kinds of food produced in these prefectures by comparing DILs.

To assess the effectiveness of the food restriction policy as a countermeasure in radiological emergency situations, we estimated retrospectively committed equivalent doses to the thyroid caused by I-131 and effective doses (to the total body) caused by I-131, Cs-134 and Cs-137 due to ingestion immediately after the accidental releases was estimated by using measured food data. Here we discuss the purpose of dose estimation and the issues to be solved.

Table 1 Derived intervention levels (DILs) on food and drink ingestion

Nuclide	Index values relating to ingestion limits in guidelines for coping with disasters at nuclear facilities (Bq/kg)	
Radioactive iodine (Representative radionuclides among mixed radionuclides: [131]I)	Drinking water	300
	Milk, dairy products*	
	Vegetables (Except root vegetables and tubers)	2,000
Radioactive cesium	Drinking water	200
	Milk, dairy products	
	Vegetables	500
	Grains	
	Meat, eggs, fish, etc.	

* Provide guidance so that materials exceeding 100 Bq/kg are not used in milk supplied for use in powdered baby formula or for babies to drink directly.

2. Methods

2.1. Age group

The population was divided into 1- to 6-year-old children, 7- to 12-year- old children, 13- to 18-year-old children and adults. The population of children less than 1 year old was not considered in this estimation because food consumption data is not available for this age group in the Japanese national food consumption survey. For 1-year-old children who ingest mother's milk, it would be possible to estimate the ingestion dose by considering ingested radioactivity by mothers[3].

2.2. Radioactivity concentration in food

A food monitoring dataset provided by the MHLW up to April 18, 2011 (*N*=1,752) was used for this study. The dataset reflects the concentrations of radioactivity in food mainly from Fukushima and 16 neighboring prefectures. Each sample was measured at 'ready to cook' status, and weight was indicated at wet status not dried status. All samples were measured by using Ge semiconductor detectors. Results reported to be below the level of detection were assumed to be 10 Bq/kg. For the unmonitored food category, concentrations were assumed to be 0 Bq/kg. Food restrictions were introduced in Japan with the aim of banning certain food items from the market; those food commodities produced in highly contaminated areas would not be circulated on the market. In addition, seafood in Fukushima was not circulated on the market during this period due to fishery restraints implemented by the prefectural government; the dataset includes both measurements that are in excess of the food restriction levels and seafood in Fukushima.

2.3. Consumption of each food category

Food consumption by 99 food categories was made available by using the original data of the Japanese national food consumption survey in 2009. The usage of these data was permitted by the MHLW. The sample size was 9,942, and 9,006 of the sets of data were available for calculation of food consumption. The mean consumption of spinach and milk is shown in Table 2.

2.4. Method for dose estimation

Food concentration and consumption in each food category were combined to calculate the consumption activities every 4 days by using random sampling by considering a limited number of samples and the decay of radioactive iodine. Food consumption data of each food category for each person was randomly sampled for each calculation in each age-sex group. These activities were summed for one month and then converted to the equivalent dose to the thyroid and the effective dose to the thyroid. The number of executions was 100,000 for each calculation by using R software version 2.14.1.

2.5. Ingestion dose coefficients

The values of the ingestion dose coefficients used for equivalent doses to the thyroid were taken from the ICRP Database[4].

2.6. Specific food

It was assumed that 10 grams of tea leaves are used for 500 *ml* of tea.

Table 2 Mean daily consumption of spinach and milk [g/d]

Age group	Available number of data		Spinach		Milk	
(y)	Male	Female	Male	Female	Male	Female
1-6	238 (259)	229 (248)	6[0]	8[0]	25[19]	22[17]
7-12	277 (313)	284 (315)	10[0]	9[0]	29[22]	33[26]
13-18	278 (321)	249 (280)	15[0]	13[0]	50[45]	43[39]
19-	3,387 (3,755)	4,064 (4,451)	18[0]	18[0]	55[37]	32[28]

Sampled number of national nutrion survey is indicated in parentheses.
Median consumption is indicated in square brackets.

3. Results

3.1. Daily concentration of I-131

The daily concentration of I-131 in food up to April 18, 2011 is shown in Figure 1 (vegetables), Figure 2 (milk), Figure 3 (fish) and Figure 4 (meat and eggs). The concentrations were measured at 'ready to cook' status. This means that measurement was performed after washing vegetables. The number of samples and minimum, first quartile, median, mean, third quartile and maximum concentration of I-131 in vegetables, milk, fish, and meat are shown in Table 3.
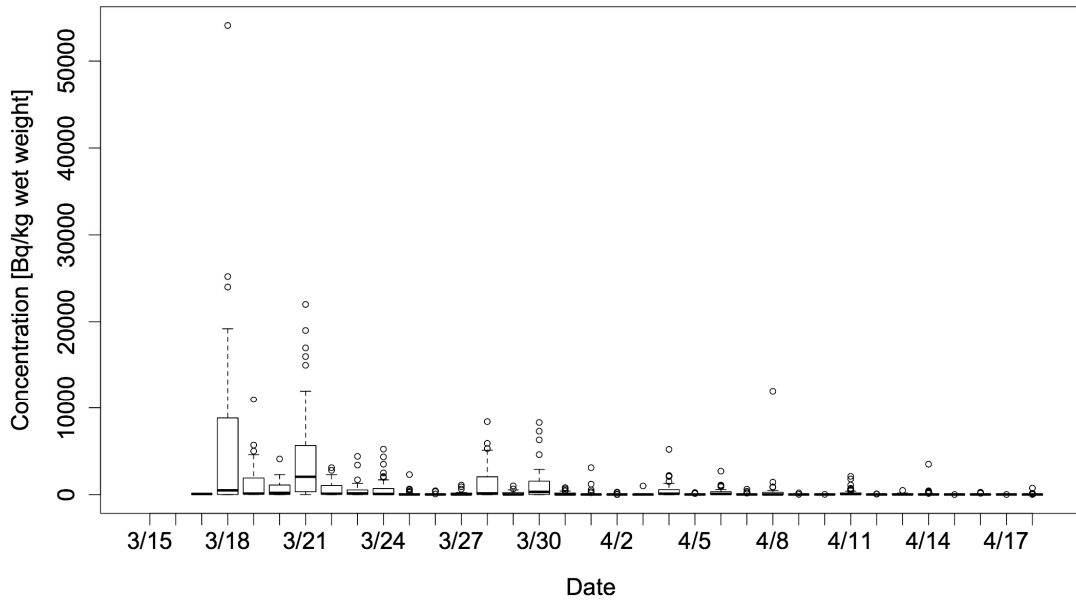
Figure 1. Concentration of I-131 in vegetables up to April 18, 2011
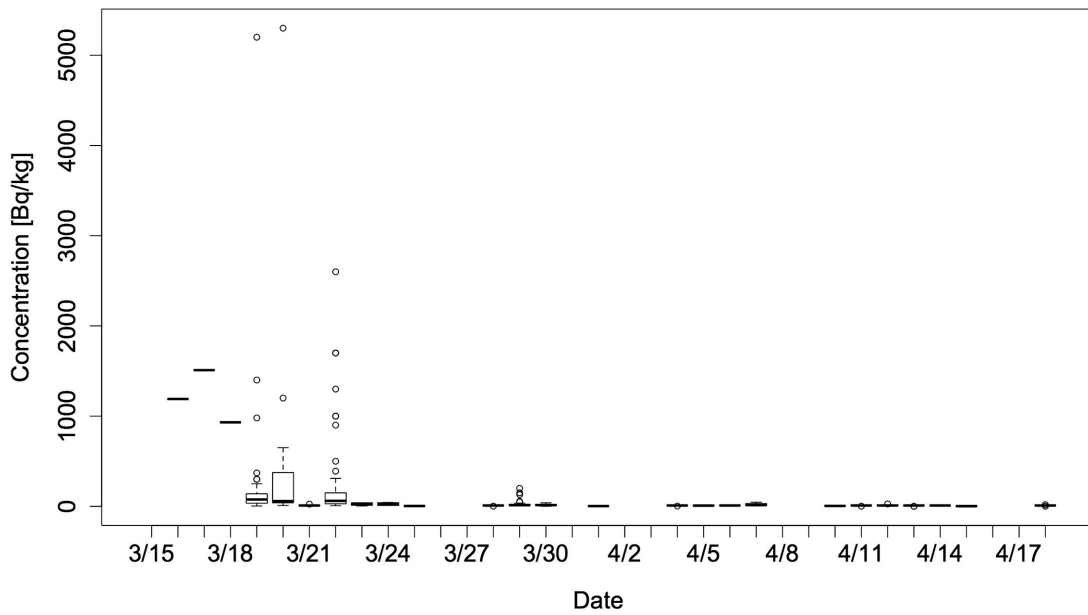
Figure 2. Concentration of I-131 in milk up to April 18, 2011
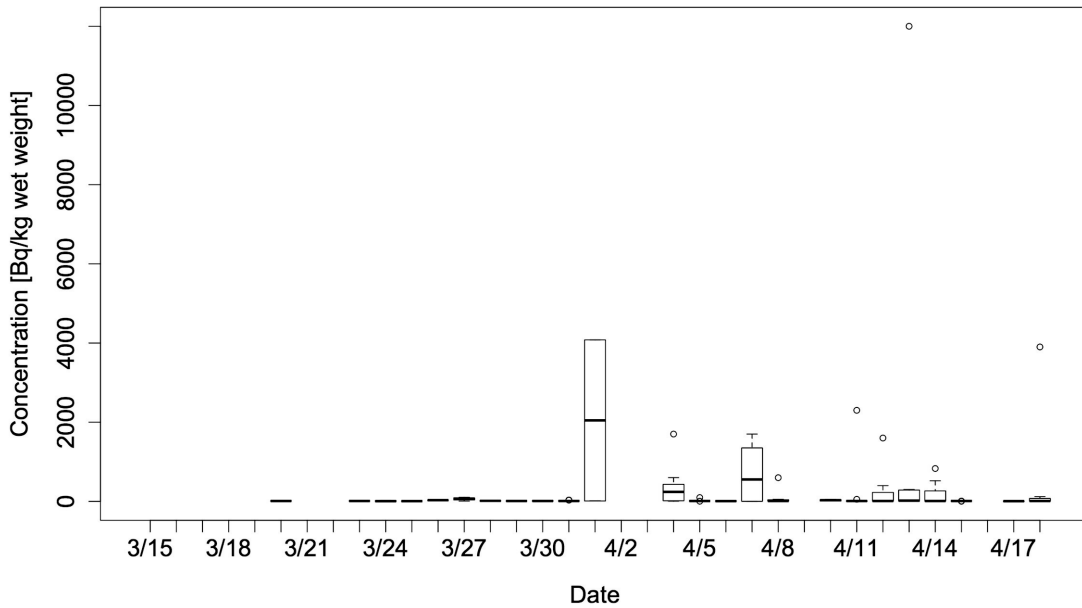
Figure 3. Concentration of I-131 in fish up to April 18, 2011
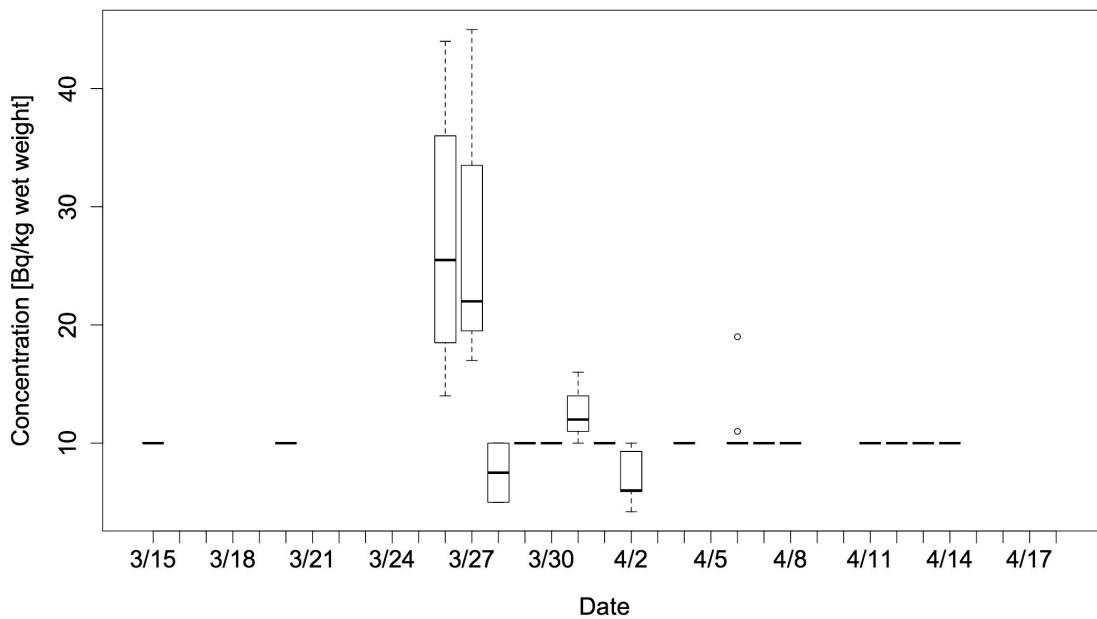
Figure 4. Concentration of I-131 in meat and eggs up to April 18, 2011

These data include test samples that were not intended for distribution in the market but only for monitoring. The vegetable with the highest level was spinach sampled on March 18 in Ibaraki Prefecture, and the concentration was 54.1 kBq/kg. As the Ibaraki prefectural government restricted the distribution of spinach into the market from March 19, this sample was categorized as not for market.Box plots in this paper show lower quartile, median, upper quartile as a box, and the maximum length of each whisker is 1.5 times the interquartile range (IQR).

87

Table 3(1) Concentration of I-131 for each food category during March 15, 2011 –
April 18, 2011[Bq/kg, wet weight]

	Vegetables	Milk	Fish	Meat and eggs
Number of samples	1,303	251	126	71
Number of undetectable samples	459	54	47	33
Minimum	1.0	0.36	1.3	10
1st Quartile	10	10	10	20
Median	27	18	10	20
Mean	685	159	293	27
Third Quartile	270	60	28.0	20
Max	54,100	5,300	12,000	510

Table 3 (2)   March 15 – March 18, 2011

	Vegetables	Milk	Fish	Meat and eggs
Number of samples	43	3	0	2
Minimum	10	932	NA	10
1st Quartile	15	1061	NA	10
Median	356	1190	NA	10
Mean	5841	1211	NA	10
Third Quartile	8625	1350	NA	10
Max	54100	1510	NA	10

Table 3(3)   March 19 – March 22, 2011

	Vegetables	Milk	Fish	Meat and eggs
Number of samples	166	111	1	7
Minimum	6.6	4	10	10
1st Quartile	25.3	28	10	10
Median	450	60	10	10
Mean	1920	305.1	10	10
Third Quartile	2100	150	10	10
Max	22000	5300	10	10

Table 3(4) March 23 – March 26, 2011

	Vegetables	Milk	Fish	Meat and eggs
Number of samples	183	17	7	4
Minimum	3.28	3	2.5	14.0
1st Quartile	10	9.6	4.6	25.5
Median	36	15	5.9	20.8
Mean	381.9	21.4	12.1	27.3
Third Quartile	405	39	19	32
Max	5230	43	29	44

Table 3(5) March 27 – March 30, 2011

	Vegetables	Milk	Fish	Meat and eggs
Number of samples	169	45	12	16
Minimum	1	1.1	6.3	5.0
1st Quartile	10	10	10	10
Median	130	11	10	10
Mean	859.6	25.1	22.8	13.1
Third Quartile	770	20	13.8	10
Max	8400	200	103	45

Table 3(6) March 31 – April 3, 2011

	Vegetables	Milk	Fish	Meat and eggs
Number of samples	127	1	12	13
Minimum	4.91	3.2	10	4.2
1st Quartile	10	3.2	10	6.0
Median	10	3.2	10	9.3
Mean	117.5	3.2	353.5	8.7
Third Quartile	49.5	3.2	17.5	10
Max	3100	3.2	4080	16

3.2. Estimated committed equivalent dose to the thyroid due to I-131 in food

The estimated committed equivalent dose to the thyroid due to I-131 in food by using all sample data is shown in Table 4 (N=1,752). These results did not take food restrictions into account. Table 5 shows the estimated committed equivalent dose to the thyroid excluding samples over DILs (N=1,548). The estimated dose distribution for 1- to 6-year-old male children is shown in Fig 5. By using the mean concentration during the first month and the mean consumption for each food category, we calculated the mean doses for each age group (Table 6). The 90% confidence intervals for estimation at adult males were 0.05 - 0.05 for median, 0.13 - 0.13 for 90%tile, 0.17 - 0.17 for 95%tile, 0.26 - 0.26 for 99%tile, 0.37 - 0.39 for 99.9% and 0.44 - 0.47 for 99.99% when food restrictions were taken into account.

1) Estimation by only food concentration in Fukushima
    The estimated percentiles of dose [mSv/month consumption] for 1- to 6-year-old males by only food concentration in Fukushima when taking food restrictions into account are indicated in Table 7

2) Estimation by different period lengths
    The estimated percentiles of dose [mSv/month consumption] for 1- to 6-year-old males by 3-day period and 5-day period are indicated in Table 7.

3.3. Estimated committed effective dose due to I-131, Cs-134 and Cs-137 in food

Table 8 shows the estimated committed effective dose due to I-131, C-134 and Cs-137, excluding samples over DILs (N=1,548).

Table 4 Estimation of the committed equivalent dose to thyroid from ^{131}I in the initial month without taking food restrictions into account [mSv/first month intake]

Age	Sex	50%	90%	95%	99%	99.9%	99.99%
1-6	Male	2.4	7.8	10.5	16.0	24.2	32.9
	Female	2.5	8.5	11.4	18.3	29.8	36.7
7-12	Male	1.3	3.6	4.7	7.1	10.3	12.5
	Female	1.2	3.4	4.6	7.1	10.2	12.5
13-18	Male	0.9	3.2	4.5	6.9	9.9	14.5
	Female	0.7	2.6	3.5	5.5	9.9	13.4
19-	Male	0.4	1.6	2.2	3.5	6.3	8.4
	Female	0.6	2.2	3.0	4.6	6.4	6.6

Note: ICRP ingestion dose coefficients used to derive the dose to the thyroid are not sex specific.
Therefore, doses given are not accurate estimates of doses received by males and females, respectively.

Table 5 Estimation of the committed equivalent dose to the thyroid from ^{131}I in the initial month, taking food restrictions into account [mSv/first month intake]

Age	Sex	50%	90%	95%	99%	99.9%	99.99%
1-6	Male	0.5	1.3	1.5	2.2	3.1	3.7
	Female	0.6	1.3	1.6	2.3	3.3	4.0
7-12	Male	0.3	0.5	0.7	0.9	1.3	1.5
	Female	0.3	0.5	0.7	1.0	1.4	1.5
13-18	Male	0.2	0.5	0.6	0.9	1.2	1.5
	Female	0.2	0.4	0.5	0.7	1.1	1.4
19-	Male	0.1	0.3	0.4	0.7	1.1	2.0
	Female	0.1	0.3	0.4	0.7	1.1	1.6

Note: ICRP ingestion dose coefficients used to derive the dose to the thyroid are not sex specific.
Therefore, doses given are not accurate estimates of doses received by males and females, respectively.
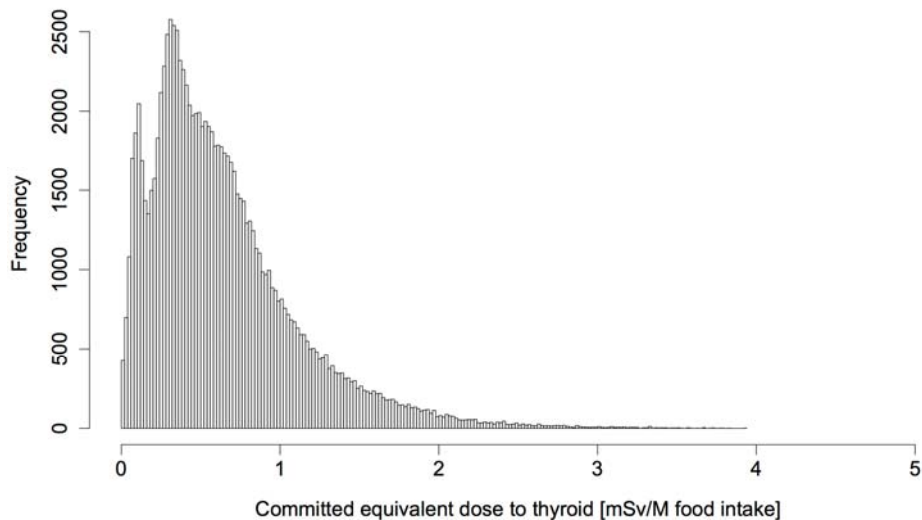
Figure 5. Estimated equivalent dose distribution to the thyroid for 1- to 6-year-old male children due to I-131 in food during the -first month of consumption following the accident on March 11, 2011

Table 6 Estimated committed equivalent dose to the thyroid from ^{131}I in the initial month by using the mean concentration and mean consumption in each food category, taking food restrictions into account [mSv/first month intake]

Age		1-6	7-12	13-18	19-
Sex	Male	1.8	0.85	0.64	0.40
	Female	1.8	0.83	0.56	0.39

Table 7 Estimation of the committed equivalent dose to the thyroid in 1- to 6-year-old males from ^{131}I in the initial month using various conditions, taking food restrictions into account [mSv/first month intake]

Location	Sampling period	50%	90%	95%	99%	99.9%	99.99%
Fukushima	4 day	0.4	1.1	1.4	2.2	3.2	3.8
Japan	3 day	0.6	1.6	2.0	3.0	4.5	5.3
Japan	5 day	0.5	1.1	1.4	2.2	2.9	3.7

Table 8 Estimation of the committed effective dose in the initial month, taking food restrictions into account [mSv/first month intake]

Age	Sex	50%	90%	95%	99%	99.9%	99.99%
1-6	Male	0.01	0.02	0.03	0.04	0.06	0.10
	Female	0.01	0.02	0.03	0.04	0.06	0.09
7-12	Male	0.01	0.02	0.03	0.04	0.07	0.09
	Female	0.01	0.02	0.03	0.04	0.07	0.10
13-18	Male	0.01	0.02	0.03	0.04	0.06	0.10
	Female	0.01	0.02	0.03	0.04	0.07	0.10
19-	Male	0.01	0.02	0.03	0.04	0.07	0.12
	Female	0.01	0.02	0.03	0.04	0.07	0.10

4. Discussion

4.1. Characteristics of dose distribution and ingestion dose

The distribution of the dose concentration in food each day has a skewed right tail. The arithmetic mean of each major food category (vegetables, milk, fish and meat) was larger than in the third quartile. According to this characteristic of concentration distribution, the dose distribution would also have a skewed right tail.

This result is consistent with the results of *in vivo* monitoring using external body measurement taken by Tokoname from April 12 to 16, 2011 [5] and by the local nuclear emergency response headquarters from March 26 to 30 and monitoring of human breast milk[6].

4.2. Underestimation factors

The distribution of the dose concentration in food may have been underestimated for several reasons.

1) Local residents who consume homegrown vegetables
   Although both food distribution restrictions and food consumption restrictions have been in

place since the accident, the dataset consists mainly of food for marketing, because homegrown vegetables are not regulated by food safety law but only by the Act on Special Measures Concerning Nuclear Emergency Preparedness. For this reason, a unified dataset covering both food for marketing and homegrown food was not available, although homegrown vegetables were also measured by cities, towns and villages. As indicated Tables 5 and 7, the concentration distribution in Fukushima was not significantly different from that in the other 15 monitored prefectures. The purpose of food sampling in each prefecture is to determine whether a food restriction should be implemented and to estimate ingestion doses due to marketed food.

Consequently, for those who consumed highly contaminated homegrown vegetables, the doses might be underestimated. The wild plant with the highest concentration was 2,540 kBq/kg sampled on 20 March 2011 at 42 km northwest of the Fukushima Dai-ichi Nuclear Power Plant. The vegetable with the highest concentration of radioactive materials was spinach sampled on March 18 in Ibaraki Prefecture, and the concentration was 54.1 kBq/kg. Assuming that the radioactive iodine concentration in vegetables was 60 kBq/kg and the daily consumption of vegetables was 100 g/d for 1-year-old children, the committed equivalent dose to the thyroid would be 150 mSv for one-week consumption. To ascertain doses to these residents, it would be helpful to have a survey on food consumption behavior at that time for concerned persons and information to estimate homegrown vegetables such as simulation on radionuclides in the environment and monitored data on wild grass and fall-out density of radionuclides.

2) Consumption of food with a high concentration of radioactive materials

For those who consumed food with a high concentration of radioactive materials continuously, doses would be underestimated. Due to the great earthquake, almost no commercial milk was available in Fukushima immediately after the accident. However, as tap water would be perceived as dangerous by local residents and stores were closed due to earthquake damage, farmers might have provided milk for consumption in their own neighborhoods as an exceptional case. To ascertain doses to these residents, more precise concentration data in local areas and consideration of food consumption patterns during this emergency situation would be helpful.

3) Sampling bias

Although local governments tried to sample the most contaminated food in each area,[7] lack of information and resources may have led to incomplete food sampling. Furthermore, it was not possible to sample every small food category each day. Especially in Fukushima, data collection immediately after the accidental radiation releases was limited. To reduce underestimation due to sampling size, concentration data were obtained 4-day pools of data. To decrease uncertainty about the estimation of the ingestion dose distribution in a target population, appropriate modeling would be helpful.

4) Incompleteness of food restrictions

According to the results of spot checks in shops, the ratio of restricted food appearing on the market was small. However, immediately after the accidental releases it seems that data on this issue was limited.

5) Foods that accumulate high levels of radiation

Iodine accumulates in seaweed and is detectable in a normal exposure situation.[8] Higher levels of iodine were detected in seaweed after the nuclear accident. Therefore, consumption of seaweed would be a route of transmitting a dose of iodine to the thyroid after the first month. However the mean consumption of seaweed is 6 g/day in 1- to 6-year old children, and the physical half-life of I-131 is 8.0 days, so that the attribution in this pathway would be limited.

6) Lack of restrictions on drinking water and water for cooking

Although tap water was restricted during the highly contaminated period, the restriction was not perfect. Furthermore, some rural areas in Fukushima have private water-providing systems using natural springs or surface water, and a dose might be ingested from contaminated water. To

ascertain doses to these residents, a survey on water consumption behavior immediately following the accident would be helpful.

7) Concentrations in the unmonitored food category

In this calculation, concentrations were assumed to be 0 Bq/kg for the unmonitored food category. This is probably an underestimation. A total diet study including the market basket method would provide quantitative assessment for the unmonitored food category. However, immediately after the accidental radiation releases, the data was limited. Therefore, we did not discuss this factor quantitatively in this paper.

8) Representativeness of food monitoring for estimation of areas that were most affected

For residents who consumed local food in areas that were most affected, the results are likely to be underestimated significantly, because estimations were calculated based on the assumption that the food comes randomly from everywhere in 16 prefectures, including less contaminated areas, and the data was scarce immediately after the accident in the most contaminated area. Therefore, the results should be interpreted carefully in terms of risk assessment, since the distribution of doses might include a significant underestimation of the doses received by the most exposed people.

9) Contamination of food during storage

Food may be contaminated during storage. Immediately after the accidental radiation releases, many local residents had to accept stored food as evacuees. Precise interviews are necessary to clarify this factor.

4.3. Overestimation factors

The distribution of the dose concentration in food may have been overestimated for several reasons.

1) Sampling bias of radioactivity concentration monitoring of food

As described above, local governments attempted to sample the most contaminated food in each area.

2) Cooking loss

Each sample was measured at 'ready to cook' not 'ready to eat' status as measured in the total diet study.

3) Ingestion dose coefficients

The ICRP ingestion dose coefficients might result in overestimation, because the high iodine content of the Japanese diet may to some extent block the uptake of radioactive iodine by the thyroid gland.

4) Imported food

Imported food was not monitored in this system. The Import Dependency Ratio of food in Japan is 61% (2011, calorie basis). As the food imported from areas outside the 16 prefectures is likely to be less contaminated, the calculated results in this study are probably an overestimation of the doses.

4.4. Other factors possibly caused by uncertainty

1) Seasonal variation of food consumption

The national food consumption survey is based on one-day consumption in November. Seasonal variation of food consumption is not considered in this study. Consumption of food such as spinach is different in spring and fall, and thus seasonal variation of food consumption would cause under- or overestimation depending on the food category.

2) Results reported to be below the level of detection

About one-third of the results (N=596) were reported to be below the level of detection. Among these, only two samples were indicated with the detection level of the measurements as 1.8 and 50 Bq/kg, respectively. Therefore, assumption of the detection level in this study would cause both over- and underestimations. As all measurements were made using a Ge semiconductor detector and this method would likely provide lower detection level of the measurements, the assumption of the detection level might cause overestimation.

3) Sampling period of food concentration

In order to consider a limited number of samples and to take into account the decay of radioactive iodine, a 4-day period has been selected. With a shorter period, uncertainty would be increased because of smaller sample size. With a longer period, the time trend on the sampling number per day and the decay of radionuclides would cause larger uncertainty. To discuss the optimization of sampling period, appropriate modeling should be considered regarding weekly pattern of sampling and other options.

5. Conclusions

The committed equivalent dose to the thyroid and the committed effective dose due to the food ingestion in the first month after the Fukushima nuclear power plant accident in east Japan were evaluated by using a food monitoring data set provided by MHLW. Assuming that food was randomly selected from monitored food, the 90%tile of equivalent dose to the thyroid and the effective dose to the thyroid in 1- to 6-year-old children were estimated to be around 1 mSv and 0.07 mSv, respectively.

Acknowledgement

Funding

References

1) Yamaguchi I. Radioactive concentration of food caused by Fukushima Nuclear Power Plant disaster and new radiological standards for foodstuffs in the existing exposure situation in Japan after a severe nuclear accident. Jpn. J. Health Phys., 47(2), (2012), 144-147.
2) Hamada N, Ogino H. Food safety regulations: what we learned from the Fukushima nuclear accident. J. Environ. Radioact., 111, (2012), 83-99.
3) ICRP. Doses to the embryo and fetus from intakes of radionuclides by the mother. ICRP Publication 88, Ann. ICRP 31(1-3), Pergamon Press (2001).
4) ICRP. Database of dose coefficients: workers and members of the public (1999).

5) Tokonami S, Hosoda M, Akiba S, Sorimachi A, Kashiwakura I, Balonov M. Thyroid doses for evacuees from the Fukushima nuclear accident. Nature (2012) doi:10.1038/srep00507

6) Unno N, Minakami H, Kubo T, Fujimori K, Ishiwata I, Terada H, Saito S, Yamaguchi I, Kunugita N, Nakai A, Yoshimura Y. Effect of the Fukushima nuclear power plant accident on radioiodine ([131] I) content in human breast milk. J. Obstet. Gynaecol. Res. 38(5), (2012), 772-9.

7) MHLW. The Revision of the "Concepts of Inspection Planning and the Establishment and Cancellation of Items and Areas to which Restriction of Distribution and/or Consumption of Foods concerned Applies". (2011)
Available at http://www.mhlw.go.jp/english/topics/2011eq/dl/food-120312.pdf

8) Morita T, Niwa K, Fujimoto K, Kasai H, Yamada H, Nishiutch K, Sakamoto T, Godo W, Taino S, Hayashi Y, Takeno K, Nishigaki T, Fujiwara K, Aratake H, Kamonoshita S, Hashimoto H, Kobayashi T, Otosaka S, Imanaka T. Detection and activity of iodine-131 in brown algae collected in the Japanese coastal areas. Sci. Total Environ. 408(16), (2010), 3443-7.

Summary of Session 1-2

S. TOLMACHEV

Talk by Masahiro HOSODA

Questions/Comments
(1)Bouville A. brought a philosophical problem: mGy *vs* mSv. In 'epidemiological world' it is better to operate with mGy (that defines physical quantity) instead of mSv ('invented' quantity), to eliminate uncertainties associated with use of 'weighting factors'. M. Balonov supported the use of ICRP recommended weighting factors.
(2) Dr. Suzuki recommended to use geometric mean value instead of max for ^{131}I atmospheric concentration for thyroid dose calculation.

Talk by Jun TAKADA

Questions/Comments
Q1 by Osamu Kurihara: How did you define/treat background measurements?
A: Direct measurement of none exposed individuals is a better way to account for the background contribution rather than to use instrumental background (activity measured in the ambient air). Instrumental background does not account for detector's shielding by human body.
Talk by Dr. Suzuki
(Q1) M. Bolonov. What were ambient dose rates?
(A1) Between 0.1 – 0.22 μSv/h
(Q2) A. Bouville. What was calculated chronic intake of ^{131}I?

Talk by Takumaro MOMOSE

Questions/Comments
(Q1) M. Balonov interested in dose reconstruction approaches.
(Q2) A. Bouville. What type of calibration phantom was used for children measurement?
(Q3) A. Bouville. Are any plans to perform follow up study for the same group?

Talk by Ichiro YAMAGUCHI

Questions/Comments
(Q1) M. Balonov. On plots, Cs concentration is that national average or just for a local area (Tohoku pref)
(A1) Average for 17 prefectures.
Dr. Bouville pointed that ingestion route should be used for intake calculations.
Dr. Ban: What was food consumption partent?

General Discussion (Chaired by N. BAN)

M. Balonov pointed that 'most reasonable approach' needs to be taken for dose reconstruction. He shared his knowledge and methodology used after on Chernobyl accident. He stressed on the importance of individual measurements in the initial stage. Individual measurements vs model predictions.

Dr. Momose clarified that acute inhalation scenario was used to avoid under estimation of intake (dose) during early stage. From February 2012 'chronic ingestion' is considered as a main route of intake.

Dr. Momose mentioned that besides external measurements JAEA collected 150 bioassay samples those provide more accurate information on internal radionuclides deposition.

Dr. Solomon pointed out that it is very important to create central database where all result can be collected and QA/QC'ed. Dr. Momose agreed.

However Dr. Ban pointed that Fukushima Pref. doesn't want to open the data collected by Prefecture. Thus, limiting availability of data for the scientific community.

Dr. Osturu pointed that database needs to be validated before opening to the scientific community.

Dr. Solomon strongly agreed with Dr. Otsuru and said that UNSCEAR has to trust data before it is going to use them.

Dr. Nagataka asked: Can we confirm the fact that dose to thyroid was below 50mSv and distribution of KI pills was not necessary?

Session 2

Measurement of Radioactivity in the Environment

Chair   :   T. NAKAMURA
Co-chair   :   M. BALONOV
Rapporteur :   K. THIESSEN

Summary of Atmospheric Measurements and Transport Pathways of Radioactive Materials Released by the Fukushima Daiichi Nuclear Power Plant Accident

Haruo TSURUTA[1], Masayuki TAKIGAWA[2], Teruyuki NAKAJIMA[1]

[1]*Atmosphere and Ocean Research Institute, The University of Tokyo, 5-1-5 Kashiwanoha, Kashiwa, CHIBA, 277-8568, Japan*
[2]*Japan Agency for Marine-Earth Science and Technology, 2-15 Natsushima, Yokosuka, KANAGAWA, 237-0061, Japan*

Abstract

After the Fukushima Daiichi Nuclear Power Plant (FD1NPP) accident, a continual monitoring of atmospheric radionuclides was independently carried out at several stations by different research institutions in the Kanto area south of Fukushima prefecture. No such measurements were made in the Fukushima area. Although the sampling methodology varied from one station to the next, the following results were found by the analysis of these data during March 13-31, 2011. High concentrations of ^{131}I, ^{134}Cs, and ^{137}Cs in the atmosphere were observed in the first period (March 15-16, 2011) and the second period (March 20-23, 2011). According to a numerical simulation by an atmospheric transport model, these radionuclides were directly transported to the stations from the FD1NPP. The ratio of ^{131}I to ^{137}Cs in the atmosphere was around 10 in the first period and on March 20-21, while the ratio in the periods outside the first period and the March 20-21 was around 100. According to the measurements of gaseous ^{131}I (^{131}I$_{(g)}$) and particulate ^{131}I (^{131}I$_{(a)}$) which were performed separately at two stations, at least half of the total ^{131}I (the sum of ^{131}I$_{(g)}$ and ^{131}I$_{(a)}$) sampled was particulate ^{131}I in the first and second periods, although ^{131}I$_{(a)}$ was 20-40% of the total ^{131}I in the periods outside the first and second periods.

Keywords: continuous measurement; atmospheric radionuclides; ^{137}Cs; gaseous and particulate ^{131}I; Kanto area

1. Introduction

A large amount of radioactive materials was released into the atmosphere by the accident at the Tokyo Electric Power Company (TEPCO) Fukushima Daiichi Nuclear Power Plant (FD1NPP), caused by the Tohoku Earthquake and Tsunami on March 11, 2011. These materials were transported over eastern Japan and deposited to the land surface on a regional scale. The continuous analysis of the data of radioactive nuclides measured in the atmosphere is needed, to evaluate the human internal exposure dose, to estimate the release rate of radionuclides into the atmosphere, and to validate the results of numerical simulation of transportation and dry/wet deposition by atmospheric transport models. In the Fukushima area, however, atmospheric data of radioactive nuclides measured after the accident is very limited. Only a sparse dataset in time and space is available from a short sampling of ambient air for 10-40 minutes once or twice per day at more than 10 sites outside the FD1NPP by the Environmental Radioactivity Monitoring Center of Fukushima, the Ministry of Education, Culture, Sports, Science and Technology (MEXT), and inside the FD1NPP by TEPCO. In contrast, radionuclides in the atmosphere have been continuously measured since the FD1NPP accident and have already been reported by several institutions/universities in the Kanto area south of Fukushima prefecture. To date, however, no study has been made to compare all the results with each other. The purpose of this paper is to discuss the dynamical behavior of radioactive materials on a regional scale for improving our understanding on the spatio-temporal distribution of the radioactive concentration of ^{131}I, ^{134}Cs and ^{137}Cs in the Fukushima and adjacent areas in the future.

2. Dataset for analysis

In the Kanto area, seven institutions independently measured radionuclides in the atmosphere after the accident, and their results and/or datasets have already been reported [1-9]. The sampling sites are shown in Figure 1, and the institutions and their methods for measuring radionuclides such as gaseous/particulate ^{131}I are listed in Table 1. Sampling equipment was divided into three groups: low-volume air samplers, high-volume air samplers, and the equipment specific to Comprehensive Nuclear Test Ban Treaty Organization (CTBTO) stations. At the Tokai-mura, Chiba, and Tsukuba stations, particulate and gaseous ^{131}I was separately collected on a series of two filters, while radionuclides at Chiba were not measured separately, but simultaneously measured as one set for two filters, for quick measurement of many samples. The filters used varied among stations. Sampling duration at the seven institutions covered a range from a half hour to two days. It was much shorter at Setagaya than at the other stations, where it was usually one-day sampling. Data quality was carefully checked, because each measurement was independently conducted following the institution's own methodology. At Setagaya station (TMITRI), the detection limit for ^{137}Cs was much higher than at the other stations, because the data had to be sent to the related administrative office so quickly that the measurement time was usually 1000 seconds for the filters with a sampling duration of 1-3 hours [5]. The measurement of radionuclides with a Ge semiconductor detector at Tajima in Kawasaki City was made about one or two months after the sampling time. In this paper, the data measured at Takasaki, a CTBTO site, was not used because of contamination of the sampling/measurement system [3].
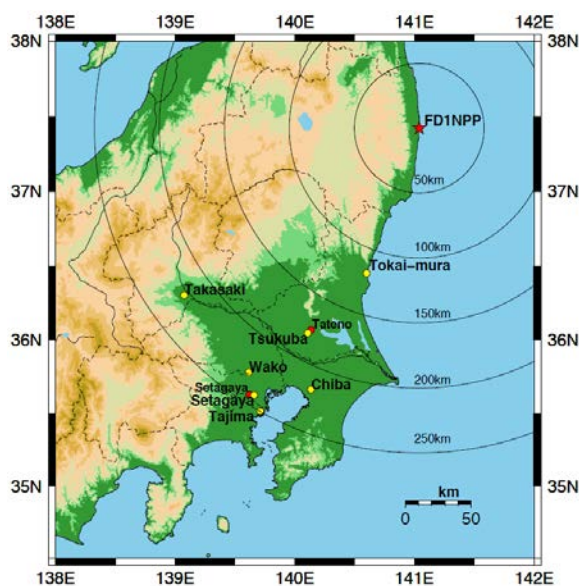
Figure 1. Seven sites of atmospheric measurement of radionuclides and an AMeDAS station of Tateno and Setagaya in the Kanto area

Radiation dose rates [1, 4, 7, 10] measured at or near six of the seven stations (Table 1) were used in our analysis. Meteorological data such as precipitation measured at the Automated Meteorological Data Acquisition System (AMeDAS) station of Tateno and Setagaya (by the Japan Meteorological Agency (JMA)), located 1 km northeast of the Tsukuba station and 4 km west of the Setagaya station, respectively, was also used for analysis. A numerical simulation of radioactive materials in the atmosphere was made by using an atmospheric transport model for radionuclides based on the regional chemical transport model of WRF/Chem [11]. The model domain covers the east side of Honshu Island in Japan, and the horizontal resolution is 3 km (250 x 250 grids). The initial and lateral boundary for the meteorological field is taken from the mesoscale model datasets constructed by the JMA. Two radionuclides (^{137}Cs and ^{131}I) are taken into account in the model, and the release rates of them are based on the estimation of JAEA [12]. The WRF/Chem is an online

model, and the transport and deposition processes are calculated using the meteorological fields such as wind fields and precipitation calculated at every model time step (10 seconds) in the model.

Table 1 Measurements of atmospheric radionuclides at 7 stations in the Kanto area

No.	Sampling station (Sampling/Measurement Org.)	Sampling equipment (Filters)	^{131}I for aerosols (A) & gases (G)	Sampling duration (hours or days)	Ref.
1	Tokai-mura (Ibaraki pref.) (JAEA-TRDC)	L.V. (HE-40T & CHC-50)	A & G (separated)	3-12h	Furuta et al. (2011)[1]
2	Tsukuba (Ibaraki pref.) (NIES/KEK)	H.V. (QF & ACF-KF1700)	A & G (separated)	3h-2d	Masumoto et al. (2011)[2] Data:Web of KEK
3	Takasaki (Gunma pref.) (CTBTO)	RASA (PP-filter)	A	1d	Yonezawa and Yamamoto (2011)[3] Data: Web of CTBTO
4	Wako (Saitama pref.) (RIKEN)	L.V. (HE-40T)	A	0.5h-1d	Haba et al. (2012)[4]
5	Setagaya (Tokyo M.) (TMITRI)	H.V. (GB100R)	A	1-8h	Nagakawa et al. (2011)[5] Data: TMITRI (2012)[6]
6	Chiba (Chiba pref.) (JCAC)	L.V. (HE-40T & CP-20)	A + G (total)	1d	Amano et al. (2012)[7] Nagaoka et al. (2012)[8]
7	Tajima (Kawasaki City) (KMRIEP & AORI (Univ. of Tokyo)/Osaka Univ.)	H.V. (QF)	A	1d	Kawasaki City (2012)[9] Data: Web of JpGU

JAEA-TRDC : Japan Atomic Energy Agency, Tokai Research and Development Center. NIES: National Institute for Environmental Studies. KEK: High Energy Accelerator Research Organization. CTBTO: Comprehensive Nuclear Test Ban Treaty Organization. RIKEN: RIKEN Wako Institute. JCAC: Japan Chemical Analysis Center. TMITRI: Tokyo Metropolitan Industrial Technology Research Institute. KMRIEP: Kawasaki Municipal Research Institute for Environmental Protection. AORI: Atmosphere and Ocean Research Institute. JpGU: Japan Geoscience Union. L. V.: Low-volume air sampler. H. V.: High-volume air sampler. QF: Quartz fiber. ACF: Activated carbon fiber

3. Results and discussion

3.1. Time series and transport pathways of radionuclides in the atmosphere

Time series of the atmospheric concentrations of ^{131}I and ^{137}Cs, and of the hourly radiation dose rate and precipitation at Tokai-mura, Tsukuba, Wako, Setagaya, Tajima, and Chiba are shown in Figures 2a and 2b (1)-(6). At most stations, high levels of radionuclides of ^{131}I, ^{134}Cs, and ^{137}Cs in the atmosphere were measured in the first period, March 15-16, and the second period, March 20-23, 2011. Only the data of ^{131}I and ^{137}Cs are shown in the figures, because the atmospheric concentration of ^{134}Cs was almost equal to that of ^{137}Cs. Although a part of the data provided in this paper has already been investigated in the previous paper [13], further analyses were made as described below.

3.1.1. Peak time of radiation dose rate

The peak time of hourly radiation doses is shown in Table 2. Since the sampling duration of continuous measurement was mostly longer than one hour, except for that at Setagaya, the peak time of radionuclides could not be exactly identified from the data for continuous measurement. In the first period when no rain was observed in the Kanto area, every peak was so short and clear that the data can be interpreted as being due to a plume release travelling southwards and impacting the various stations in an appropriate time sequence, because the wind direction shifted clockwise.

In contrast, during the second period, March 21-23, when most of the Kanto area was experiencing rain, the hourly radiation dose rate slowly increased from the beginning of rain around 08:00 on the morning of March 21, when the polluted air masses were transported to the Kanto area. As a result, a portion of the radionuclides was deposited on the land surfaces by rain, and the peak of the radiation dose rate was not sharp, due to the influence of surface radioactive contamination on the dose rate. We will discuss the behavior of the radionuclides in the next section, mainly focusing on peaks No.2, No.8 and No.10 (Table 2).
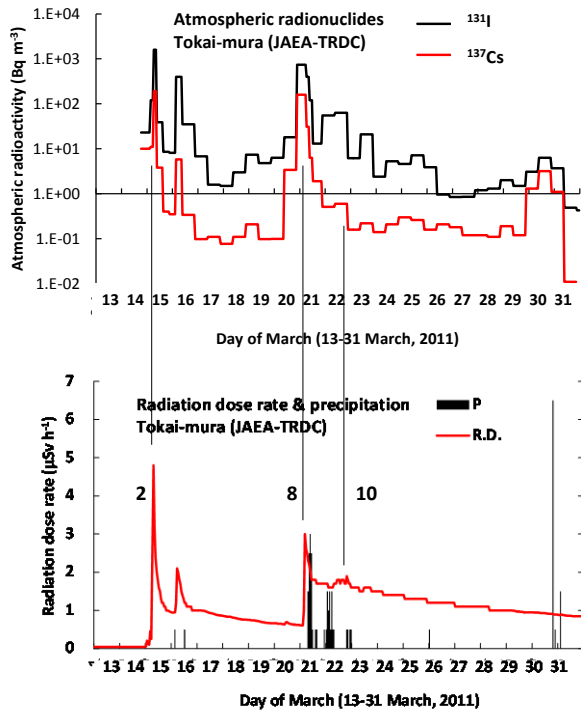
(1) Tokai-mura (JAEA-TRDC)
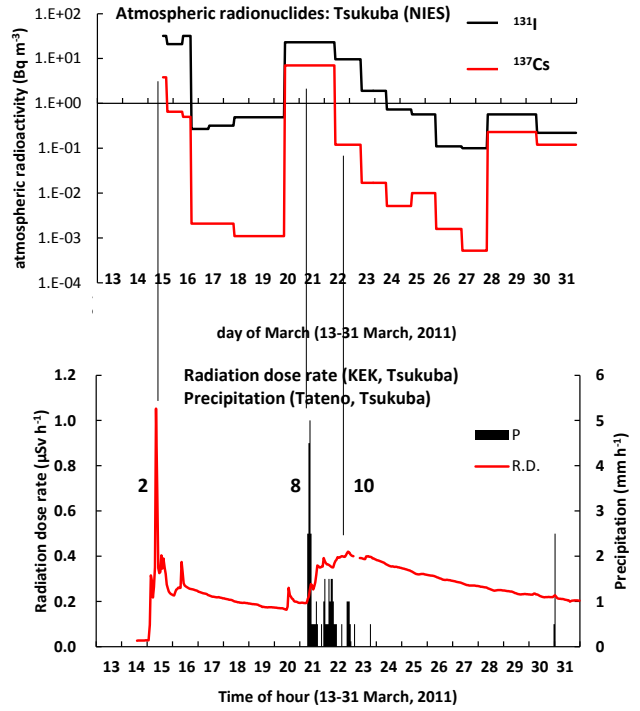
(2) Tsukuba (NIES)
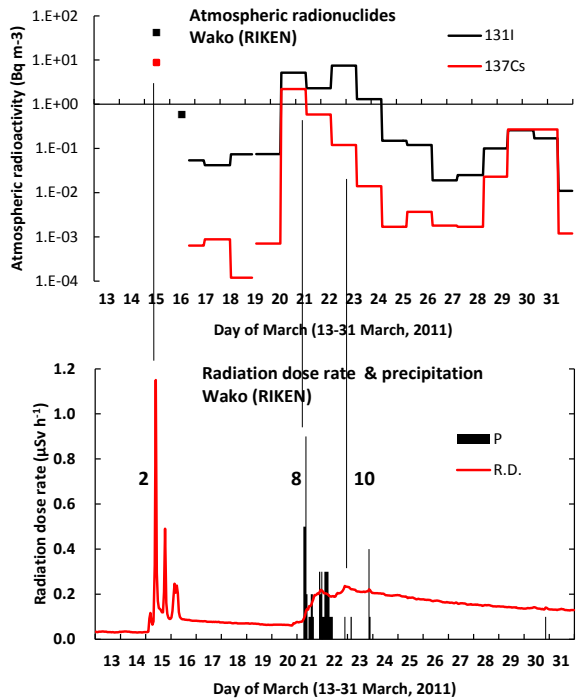
(3) Wako (RIKEN)
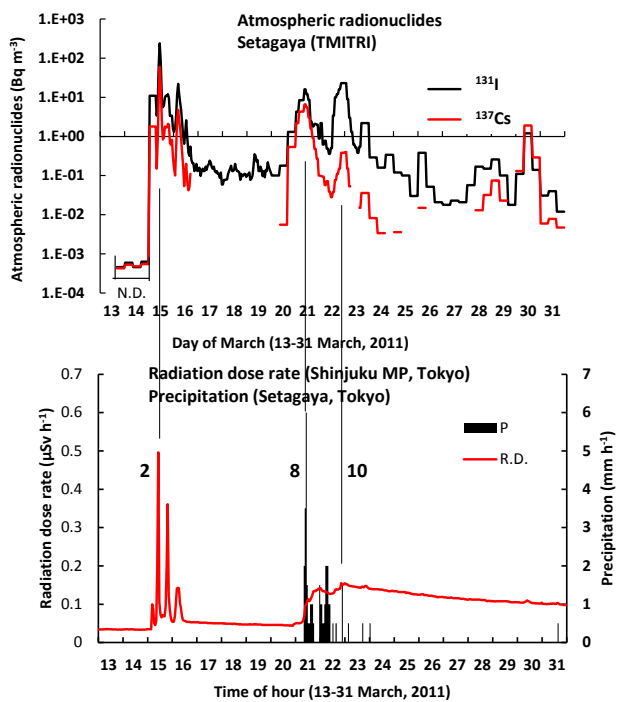
(4) Setagaya (TMITRI)

Figure 2a. Time series of air concentration of ^{131}I and ^{137}Cs (upper half) and radiation dose rate (R.D.) and precipitation (P) (lower half) at different stations: (1) Tokai-mura, (2) Tsukuba, (3) Wako, and (4) Setagaya. The numbers in the figure are the peak numbers in Table 2 (March 13-31, 2011).
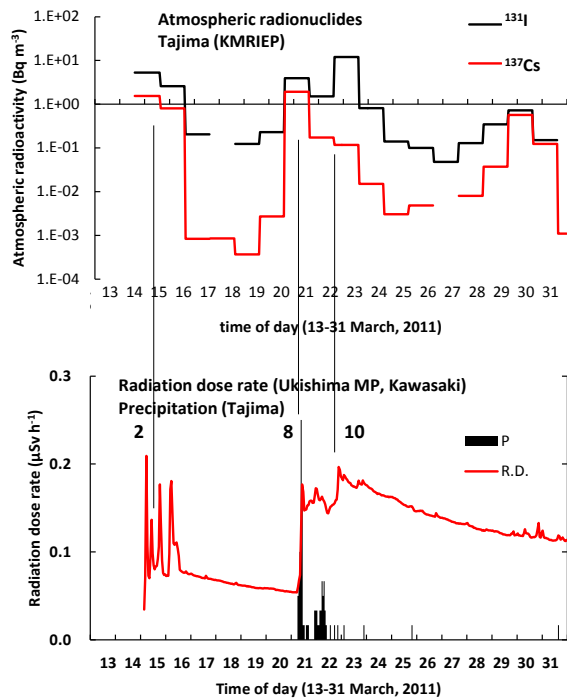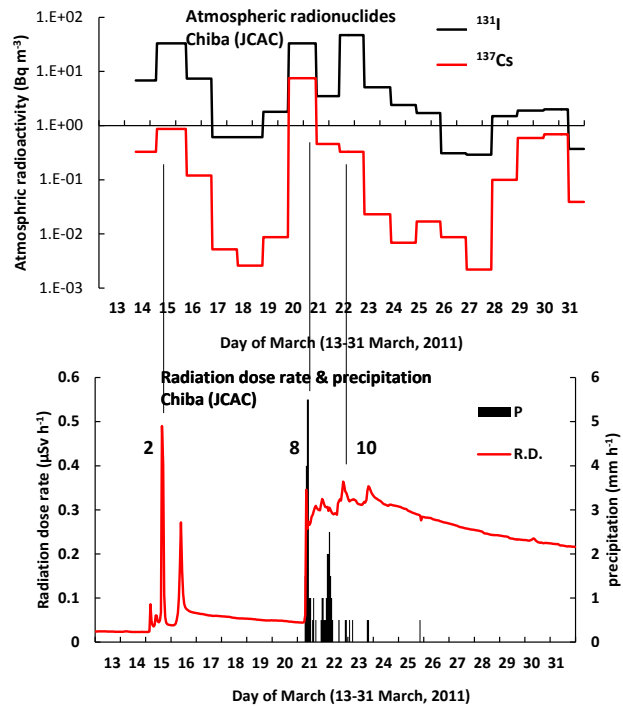
(5) Tajima (KMRIEP)   *(6) Chiba (JCAC)*

Figure 2b. The same as Figure 2a, but at (5) Tajima and (6) Chiba (March 13-31, 2011).

Table 2 Peak time of radiation dose rate at or near each station (March 15-23, 2011)

Station or	Day of March, 2011											Ref.
(Monitoring Post)	15	15	15	15	16	16	20	21	21	22	23	
Tokai-mura	1-2, 4-5	7-8***				5-7	11-12	4-5		19-20		1), #
Tsukuba	3-4*	8-9***	13-16			8-9	13-14	7-8	22-23	21-22		10)
Wako	4-5**	9-10***		18-19	3-6			5-6	22-24	21-22	20-21	4)
Tokyo (Shinjuku)	4-5	10-11***		19-20	4-6			7-8	22-01	20-21	20-21	##
Chiba	4-5	9-11	15-16+***			9-10		8-9	23-24	19-20	19-20	7)
Kawasaki (Ukishima)	5-6***	10-11		18-19	5-6			10-11	23-24	21-22	16-17,20-21	###
Peak No.	1	2	3	4	5	6	7	8	9	10	11	

*3-4 means the hour from 03:00 to 04:00. ** 4-5 means the lowest peak was during the hour from 04:00 to 05:00 at the station/monitoring post (MP) on March 15-16.

***5-6 means the highest peak was during the hour from 5:00 to 6:00 at the station/MP on March 15-16.

15-16+: The major radionuclide was ^{133}Xe [8].

The data measured at MP2 was used, because it was the most closely located MP to the dust sampling site among 8 MPs at the Tokai-mura station.

Shinjuku in Tokyo M.: An MP run by MEXT, 10 km north of Setagaya station (TMITRI).

Ukishima in Kawasaki City: An MP of Kanagawa pref., 5 km east of Tajima station (KMRIEP).

3.1.2. The first period (March 15-16, 2011)

In the first period, the highest ^{131}I concentration of 1,600 Bq m^{-3} was measured at Tokai-mura during sampling from 06:00 to 09:00 (JST) on March 15, including peak No. 2 in Table 2. At Setagaya, a high ^{131}I peak of 240 Bq m^{-3} was also measured in a sampling from 10:00 to 11:00 (JST). Figure 3 shows a regional map of the atmospheric concentration of ^{131}I at 04:00 and 10:00 (JST) on March 15, simulated by the WRF/Chem [11]. The model well simulated the transport pathway of atmospheric radionuclides for peak No.2, that the radioactive materials released from the FD1NPP at 02:00 to 03:00 on March 15 were transported southwards through Tokai-mura (point B in Figure 3) between 06:00 and 07:00 as a plume carried by northeasterly wind, and then to Setagaya (point G), arriving between 09:00 and 10:00. The atmospheric concentrations of ^{131}I simulated by the model, however, were underestimated compared with those observed at

Tokai-mura. This discrepancy between the observation and the model may have been caused by the insufficient reproduction of meteorological fields in the model, and, an uncertainty of the release rates [12, 14, 15] of radionuclides from the FD1NPP. The second ^{131}I peak of 400 Bq m[-3] at Tokai-mura was measured during sampling from 03:00 to 09:00 on March 16, while at Setagaya, the second ^{131}I peak of only 22 Bq m[-3] was found during sampling from 04:00 to 05:00 on March 16. This peak at Setagaya corresponded to peak No. 5 in Table 2 which was also detected at Wako and Kawasaki. Considering the peak time (05:00-07:00 on March 16) of the radiation dose rate at Tokai-mura, and the long distance from Tokai-mura to Setagaya, these two peaks were possibly caused by different polluted air masses. According to the model result, the high radionuclides in the second peak at Tokai-mura were directly transported from the FD1NPP southwards along the east coast of the Kanto area by the northerly wind. In contrast, at Setagaya, the second ^{131}I peak was possibly caused by the aged radionuclides, which were directly transported from the FD1NPP in the morning of March 15, moved northwards by the southerly wind in the afternoon, and returned again from the north by the northerly wind in the early morning of March 16.
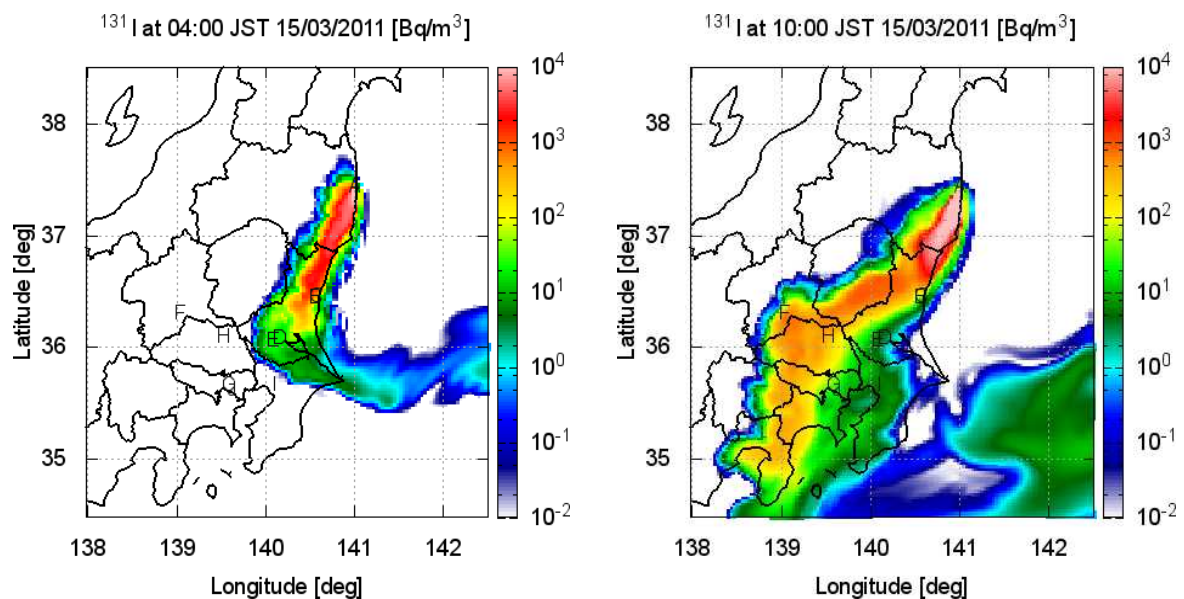
Figure 3. Contour map of the atmospheric concentration of ^{131}I near the surface. Results of a numerical simulation by using WRF/Chem [11]. (Reft) 04:00 and (right) 10:00 (JST) on March 15, 2011. B: Tokai-mura, D: Tsukuba, G: Setagaya, I: Chiba.

3.1.3. The second period (March 20-23, 2011)

In the second period, all the stations had a peak of ^{131}I and ^{137}Cs on March 21-22, which corresponds to peaks No. 8 and No. 10 in Table 2, respectively. The highest ^{131}I peak of 740 Bq m[-3] was measured at Tokai-mura in the sampling period from 21:00 (March 20) to 06:00 (March 21), while further downwind, such as at Setagaya in Tokyo, only a small ^{131}I peak of 16 Bq m[-3] was found between 08:00 and 10:00. Figure 4 shows a regional map of the atmospheric ^{131}I concentration at 08:00 and 12:00 of March 21, simulated by the model [11]. In this case, the transport pathway of radioactive materials from the FD1NPP to Tokai-mura was similar to that on 15 March, but the peak time was a few hours later than in the field measurement.

At Setagaya, however, a slightly higher ^{131}I concentration of 23 Bq m[-3] was measured in the period from 20:00 (March 22) to 02:00 (March 23) compared to that on March 21, while the ^{137}Cs concentration was much lower than that on March 21. This large difference in the concentrations of ^{131}I and ^{137}Cs between peaks No. 8 and 10 was found at all the stations, as shown in Figures 2a and 2b. This possibly reflects the difference in the release rate of ^{131}I and ^{137}Cs from the FD1NPP, although there is no reliable information about exactly what happened in the reactor units of the FD1NPP on those days.

3.1.4. The other periods (17-19 March and 24-27 March 2011)

In the periods (March 17-19 and March 24-27) outside of the first and second periods, however, surface wind in the Kanto area came from the northwest by winter monsoon, or from the south, and radioactive materials were not transported directly to the area from the continued release by the FD1NPP. The concentration of ^{131}I right after the second period (March 24-25) was still high, and gradually decreased, compared with that right after the first period (March 17-19). Possible reasons for this difference in the ^{131}I concentration between the two periods have not been clarified yet.
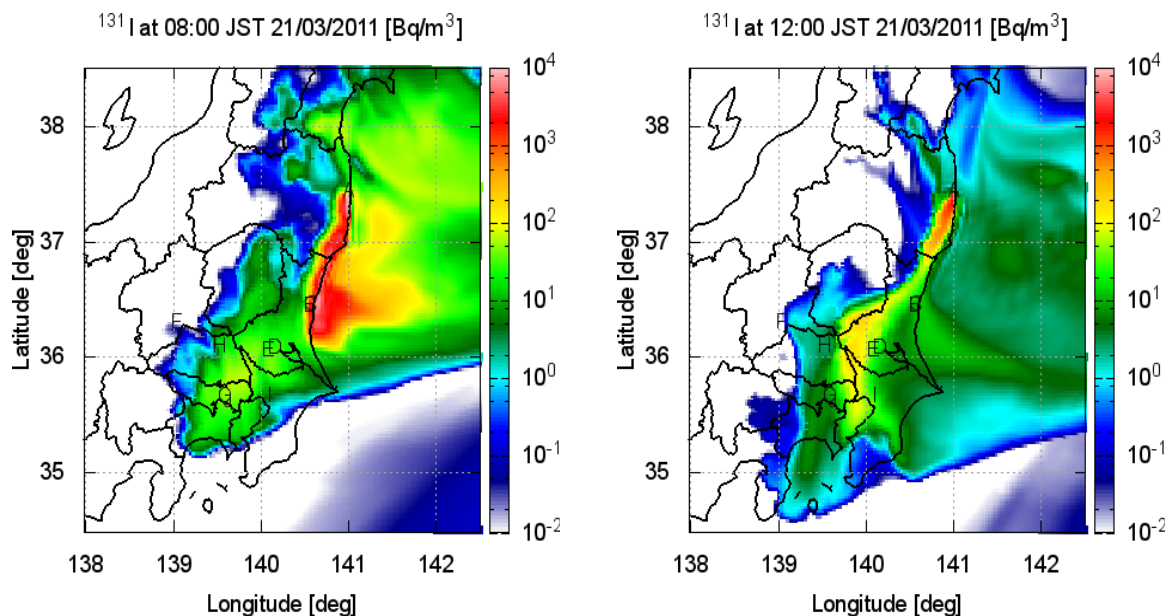
Figure 4. Contour map of the atmospheric concentration of ^{131}I near the surface. Results of a numerical simulation made using WRF/Chem[11]. (Left) 08:00 and (right) 12:00 (JST) on March 21, 2011.
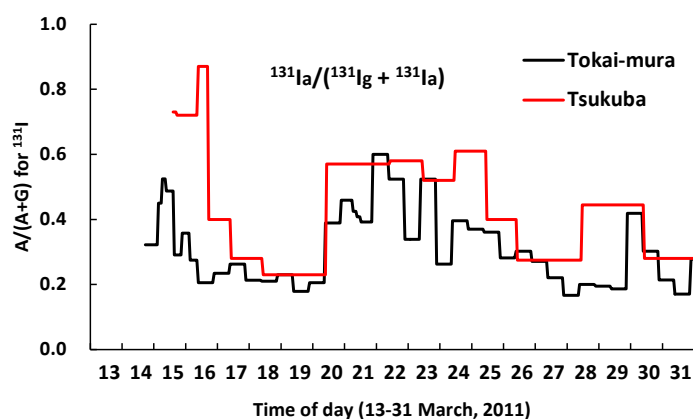
Figure 5. Time series of the ratio of ^{131}I(a) in aerosols to the total ^{131}I ($=^{131}$I(a)$+^{131}$I(g)) measured at Tokai-mura and Tsukuba (March 13-31, 2011). The value for Tsukuba was calculated from data published previously[2].

3.2. Ratio of ^{131}I in aerosols to the sum of ^{131}I in aerosols and gases

At Tokai-mura and Tsukuba, where ^{131}I was separately measured in aerosols (^{131}I(a)) and gas phase (^{131}I(g)), the time series of the ratio of ^{131}I(a) to the sum of ^{131}I(a) and ^{131}I(g) was similar between these two stations, as shown in Figure 5. This ratio was higher at Tsukuba than at

Tokai-mura, for the most part, which may have occurred because of the use of a filter without loading of Triethylenediamine (TEDA) at Tsukuba, while a filter with TEDA was used at Tokai-mura and Chiba to increase the collection efficiency of gaseous ^{131}I [16]. The ratio was higher (0.5-0.8) in the first and second periods at both of Tokai-mura and Tsukuba stations when compared to 0.2-0.4 in the other periods, while the filters used in the sampling were different as shown in Table 1, and these two stations are located at a long distance (65 km) with each other. In early May 2011, the atmospheric concentration of ^{131}I$_{(a)}$ and ^{131}I$_{(g)}$ was measured with the filters of quartz fiber and activated carbon fiber (Type-K, Toyobo Co., Ltd.) with loading of TEDA, by a high-volume air sampler at Kashiwa, 20 km southwest of the NIES in Tsukuba. An average range of the ratio was 0.1-0.3 [17], almost equal to that measured in the Kanto area in the periods of March 2011 outside of the first and second periods.

After the Chernobyl accident in 1986, the atmospheric radionuclides of ^{131}I$_{(a)}$ and ^{131}I$_{(g)}$ were measured in Europe [16]. The highest ratio of ^{131}I$_{(a)}$ to the sum of ^{131}I$_{(a)}$ and ^{131}I$_{(g)}$ was 0.4, which was measured in Germany four days after the accident and before rain, and the other instances of the ratio ranged from 0.06 to 0.25, measured later in Germany, Sweden, and Finland. The ratios measured in Kanto and Europe strongly suggest that at least half of the ^{131}I radionuclide released into the atmosphere could exist as aerosols within a few days just after the accident in case of no rain, compared with that in gas phase. Since there is an uncertainty of the collection efficiency of ^{131}I in submicron aerosols and gaseous ^{131}I due to the filters used at Tsukuba and Tokai-mura, and no data has been available to indicate the size distribution of radionuclides just after the accident, further research is needed to understand the possible mechanism for the difference in the ratio of ^{131}I$_{(a)}$ to the sum of ^{131}I$_{(a)}$ and ^{131}I$_{(g)}$.

3.3. Radioactivity ratio of ^{131}I to ^{137}Cs in the atmosphere

The atmospheric concentration of ^{131}I was always higher than that of ^{137}Cs, except for a few of the measurements recorded on March 29 at Wako and Setagaya, and most of the ratio of ^{131}I to ^{137}Cs was much higher than 1, as shown in Figure 6. The ratio was around 10 in the polluted air rich in both ^{131}I and ^{137}Cs on March 15 and March 20-21. According to a calculated core inventory [18] made by using ORIGEN code, the ratio of ^{131}I/^{137}Cs was 7-10 in the containment drywell with no water and high temperature among four reactor units of the FD1NPP on the day of the accident, March 11, 2011. The ratios at the measurement stations on March 15 and March 20-21 are nearly equal to the inventory data, and which suggests that the radioactive nuclides were possibly released into the atmosphere in dry conditions. If the radionuclides would be released from the pressure suppression chamber partly filled with water, the ratio would be changed due to the removal of particulates such as ^{137}Cs through the water. In contrast, the ratio was around 100 in polluted air rich in only ^{131}I on March 22-23, and on the other days (March 24-27) when both ^{131}I and ^{137}Cs were very low. Possible reasons for the difference in the concentration of ^{131}I and ^{137}Cs between the two periods have still remained unknown.
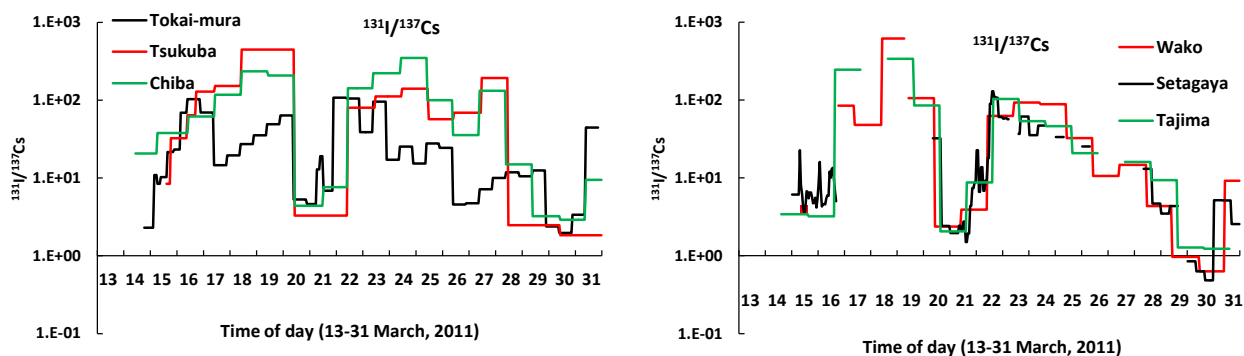
Figure 6. Time series of the ratio of ^{131}I to ^{137}Cs in the atmosphere at Tokai-mura, Tsukuba, and Chiba (left) and at Wako, Setagaya, and Tajima (right) (March 13-31, 2011).

As shown Figure 6, time series of the ratio at three stations (Wako, Setagaya, and Tajima) almost matched one another, while they showed large variation during March 17-19 because the ^{137}Cs concentrations were very low and near the detection limit. In addition, the ratio at these three stations on March 15 and March 20 was lower than that at Tokai-mura, because only ^{131}I(a) was measured, while the sum of ^{131}I(a) and ^{131}I(g) was measured at Tokai-mura. Supposing that the ratio of ^{131}I(a) to the sum of ^{131}I(a) and ^{131}I(g) is 0.5, then the ratio of the sum of ^{131}I to ^{137}Cs at Setagaya at 10:00-11:00 on March 15 was 8.0, almost equal to the ratio of 8.4 at Tokai-mura at 06:00-09:00 on March 15. This suggests that the high level of atmospheric radionuclides measured at Setagaya on March 15 were in the same air masses as those previously transported through Tokai-mura from the FD1NPP. Therefore, it should be carefully checked whether both ^{131}I(a) and ^{131}I(g) were measured, before making a quantitative comparison of ^{131}I results among the stations.

Day-to-day variations in the ratio were very similar among five stations except the Tokai-mura station where some contamination of the measurement system may have influenced the ^{137}Cs concentration, compared with the spatial variation of the radionuclides, as shown in Figure 6. This could be attributed to the large day-to-day difference in the release rate of radioactive materials into the atmosphere [12, 14, 15], and to the likelihood that the polluted air masses released from the FD1NPP on the early morning of March 15 and March 21 were transported to almost all of the stations on the same day. A new approach to the reconstruction of the release rate of radionuclides is needed, in which all of the data such as pressure, temperature, and radiation dose rate in the reactor units of the FD1NPP are analyzed.

4. Conclusions

Analyzing the continuous data of atmospheric ^{131}I and ^{137}Cs measured at six stations in the Kanto area during March 13-31, 2011, after the accident at FD1NPP, led to the new findings summarized as follows:

(1) High concentrations of ^{131}I and ^{137}Cs in the atmosphere were observed at all the stations during March 15-16, 2011 (the first period) and March 20-23, 2011 (the second period).
(2) A numerical simulation by an atmospheric transport model showed that the polluted air masses with high levels of radionuclides ^{131}I and ^{137}Cs were directly transported to the Kanto area from the FD1NPP by northeasterly wind during the first and second periods.
(3) According to two stations where ^{131}I was separately measured as gases (^{131}I(g)) and aerosols (^{131}I(a)), the ratio of ^{131}I(a) to the sum of ^{131}I(a) and ^{131}I(g) was 0.5-0.8 in the first and second periods, which was much higher than the ratio of 0.2-0.4 in the other periods. This strongly indicates that at least half of ^{131}I could exist as aerosols within a few days after radioactive materials were released into the atmosphere. It is still unknown whether ^{131}I was directly released as aerosols or ^{131}I(a) was produced in the atmosphere.
(4) Regarding the ratio of ^{131}I to ^{137}Cs, day-to-day variation was much larger than the spatial variation among the six stations. The ratio was around 10 in the first period and during March 20-21 in the second period. The ratio was nearly equal to the ratio in the reactor units of the FD1NPP on the day of the accident, according to the core inventory analysis, and it could directly reflect the condition in the reactor units. In contrast, the ratio was around 100 during March 22-23 and in the other periods (March 17-19 and March 24-27) where the level of ^{137}Cs was very low.

Studying these results in detail may clarify what happened in the reactor units and also allow us to estimate more reliable amounts of the radionuclides released from each reactor unit, in combination with an analysis of all the data available for the reactor units such as pressure, temperature, and radiation dose rates for this purpose.

Acknowledgement

References

1) Furuta, S., Sumiya, S., Watanabe, H., Nakano, M., Imaizumi, K., Takeyasu, M., Nakada, A., Fujita, H., Mizutani, T., Morisawa, M., Kokubun, Y., Kona, T., Nagaoka, M., Yokoyama, H., Hokama, T., Isozaki, T., Nemoto, M., Hiyama, Y., Onuma, T., Kato, C., and Kurachi, T. Results of the environmental radiation monitoring following the accident at the Fukushima Daiichi Nuclear Power Plant-Interim report (Ambient radiation dose rate, radioactivity concentration in the air and radioactivity concentration in the fallout), JAEA Review, 2011-035, (2011). (in Japanese with English abstract)

2) Masumoto, K., Toyoda A., Doi, T., Tanaka, A., Ban, S., Hirayama, H., and Shibata, Y. Radionuclides in aerosol samples collected at Tsukuba, Ibaraki prefecture after the accident in Fukushima Daiichi nuclear power plant, International Congress for Analytical Sciences 2011 (ICAS2011), Kyoto, 23-24 May 2011.

3) Yonezawa, C., and Yamamoto, Y. Measurement of atmospheric radionuclides in the CTBT network, Bunseki, 8, (2011), 451-458. (in Japanese)

4) Haba, H., Kanaya, J., Mukai, H., Kambara, T., and Kase, M. One-year monitoring of airborne radionuclides in Wako, Japan, after the Fukushima Dai-ichi nuclear power plant accident in 2011. Geochemical Journal, 46, (2012), 271-278.

5) Nagakawa, Y., Suzuki, T., Kinjo, Y., Miyazaki, N., Sekiguchi, M., Sakurai, N., and Ise, H. (2011) Measurement of the ambient radioactivity and estimation of human radiation exposure dose in Tokyo with regard to the radioactive substance leakage due to the Fukushima Daiichi Nuclear Power Plant accident, RADIOISOTOPES, 60, (2011), 467-472. (in Japanese with English abstract)

6) Tokyo Metropolitan Industrial Technology Research Institute (TMITRI), Research report of radioactive materials in the atmospheric dust released by the Fukushima Daiichi Nuclear Power Plant accident, TMITRI, (2012). (in Japanese)

7) Amano, H., Akiyama, M., Chunlei, B., Kawamura, T., Kishimoto, T., Kuroda, T., Muroi, T., Odaira, T., Ohta, Y., Takeda, K., Watanabe, Y., and Takao, M. Radiation measurements in the Chiba metropolitan area and radiological aspects of fallout from the Fukushima Dai-ichi Nuclear Power Plants accident. J. Environ. Radioact., 111, (2011),42-52.

8) Nagaoka, K., Sato, S., Araki, S., Ohta, Y., and Ikeuchi, Y. Changes of radionuclides in the environment in Chiba, Japan, after the Fukushima Nuclear Power Plant accident, Health Physics, 102, (2012), 437-442.

9) Safety Measure Council for Nuclear Power Facility in Kawasaki City. Report of environmental radioactivity survey in Kawasaki City, 50, (2012), 16-18. (in Japanese)

10) Sanami, T., Sasaki, S., Iijima, K., Kishimoto, Y., and Saito, K. Time variations in dose rate and g spectrum measured at Tsukuba City, Ibaraki, due to the accident of Fukushima Daiichi Nuclear Power Station, Transactions of the Atomic Energy Society of Japan, 10, (2011), 163-169. (in Japanese with English abstract)

11) Takigawa, M. Estimation of transport and deposition of Caesium from the Fukushima accident by using a regional atmospheric transport model. Proceedings of 92nd American Meteorological Society, New Orleans, US., 21-26 January 2012.

12) Katata, G., Ota, M., Terada, H., Chino, M., and Nagai, H. Atmospheric discharge and dispersion of radionuclides during the Fukushima Dai-ichi Nuclear Power Plant accident: Part I: Source term estimation and localscale atmospheric dispersion in early phase of the accident. Journal of Environmental Radioactivity, 109, (2012), 103-113.

13) Tsuruta, H., and Nakajima, T. Radioactive materials in the atmosphere released by the accident of the Fukushima Daiichi Nuclear Power Plant, Chikyukagaku (Geochemistry), 46, (2011), 99-111. (in Japanese with English abstract)

14) Chino, M., Nakayama, H., Nagai, H., Terada, H., Katata, G., and Yamazawa, H. Preliminary estimation of release amounts of ^{131}I and ^{137}Cs accidentally discharged from the Fukushima Daiichi nuclear power plant into the atmosphere. Journal of Nuclear Science and Technology, 48, (2011), 1129-1134.

15) Terada, H., Katata, G., Chino, M., Nagai, H. (2012) Atmospheric discharge and dispersion of radionuclides during the Fukushima Daiichi Nuclear Power Plant accident. Part II: Verification of the source term and regional-scale atmospheric dispersion. J. Environ. Radioact., 112, (2012), 141-154.

16) Ministry of Education, Culture, and Sports. A technical report on monitoring of radioactive materials in the atmosphere, Japan Chemical Analysis Center, (2003), 67-70. (in Japanese)

17) Tsuruta, H., and Higaki., S. Unpublished data.

18) Nishihira, K., Yamagishi, I., Yasuda, K., Ishimori, K., Tanaka, K., Kuno, T., Inada, S., and Gotoh, Y. Radionuclide release to stagnant water in Fukushima-1 Nuclear Power Plant, Transactions of the Atomic Energy Society of Japan, 12, (2012), 13-19, doi:10.3327/taesj. J11.040 (in Japanese with English abstract).

Radiation and Radioactivity Monitoring in the Surrounding Environment after the Fukushima Daiichi Nuclear Power Plant Accident
- Overview -

Takashi NAKAMURA

Professor Emeritus of Tohoku University
Shimo-Shakujii 6-43-5, Nerima-ku, TOKYO, 177-0042, Japan

Abstract

After the explosion of the Fukushima Daiichi nuclear power plants on March 14, radiation surveys were conducted by airplane by the US DOE (Department of Energy) and MEXT of Japan (Ministry of Education, Culture, Science, Sports and Technology) within an approximately 100 km radius of the power plant. At the end of May, MEXT formed a committee on radiation and radioactivity mapping in this area, the behavior of radioactive materials in the forest and their transfer to the river. Twice from June to July, the radio-activities of soils were measured at more than 2000 points spaced at 2 km intervals at a radius of 80 km and at 10 km intervals at a radius of from 80 to 100 km from the power plant, and the radiation levels at those points were monitored by about 90 organizations. The same groups have also been conducting road-based surveys by car. The results of these investigations indicated that the explosion of the power plants on March 15 to 16 emitted large amounts of numerous radioisotopes, including I-131, Te-132, Cs-134 and Cs-137, into the atmosphere. Volatile iodine isotopes were predominant, of which activities were approximately 100 times larger than cesium isotopes, were predominant in more of the total activity of emitted radioisotopes than cesium isotopes, but two months after the accident, cesium isotopes have become dominant. Activities of Sr-89 and Sr-90 were about 1/1000 to cesium isotopes due to higher melting and boiling points than cesium isotopes. Several research groups have continued to monitor the behavior of these isotopes in the forest and their transfer into the rivers and wells. Monitoring of the time-sequential variation of these deposited radioisotopes will continue.

Keywords: Environmental monitoring;Fukushima Daiichi NPP accident; radiation mapping; radioactivity mapping; migration

1. Introduction

After the explosion of the Fukushima Dai-ichi nuclear power plants on March 14, 2011, radiation surveys were conducted by airplane by the US DOE (Department of Energy) and MEXT of Japan (Ministry of Education, Culture, Science, Sports and Technology) within an approximately 100 km radius of the power plant. The Tokyo Electric Power Company (TEPCO) is also monitoring the radiation levels around the power plant up to a radius of 20 km with the help of other power companies and institutes, and the Fukushima local government continues to monitor radiation levels at more than 2000 points. At the end of May, MEXT formed a committee to investigate radiation and radioactivity mapping in this area, as well as the behavior of radioactive materials in the forest and their transfer to the river. Twice from June to July, the radio-activities of soils were measured at more than 2000 points spaced at 2 km intervals at a radius of 80 km and at 10 km intervals at a radius of from 80 to 100 km from the power plant, and the radiation levels at those points were monitored by about 90 organizations. The same groups have also been conducting road-based surveys by car. The radio-activities of soils and dusts have been measured at various points by several organizations working in tandem with MAFF of Japan (Ministry of Agriculture, Forestry and Fisheries).

The Nuclear and Industrial Safety Agency (NISA) and Nuclear Safety Commission (NSC) announced that the total amounts of radioactive materials discharged into the atmosphere were 1.5 to 1.6×10^{17} Bq of ^{131}I and 1.2 to 1.5×10^{16} Bq of ^{137}Cs. These amounts are roughly 1/10 of radioactive materials emitted at the Chernobyl accident. They also announced that highly contaminated water with a radiation level of over 1000 mSv/h was discovered flowing into the seawater and the total amount of radioactive materials discharged in this manner was estimated to be 4.7×10^{15} Bq; and that low-level contaminated water was discharged into the seawater from April 4 to 10 in order to secure storage capacity for contaminated water and the total amount of radioactive materials discharged in this manner was estimated to be 1.5×10^{11} Bq.

Several research groups have continued to monitor the behavior of these isotopes in the forest and their transfer into rivers and wells. Comprehensive and long-term monitoring of the time-sequential variation of these deposited radioisotopes is being conducted by many institutes and universities in conjunction with the JAEA (Japan Atomic Energy Agency) in an ongoing manner, so this paper will provide only an overview of these monitoring activities. A detailed report on these works has already been published onto the MEXT website [1, 2].

2. Observed radio-nuclides emitted from the power plants

Radio-nuclides emitted into the atmosphere from the explosion of the power plants, especially on March 15 to 16, were observed by various groups with Ge detectors. The observed radio-nuclides were ^{131}I, ^{132}Te, ^{133}I, ^{134}Cs, ^{136}Cs, ^{129m}Te, ^{137}Cs, ^{99}Mo and ^{140}Ba. Iodine isotopes of which activities were approximately 100 times larger than cesium isotopes, were predominant in more of the total activity of emitted radioisotopes than cesium isotopes, but two months after the accident, cesium isotopes have become dominant, since the longest half life of iodine isotopes is 8 days for ^{131}I, while those of ^{134}Cs and ^{137}Cs are 2 years and 30 years, respectively. Activities of Sr-89 and Sr-90 were about 1/1000 to cesium isotopes due to higher melting and boiling points than cesium isotopes. Trace amounts of plutonium isotopes of ^{238}Pu, ^{239}Pu, ^{240}Pu and ^{241}Pu were detected at several sites close to the power plants.

3. Environmental radiation monitoring around the power plants

Ambient dose equivalent rates both inside and outside of the 20 km zone of the power plants, which is the evacuation area, have been continuously measured after the accident at monitoring posts. Radioactive concentrations in dust samples, soil samples and other environmental samples were also measured both inside and outside the power plants. Air-borne monitoring within a 100 km radius zone has been performed by the airplanes of the DOE and MEXT from the beginning of the accident.

Comprehensive monitoring survey started twice from June to August, 2011 and is still going on from December by MEXT under the initiative of JAEA with cooperation of various universities and research institutes, including the Fukushima local government. Based on the results of airborne monitoring and other environmental monitoring, the areas within an 80 km radius from the Fukushima Dai-ichi NPP were divided into 2 km×2 km grids, whereas the areas between 80 km and 100 km and the other areas of Fukushima prefecture were divided into 10 km×10 km grids. Ambient dose equivalent rates were measured at a height of 1m above the ground surface at one location each in these divided grids (nearly 2,200 locations in total) by using calibrated NaI(Tl) scintillators and ionization chamber-type survey meters, and soil samples were collected at five points in principle at each location. With regard to the approximately 11,000 soil samples, the deposited amounts (radiation levels per unit area) of five gamma-emitting nuclides (Cs-134, Cs-137, I-131, Te-129m, and Ag-110m) were measured

by using germanium semiconductor detectors. With regard to soil samples collected at 100 locations out of around 2,200 monitoring points within the 100-km from the Fukushima Dai-ichi NPP and within the other areas of Fukushima prefecture   radiochemical analysis was conducted for Pu-238 and Pu-239+240 (alpha-emitting nuclides) and Sr-89 and Sr-90 (beta-emitting nuclides) to obtain their deposition amounts by the Japan Chemical Analysis Center. In order to ascertain the distribution of radioactive materials around roads in detail, a car survey was also conducted by using the KURAMA (Kyoto University RAdiation MApping) system [3] in the targeted area, and was later expanded over the northern and southern areas in Japan.

Figure 1 shows the distribution map of ambient dose equivalent rates measured at soil sampling points converted on June 14, 2011. Figures 2 and 3 illustrate the deposition densities of ^{137}Cs and ^{131}I isotopes in Bq/m^2 converted on June 14, 2011, respectively. These figures clarify the higher values of dose rates (the highest value was about 55 μSv/h) and deposition in the area northwest of the power plants. The highest integrated dose from March 23 to June 30 was observed to be 47 mSv at a point about 30 km northwest of the power plants.
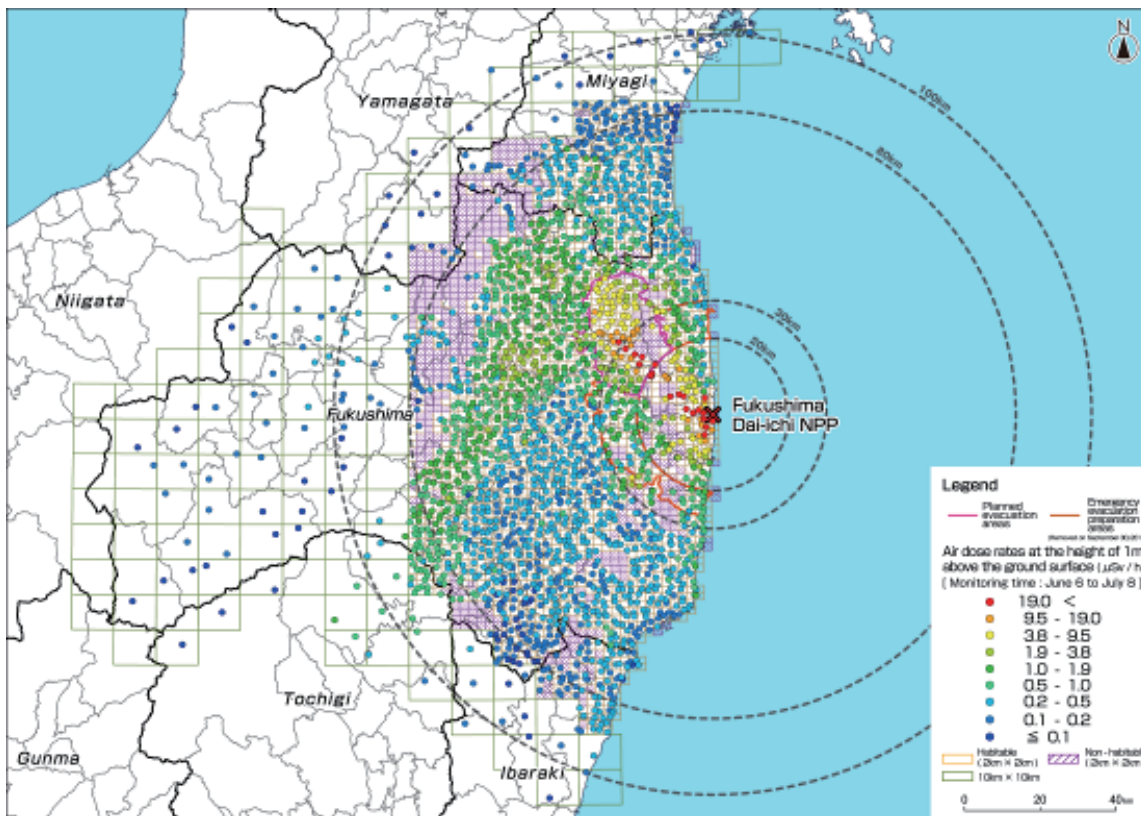
Figure 1. Distribution map of ambient dose equivalent rates at soil sampling points converted at June 14, 2011
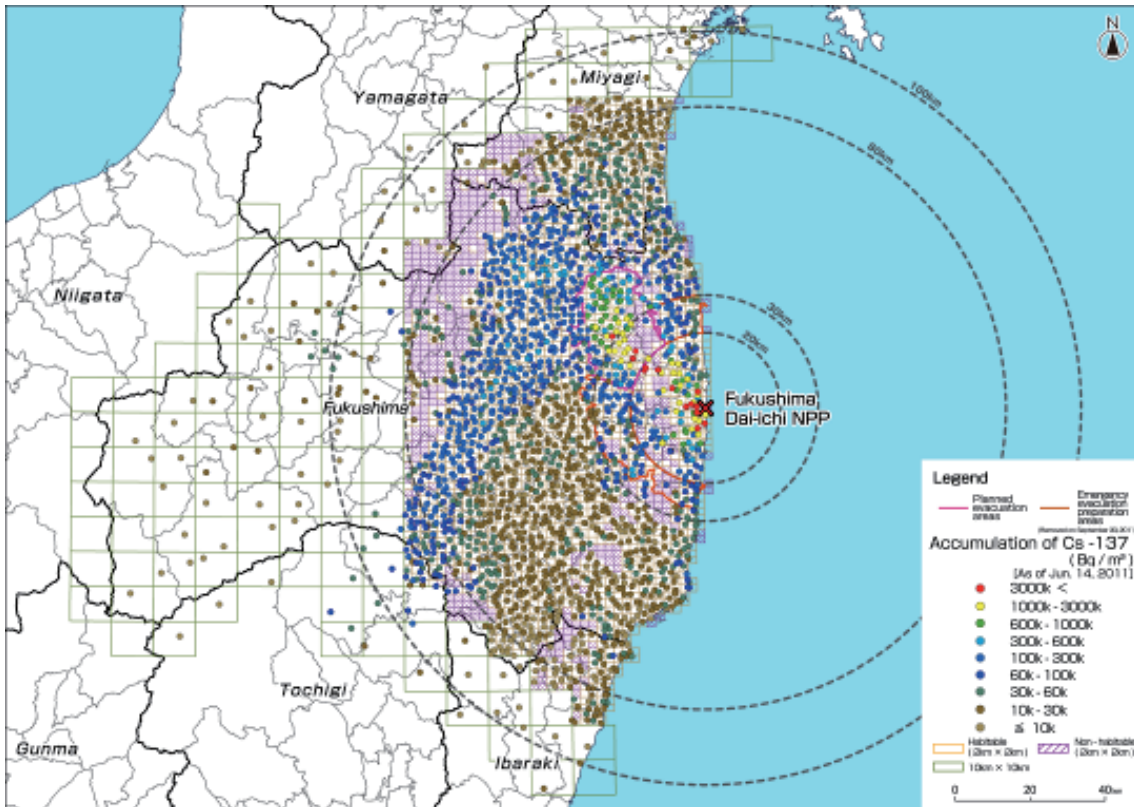
Figure 2. Map of Cs-137 deposition density in soil converted at June 14, 2011
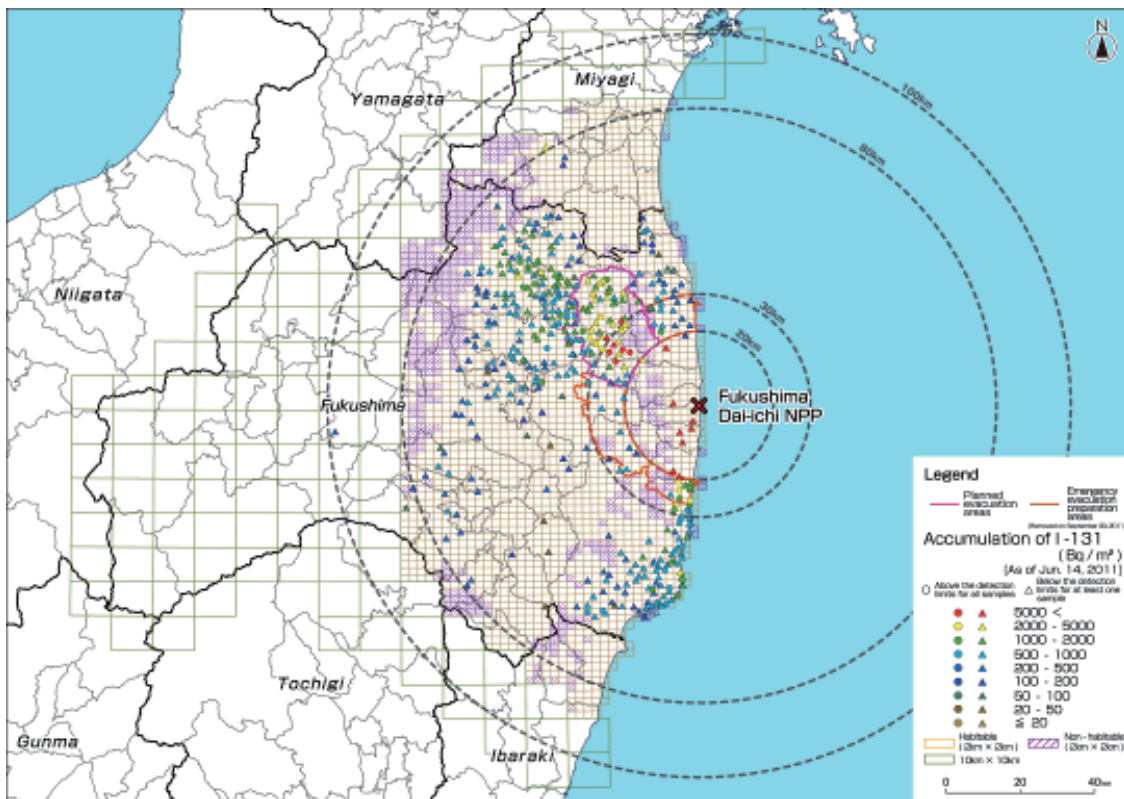
Figure 3. Map of I-131 deposition density in soil converted at June 14, 2011

In order to examine the movement of radioactive materials discharged due to the accident at the Fukushima Dai-ichi NPP, MEXT conducted research surveys on the following individual themes of great importance as research relating to the distribution maps of radiation doses.

 (i) Distribution of radioactive materials within a narrow area in soil by Haruyasu Nagai (Japan Atomic Energy Agency), et al.

 (ii) Vertical distribution of radioactive materials in soil using Geoslicers by Kazuhiro Aoki (Japan Atomic Energy Agency), et al. and using iron pipes by Isao Tanihata (Osaka University), et al.

 (iii) Trends in deposition density levels of radioactive materials in rivers and well water by Yoshihiro Ikeuchi (Japan Chemical Analysis Center), et al.

 (iv) Comprehensive migration of radioactive materials in the model area by Yuichi Onda (Tsukuba University), et al.

The vertical distribution of radioactive cesium in farmland soil was also investigated in Miyagi, Fukushima, Tochigi, Gunma, Ibaraki, and Chiba prefectures. This project was consigned by the Ministry of Agriculture, Forestry and Fisheries (MAFF) and was conducted with the cooperation of the National Institute for Agro-Environmental Sciences, universities, and related parties of the respective prefectures.

All data in these figures were taken from the MEXT website [1].

Further measurements were performed by car in a road-based survey over two separate periods, from December 5 to 28, 2011 and from March 13 to 30 2012, and by an in-situ Ge spectrometry method between December 2011 and May 2012 over an expanded area of about 250 km radius around the power plants. Figure 4 (a) shows the distribution map of the ambient dose equivalent rates in μSv/h from the two road-based surveys. The air-borne monitoring has continued and has been expanded to cover the airspace over all of Japan. Figure 4 (b) shows the sum of the deposited radio-activities in Bq/m^2 of ^{134}Cs and ^{137}Cs over eastern Japan obtained from air-borne monitoring as of November 5, 2011.
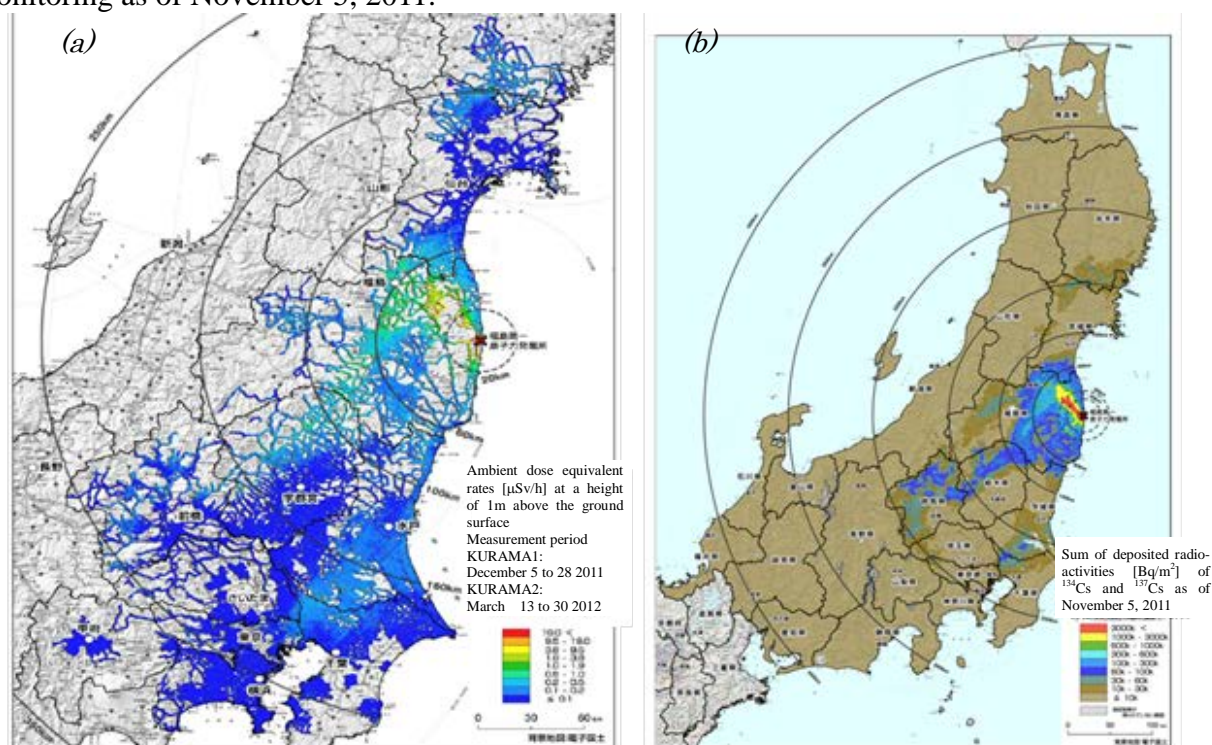
Figure 4. Distribution map of (a) the ambient dose equivalent rates in μSv/h from the two road-based surveys. (b) the sum of the deposited radio-activities in Bq/m^2 of ^{134}Cs and ^{137}Cs over eastern Japan obtained from air-borne monitoring as of November 5, 2011.

The data from the first road-based survey gathered in June 2011 were compared with those from the second road-based survey in December 2011. This comparison clarified that the ^{137}Cs and ^{134}Cs activities in December decreased by about 82% and 72% from June, respectively. These decreases were much faster than the physical decay (30.2 y of ^{137}Cs and 2.06 y of ^{134}Cs), which means that the Cs isotopes were washed out or transferred.

4. Estimated effective doses of each radionuclide over 50 years as determined using IAEA-TECDOC-1162 conversion factors

In order to ascertain the effects of exposure to each radionuclide detected in this monitoring survey, MEXT calculated the possible external exposure and committed effective doses due to resuspension under the assumption that an individual will remain on the ground surface where radionuclides are deposited for 50 years beginning on June 14, 2011 (hereinafter referred to as the "estimated effective doses over 50 years") by using conversion factors defined in the method of exposure assessment in an emergency as proposed by IAEA (IAEA-TECDOC-1162) [4].

Table 1 shows the estimated effective doses over 50 years under the safe-side assumption that an individual will remain for 50 years at the point where the maximum amount of each radionuclide was detected and normalized on June 14, 2011. Because the amounts of radioactive cesium discharged and deposited due to the Fukushima Dai-ichi NPP accident were much larger than those of the other nuclides shown in Table 1, compared with estimated effective doses over 50 years for ^{134}Cs and ^{137}Cs, those for the other nuclides were very small. Based on further measurement data, the estimated effective doses over 50 years were 1200 mSv for the ^{137}Cs isotope and 33 mSv for the ^{134}Cs isotope when normalized on March 1, 2012.

Therefore, it will be appropriate to focus on deposition amounts of ^{134}Cs and ^{137}Cs when assessing exposure levels and taking decontamination measures in the future.

Table 1 Estimated effective dose over 50 years at points where the maximum amount of each type of radionuclides was detected

Radionuclide	Half-life period	Maximum deposition density level[*1] (Bq/m^2)	Estimated effective dose over 50 years	
			Conversion factor $(\mu Sv/h)/(Bq/m^2)$	Obtained results (mSv)
Cs-134	2.065 years	1.4×10^7	5.1×10^{-3}	71
Cs-137	30.167 years	1.5×10^7	1.3×10^{-1}	2000 (2.0Sv)
I-131	8.02 days	5.5×10^4	2.7×10^{-4}	0.015
Sr-89	50.53 days	2.2×10^4	2.8×10^{-5}	0.00061 (0.61μSv)
Sr-90	28.79 years	5.7×10^3	2.1×10^{-2}	0.12
Pu-238	87.7 years	4.0	6.6	0.027
Pu-239+240	2.411×10^4 years	15.0	8.5	0.12
Ag-110m	249.95 days	8.3×10^4	3.9×10^{-2}	3.2
Te-129m	33.6 days	2.7×10^6	2.2×10^{-4}	0.6

*1: Converted to radiation levels as of June 14, 201

5. Website for comprehensive monitoring data

In order to allow individuals to ascertain the effects of radioactive materials discharged from the Fukushima Dai-ichi NPP in more detail, MEXT prepared a website with detailed information on the comprehensive monitoring data, where users can freely obtain distribution maps of radiation doses (distribution maps of ambient dose equivalent rates and soil deposition density maps of radioactive cesium) and other maps showing the results of various monitoring surveys that MEXT has conducted so far. This database can be managed and operated with high security, by compiling these past measurement results and by adding assorted information, such as the measurement methods, analysis methods, and measurement accuracy, with the aim of enabling administrative officials and the general population, including the residents of affected municipalities, to confirm them easily and for researchers worldwide to utilize them for the examination of the Fukushima Dai-ichi NPP accident. This website has just been opened to the public [5] and more data will be added when available.

6. Future plans

In cooperation with other groups, MEXT is continuing its follow-up actions to clarify the comprehensive behavior and migration of deposited radionuclides in the environment, including in soil and sediment samples, and river and forest sites.

References

1) http://www.mext.go.jp
2) Summarized Version of the "Results of the Research on Distribution of Radioactive Substances Discharged by the Accident at TEPCO's Fukushima Dai-ichi NPP", Emergency Operation Center, Ministry of Education, Culture, Sports, Science and Technology (MEXT) and Agriculture, Forestry and Fisheries Research Council, Ministry of Agriculture, Forestry and Fisheries (MAFF), March 13, 2012, in Japanese, http://radioactivity.mext.go.jp/en/contents/1000/294/24/PressR04%200802s.pdf
3) http://www.rri.kyoto-u.ac.jp/kurama/index.html
4) IAEA, Generic procedures for assessment and response during a radiological emergency, IAEA-TECDOC 1162 (2000)
5) http://radb.jaea.go.jp/ or http://radioactivity.mext.go.jp/ja/list/338/list-1.html

Summary of Session 2

K.THIESSEN

Session 2　　　Measurement of Radioactivity in the Environment

The aims of this session were provided by the chairman, Dr. Nakamura.　Three areas of work were described:

(1) Collection of environmental data for use in estimating internal dose
(2) Monitoring of radioactivity in the environment
(3) Retrospective evaluation of the deposition based on measurements

The goal of all of these areas of work is the estimation of the distribution of radioiodine in the early phase after the accident, for use in estimating the early internal dose.

Presentation 1　　　Haruo TSURURA
"Summary of atmospheric measurements of radioactive materials released by the Fukushima Daiichi Nuclear Power Plant accident and their transport pathways"

Dr. Tsuruta described the available atmospheric measurements after the accident.　These are needed both to evaluate internal exposure dose due to inhalation and to calibrate or validate modeling results of atmospheric transport and deposition.　The goal is to develop a time-spatial map of the activity concentrations of I-131 and Cs-137 in the area of concern, in and near Fukushima.

Three data sets are available so far:
(1) Spot and short sampling data in and near the power plant site (ERMCF, MEXT, TEPCO)
(2) Raw spectrometer data at several monitoring sites (ERMCF)
(3) Continuous measurements at several locations (several institutions and universities)

These data sets include atmospheric dust samples, 10-40 minutes per sample, and include radioiodine and radiocesium.

At various stations in the Kanto area (south of Fukushima), time series are available, with sharp peaks corresponding to rainfall events.

Contour maps of atmospheric I-131 at different times have been produced with computer models.

The ratios of I-131 to Cs-137 concentrations show wide variability, with I-131 from 1 to 1000 times as high as the Cs-137.　This variability is probably due to day-to-day variations in the release rates, variability of the meteorological conditions (especially whether or not there was precipitation), and to the chemical form of the iodine.　The peaks (corresponding to rain events) included mostly aerosols, otherwise the gaseous form dominated.

The authors are still looking for additional data or unmeasured samples that might become available.

Questions following the talk:

(Yamazawa?) On days with low concentrations, were the measured concentrations from the plume or from resuspension?

(Bouville) If time-integrated concentrations are looked at, is there still variation in the iodine-cesium ratio?

Presentation 2   Yasuyuki MURAMATSU
"Retrospective evaluation of I-131 deposition following the Fukushima accident through the analysis of I-129 in soil samples"

Dr. Muramatsu described ongoing analyses using neutron activation and mass spectrometry of iodine isotopes.   The methods have been developed for determining I-129/I-127 ratios in the environment and are very accurate and very sensitive.   The methods have been used for estimation of I-131 deposition densities after the Chernobyl accident.   The goal now is to be able to estimate the deposition density of I-131 released from Fukushima by analyzing the data for I-129.   So far, the data indicate a good correlation between I-131 and I-129, much better than the correlation between I-131 and Cs-137.   The ratio of I-131 and Cs-137 varied spatially, making it more difficult to use the Cs-137 measurements to estimate the I-131 deposition densities.   The I-129/I-131 ratios do not show much variability across sampling locations.

Comments following the talk:

(Balonov) The eventual goal is internal exposure (from the air), so deposition density is not as relevant as it would be for exposure pathways involving soil.

(Muramatsu) It will require a model to estimate air concentrations and doses from the soil data.

(Akashi, Muramatsu) There are food samples and a few human thyroid samples available, and the I-129/I-131 ratios will be estimated for those as well as the soil samples.

Presentation 3   Takashi NAKAMURA
Radiation monitoring in the environment around Fukushima

Dr. Nakamura described various sampling and surveying that has been done by MEXT.   This was started in June 2011 and involves 2200 locations.   Within 80 km of Fukushima, the sampling was done on a 2 km x 2 km grid.   From 80-100 km, a 10 km x 10 km grid was used.   A report was published in March 2012 (March 14, 2012) describing the results of the surveying, in terms of the distribution of radioactive substances.   The measured dose rates (both at fixed locations and from vehicles), soil samples, etc. are combined with GPS data to produce maps.   The maximum dose rate is 55 µSv/h.   The dose rate is attributed primarily to Cs-134 and Cs-137.   (The survey was started in June 2011, too late for I-131 to be a major contributor.)   The data will be compared with I-129 data to estimate the contribution from Te-129m.   For the most part, the dose rate correlates with Cs-137. The dose rate data will be used to estimate the Cs-137 deposition densities.   The deposition densities of plutonium and strontium are expected to be correlated with the Cs-137.   Cs-137 is estimated to contribute 96% of the 50-y dose (2000 mSv), and Cs-134 to contribute 4% (71 mSv).

A database of results (maps) will be available at http://ramap.jaea.go.jp/map/ (in Japanese).

MAFF has data on the activity in farmland soil.   From a comparison of Fukushima with Chernobyl, it is estimated that Fukushima released about 1/10 of the radioiodine and radiocesium as Chernobyl did. Thus, the effects are expected to be about 10 x larger for Chernobyl than for Fukushima.

Further work by MEXT and MAFF will include a larger area (larger radius) and more data.

Question following the talk:
(Tolmachev) Are there any data on Pu-239/240?   Plutonium data (241, 238, 239+240) are now being measured.

General Discussion (comments and observations from various individuals)

(Balonov) This is important work.

(Bouville) The I-131/Cs-137 ratios vary in different areas, for example between north and south of the release point.

(Tsuruta) The source term varied, and the precipitation (rain, snow) varied.

(Kajimoto) Iodine was released more quickly early on, less in the later phase.   There will be more source term information in a few weeks.

(Tolmachev) Iodine speciation is important for dose estimation.

(Nasstrom) There may be different chemistry in the reactors, gas vs. aerosol.

(Tsuruta) Wet vs. dry wind is probably important--we need details about what happens in the atmosphere.

(Kajimoto) Iodine is released in aerosol form, then there are reactions in the atmosphere.

(Balonov) Which reactors had releases when?

(answer) March 12-13 was #1.   March 15 was #3.   Later on was #2.   Possibly the releases from each could be different (because of the timing).

(Kajimoto) Three hours after the reactor shut down.   The times are different for each reactor.

(Homma) March 15 was the heaviest release.   The early part of that one was directed to the south, and the weather was dry.   In the afternoon things were different.   Therefore there could be differences between chemical forms on the same day.

Question about ionic iodine.

(Kajimoto) Most iodine released as aerosol (I and Cs), due to high temperature conditions.   This applies for the releases at the top flange of unit 2, possibly also to unit 3.   Conversion to ionic iodine is not dominant.

(Muramatsu) There were German studies after Chernobyl.   The guess is that gaseous iodine was greater than particulate.

(Tolmachev) The organic bound iodine was measured months later--what happened during the early phase?

(Solomon) The goal of a lot of the work is to produce air concentrations from the available data.   Both the time and spatial distributions are important.   There needs to be thought as to how to publish this information in useful form.

(Kurihara) NIRS will publish a proceedings of this symposium.

(Muramatsu) There are important differences (environmental differences) between Chernobyl and Japan, e.g., bamboo.   There are big questions about snowfall, e.g., is deposition higher with snow?

(Tolmachev, Solomon) Snow is important.   The scavenging could be different for snow vs. rain.   The chemical forms could be different, etc.

Rapporteur's Summary
A variety of valuable environmental data are available in and near the Fukushima area, including some atmospheric data, soil measurements, and dose rate measurements.   The goal is to reconstruct the radionuclide concentrations in air as a function of time and location, from the available data.   The I-131/Cs-137 ratios are highly variable, due to differences in the source term with time and to differences in weather conditions.   The I-131/I-129 ratios appear to be stable, but the analyses are more difficult.   Iodine speciation and chemistry are important.   While reproducing the deposition measurements is important, the air concentrations are more important for the assessment than the deposition densities.   Therefore, the uncertainty in estimating air concentrations from deposition (or from source term estimates) will be extremely important in estimating the uncertainty in inhalation doses.

Session 3

Atmospheric Dispersion Simulations for Radionuclides

Chair   :   H. YAMAZAWA
Co-chair   :   G. SUGIYAMA
Rapporteur :   J. NASSTROM

Resulting from the Fukushima Daiichi Nuclear Power Plant Accident

Masamichi CHINO [1], Hiroaki TERADA [1], Genki KATATA [1], Haruyasu NAGAI [1],
Hiromasa NAKAYAMA [1], Hiromi YAMAZAWA [2], Shigekazu HIRAO [2], Toshimasa OHARA [3],
Masayuki TAKIGAWA [4], Hiroshi HAYAMI [5], Michio AOYAMA [6]

[1] *Japan Atomic Energy Agency, 2-4 Shirakata-shirane, Tokai-mura, IBARAKI, 319-1195, Japan*
[2] *Nagoya University, Furo-cho, Chikusa-ku, Nagoya, AICHI, 464-8601, Japan*
[3] *National Institute for Environmental Studies, 16-2 Onogawa, Tsukuba, IBARAKI, 305-8506, Japan*
[4] *Japan Agency for Marine-Earth Science and Technology, 2-15 Natsushima-Cho, Yokosuka, KANAGAWA, 237-0061, Japan*
[5] *Central Research Institute of Electric Power Industry, 1646 Abiko, Abiko, Chiba, 270-1194, Japan*
[6] *Meteorological Research Institute, 1-1 Nagamine, Tsukuba, IBARAKI, 305-0052, Japan*

Abstract

The release rates and total amounts of ^{131}I and ^{137}Cs discharged into the atmosphere as a result of the nuclear accident at the Fukushima Daiichi Nuclear Power Plant were estimated for March 12 to April 5, 2011. The applied method was a reverse estimation by coupling environmental monitoring data with atmospheric dispersion simulations under the assumption of the unit release rate (1 Bq h^{-1}). The estimated temporal variation in the releases indicated that a significant release of greater than 10^{15} Bq h^{-1} of ^{131}I occurred on March 15, followed by relatively small releases on the order of 10^{13} Bq h^{-1}, while the release rates from March 16 until March 24 were estimated to be rather constant on the order of 10^{14} Bq h^{-1}. The release rates decreased with small day-to-day variations to approximately 10^{11}-10^{12} Bq h^{-1} of ^{131}I at the beginning of April. The estimated source term was then examined on the basis of a comparison to other results. In addition, the ground depositions of ^{137}Cs calculated using various atmospheric dispersion models with the estimated source term in this study were compared with observed values. These examinations indicated that the estimated source term was reasonably accurate at least during the period when the plume flowed over the land in Japan.

Keywords: Fukushima; source term; atmosphere; reverse estimation; atmospheric transport simulation; ^{131}I ; ^{137}Cs; Monitoring; SPEEDI; WSPEEDI

1. Introduction

In the early stage of the nuclear accident at the Fukushima Daiichi Nuclear Power Plant (FDNPP) in March 2011, the source term for the atmospheric releases of radionuclides was unknown. Estimation of the source term was urgently needed to evaluate the scale of the accident and radiation doses to the public. Chino et al. [1] conducted a preliminary estimation of the source terms of ^{131}I and ^{137}Cs using a reverse estimation method that combined atmospheric dispersion simulation and monitoring data. This preliminary estimation was revised several times as new monitoring data became available [2, 3]. The most current source term is described in detail by Terada et al. [4]

Estimation of the source term and atmospheric dispersion has been performed by various researchers in Japan and abroad, and the first comparison of these studies was conducted at an open workshop entitled ''Reconstruction of environmental releases and dispersion processes due to the Fukushima Daiichi Nuclear Power Plant accident'' on March 6, 2012, organized by the Japan Atomic Energy Agency (JAEA) [5]. At the workshop, the source terms derived by Terada et al. (hereafter described as the source terms by the JAEA) were examined by several methods. This paper addresses the source term estimation method and the verification of the results at the workshop.

2. Reverse estimation method

Detailed descriptions of the reverse estimation method for examining the source terms, monitoring data, and atmospheric simulation models are given in the literature [1-4], and, thus, only an outline of them is presented below.

The reverse estimation method calculates release rates of radionuclides (Bq h^{-1}) by coupling environmental monitoring data with atmospheric dispersion simulations, assuming the unit release rate (1 Bq h^{-1}). The release rates are obtained by dividing measured air concentrations of ^{131}I and ^{137}Cs into calculated ones at sampling points, as follows:

$$Q_i = M_i/C_i,\qquad(1)$$

where Q_i is the release rate (Bq h^{-1}) of nuclide i when discharged into the atmosphere, M_i is the measured air concentration (Bq m^{-3}) of nuclide i, and C_i is the dilution factor (h m^{-3}) of nuclide i, which is equal to the air concentration calculated under the assumption of the unit release rate. When air concentration data are not available, the release rates can also be estimated by comparing measured air dose rates due to radionuclides on the ground surface with calculated ones derived from simulations with the unit release rate, assuming the composition of tellurium, iodine, and cesium.

The total release amounts are estimated by the time integration of release rates, as follows:

$$S_i = \sum \left[Q_{i,j} \times T_j \right],\qquad(2)$$

where S_i is the total release amount (Bq) of nuclide i, and $Q_{i,\,j}$ is the release rate (Bq h^{-1}) of nuclide i at time j of which the duration is T_j (h).

2.1. Environmental monitoring data

For the source term estimation, researchers mainly used environmental monitoring data for the air concentrations of iodine and cesium (hereafter, dust sampling data). Gaseous and particulate iodine were expected to be sampled according to the guideline for environmental radiation monitoring from the Nuclear Safety Commission of Japan (NSC) [6], which recommends the use of dust samplers with charcoal cartridges for monitoring gaseous iodine. The data used in the estimation are from the websites of the Ministry of Education, Culture, Sports, Science and Technology (MEXT) [7], the Japan Chemical Analysis Center (JCAC) [8], and the JAEA [9, 10]. Air dose monitoring data from MEXT [7], the Nuclear and Industrial Safety Agency (NISA) [11], and Fukushima Pref. [12] indicate that the atmospheric release of radionuclides caused a large amount of ground deposition after the hydrogen explosion at Unit 1 on March 12 and in the daytime of March 15, resulting in high dose rates in the sectors to the north and northwest of the plant, respectively. However, because no dust sampling data were available, the release rates of ^{131}I and ^{137}Cs during these periods were estimated from a comparison of the measured air dose rate pattern due to ground shine with a calculated pattern, after the plume moved away from these regions.

2.2. Atmospheric dispersion simulation

The System for Prediction of Environmental Emergency Dose Information (SPEEDI) network system [13] and the Worldwide version of SPEEDI (WSPEEDI) [14] developed by the JAEA were used for calculating air concentrations and dose rates. SPEEDI and WSPEEDI consist of similar numerical models, i.e., the meteorological condition is calculated by atmospheric dynamic models and air concentration, deposition, and radiological doses are calculated by particle dispersion models. Both input meteorological forecasts from the Japan Meteorological Agency as initial and boundary

conditions and consider the terrain effect on transport and diffusion. The difference is that SPEEDI is customized for Japanese nuclear sites and in practical use, while WSPEEDI can treat nuclear accidents around in the world. The simulation results from SPEEDI now operated by MEXT were furnished from NSC for the purpose of the source term estimation.

3. Results

Figure 1 shows the estimated temporal variation in the release rates of ^{131}I and ^{137}Cs. When dust sampling data were used, the release rates of ^{131}I were estimated using the reverse estimation method and the release rates of ^{137}Cs were derived based on the radioactivity ratios of ^{131}I to ^{137}Cs of dust sampling data. The release due to the hydrogen explosion at Unit 3 was simply assumed to be the same as that at Unit 1, because the wind was toward the Pacific Ocean and no environmental data were available. When several sets of dust sampling data were available for the estimation on the same day, the highest value of the release rates for the day is applied.
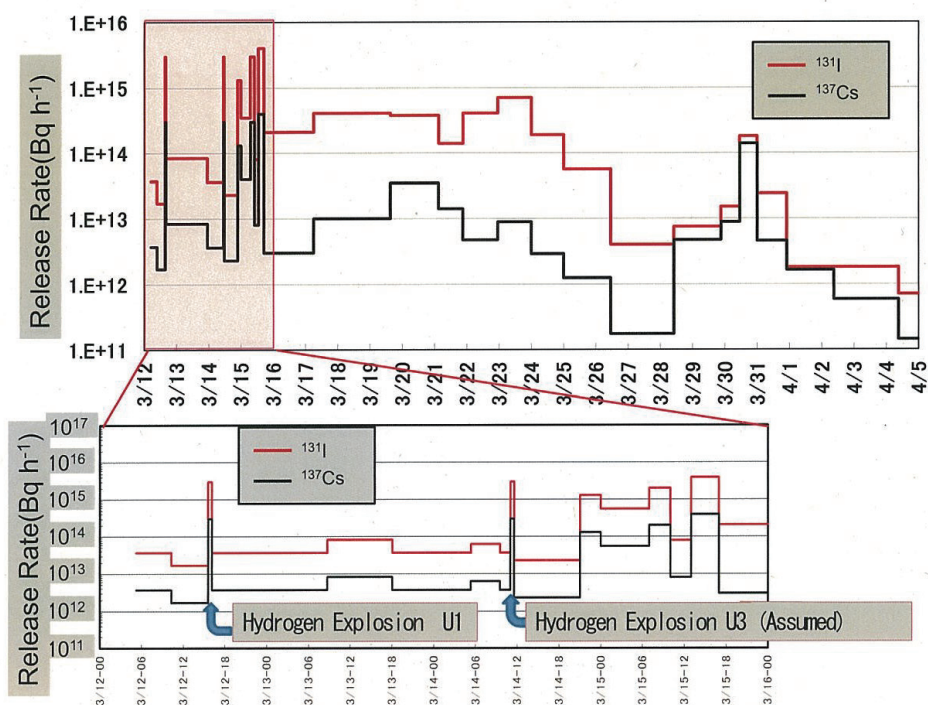
Figure 1. Temporal variation in the estimated release rates of ^{131}I and ^{137}Cs (a) from 5 JST on March 12 to 0 JST on April 5 and (b) from 5 JST on March 12 to 0 JST on March 16

The temporal variation indicates that a significant release of over 10^{15} Bq h^{-1} of ^{131}I occurred on March 15, followed by relatively small releases, on the order of 10^{13} Bq h^{-1}, but the release rates from March 16 until March 24 were estimated to be rather constant on the order of 10^{14} Bq h^{-1}. The release rates then decreased with small day-to-day variations to 10^{11}-10^{12} Bq h^{-1} of ^{131}I at the beginning of April. The release rate of ^{137}Cs follows a similar trend, with fluctuations of the ^{131}I/^{137}Cs ratio in the range from 1 to 100.

According to Eq. (2), the total amounts of ^{131}I and ^{137}Cs discharged into the atmosphere from 05 JST (Japanese Standard Time JST=UTC+9) March 12 to 0 JST April 1 were approximately 1.2×10^{17} Bq and 0.9×10^{16} Bq, respectively.

4. Verification

The estimated source terms were examined by the comparison with other estimations of the time trends and total releases of ^{131}I and ^{137}Cs. Furthermore, the ground depositions of ^{137}Cs calculated by using various atmospheric dispersion models with the estimated source term in this study were compared with observed values. A summary of the verification studies is in Table 1.

Table 1 Summary of verification studies.

	Method	Simulation model	Used data
JAEA	Reverse estimation of time trend of releases of ^{131}I and ^{137}Cs	WSPEEDI: GPV/MSM[15]+MM5[16] +GEARN	Mainly dust sampling data in Fukushima Pref.
Hirao, et al.	Reverse estimation of time trend of releases of ^{131}I and ^{137}Cs	GPV/MSM+MM5+ Lagrangian model	Dust sampling and deposition data in East Japan
Ohara et al. Takigawa Hayami	Atmospheric dispersion and deposition simulations using source term from Terada et. al.	GPV/MSM+WRF[17]+CM AQ[18] GPV/MSM+WRF/Chem[19] MANAL+WRF+CAMx[20]	Comparison with observed deposition map of ^{137}Cs and fallout of ^{131}I and ^{137}Cs in the East Japan
Aoyama et al.	Reverse estimation of total releases of ^{137}Cs	Atmospheric and oceanic dispersion models	^{137}Cs concentration in marine and ground surfaces

*The full text of acronyms in the simulation model is shown at the end of the paper.

4.1. Time trend

Hirao et al. estimated the source terms for ^{131}I and ^{137}Cs based on their original reverse estimation method [21] and monitoring data different from those used by the JAEA, e.g., air concentrations and depositions on the ground over eastern Japan. On the other hand, the JAEA mainly used air concentrations and air dose rates in the local area within 100 km of the FDNPP. Figure 2 compares the release rates of ^{131}I and ^{137}Cs by Hirao et al. and the JAEA. Note that the plots from Hirao et al. are limited when the plume flowed over the land. The results are in good agreement during the period when the plume flowed over the land after the evening of March 14.
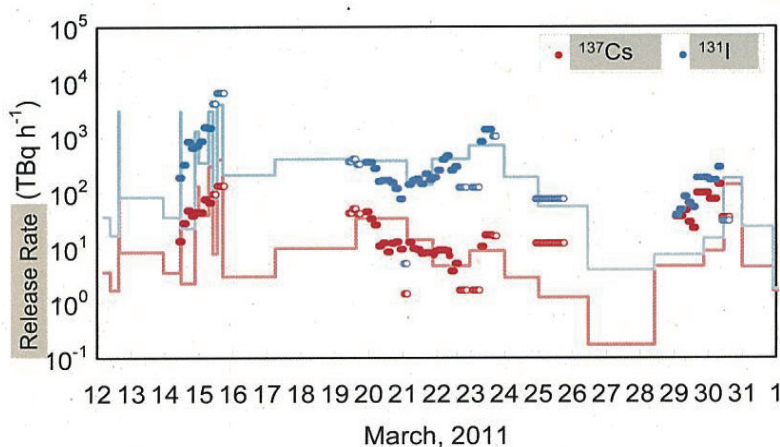
Figure 2. Comparison of the release rates of ^{131}I and ^{137}Cs determined by the JAEA and Hirao et al.[22]

4.2. Ground depositions of ^{137}Cs

Ohara et al., Takigawa, and Hayami calculated the atmospheric dispersions and depositions using their atmospheric dispersion models and the source terms by the JAEA, and evaluated the accuracy of the results by comparing them with a contamination map of ^{137}Cs obtained from an aerial survey by MEXT [23]. Figure 3 shows the comparison results. The results from the three simulations agreed well with the contamination map both qualitatively and quantitatively, though three different atmospheric dispersion models were used. In particular, the result of Ohara et al. showed fairly good agreement with the results of the aerial survey by MEXT [23]. The discrepancies among the simulation results were probably due to the difference in the wet deposition model. Ohara et al. and Nagai compared the calculated daily fallout of ^{131}I and ^{137}Cs over eastern Japan with measurements. The results are shown in Fig. 4. Here, it should be noted that the measurements of daily fallouts began on March 18, 2011, and actual increases were from March 20. In both cases, the calculated results were in good agreement with the measured values within a factor of 10 and had no bias. Considering that atmospheric transport models generally have uncertainty of around a factor of 2 to 5, the accuracy of the source terms estimated by the JAEA is within a factor of 2 to 5 at least after March 20.
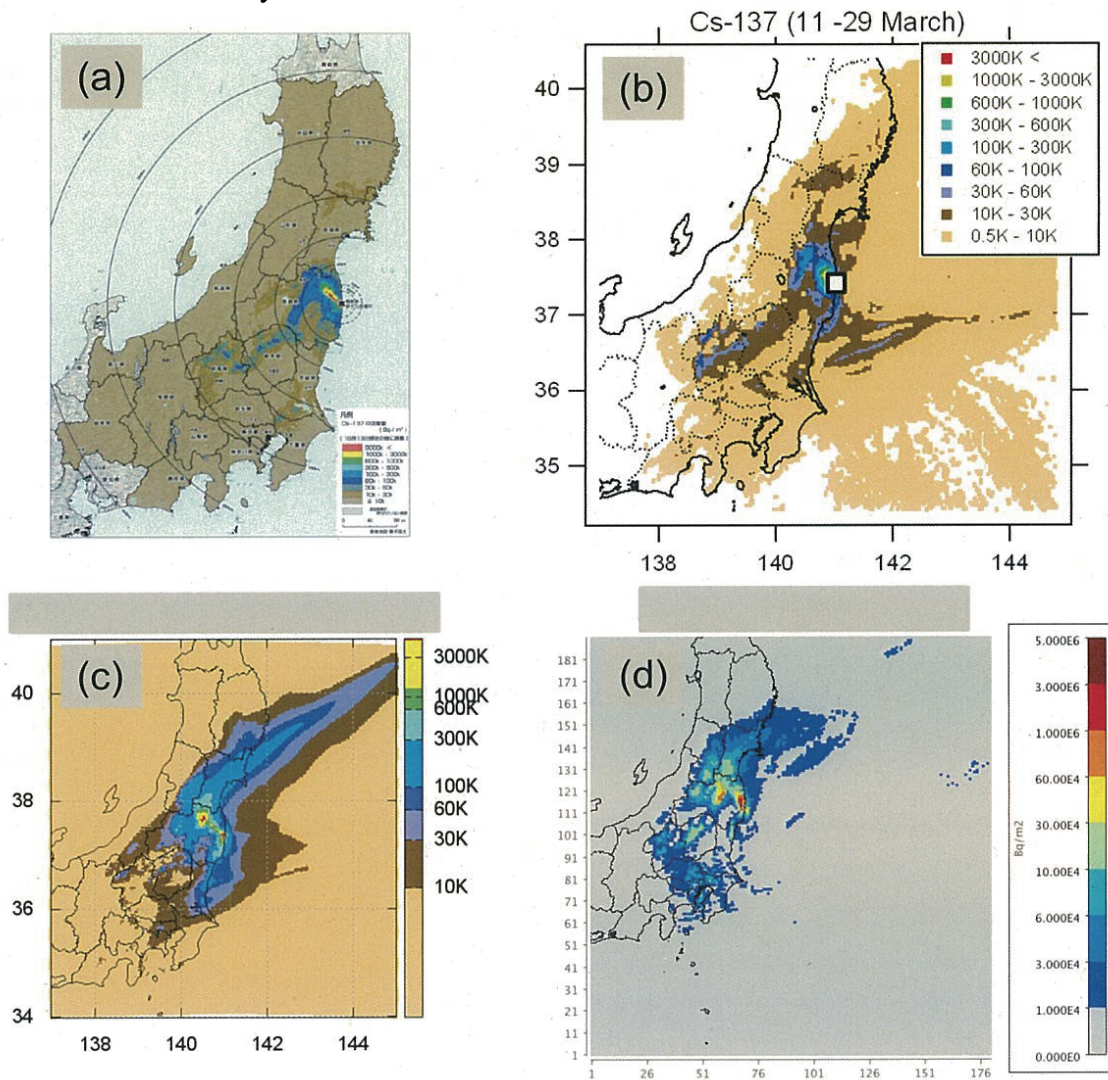
Figure 3. Comparison of ^{137}Cs deposition maps for three atmospheric dispersion models by using the source terms of the JAEA and the aerial survey by MEXT. (a) Aerial survey by MEXT[23], (b) Ohara et al. [24], (c) Takigawa [25], and (d) Hayami [26].
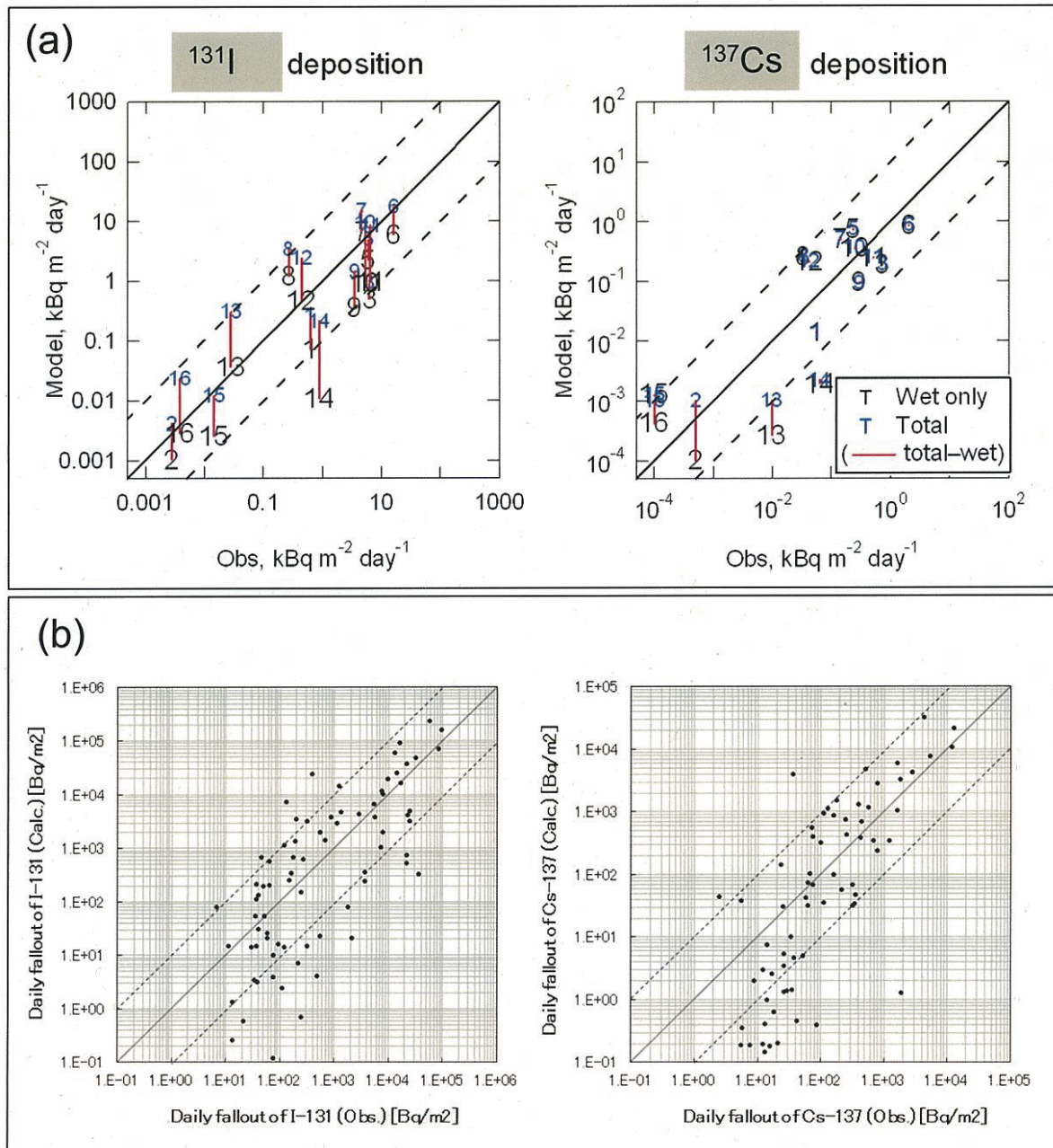
Figure 4. Comparison of ^{131}I and ^{137}Cs fallouts calculated with two atmospheric dispersion models and daily observations over eastern Japan after March 18 by (a) Ohara et al.[27] and (b) Nagai et al.[28]

4.3. Total release

Aoyama et al.[29] estimated the total release of ^{137}Cs by comparing the simulation results from a combination of atmospheric and oceanic dispersion models with the observed deposition of ^{137}Cs on the ground and the concentrations of ^{137}Cs in marine surface water. The total release of ^{137}Cs estimated by the JAEA was compared with other total releases estimated by reverse estimation, severe accident analysis, and so on. Stohl et al.[30] estimated the source terms for ^{133}Xe and ^{137}Cs by the reverse estimation method using the monitoring data from the Comprehensive Nuclear-Test-Ban Treaty Organization (CTBTO). NISA estimated the source term on the basis of severe accident analysis[31]. The French Institute for Radiological Protection and Nuclear Safety (IRSN) also posted an analysis of

the source terms for noble gases, iodine, and cesium on its website [32], although the details of the estimation method are not clear. Furthermore, Tokyo Electric Power Company (TEPCO) estimated the source terms for noble gases, iodine, and cesium using a combination of severe accident analysis and reverse estimation [33].

The results of these studies are shown in Table 2. According to the table, the total release of ^{131}I was in the range from 0.9 to 5.0×10^{17} Bq, but it was in the range from 0.9 to 1.6×10^{17} Bq when extremely large values were excluded. Likewise, the total release of ^{137}Cs was from 0.6 to 3.7×10^{16} Bq, but from 0.6 to 2.0×10^{16} Bq when large values were excluded. The source term for ^{137}Cs as determined by the JAEA is small considering the range of the results presented in Table 2. Because the results discussed in 4-1 and 4-2 are for the source terms for ^{131}I and ^{137}Cs during the period when the plume flowed over the land, they are probably appropriate, and underestimation of the source terms when the plume flowed toward the Pacific Ocean may have occurred. While it is not critical to estimate the radiological doses to the domestic public, these values should be estimated in the future.

Table 2 Comparison of the estimated total releases of ^{131}I and ^{137}Cs

	^{131}I (Bq)	^{137}Cs (Bq)
JAEA Chino et al.[1] Katata et al.[3] Terada et al.[4]	1.5×10^{17} 1.3×10^{17} 1.2×10^{17}	1.3×10^{16} 1.1×10^{16} 0.9×10^{16}
Aoyama et al.[29]	-	$1.5\text{-}2.0\times10^{16}$
Stohl et al.[30]	-	3.7×10^{16}
NISA[31] April 12, 2011 June 6, 2011	1.3×10^{17} 1.6×10^{17}	0.6×10^{16} 1.5×10^{16}
IRSN (France)[32]	0.9×10^{17}	1.0×10^{16}
TEPCO[33]	5.0×10^{17}	1.0×10^{16}

5. Conclusion

The source terms for ^{131}I and ^{137}Cs discharged from the FDNPP accident were estimated and verified by using several methods. The verification results indicated that the estimated source terms were reasonably accurate during the period when the plume flowed over the land in Japan, with an error factor of approximately 2 to 5. However, the source terms when the plume flowed toward the Pacific Ocean, e.g., from the evening of March 13 to the evening of March 14 and from the afternoon of March 16 to the early morning of March 20, are still interpolated values. Thus, the source term for these periods should be examined as a future task.

References

1) M. Chino, H. Nakayama, H. Nagai, H. Terada, G. Katata, H. Yamazawa, J. Nucl. Sci. Technol., 48, (2011), 1129-1134.
2) G. Katata, H. Terada, H. Nagai, M. Chino, J. Environ. Radioactiv., 111, (2012), 2-12.
3) G. Katata, M. Ota, H. Terada, M. Chino, H. Nagai, J. Environ. Radioactiv., 109, (2012) , 103-113.
4) H. Terada, G. Katata, M. Chino, H. Nagai, J. Environ. Radioactiv., 112, (2012), 141-154.

5) JAEA, the open workshop 'Reconstruction of environmental releases and dispersion processes due to the Fukushima Daiichi Nuclear Power Plant accident' , http://nsed.jaea.go.jp/ers/environment/envs/FukushimaWS/index.htm, (2012) , [in Japanese].

6) NSC, The guideline for environmental radiation monitoring, http://www.nsc.go.jp/shinsajokyo/pdf/100327_kankyo_monita.pdf, (2010), [in Japanese].

7) MEXT, http://radioactivity.mext.go.jp/en/ , (2011).

8) JCAC, http://www.jcac.or.jp/lib/senryo_lib/taiki_kouka.pdf, (2011), [in Japanese].

9) T. Ohkura, T. Oishi, M. Taki, Y. Shibanuma, M. Kikuchi, et al., Emergency Monitoring of Environmental Radiation and Atmospheric Radionuclides at Nuclear Science Research Institute, JAEA Following the Accident of Fukushima Daiichi Nuclear Power Plant, JAEA-Data/Code 2012-010, JAEA, (2012).

10) S. Furuta, S. Sumiya, H. Watanabe, M. Nakano, K. Imaizumi, et al., Results of the Environmental Radiation Monitoring Following the Accident at the Fukushima Daiichi Nuclear Power Plant, JAEA-Review 2011-035, JAEA, (2011), [in Japanese].

11) NISA,http://www.meti.go.jp/press/2011/06/20110603019/20110603019.html,(2011), [in Japanese].

12) Fukushima Prefecture, http://www.pref.fukushima.jp/j/ , (2011), [in Japanese].

13) H. Nagai, M. Chino, H. Yamazawa, J. At. Energy Soc. Japan, 41, (1999), 777-785, [in Japanese].

14) H. Terada, M. Chino, J. Nucl. Sci. Technol., 45, (2008), 920-931.

15) Japan Meteorological Business Support Center, http://www.jmbsc.or.jp/index.html, (2012) [in Japanese].

16) G. A. Grell, J. Dudhia, D. R. Stauffer, A Description of the Fifth-generation Penn State/NCAR Mesoscale Model (MM5), NCAR Tech. Note NCAR/TN-3921STR, NCAR, (1994), 122 pp.

17) W. C. Skamarock, J. B. Klemp, J. Dudhia, D. O. Gill, D. M. Barker, M. G. Duda, X. Y. Huang, W. Wang, J. G. Powers, A Description of the Advanced Research WRF Version 3, NCAR Tech. Note NCAR/TN-475+STR, National Center for Atmospheric Research, (2008), 125 pp.

18) D. Byun, and K. L. Schere, Review of the governing equations, computational algorithms, and other components of the models-3 Community Multiscale Air Quality (CMAQ) modeling system, Appl. Mech. Rev., 59, (2006), 51-77.

19) G. A. Grell, S. E. Peckham, R. Schmitz, and S. A. McKeen, G Frost, W. C. Skamarock, B. Eder, Fully coupled "online" chemistry in the WRF model. Atmos. Environ., 39, (2005), 6957-6975.

20) ENVIRON, Users Guide: Comprehensive Air Quality model with Extensions (CAMx) Version 5.40, ENVIRON International Corporation, Available at http://www.camx.com (2011), 306 pp.

21) S. Hirao, H. Yamazawa, J. Nucl. Sci. Technol., 47, (2010), 20− 30.

22) S. Hirao, H. Yamazawa, http://nsed.jaea.go.jp/ers/environment/envs/FukushimaWS/taikihoushutsu1.pdf, pg. 8, (2012), [in Japanese].

23) MEXT, http://radioactivity.mext.go.jp/ja/contents/5000/4901/24/1910_1216.pdf, (2011), [in Japanese].

24) T. Ohara, Y. Morino, http://nsed.jaea.go.jp/ers/environment/envs/FukushimaWS/taikikakusan1.pdf, pg. 19, (2012), [in Japanese].

25) M. Takigawa, http://nsed.jaea.go.jp/ers/environment/envs/FukushimaWS/taikikakusan2.pdf, p.14, (2012), [in Japanese].

26) H. Hayami, http://nsed.jaea.go.jp/ers/environment/envs/FukushimaWS/taikikakusan3.pdf, (2012), [in Japanese].

27) T. Ohara, Y. Morino, http://nsed.jaea.go.jp/ers/environment/envs/FukushimaWS/taikikakusan1.pdf, pp.11-12, (2012), [in Japanese].

28) H. Nagai, M. Chino, H. Terada, G. Katata, H. Nakayama, et al.,: http://nsed.jaea.go.jp/ers/environment/envs/FukushimaWS/jaea2.pdf, pg. 11, (2012), [in Japanese].

29) M. Aoyama, M. Kajino, T. Tanaka, T. Sekiyama, D. Tsumune, et al.,

http://nsed.jaea.go.jp/ers/environment/envs/FukushimaWS/souhoushutsu.pdf, (2012).
30) A. Stohl, P. Seibert, G. Wotawa, D. Arnold, J.F. Burkhart, et al., Atmos. Chem. Phys., 12, (2012), 2313-2343.
31) NISA,
http://www.meti.go.jp/press/2011/06/20110606008/20110606008.html,
http://www.meti.go.jp/press/2011/04/20110412001/20110412001.html, (2011), [in Japanese].
32) IRSN,
http://www.irsn.fr/EN/news/Documents/IRSN_fukushima-radioactivity-released-assessment-EN.pdf#search='IRSN, (2011).
33) TEPCO, Report of Fukushima Nuclear Accidents Investigation, (2012), [in Japanese].

Full text of acronyms in Table 1

GPV: Japan Meteorological Agency Grid Point Value
MSM: Japan Meteorological Agency Meso-Scale Model
MM5: the Fifth-generation Penn State/NCAR Mesoscale Model
GEARN: Global Environmental Assessment for Reactor accident –New version
WRF: The Weather Research & Forecasting Model
WRF/Chem: The Weather Research and Forecast (WRF) model coupled with Chemistry
CMAQ: Community Multi-scale Air Quality
MANAL: Japan Meteorological Agency Meso-Scale Analysis
CAMx: Comprehensive Air Quality model with Extensions (CAMx)

Atmospheric Dispersion Simulations of Radioactive Materials Discharged from the Fukushima Daiichi Nuclear Power Plant due to Accident: Consideration of Deposition Process

Haruyasu NAGAI, Masamichi CHINO, Hiroaki TERADA, Genki KATATA

Japan Atomic Energy Agency
2-4 Shirakata-shirane, Tokai-mura, IBARAKI, 319-1195, Japan

Abstract

In order to assess the radiological dose to the public resulting from the Fukushima Daiichi Nuclear Power Plant accident in Japan, the spatial and temporal distribution of radioactive materials in the environment have been analyzed by computer simulations. As the first step, the source term of radioactive materials discharged into the atmosphere was estimated by coupling environmental monitoring data with atmospheric dispersion simulations by the System for Prediction of Environmental Emergency Dose Information (SPEEDI) and the Worldwide version of SPEEDI (WSPEEDI-II). By using the estimated source term, detailed analysis on the local dispersion around the plant and regional scale dispersion over the eastern Japan area were carried out by WSPEEDI-II simulations. The formation processes of high dose rate zone around north-west direction from the plant and deposition over the eastern Japan area were reproduced in these simulations. However, there were some discrepancies between calculation and airborne monitoring of surface deposition of ^{137}Cs, and the cause of these discrepancies was investigated. The result of parametric study indicated that the model can reproduce the spatial and temporal distribution of radioactive materials in the environment more accurately by using different wet deposition schemes considering rainout/washout, ice/liquid phases, and fog deposition.

Keywords: Fukushima Daiichi Nuclear Power Plant accident; numerical simulation; environmental transport; WSPEEDI-II; SPEEDI-MP

1. Introduction

The Fukushima Daiichi Nuclear Power Plant accident in Japan triggered by a magnitude 9.0 earthquake and resulting tsunami on 11 March, 2011 caused the month-long discharge of radioactive materials into the atmosphere. It is urgent to assess the radiological dose to the public resulting from this release. In order to do this task, the spatial and temporal distribution of radioactive materials in the environment needs to be determined although this is difficult to obtain considering the limited measurement data. Computer simulations based on dispersion modeling are very useful and effective to provide the spatially and temporally 4-dimensional distribution of radioactive materials in the environment by connecting fragmentary measured data in space and time.

Japan Atomic Energy Agency (JAEA) has been developing numerical simulation system to predict the environmental transport of radioactive materials. Starting from System for Prediction of Environmental Emergency Dose Information (SPEEDI), which is currently operational as a nuclear emergency response system of Ministry of Education, Culture, Sports, Science and Technology (MEXT) [1], and Worldwide version of SPEEDI (WSPEEDI-II) [2], we are constructing new numerical simulation system for material transport in the atmospheric, terrestrial, and oceanic environments, SPEEDI-MP (SPEEDI Multi-model Package) [3]. These numerical simulation systems have been and are planning to be applied to predict the environmental transport of radioactive materials discharged due to the Fukushima Daiichi nuclear power plant accident.

As the first step, the source term of radioactive materials discharged into the atmosphere was estimated by coupling environmental monitoring data with atmospheric dispersion simulations [4-7]. The atmospheric dispersion models used for this task are SPEEDI and WSPEEDI-II. By using the estimated source term, detailed analyses on the local dispersion around the plant and regional scale dispersion over the eastern Japan area were carried out by WSPEEDI-II simulations. The formation processes of high dose rate zone around north-west direction from the plant and deposition over the eastern Japan area were reproduced in these simulations [5-7]. However, there were some discrepancies between calculation and airborne monitoring of surface deposition of ^{137}Cs, e.g., underestimations in Tochigi and Gunma Prefectures, and overestimations in Miyagi and Iwate Prefectures [7].

The cause of discrepancies between calculated and measured surface depositions of ^{137}Cs was investigated in this study. Uncertainties in the used source term, predicted meteorological field, and deposition process treated in dispersion calculations were conceivable factors for the discrepancies. In these factors, the source term for the period relating to these discrepancies was verified by the local-scale analysis [6], and the predicted meteorological field was confirmed to some extent by comparing with surface meteorological measurements and further improvements of the prediction seemed to be difficult. Thus, we carried out preliminary parametric study to find out a possible cause of the discrepancies with focus on uncertainties due to the deposition process in the dispersion model.

2. Simulation model

JAEA has been developing numerical simulation system to predict the environmental transport of radioactive materials. At first, SPEEDI was developed and it is currently operational as a nuclear emergency response system of MEXT. By expanding the function of SPEEDI, WSPEEDI and its second version (WSPEEDI-II) have been constructed [2]. WSPEEDI-II uses a combination of non-hydrostatic mesoscale atmospheric model MM5 [8] and Lagrangian particle dispersion model GEARN [9]. MM5 is a community model having many users all over the world and is used for the official weather forecast by some countries. It has many useful functions such as nesting calculations, four-dimensional data assimilation, and many options of parameterizations for cloud micro-physics, cumulus cloud, planetary boundary layer (PBL), radiation, and land surface scheme. MM5 predicts three-dimensional fields on wind, precipitation, diffusion coefficients, etc. based on atmospheric dynamic equations with appropriate spatial and temporal resolution, by using a domain nesting method.

GEARN calculates the atmospheric dispersion of radionuclides by tracing the trajectories of a large number (typically a million) of marker particles discharged from a release point. The horizontal model coordinates are the map coordinates, and the vertical coordinate is a terrain-following coordinate (z*-coordinate). Using meteorological fields predicted by MM5, GEARN calculates the movement of each particle affected by both advection due to mean wind and sub-grid scale turbulent eddy diffusion. The turbulent eddy diffusion is calculated by using the horizontal diffusion coefficient based on empirical formulations and vertical diffusion coefficient provided by MM5. The random movements of eddy diffusion are determined by a uniform random number. GEARN can work on two domains corresponding to MM5 nests. These two nested domains are calculated concurrently by different executables on a parallel computer, while marker particles moving across the domain boundary are exchanged between domains.

A part of the radioactivity in the air is deposited on the ground surface by turbulence and other dry processes (dry deposition) and precipitation (wet deposition). The decrease in radioactivity due to dry deposition is calculated for each particle with the dry deposition velocity (set as 3×10^{-3} m s^{-1} for iodine and 10^{-3} m s^{-1} for caesium and other nuclides based on the experimental data [10] without consideration of chemical form and particle size). The decrease in radioactivity of each particle by wet deposition is calculated by using the scavenging coefficient. Values and spatial distributions of

scavenging coefficient are determined from the precipitation intensity and distributions of rain, snow, and cloud predicted by MM5.

The air concentration in each Eulerian cell and total surface deposition are calculated by summing up the contribution of each particle to the cell at each time step, then averaged over and accumulated during the output time interval, respectively. The radioactive decay is calculated at each output time and integrated in both air concentration and surface deposition calculations, although decay chains are not considered. The radiological doses are calculated by multiplying the air concentration and deposition by conversion factors [11].

3. Analyses on the local and regional scale dispersions

3.1. Local scale dispersion

The formation process of high dose rate zone around north-west direction from the plant, which was clarified by aerial monitoring carried out after 16 March [12], was investigated by reconstructing the atmospheric dispersion of radionuclides during the period from 15 to 16 March, 2011 [5]. Three nested domains (domain-1: 100×100 grids with 9 km resolution, domain-2: 130×190 grids with 3 km resolution, domain-3: 190×190 grids with 1 km resolution) were used for MM5 calculation, and GEARN used inner two domains of MM5. Major radioactive species of ^{131}I, ^{132}Te (^{132}I), ^{134}Cs and ^{137}Cs (radioactivity ratio 1:2:0.1:0.1 assumed based on air sampling data) were considered in the calculation. GEARN code was modified to treat ^{132}I as ^{132}Te progeny nuclide and radioactive equilibrium between ^{132}Te and ^{132}I is assumed. The dry deposition velocity in GEARN was also modified to have five times larger value at grids with forested land surface considering the particle capture efficiency of tall canopy [13]. In the reconstruction of the event, revisions of MM5 and GEARN calculations were repeated by changing nudging parameters of four-dimensional data assimilation in MM5 and modifying temporal variation in release rates of radioactive materials manually until the simulation results of meteorological field and air dose rate became consistent with most of the measurements (Figure 1).

The simulation results revealed that two significant releases, 3×10^{15} Bq h^{-1} of ^{131}I from 7 to 10 Japan Standard Time (JST) and 4×10^{15} Bq h^{-1} of ^{131}I from 13 to 17 JST on 15 March, were necessary to reproduce the spatial distribution and temporal changes of measured air dose rates. Increases in air dose rates at the monitoring posts at the southwest and west directions of the plant were caused by the high-concentration plume released in the morning (Figure 1). The plume represented by concentration contours of radionuclides distributed in the southwest direction of the plant around 12 JST (Figure 2 (a)). At 14 JST, the plume encountered the rainband that covered the west and central areas, and caused some amounts of wet deposition around the middle area of Fukushima Prefecture. Southeasterly wind carried the plume discharged in the afternoon to the northwest of the plant (Figure 1). The precipitation covering the northern part of Fukushima scavenged this high-concentration plume and produced a significant amount of surface deposition at the northwest region of the plant in the evening (Figure 2 (b)). It is noted that the air dose rates rose up when the plume covered the posts and, even after the passage of plume, higher levels of air dose rates continued than those before the passage of plume (Figure 1). This fact means that radionuclides depositing on the ground surface maintain the high dose rate zones.

The dry deposition was dominant in the southwest region of the plant where no rainfall area appeared during the passage of plume. It gradually decreased with distance from the plant, i.e., with the decrease of ground-level concentration due to atmospheric dispersion. In contrast, the wet deposition dominated the high dose rate zones in the northwest region of the plant and the middle area of Fukushima Prefecture. These results indicate that the dry deposition contributes to the formation of

high dose rate zones close to the release point along the passage of plume and the wet deposition due to rainfall plays an important role in the formation of wide and heterogeneous high dose rate zones. It corresponds to the prior observational study on the Chernobyl nuclear accident addressing that the geographic pattern of deposited ^{137}Cs was closely related to that of rainfall[14].
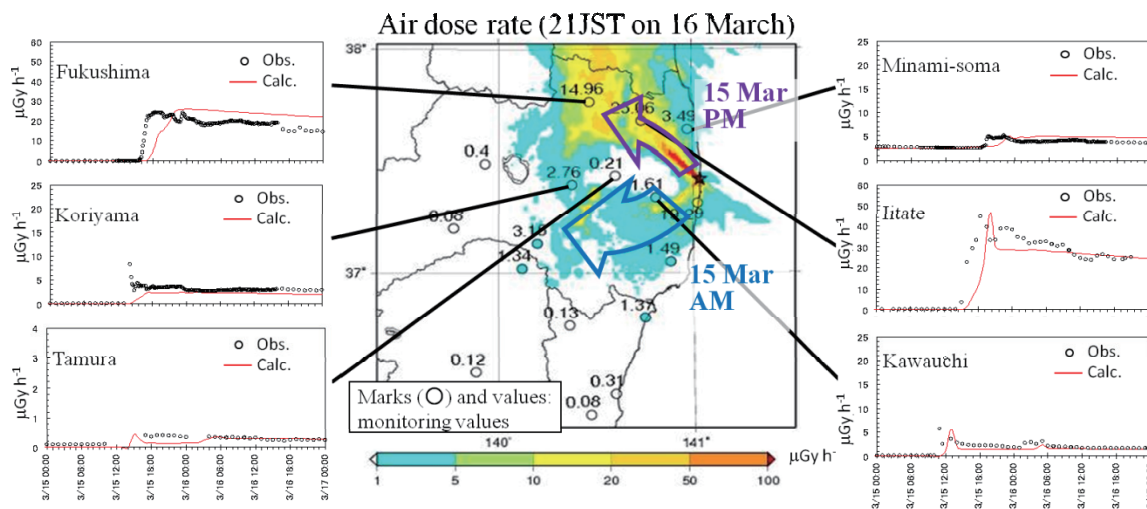
Figure 1. Distribution of air dose rate by calculation (shaded area) and monitoring (circles with values) at 21 JST on 16 March and comparisons of temporal changes of air dose rates between calculations and measurements at several monitoring posts. Arrows show movements of high concentration plumes discharged in the morning and afternoon on 15 March.
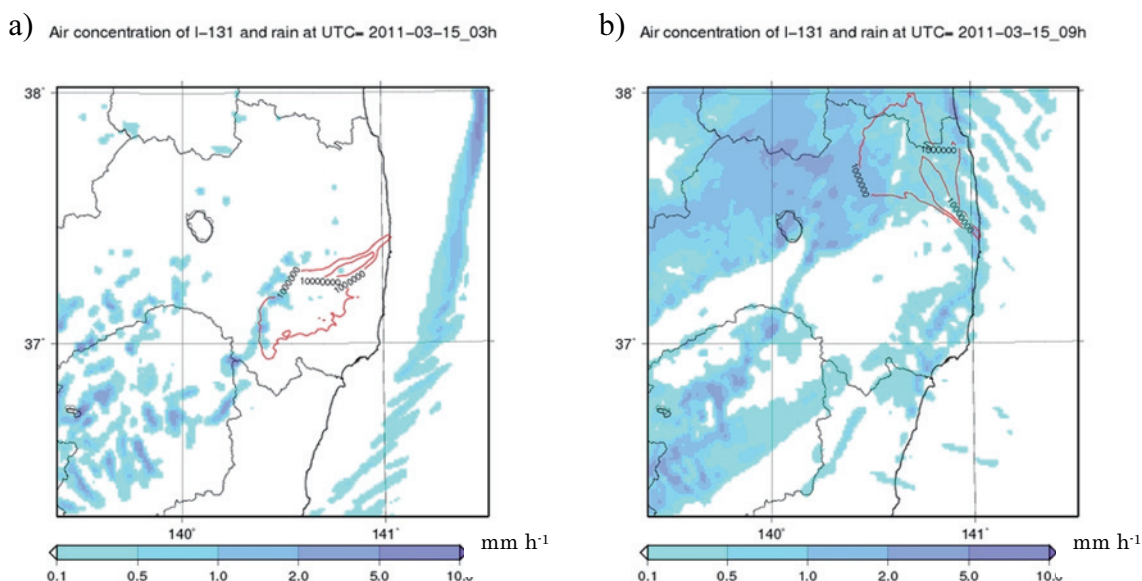
Figure 2. Vertical accumulated concentration (line contours (Bq m^{-2})) and rain intensity (shaded area) by calculation at (a) 12 JST and (b) 21 JST on 15 March

3.2. Regional scale dispersion

With the above analysis and further analysis for the early phase of the accident from 12 to 14 March, 2011[6], the release rates and total amounts of ^{131}I and ^{137}Cs discharged into the atmosphere were re-estimated for the period from 12 to 15 March, 2011. The preliminary estimated source term[4] was

revised by using the re-estimated one for this period. The validity of revised source term was also examined by comparing daily and monthly surface deposition (fallout) over land in eastern Japan between measurements and outputs from the regional scale atmospheric dispersion simulation by WSPEEDI-II [7]. The calculation period in the present study was from 5 JST on 12 March to 0 JST on 1 May. The computational domain (230×320 grids with 3 km resolution) includes the eastern area of Japan's main island, Honshu (Figure 3). The site of Fukushima Daiichi Nuclear Power Plant is located along the Pacific coast on the eastern edge of Fukushima Prefecture. To improve the prediction accuracy of meteorological fields, the four-dimensional data assimilation method using meteorological observation data was employed in the model calculations. Wind speed and direction observed at the Fukushima Daiichi and Fukushima Daini Nuclear Power Plants, and surface weather stations were used for data assimilation.

No.	Monitoring point (City)	Prefecture
1	Aomori	Aomori
2	Morioka	Iwate
3	Akita	Akita
4	Yamagata	Yamagata
5	Fukushima	Fukushima
6	Hitachinaka	Ibaraki
7	Utsunomiya	Tochigi
8	Maebashi	Gunma
9	Saitama	Saitama
10	Ichihara	Chiba
11	Shinjuku	Tokyo
12	Chigasaki	Kanagawa
13	Niigata	Niigata
14	Minami-uonuma	Niigata
15	Kofu	Yamanashi
16	Omaezaki	Shizuoka
17	Imizu	Toyama
18	Kakamigahara	Gifu
19	Yokkaichi	Mie
20	Fukui	Fukui

Figure 3. The simulation area and locations of the environmental monitoring points used for verification. Circles on the map indicate the sampling points for daily surface deposition in the area. Triangles show monitoring points for air dose rate used in section 4. Color shaded area shows the ground elevation. Solid lines over land in Japan show boundaries of prefectures. The names of the monitoring points and of prefectures where the monitoring points exist are denoted in the table.

Scatter diagrams and statistics of the daily surface deposition of ^{131}I and ^{137}Cs for calculations and for measurements from 18 to 31 March are shown in Figure 4 and Table 1, respectively. To evaluate the accuracy of the initial source term, statistics were calculated for data points for which calculations reproduced observed daily surface depositions greater than 0.1 Bq m^{-2}. The threshold value of 0.1 Bq m^{-2} was determined from the minimum values of measurements in the simulation area.
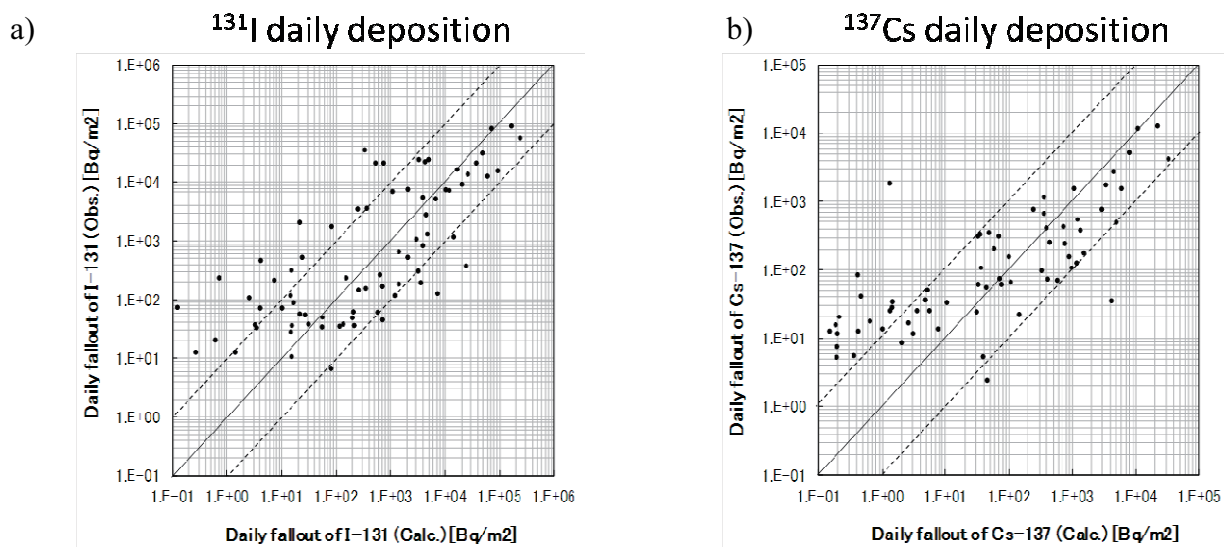
Figure 4. Scatter diagrams of the daily surface deposition of (a) ^{131}I and (b) ^{137}Cs (Bq m^{-2}) comparing measurements and calculations. Solid lines show 1:1 lines, and the areas between two dashed lines indicate the bands within a factor of 10.

Table 1 Statistics of daily surface deposition of ^{131}I and ^{137}Cs calculated from data points, for which both measured and calculated values were larger than 0.1 Bq m^{-2} during the period from 18 to 31 March, 2011. The values of FA2, FA5, and FA10 denote the percentage of calculations within factors of 2, 5, and 10 of the measurements, respectively.

Radionuclides	FA2 (%)	FA5 (%)	FA10 (%)	Correlation coefficients
^{131}I	22.4	48.7	65.8	0.75
^{137}Cs	26.5	48.5	70.6	0.72

It is shown that no apparent biases of under- or overestimation are seen in the scatter diagrams, except for calculated results with small amounts (less than 10 Bq m^{-2}) of surface deposition (Figure 4). The underestimation of these small values is considered to be caused mainly by errors in the meteorological and atmospheric dispersion calculations. Atmospheric dispersion simulations have uncertainties of at least a factor of 5 according to prior studies[15]. Considering these errors, it can be concluded that the source term is reasonable for the period when the radionuclides were dispersed and deposited over land in Japan. Figure 5 shows a comparison of calculations and measurements of the cumulative surface ^{137}Cs deposition from 5 JST on 12 March to 0 JST on 1 April. The calculations agreed well with the measurements at the sampling points.

The calculated cumulative surface ^{137}Cs deposition was also compared with that from the airborne monitoring [12]. The distribution of surface deposition, observed by airborne monitoring, were roughly reproduced, although some discrepancies were seen between calculations and measurements, e.g., it was underestimated in Tochigi and Gunma Prefectures, and overestimated in the north central part of the Fukushima Prefecture, the Miyagi Prefecture, in the southern part of the Iwate Prefecture, in particular. These discrepancies are thought to be caused mainly by errors in the meteorological and atmospheric dispersion calculations when the plume encountered precipitation in areas distant from the Fukushima Daiichi Nuclear Power Plant on 15 March. The cause of these discrepancies is discussed in the following section.

Deposition until the end of March
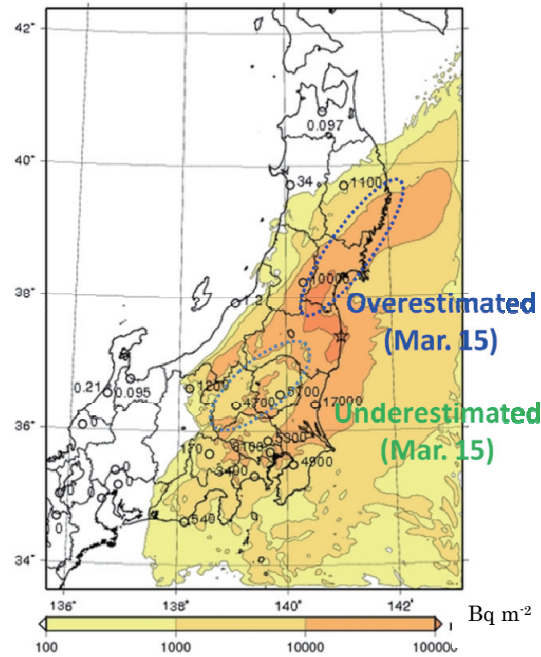
Figure 5. Comparison of the cumulative surface ^{137}Cs deposition (Bq m^{-2}) from calculations (colored shades) with the corresponding measurements (colored circles and values) during the period from 5 JST on 12 March to 0 JST on 1 April, 2011. Observation results that were not detectable are shown as 0 in the figures.

4. Consideration of deposition process

The cause of discrepancies between calculated and measured surface depositions of ^{137}Cs in section 3 was investigated. Uncertainties in the used source term, predicted meteorological field, and deposition process treated in dispersion calculations were conceivable factors for the discrepancies. In these factors, the source term for the period relating to these discrepancies was verified by the local-scale analysis [6], and the predicted meteorological field was confirmed to some extent by comparing with surface meteorological measurements and further improvements of the prediction seemed to be difficult. Thus, we carried out some parametric study to find out the main cause of the discrepancies with focus on uncertainties due to the wet deposition process in the dispersion model.

The wet deposition process is treated in the dispersion model GEARN in WSPEEDI-II as follows. The decrease in radioactivity of each particle (q_n) by wet deposition is calculated by

$$\frac{dq_n}{dt} = -\Lambda q_n \qquad (1)$$

where Λ is the scavenging coefficient based on the study by Brenk and Vogt[16], calculated at each grid cell for any nuclides except for noble gases in GEARN as

$$\Lambda = \alpha\left(F_c I_c + F_n I_n\right)^\beta \tag{2}$$

where α (=5×10^{-5}) and β (=0.8) are the empirical constants, I_c and I_n are precipitation intensities (mm h^{-1}) for convective and non-convective rains, respectively, predicted by MM5. F_c and F_n are unity at grid sells below convective and non-convective cloud heights, respectively, and zero at other grid cells. This formulation does not consider variations in scavenging coefficient due to not only chemical form and particle size of radionuclide but also rainout/washout and ice/liquid phases. Here, we focus on the influence of meteorological condition on scavenging process, i.e., consideration of rainout/washout, ice/liquid phases, and fog deposition. Although the scavenging process by ice/liquid phase for radionuclides is poorly known, the collection efficiency of aerosol particles by snow is generally considered to be smaller than that for rain [17], indicating the lower value of scavenging coefficient for ice phase. The fog deposition is not measured as precipitation in usual case and is not considered in GEARN calculation, although its amount and efficiency to carry airborne substances to the ground surface are substantially large over mountain forests [18-20].

As a preliminary evaluation of the influence of meteorological condition on scavenging process, test simulations were carried out by changing the scavenging coefficient in GEARN depending on the physical state of air moisture at each grid cell calculated by MM5. GEARN calculations were carried out by using the following temporal settings for the scavenging coefficient without changing any other conditions.

- Test 1: To consider the smaller scavenging by ice phase process, the scavenging coefficient had a smaller value ($\Lambda\times0.1$) at cells with ice phase of moisture.
- Test 2: To consider the larger scavenging by rainout process, the scavenging coefficient had a larger value ($\Lambda\times10$) at cells with cloud water.
- Test 3: To consider the fog deposition, the rain intensity was increased to have a value (0.5 mm h^{-1}) at cells where the air moisture had potential of fog occurrence and the rain intensity was smaller than 0.5 mm h^{-1}. In this test, the fog deposition was not treated actually but expressed its effect by increasing rain intensity.

Cumulative surface ^{137}Cs depositions during the 5-day period from 5 JST on 12 March to 9 JST on 17 March and those for the 20-day period from 5 JST on 12 March to 5 JST on 1 April calculated by the original GEARN, setting of Test 1, setting of Test 1+2, and setting of Test 1+2+3 are shown in Figures 6 and 7, respectively. By considering smaller scavenging by ice phase process (Test 1: comparisons between panels (a) and (b) in Figures 6 and 7), overestimation around the area from Miyagi Prefecture to the south of Iwate Prefecture was reduced. This improvement was attributed mainly to the smaller scavenging from the plume passing over this area at high altitude during the period from 15 to 16 March. The lower ^{137}Cs deposition at high elevation terrains by airborne monitoring [12] can be explained as the result of smaller scavenging by ice phase of moisture at the high altitude. The possibility that the plume did not flow over mountains due to the capping inversion may not be true at some areas, e.g., mountains around the border of Gunma and Niigata Prefectures, considering the fact that the plume passage with the same level of air dose rate was measured at both side of the mountains (Maebashi in Gunma Prefecture in the afternoon on 15 March [21] and Minami-uonuma in Niigata Prefecture in the late night on 15 March [22]). Despite the plume passage, higher ^{137}Cs deposition area was not shown at the high elevation mountains in Gunma Prefecture and all over Niigata Prefecture, where precipitation (mostly snowfall) was observed during the passage of plume. This deposition pattern can be also explained as the result of smaller scavenging by ice phase of moisture.

Surface deposition of Cs-137 at UTC=2011-03-17_00h

(a) *(b)*

Bq/m^2

10000 30000 60000 100000 300000 600000 1000000 3000000

Bq/m^2

10000 30000 60000 100000 300000 600000 1000000 3000000

Surface deposition of Cs-137 at UTC=2011-03-17_00h

Surface deposition of Cs-137 at UTC=2011-03-17_00h

(c) *(d)*

Bq/m^2

10000 30000 60000 100000 300000 600000 1000000 3000000

Bq/m^2

10000 30000 60000 100000 300000 600000 1000000 3000000
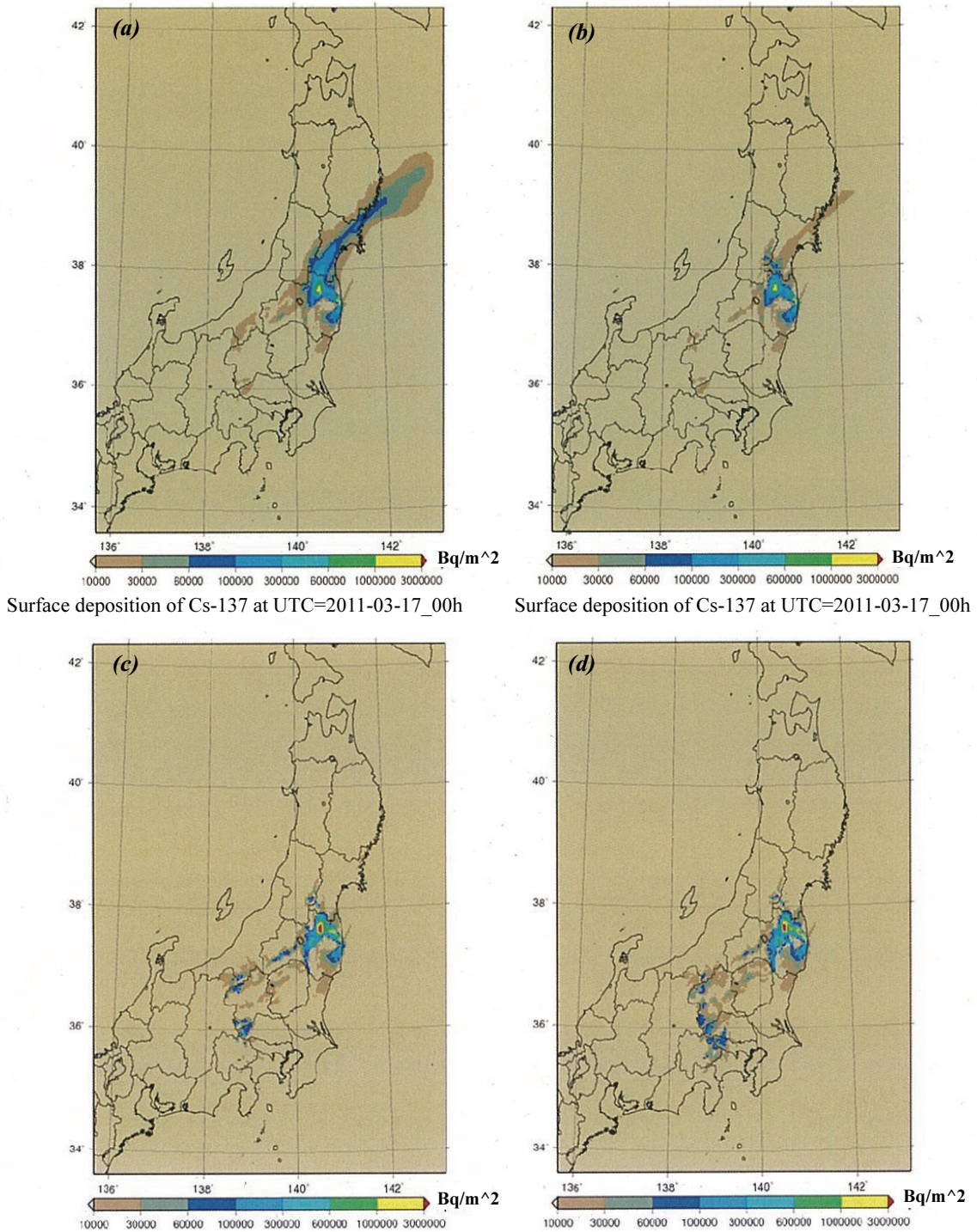
Figure 6. Cumulative surface ^{137}Cs deposition (Bq m^{-2}) during the period from 5 JST on 12 March to 9 JST on 17 March, 2011 calculated by (a) the original GEARN, (b) setting of Test 1, (c) setting of Test 1+2, and (d) setting of Test 1+2+3.

Surface deposition of Cs-137 at UTC=2011-03-31_20h   Surface deposition of Cs-137 at UTC=2011-03-31_20h
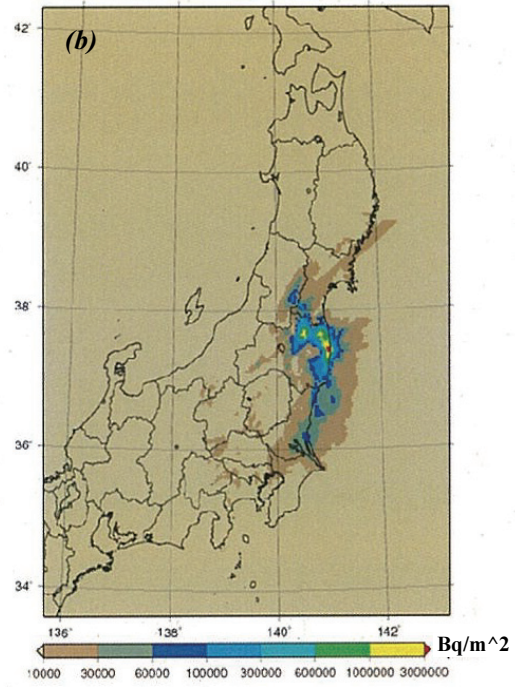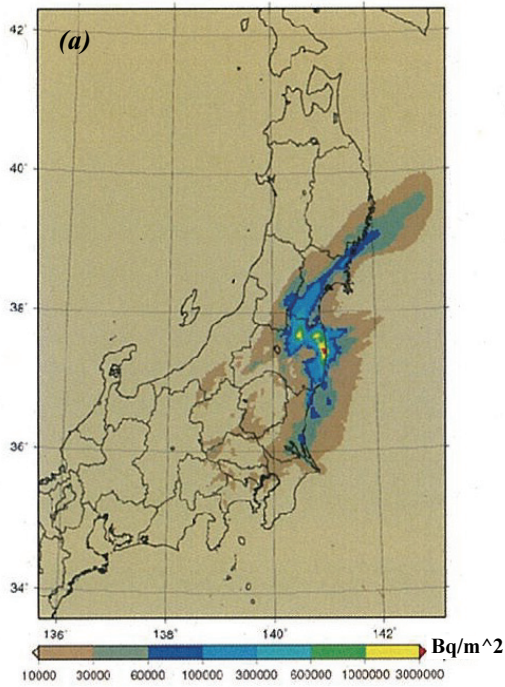
Surface deposition of Cs-137 at UTC=2011-03-31_20h   Surface deposition of Cs-137 at UTC=2011-03-31_20h
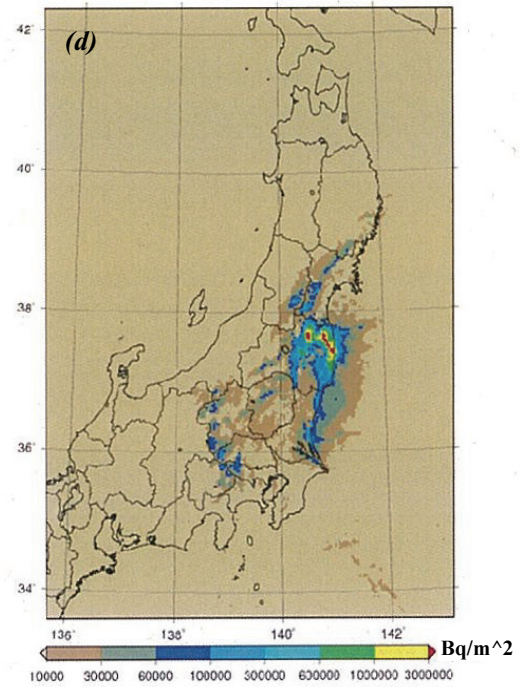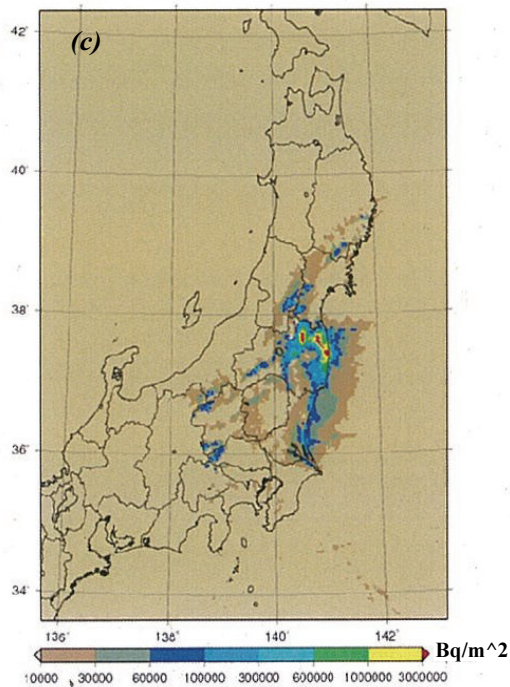
Figure 7. Cumulative surface ^{137}Cs deposition (Bq m^{-2}) during the period from 5 JST on 12 March to 5 JST on 1 April, 2011 calculated by (a) the original GEARN, (b) setting of Test 1, (c) setting of Test 1+2, and (d) setting of Test 1+2+3.

Changes in calculated ^{137}Cs deposition due to consideration of larger scavenging by rainout process (Test 2) is shown as the difference between panels (b) and (c) in Figures 6 and 7. By using large scavenging coefficient for cells with cloud water calculated by MM5, i.e., potential cells with rainout, underestimations of ^{137}Cs deposition in Tochigi and Gunma Prefectures on 15 March (Figure 6(b) and (c)) and those around the border between Miyagi and Iwate Prefectures, which was attributed to the deposition on 20 March, (Figure 7(b) and (c)) were reduced. However, the underestimation in Tochigi and Gunma Prefectures was still remained and much more ^{137}Cs deposition was necessary to better reproduce the ^{137}Cs deposition distribution by airborne monitoring. Therefore, another possible deposition process, i.e., fog deposition was considered in Test 3 (Figures 6 (d) and 7(d)). Since the meteorological conditions and low values in visibility data observed at the meteorological stations of Japan Meteorological Agency in Tochigi and Gunma Prefectures on 15 March indicated the fog occurrence, there was a possibility that the fog deposition contributed significantly to the formation of ^{137}Cs deposition distribution around this region. By comparing panels (c) and (d) in Figure 6, ^{137}Cs deposition in Tochigi and Gunma Prefectures increased with test 3, and this result indicated the importance of fog deposition. However, the fog deposition was not treated appropriately in this test calculation and it was difficult to evaluate the effect of fog deposition properly. Here, we only point out the necessity of adequate deposition modeling for fog deposition as the future work.

5. Conclusions

In order to assess the radiological dose to the public resulting from the Fukushima Daiichi nuclear power plant accident in Japan, the spatial and temporal distribution of radioactive materials in the environment have been reconstructed by WSPEEDI-II simulations. The formation processes of high dose rate zone around north-west direction from the plant and deposition over the eastern Japan area were reproduced by using the source term estimated by our previous studies. It was also shown in this study that most discrepancies between calculation and airborne monitoring of surface deposition of ^{137}Cs were reduced by modifying wet deposition processes from simple ones originally used in the dispersion model of WSPEEDI-II without changing any other conditions. These results indicated that the source term used in our simulations was reasonable and the model can reproduce the spatial and temporal distribution of radioactive materials in the environment more accurately by using different wet deposition scheme considering rainout/washout, ice/liquid phases, and fog deposition. Further examinations including parametric study on meteorological prediction are necessary to quantify and formulate wet deposition processes properly and to provide more accurate simulation for assessment of the radiological dose to the public, especially for the early phase of the accident when environmental monitoring was not carried out sufficiently.

References

1) MEXT, SPEEDI System for Prediction of Environmental Emergency Dose Information, Pamphlet of SPEEDI (2007).

2) H. Terada, H. Nagai, A. Furuno, T. Kakefuda, T. Harayama, M. Chino, Development of worldwide version of system for prediction of environmental emergency dose information: WSPEEDI 2nd version, Trans. At. Energy Soc. Jpn., 7 (2008) 257-267 [in Japanese].

3) H. Nagai, M. Chino, H. Terada, T. Harayama, T. Kobayashi, K. Tsuduki, K. Kim, A. Furuno, Numerical simulation system for environmental studies: SPEEDI-MP, JAEA-Research 2006-057, Japan Atomic Energy Agency (2006) [in Japanese].

4) M. Chino, H. Nakayama, H. Nagai, H. Terada, G. Katata, H. Yamazawa, Preliminary estimation of release amount of ^{131}I and ^{137}Cs accidentally discharged from the Fukushima Daiichi Nuclear Power Plant into the atmosphere, J. Nucl. Sci. Technol., 48 (2011) 1129-1134.

5) G. Katata, H. Terada, H. Nagai, M. Chino, Numerical reconstruction of high dose rate zones due to the Fukushima Dai-ichi Nuclear Power Plant accident, J. Environ. Radioactiv., 111 (2012) 2-12.

6) G. Katata, M. Ota, H. Terada, M. Chino, H. Nagai, Atmospheric discharge and dispersion of radionuclides during the Fukushima Dai-ichi Nuclear Power Plant accident. Part I: Source term estimation and local-scale atmospheric dispersion in early phase of the accident, J. Environ. Radioactiv., 109 (2012) 103-113.

7) H. Terada, G. Katata, M. Chino, H. Nagai, Atmospheric discharge and dispersion of radionuclides during the Fukushima Dai-ichi Nuclear Power Plant accident. Part II: Verification of the source term and analysis of regional-scale atmospheric dispersion, J. Environ. Radioactiv., 112 (2012) 141-154.

8) G. A. Grell, J. Dudhia, D. R. Stauffer, A description of the fifth-generation Penn State/NCAR Mesoscale Model (MM5), NCAR Tech. Note, NCAR/TN-398+STR, National Center for Atmospheric Research (1994).

9) H. Terada, M. Chino, Development of an atmospheric dispersion model for accidental discharge of radionuclides with the function of simultaneous prediction for multiple domains and its evaluation by application to the Chernobyl nuclear accident, Journal of Nucl. Sci. Technol., 45 (2008) 920-931.

10) G. A. Sehmel, Particle resuspension: a review, Environ. Int., 4 (1980) 107-127.

11) ICRP, Age-dependent Doses to Members of the Public from Intake of Radionuclides: Part 4 Inhalation Dose Coefficients, ICRP Publication 71, Ann. ICRP 25 (3-4) (1995).

12) MEXT and DOE, MEXT and DOE Airborne Monitoring, MEXT Web page, http://radioactivity.mext.go.jp/en/list/203/list-1.html (accessed 31 July 2012).

13) B. Sportisse, A review of parameterizations for modelling dry deposition and scavenging of radionuclides, Atmos. Environ., 41 (2007) 2683-2698.

14) M. J. Clark, F. B. Smith, Wet and dry deposition of Chernobyl releases, Nature, 332 (1988) 245-249.

15) H. Terada, A. Furuno, M. Chino, Improvement of Worldwide Version of System for Prediction of Environmental Emergency Dose Information (WSPEEDI), (I) New combination of models, atmospheric dynamic model MM5 and particle random walk model GEARN-new, J. Nucl. Sci. Technol., 41 (2004) 632-640.

16) H. D. Brenk, K. J. Vogt, The calculation of wet deposition from radioactive plumes, Nuclear Safety, 22 (1981) 362-371.

17) L. D. Rotstayn, U. Lohmann, Simulation of the tropospheric sulfur cycle in a global model with a physically based cloud scheme, J. Geophys. Res., 107 (2002) 4592.

18) M. Igawa, K. Matsumura, H. Okochi, High frequency and large deposition of acid fog on high elevation forest, Environ. Sci. Technol., 36 (2002) 1–6.

19) P. Herckes, R. Wendling, N. Sauret, P. Mirabel, H. Wortham, Cloud water studies at a high

elevation site in the Vosges Mountains (France), Environ. Pollut., 117 (2002) 169–177.

20) C. A. Lange, J. Matschullat, F. Zimmermann, G. Sterzik, O. Wienhaus, Fog frequency and chemical composition of fog water — A relevant contribution to atmospheric deposition in the eastern Erzgebirge, Germany, Atmos. Environ., 37 (2003) 3731–3739.
21) Gunma Prefecture, Prefectural Radiation Monitoring, Gunma Prefecture Web page, http://www.pref.gunma.jp/contents/000185131.pdf (accessed 31 July 2012).
22) Niigata Prefecture, Prefectural Radiation Monitoring, Niigata Prefecture Web page, http://www.pref.niigata.lg.jp/HTML_Article/918/480/20110425_2,0.pdf (accessed 31 July 2012).

Atmospheric Transport and Deposition Modeling of Radioactive Materials: Current Status and Future Tasks

Toshimasa OHARA, Yu MORINO

National Institute for Environmental Studies, 16-2 Onogawa, Tsukuba, IBARAKI, 305-8506, Japan

Abstract

We simulated the spatial and temporal variations of ^{131}I and ^{137}Cs around the Fukushima Daiichi nuclear power plant (FDNPP) for the period of March 11–April 30, 2011, by using a chemical transport model. The model domain covered the region of 700×700 km^2 at a 3 km grid resolution. The model reproduced the observed total amount and spatial distribution of ^{137}Cs deposition in East Japan by the airborne monitoring survey and the observed temporal variations of deposition rates and atmospheric concentration of ^{131}I and ^{137}Cs. Budget analysis indicated that approximately 12% of ^{131}I and 25% of ^{137}Cs were deposited over land in Japan, and the rest was deposited to the ocean or transported out of the model domain. Most of the radioactive materials emitted from the FDNPP were deposited or transported out of the model region within a few days. Even though there are still large uncertainties in this simulation, agreement between the observed and simulated results indicates the validity of the model, and the model developed by this study will be an important tool for understanding the behavior of radionuclides and for estimating the exposure to radiation.

Keywords: chemical transport model; radionuclide; deposition

1. Introduction

A nuclear accident in Fukushima Daiichi Nuclear Power Plant (FDNPP), accompanied with the Great Tohoku Earthquake and tsunami on March 11 2011, resulted in enormous amounts of radionuclide emissions into atmosphere and ocean. Radionuclides (particularly iodine-131 (^{131}I) and cesium-137 (^{137}Cs)) have harmful impacts on human health through the contamination of air, water, soils, and foods. To understand the spatial and temporal variations of radioactive materials in the atmosphere, numerical simulations play important roles. For example, many numerical simulations were conducted and helped to understand the atmospheric behaviors of radioactive materials after the Chernobyl nuclear accident in 1986.

In this study, we simulated transport and deposition processes of ^{131}I and ^{137}Cs using a chemical transport model for air pollutants. At first, we compared the simulated atmospheric deposition rates and atmospheric concentrations of ^{131}I and ^{137}Cs with observation and evaluated the model reproducibility. Then, we assessed the budget of radioactive materials emitted from FDNPP.

2. Methodology

We simulated distributions of ^{131}I and ^{137}Cs using a three-dimensional CTM, the Models-3 Community Multiscale Air Quality (CMAQ) [1] for the period of March 11 − April 30, 2011. In this simulation, we calculated processes of horizontal and vertical advection, horizontal and vertical diffusion, emissions, dry and wet deposition, and radioactive decay. Chemical and aerosol processes are not calculated as these processes of radioactive materials are highly unknown [2]. We assume that gaseous fraction of ^{131}I is 80%, ^{137}Cs is all in particulate phase, and diameters of particulate matters are

set to be 1 μm both for ^{131}I and ^{137}Cs based on the results of measurements at Tsukuba after the accident. Deposition rate of gaseous ^{131}I is assumed to be the same with sulfur dioxide as same with previous studies [2]. Radioactive decay of ^{131}I (half-lifetime of 8.02 days) was calculated while decay of ^{137}Cs (half-lifetime of 30.2 years) was neglected in this simulation. Model domain covers most of Tohoku (including #1 – #5 prefectures in Figure 1) and Kanto (#6 – #12 prefectures in Figure 1) regions (700 × 700 km^2) at a 3-km grid resolution and a 34-layer vertical structure with a surface layer thickness of about 60 m (Figure 1). Meteorological fields were calculated using the Weather Forecast and Research (WRF) Model version 3.1 [3]. The analysis nudging was conducted using the three-dimensional meteorological fields from Japan Meteorological Agency Meso-Scale Model datasets available with 5 × 5 km^2 horizontal resolution for every 3 h. The model and the simulation conditions are basically same as our previous paper [4] except for grid resolution. Emission data from FDNPP was taken from the Terada et al. [5]. Additionally, we used the emission data from the Stohl et al. [6] to examine the model sensitivity due to the emission data. We set that both ^{131}I and ^{137}Cs were emitted in the bottom layer of the model. Initial and boundary conditions of radioactive materials are set to zero.

Daily deposition rates of ^{131}I and ^{137}Cs are monitored over 46 prefectures over Japan from March 18, 2011, using bulk samplers by the Ministry of Education Culture Sports Science and Technology, Japan (MEXT) [7]. Each prefecture in Japan possesses one monitoring station. Bulk samplers collect materials from dry deposition in addition to those from wet deposition, though collection efficiency of bulk samplers for trace gases and submicron particles is substantially different from that of a natural landscape [8]. We consider that deposition rates measured using bulk samplers were in between wet deposition and total (i.e., dry plus wet) deposition rates [8].

In addition, atmospheric concentrations of particulate radionuclides were continuously measured at a Tsukuba site ("T" in Figure 1) from March 15 by High Energy Accelerator Research Organization [9] and at a Chiba site ("C" in Figure 1) by the Japan Chemical Analysis Center (JCAC) [10]. High-volume sampler was used for bulk aerosol sampling. The sampling periods were 3 – 48 hours at Tsukuba and 24 hours at Chiba. Also, the spatial distribution of total deposition of ^{137}Cs in East Japan was measured from October 22 to November 5, 2011, by the airborne monitoring survey by MEXT [11].
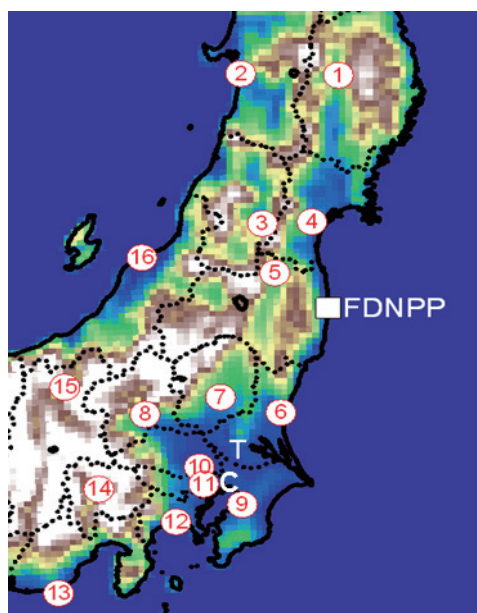
Figure 1. Model domain with terrain height. Numbered red circles are measurement sites in 16 prefectures. A white square shows the site of Fukushima Daiichi Nuclear Power Plant (FDNPP) and a white character, T and C, indicates a Tsukuba and Chiba site, respectively.

3. Results and discussion

3.1. Comparison between observed and simulated results

We compared the simulated deposition rates of ^{131}I and ^{137}Cs with observation over monitoring sites in March 2011 (Figure 2). Figure 2(b) and 2(c) shows the modeled ^{137}Cs deposition based on the emission data from Terada et al. [5] (Case T) and Stohl et al. [6] (Case S), respectively. For this comparison, we selected monitoring sites in 15 prefectures shown in Figure 1. Overall, despite some discrepancies, both the simulated total and wet deposition rates mostly agreed with observed deposition rates of ^{131}I and ^{137}Cs over the 15 prefectures within one order of magnitude. The model performance in this study is comparable to the model performance for the Chernobyl-case simulations [12, 13], although the temporal and spatial scales between this simulation and the Chernobyl-case simulations are different. For the "Case S", the model underestimates though the total ^{137}Cs emission estimated by Stohl et al. [6] is larger than that by Terada et al. [5]. This indicates the estimation of emission amount as well as temporal variation of emission is very important for the model simulation of atmospheric behaviors of radionuclides.
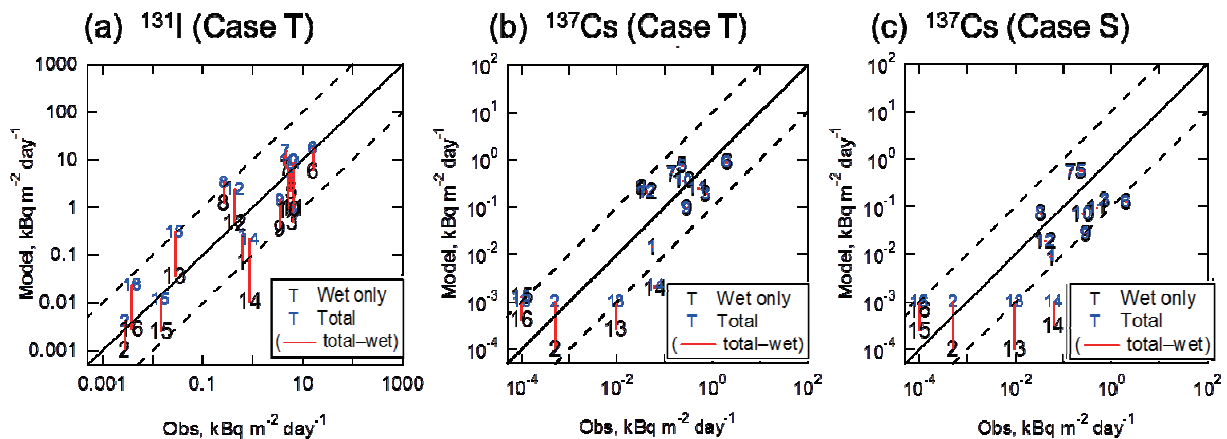
Figure 2. Observed and simulated deposition rates of ^{131}I (a) and ^{137}Cs (b, c) at measurement sites shown in Figure 1 averaged over March 11-30, 2011. Figure 2 (b) and (c) is the modeled results based on the emission estimate from Terada et al. [5] and Stohl et al. [6], respectively.

Simulated deposition rates of ^{131}I and ^{137}Cs increased in Fukushima (#5) and its adjacent prefectures (Yamagata (#3), Miyagi (#4), Ibaraki (#6), and Tochigi (#7)) on March 15–17 and 20–26 (Figure 3). During the other periods, deposition rates of ^{131}I and ^{137}Cs were low over the most observational stations. This behavior roughly agreed with the observation, although simulated deposition peak on March 15–17 cannot be verified because of lack of observation. Observed atmospheric concentrations of particulate ^{131}I and ^{137}Cs in Tsukuba showed the similar behavior (Figure 4(a)). It should be noted that the model largely underestimated observed peak of ^{137}Cs concentration on March 21–22. Similar behavior was found in deposition rates at a monitoring site in Ibaraki prefecture (#6), in which the Tsukuba site locates (Figure 1). By contrast, deposition rates of ^{137}Cs at sites in the north area of Kanto were overestimated by the model. Thus, these discrepancies between observation and the model would be partly caused by uncertainties in transport and deposition processes in addition to uncertainties in emissions. During March 15–17 and 21–23, when deposition rates increased over the areas around Fukushima, northeasterly, easterly, or southeasterly winds associated with the transient cyclone transport radioactive materials from FDNPP to inland areas. In addition, precipitations were observed on March 15–17 and 21–23, when transient cyclone passed over Japan (Figure 3), and thus,

radioactive materials effectively deposited over lands by wet processes. By contrast, on March 17–20 when anticyclone dominated over Fukushima, westerly or northwesterly dominated and radioactive materials were transported predominantly to the Pacific Ocean.

The modeled atmospheric concentrations are compared with the observation at Tsukuba and Chiba sites (Figure 4). The model can catch the temporal variation of observed atmospheric concentration though the model underestimates in the period of lower concentration of ^{131}I. The underestimation should be solved in future. There is less difference in the temporal variation of atmospheric concentration between "Case T" and "Case S".

Yamagata (#3)
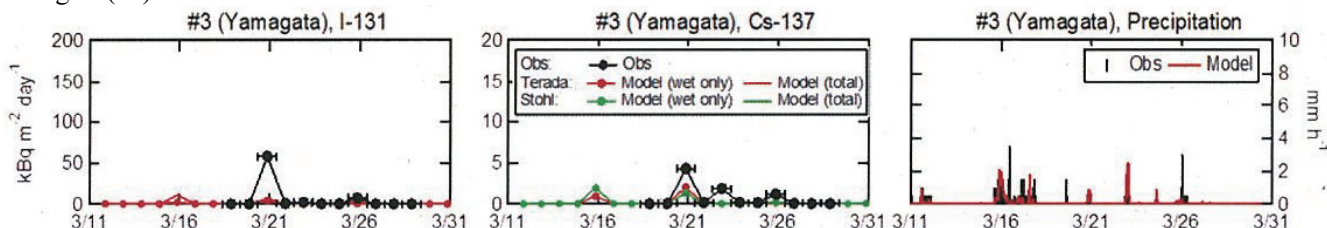
Miyagi (#4)
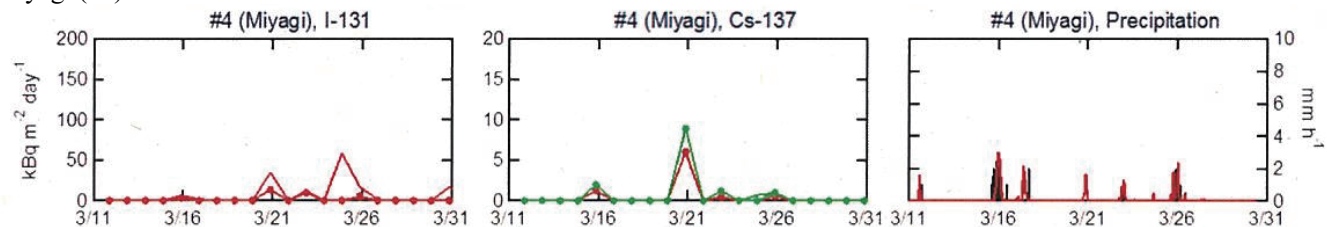
Fukushima (#5)
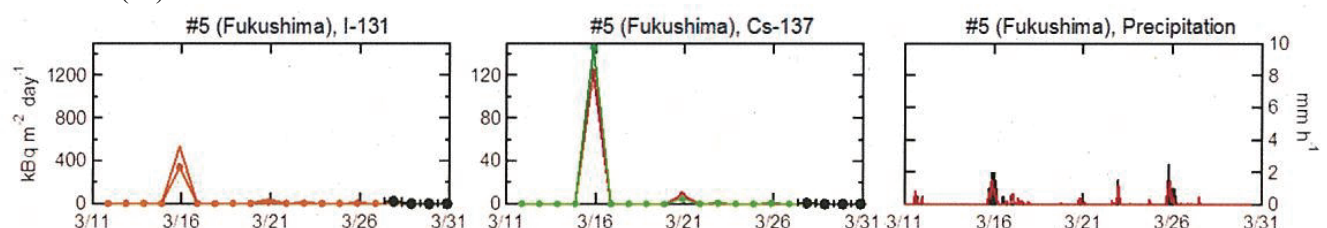
Ibaraki (#6)
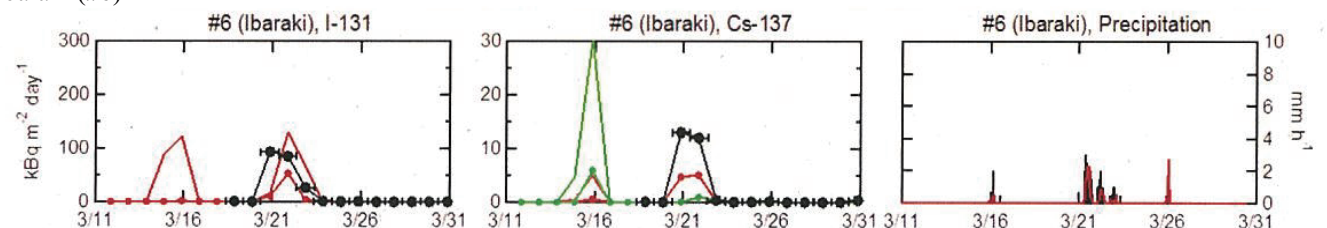
Tochigi (#7)
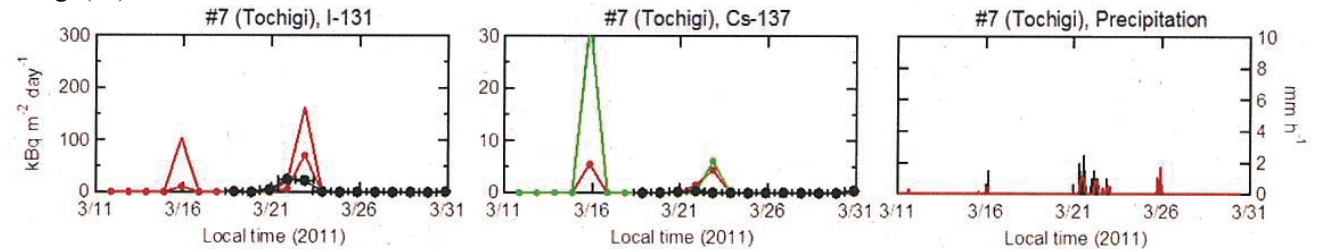
Figure 3. Observed and simulated deposition rates of ^{131}I (left) and ^{137}Cs (center) and precipitation rates (right) at measurement sites (#3 - #7 shown in Figure 1).
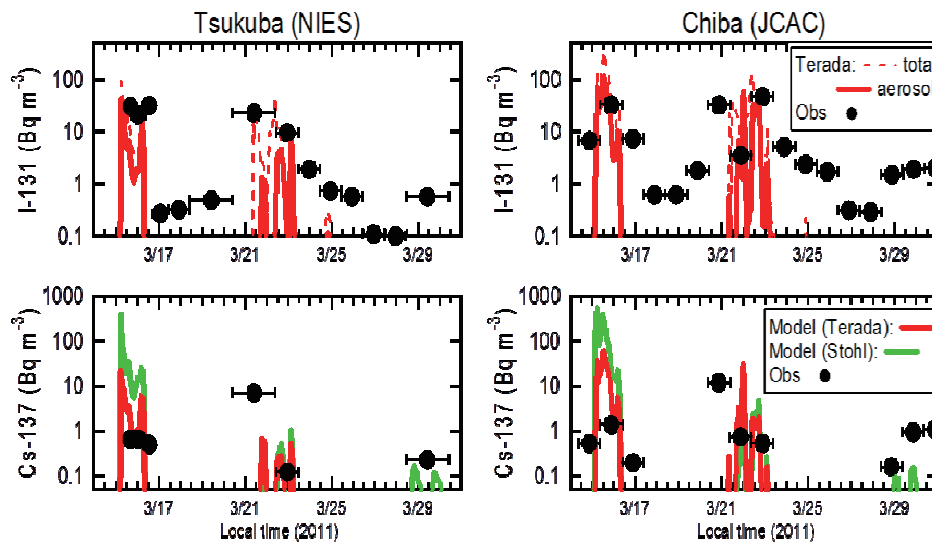
Figure 4. Observed and simulated atmospheric concentrations of ^{131}I and ^{137}Cs at measurement sites at Tsukuba and Chiba shown by a white character, T and C, in Figure 1, respectively.

3.2. Spatial distribution and budget of radioactive materials

Figure 5 demonstrates the simulated spatial distribution of average atmospheric concentrations at surface and accumulated deposition densities of ^{131}I and ^{137}Cs over March 11–April 30, 2011. Deposition densities of ^{131}I are the highest in Fukushima, followed by Ibaraki and other prefectures in Kanto Area. ^{137}Cs deposition densities were also the highest in Fukushima, and second largest in Miyagi. High deposition areas of both ^{131}I and ^{137}Cs extend from a Fukushima prefecture to northwest and southerly direction (Figure 5). This pattern reflected the wind and precipitation patterns during the period of high emissions. These patterns in the modeled spatial distribution of total deposition of ^{137}Cs are consistent with the measurement by the airborne monitoring survey by MEXT (Figure 6).

We assessed the budget of ^{131}I and ^{137}Cs in the model domain by quantifying the contributions of individual processes, such as advection, diffusion, emissions, and depositions. In the model domain, dominant loss processes of ^{131}I were dry and wet depositions on March 15 and advection after March 16. Outflow of ^{131}I from the model domain predominantly occurred through the eastern boundary, though outflow from the northern and southern boundary also occurred. Wet deposition of ^{137}Cs had large contributions on March 15–16 and 20–21, and advection dominated the loss processes during the other periods. In the "Case T", 12% of ^{131}I and 25% of ^{137}Cs emitted from FDNPP were deposited over the land of Japan in March to April 2011 (Table 1). It is found that the modeled deposited amount (2.2 PBq) for ^{137}Cs over the land in Japan is consistent with the observed value (2.7 PBq) by the airborne monitoring survey by MEXT. About 22% of ^{131}I and 25% of ^{137}Cs were deposited over ocean in the model domain, and 67% of ^{131}I and 51% of ^{137}Cs emitted from FDNPP were transported to outside of the model domain. On the other hand, the modeled results in the "Case S" shows that 13% of ^{137}Cs emitted from FDNPP were deposited over the land of Japan in March to April 2011 and the deposited amount (4.5 PBq) is overestimated (Table 1). This may suggest that the emission data by Stohl et al. [6] has some problems in the emission amount and/or temporal variation.

These fractions do not change even though total emission amount changes, while they would change if temporal emission patterns change. Temporal emission patterns had large impact on the budget of radioactive materials. On March 15–17 and 19–23, when transient cyclone passed over Japan, a large part of ^{131}I and ^{137}Cs emitted from FDNPP deposited over land in the model domain, while deposition amount over land were much smaller in the other period, when westerly wind dominated.

Thus, budget of radionuclides estimated in this study largely changes when temporal emission profiles change. Accurate estimation of emission amount and temporal variation is very important for the model simulation of atmospheric behaviors of radionuclides.
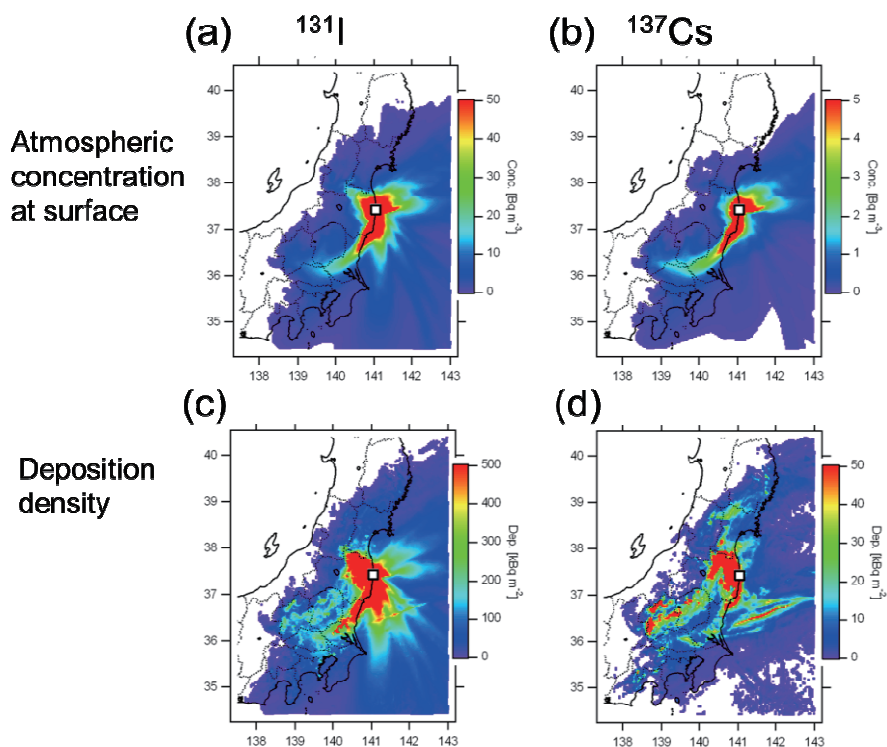
Figure 5. Spatial distributions of average atmospheric concentrations at surface and accumulated deposition densities of ^{131}I and ^{137}Cs simulated by CMAQ averaged over March 11–April 30, 2011.
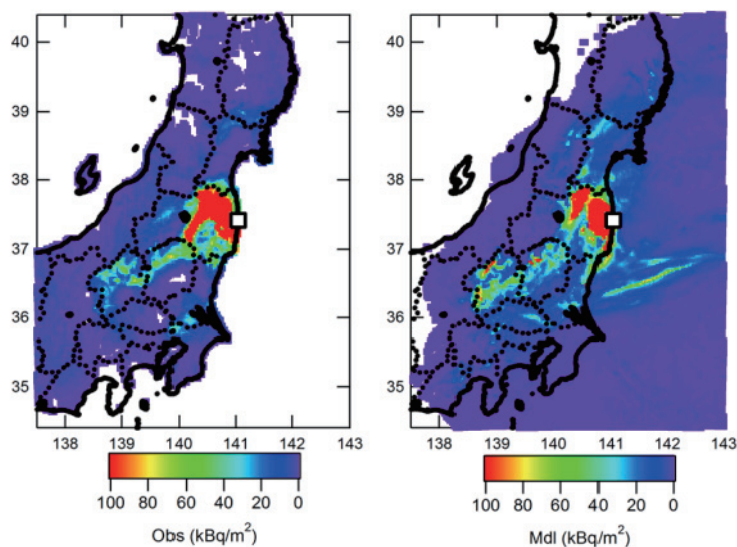
Figure 6. Observed (left) and simulated (right) distributions of accumulated deposition densities of ^{137}Cs. The observed distribution was measured by the airborne monitoring survey by MEXT. The simulated distribution was calculated by CMAQ accumulated over March 11–April 30, 2011.

Table 1 ^{131}I and ^{137}Cs budget in model domain for the period of March 11–April 30, 2011 (PBq)

	Emission data	Emission	Deposition in land	Deposition in ocean	Outflow
^{131}I	Terada et al. (2012)	117.8	14.0 (11.9%)	25.4 (21.5%)	78.4 (66.6%)
^{137}Cs	Terada et al. (2012)	8.8	2.2 (24.8%)	2.2 (24.7%)	4.4 (50.5%)
	Stohl et al. (2011)	35.8	4.5 (12.6%)	4.3 (12.0%)	27.0 (75.4%)

Note: The value in parenthesis denotes the ratio to the total emissions.

4. Conclusions

We simulated the spatial and temporal variations of ^{131}I and ^{137}Cs around the FDNPP for the period of March 11–April 30, 2011, by using a chemical transport model (CMAQ). The model domain covered most of the Tohoku region and the Kanto region of Japan (700 × 700 km^2) at a 3 km grid resolution and a 34 layer vertical structure with a surface layer thickness of about 60 m. We calculated meteorological fields by using the Weather Research and Forecasting Model (WRF) version 3.1 driven by the three-dimensional meteorological fields from the Japan Meteorological Agency Meso-Scale Model datasets. The model and the simulation conditions are basically same as Morino et al. [4] except for grid resolution. Emission data from the FDNPP were taken from Terada et al. [5] and Stohl et al. [6].

The model reproduced the fundamental feature of observed spatial distribution of total deposition of ^{137}Cs in East Japan by the airborne monitoring survey by MEXT. Additionally, the model roughly reproduced the spatiotemporal variations of deposition rates of ^{131}I and ^{137}Cs over 15 prefectures in Japan (60–400 km from the FDNPP) and the temporal variations of atmospheric concentration measured at two sites in the Kanto region, although there were some discrepancies between the simulated and observed data, most likely due to uncertainties in the treatment of emission, transport, and deposition processes in the model.

Budget analysis based on the emission estimate from Terada et al. [5] indicated that approximately 12% of ^{131}I and 25% of ^{137}Cs were deposited over land in Japan, and the rest was deposited to the ocean or transported out of the model domain. Most of the radioactive materials emitted from the FDNPP were deposited or transported out of the model region within a few days and did not stay in the atmosphere in the model domain. Even though there are still large uncertainties in this simulation, agreement between the observed and simulated results indicates the validity of the model, and the atmospheric transport and deposition model developed by this study will be an important tool for understanding the behavior of radionuclides emitted from the FDNPP and for estimating the exposure to radiation.

Acknowledgement

References

1) Byun, D., and K. L. Schere, Review of the governing equations, computational algorithms, and other components of the models-3 Community Multiscale Air Quality (CMAQ) modeling system, Appl. Mech. Rev., 59 (2006), 51-77.

2) Sportisse, B., A review of parameterizations for modelling dry deposition and scavenging of radionuclides, Atmos. Environ., 41 (2007), 2683-2698.

3) Skamarock, W. C., J. B. Klemp, J. Dudhia, D. O. Gill, D. M. Barker, M. G. Duda, X. Y. Huang, W. Wang, and J. G. Powers, A Description of the Advanced Research WRF Version 3, Rep. NCAR/TN.475+STR, Natl. Cent. for Atmos. Res. , Boulder, Colo (2008).

4) Morino, Y., T. Ohara, and M. Nishizawa, Atmospheric behavior, deposition, and budget of radioactive materials from the Fukushima Daiichi nuclear power plant in March 2011, Geophys. Res. Lett., 38 (2011), L00G11, doi:10.1029/2011GL048689.

5) Terada, H., G. Katata, M. Chino, and H. Nagai, Atmospheric discharge and dispersion of radionuclides during the Fukushima Dai-ichi Nuclear Power Plant accident. Part II: verification of the source term and analysis of regional-scale atmospheric dispersion, J. Environ. Radioact., 112 (2012), 141-154.

6) Stohl, A., P. Seibert, G. Wotawa, D. Arnold, J. F. Burkhart, S. Eckhardt, C. Tapia, A. Vergas, and T. J. Yasunari, Xenon-133 and caesium-137 releases into the atmosphere from the Fukushima Dai-ichi nuclear power plant: determination of the source term, atmospheric dispersion, and deposition, Atmos. Chem. Phys. Discuss., 11 (2011), 28319-28394.

7) Ministry of Education Culture Sports Science and Technology, Reading of radioactivity level in fallout by prefecture (March 2011), http://radioactivity.mext.go.jp/en/list/194/list-201103.html.

8) Staelens, J., A. De Schrijver, P. Van Avermaet, G. Genouw, and N. Verhoest, A comparison of bulk and wet-only deposition at two adjacent sites in Melle (Belgium), Atmos. Environ., 39 (2005), 7-15.

9) High Energy Accelerator Research Organization, Radiation monitoring at KEK, Measurement result of airborne nuclide and air radiation level in Tsukuba area (2011), http://legacy.kek.jp/quake/radmonitor/index-e.html.

10) Japan Chemical Analysis Center, http://www.jcac.or.jp/lib/senryo_lib/taiki_kouka_back.pdf, (2012). (in Japanese)

11) Ministry of Education Culture Sports Science and Technology, Results of the Fourth Airborne Monitoring Survey by MEXT (December 16, 2011), http://radioactivity.mext.go.jp/en/contents/4000/3179/24/1270_1216.pdf.

12) Brandt, J., J. H. Christensen, and L. M. Frohn, Modelling transport and deposition of caesium and iodine from the Chernobyl accident using the DREAM model, Atmos. Chem. Phys., 2 (2002), 397-417.

13) Davoine, X., and M. Bocquet, Inverse modelling-based reconstruction of the Chernobyl source term available for long-range transport, Atmos. Chem. Phys., 7 (2007), 1549-1564.

National Atmospheric Release Advisory Center Dispersion Modeling During the Fukushima Daiichi Nuclear Power Plant Accident

Gayle SUGIYAMA, John NASSTROM, Kevin FOSTER, Brenda POBANZ, Matthew SIMPSON, Phil VOGT, Fernando ALUZZI Steve HOMANN

Lawrence Livermore National Laboratory
7000 East Avenue L-103 Livermore CA 94550

Abstract

The U.S. Department of Energy / National Nuclear Security Administration (DOE / NNSA) deployed personnel to Japan and stood up expert teams to aid in assessing the consequences of releases from the Fukushima Daiichi Nuclear Power Plant. The National Atmospheric Release Advisory Center (NARAC) was activated as the DOE/NNSA's operational plume modeling capability. NARAC provides real-time atmospheric dispersion predictions of air concentrations and ground contamination as well as dose resulting from a radiological incident. This paper briefly summarizes NARAC response activities during the Fukushima emergency and then discusses NARAC source reconstruction efforts. A range of source estimates were found to be consistent with the available data, with estimates varying depending on assumptions about the release rates (e.g., time-varying vs. constant-rate), the radionuclide mix, the meteorology, and/or the radiological data used in the analysis. However, NARAC results were consistent within expected uncertainties and were found to agree with other studies that used different models, source estimation methodologies, and radiological measurement data sets. Results from a preliminary model sensitivity study of the dependence of calculated thyroid dose on iodine partitioning between gas and particulate phases also are presented in this paper.

Keywords: Fukushima Daiichi; reactor accident; atmospheric dispersion modeling; meteorological modeling; source estimation; dose exposures; environmental monitoring

1. Introduction

Following the 2011 Tohoku earthquake and tsunami, the U.S. Department of Energy / National Nuclear Security Administration (DOE/NNSA) deployed personnel to Japan and activated expert teams across the DOE laboratory complex to aid in assessing the consequences of releases from the Fukushima Daiichi Nuclear Power Plant [1]. DOE/NNSA personnel provided predictive modeling, air and ground monitoring (including the deployment of the Aerial Measuring System to Japan), sample collection, *in situ* field and laboratory sample analysis, dose assessment, and data interpretation. The National Atmospheric Release Advisory Center (NARAC) at Lawrence Livermore National Laboratory (LLNL) was activated by the DOE/NNSA on March 11, 2011. The center remained on active operations through late May when the DOE/NNSA ended its deployment to Japan. Over 32 NARAC staff members, supplemented by other LLNL scientists, invested over 5000 person-hours of time and generated over 300 analyses during the response.

NARAC simultaneously supported a number of Fukushima-related modeling activities in response to a variety of requests for meteorological and dispersion analyses including:

- Daily weather forecasts and hypothetical atmospheric dispersion predictions to provide on-going situational awareness of meteorological conditions and to inform planning for U.S. field data collection and operations

- Estimates of possible dose in Japan resulting from hypothetical scenarios developed by the U.S. Nuclear Regulatory Commission (NRC) that were used to inform U.S. federal government considerations of possible actions that might be needed to protect U.S. citizens in Japan
- Predictions of potential plume arrival times and dose for U.S. locations
- Plume model refinement and source estimation based on meteorological analyses, atmospheric dispersion modeling, and available field data

An overview of NARAC response activities including a description of the first three activities listed above is available in Sugiyama et al., 2012 [2] and will not be replicated here. This paper discusses NARAC source estimation and provides some additional material on potential dose exposures. The paper concludes with results from a preliminary investigation of changes in predicted thyroid dose resulting from different assumptions regarding iodine partitioning between gas and particle phases.

2. Source Estimation

As part of standard response procedures during a U.S. radiological release, NARAC provides preliminary model predictions to guide initial measurement surveys. In turn, field teams conduct air and ground monitoring and collect samples for laboratory analysis. These data are uploaded into DOE databases for quality assurance by the U.S. DOE/NNSA Consequence Management Home Team (CMHT) and transferred electronically to NARAC. NARAC uses specialized software to select, filter, and both graphically and statistically compare measurements and model predictions. Modeling analyses are then refined based on the available data and the new predictions are provided to the field teams. This iterative process continues until the impacts of the release are characterized. Although this standard procedure was altered during the Fukushima response due to the prioritization of other modeling requests, as well as the unique aspects of the DOE/NNSA response to the Fukushima Dai-ichi accident, NARAC conducted an initial set of source reconstruction estimates that are discussed in this paper.

NARAC analysts reconstructed source estimates by optimizing the overall graphical and statistical agreement of model predictions with dose-rate measurements by comparing data and model values paired in space and time. Source reconstruction for the Fukushima accident was complicated by the long duration of the releases, emissions from multiple reactor units, unknown reactor and spent fuel pool conditions, rapidly-changing meteorological conditions, complicated geography and land-sea interfaces, and the relatively limited measurement data available during critical stages of the releases.

2.1. Meteorological Conditions

Rapidly changing atmospheric conditions presented a significant modeling challenge during the Fukushima response. NARAC meteorological analyses were developed from observational data provided by the Japan government and/or numerical weather predictions generated using the U.S. community Weather Research and Forecast (WRF) model [3] driven by NOAA Global Forecast System (GFS) model output [4]. The WRF model was used in both pure forecast mode and in four dimensional data assimilation (FDDA) simulations that incorporated Japanese meteorological observations. The latter simulations used analysis nudging [5] for the outer model domains (27, 9, and 3 km grid spacing) and observational nudging [6] for the innermost domain (1 km grid spacing).

NARAC simulations showed that following the earthquake and tsunami, winds remained primarily off-shore until the March 14 – March 16 UTC period, during which the wind direction rotated in a clockwise direction consistent with the movement of a low pressure area. NARAC-simulated wind directions pushed modeled plumes southwards from March 14 13:00 UTC to

March 15 02:00 UTC period, rotated towards the northwest around March 15 03:00 UTC, and turned off-shore again on March 16 UTC. Winds then remained off-shore until March 21 UTC when changing conditions again sent radioactive material southward in the general direction of Tokyo.

Precipitation occurred episodically throughout the release period. NARAC investigated a variety of precipitation conditions ranging from uniform grid-wide, time-varying precipitation based on Japanese meteorological observations to WRF FDDA spatially and temporally varying precipitation [2]. Comparisons of measured and WRF FDDA modeled rates showed good qualitative agreement with precipitation data for the passage of a rain band in the March 15th UTC time frame, as did time-series comparisons of measured and predicted precipitation rates for stations located near Tokyo and Fukushima City.

Initial NARAC forecasts captured the overall pattern of winds and the occurrence of precipitation, but subsequent higher resolution (3-km) WRF FDDA simulations provided increased accuracy in modeling the timing of the wind shifts and precipitation patterns [2] and were used in the source estimation process. Wet deposition from both in-cloud and below-cloud precipitation scavenging significantly impacted NARAC estimates of downwind plume transport and deposition.

2.2. Radiological Data

The primary data available to NARAC for source estimation during the Fukushima response consisted of dose-rate measurements. The Japanese Ministry of Education, Culture, Sports, Science and Technology [7] (MEXT) provided data from its radiological monitoring stations, although most data from the prefectures closest to the Daiichi nuclear power plant were available only after March 15 0900 UTC. MEXT also collected dust sample data, but insufficient data of this type were available to NARAC for use during the response. The U.S. DOE Aerial Measuring Survey (AMS) arrived and began taking data on March 17-18 and U.S. personnel collected ground monitoring data as well as samples for laboratory analysis [1]. The center also received on-site Tokyo Electric Power Company (TEPCO) radiological measurements, although significant data gaps existed in the time period following the earthquake and tsunami and during the March 15 site evacuation. TEPCO measurements were used as qualitative guidance only, as these data were collected from locations very close to the site that were likely to have been heavily influenced by the local wind conditions and the exact location of the mobile monitor relative to the release locations. To supplement the very limited information available regarding reactor and spent fuel conditions, NARAC also drew upon U.S. Nuclear Regulatory Committee (NRC) analyses of possible nuclear reactor scenarios.

2.3. Source Reconstruction Methodology

NARAC's source estimation efforts concentrated on the critical period from March 14-16 UTC, due to DOE/NNSA interest in the relatively high deposition pattern measured by the Aerial Measuring System (AMS) to the northwest of the Fukushima Daiichi nuclear power plant. The various NARAC source estimates were based on the data and other information that were available at the time the analysis was conducted. As additional or corrected data were received, these estimates often were updated to take into account the new information. As discussed above, NARAC meteorology was derived from both weather observations and WRF FDDA simulations. Releases from all reactor units were treated as one combined source.

One of the key assumptions in NARAC's source estimation process was the selection of an appropriate radionuclide mix. Initial NARAC source estimates used a radionuclide mix of ^{133}Xe, ^{131}I, and ^{137}Cs that was provided by the DOE/NNSA CMHT based on an analysis of data provided by the USS Ronald Reagan from a location approximately 100 miles off the east coast of Japan. Later analyses incorporated three other primary radionuclide contributors to dose: ^{132}I, ^{132}Te (due to its decay

into ^{132}I), and ^{134}Cs. Typical release activity ratios for ^{133}Xe:^{131}I: ^{132}I: ^{132}Te:^{137}Cs:^{134}Cs used in NARAC's source estimation process were 100:20:20:20:1:1 or 100:10:10:10:1:1. These relative activity ratios were determined *a priori* from data provided by DOE laboratory analyses, supplemented by U.S. NRC reactor scenario radionuclide mixes. For example, DOE *in situ* field assays, later confirmed by laboratory analyses of soil samples and air filters collected over the March to May, 2011 period [8], showed that a reasonable choice for the ^{134}Cs:^{137}Cs activity ratio was 1:1, despite considerable scatter in the data.

NARAC source estimates were produced by statistically and graphically comparing data and model results paired in both space and time [9]. Input assumptions were varied to find the best fit to the data and the average measured-to-predicted value ratio was used to scale the release amounts to best match the measurements. Below-threshold measured and/or predicted values were not used in the comparisons, and outlier values were removed as appropriate. The primary statistics used in the model-data comparisons were the percentage of predicted values that fell within a factor, R, of the measured values (where $R = 2, 3, 5, 7, 10, 20, 50, 100,$ and 1000), supplemented by a bias analysis (i.e., consideration of the relative magnitude and number of values over or under predicted). Ratios of measured and computed values were used for statistical comparison of air concentration and ground deposition values that varied over many orders of magnitude. Additional statistical measures included the (absolute and signed) bias, the normalized mean square error, and the average and standard deviations of the ratios of measurements to calculated values.

3. Results

NARAC conducted a number of source reconstruction analyses using a range of possible release assumptions and meteorological conditions. Both uniform and time-varying release rates were examined and a limited investigation was made of the sensitivity to different radionuclide activity ratios, release heights, and particle-size distributions. In this paper, we will focus on the results of one source reconstruction analysis that will be designated the "baseline" estimate. Comparisons with other NARAC analyses that used different meteorology (e.g., observational data, WRF forecasts, WRF FDDA analyses), radionuclide mixes (i.e., relative activity ratios for iodine, cesium, tellurium, and xenon), and radionuclide measurement data (e.g., AMS, MEXT) are summarized in the results discussion below.

3.1. "Baseline" Case Source Estimate

The "baseline" case [2] is a constant release rate fit to the data for the March 14-16 UTC, 2011 period derived by optimizing the overall graphical and statistical agreement of model predictions with 451 MEXT dose-rate measurements from 19 stations within Fukushima and the surrounding Prefectures. The MEXT dose-rate measurements were assumed to include both air immersion and ground-shine contributions. The "baseline" case used arguably the best meteorology developed by NARAC during the response – WRF FDDA simulations at 3 km resolution, which incorporated Japanese meteorological observations. The assumed radionuclide mix for ^{133}Xe: ^{131}I: ^{132}I: ^{132}Te: ^{137}Cs: ^{134}Cs was 100:20:20:20:1:1.

Graphical comparisons from the model-data fit for the "baseline" case are shown in Figure 1 for two time example time periods - 0900 UTC and 1200 UTC on March 15. The corresponding total release estimate over the March 14 0000 UTC to March 16 0000 UTC period was 3.7×10^{15} Bq (1×10^5 Ci) each of ^{137}Cs and ^{134}Cs, 7.4×10^{16} Bq (2×10^6 Ci) each of ^{131}I, ^{132}I, and ^{132}Te, and 3.7×10^{17} Bq (1×10^7 Ci) of ^{133}Xe.
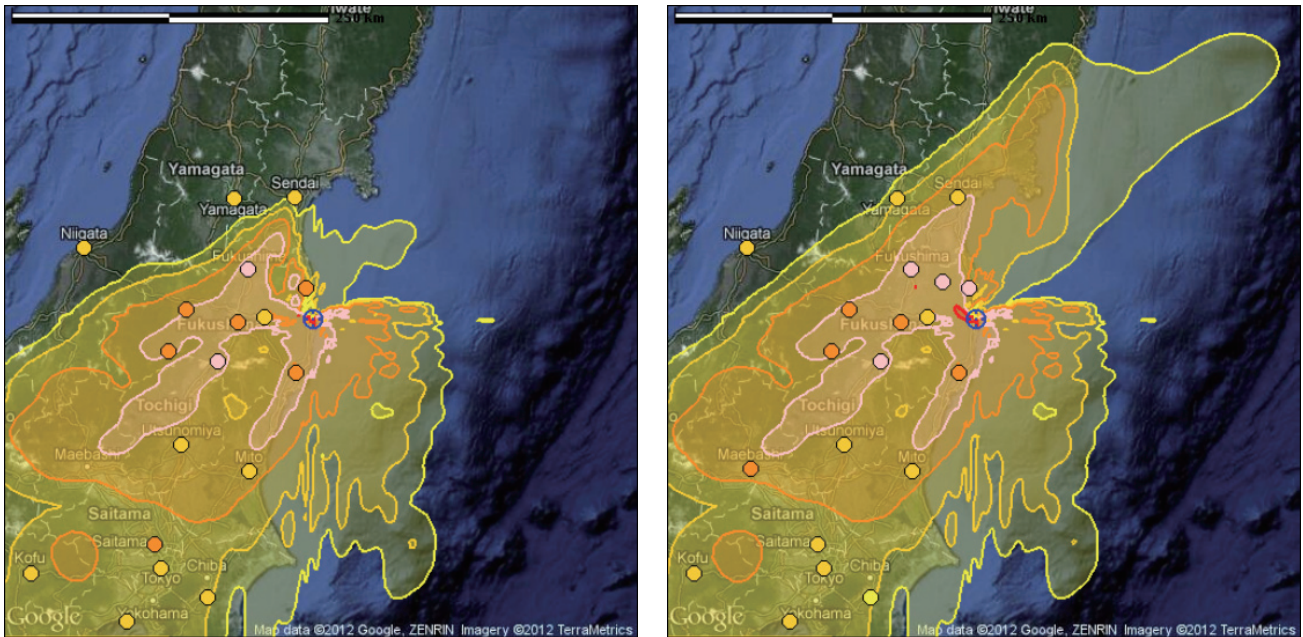
Figure 1. Dose rate results from the NARAC-modeled "baseline" case (color-filled contours) are compared with MEXT data (circles color coded to the same levels as the contours) for March 15 0900 UTC (left panel) and March 15 1200 UTC (right panel). The innermost red contour is the area where the model predicts that 120 μGy h^{-1} (12.0 mrad h^{-1}) is exceeded; pink shows 4-120 μGy h^{-1} (0.4-12.0 mrad h^{-1}), orange 0.4-4 μGy h^{-1} (0.04 – 0.4 mrad h^{-1}), light orange 0.04-0.4μGy h^{-1} (0.004-0.04 mrad h^{-1}), and yellow 0.004-0.04 μGy h^{-1} (0.0004-0.004 mrad h^{-1}). The blue circle indicates the location of the Fukushima Daiichi plant. (Background map courtesy of Google)

Over 35% of the predicted values were with a factor of 2 of the measurements, (i.e., the ratios of measured and predicted values for the same time and location were between 0.5 and 2) and 82% within a factor of 10. The agreement between predicted and measured values was slightly better for the MEXT stations located outside of Fukushima Prefecture (not shown). The NARAC "baseline" case model-predicted values also were found to fit the March 18th AMS data to a similar degree, even though these data were not used in developing the source estimate (see Figure 2).

The "baseline" case provides an interesting comparison to other NARAC analyses in which time-varying release rates were used to match the data. These results showed that the deposition pattern to the northwest of the Fukushima Daiichi nuclear power plant could be matched by different combinations of time-varying emission rates, spatially and temporally-varying precipitation, and precipitation scavenging parameters. It is unclear whether sufficient data is available to distinguish the competing contributions of these two effects, as similar deposition patterns can be derived by either increasing release rates or increasing wet deposition rates over the appropriate time periods. It also should be noted that NARAC analyses did not account for the changes in wet deposition resulting from different types of precipitation (e.g., rain, snow).
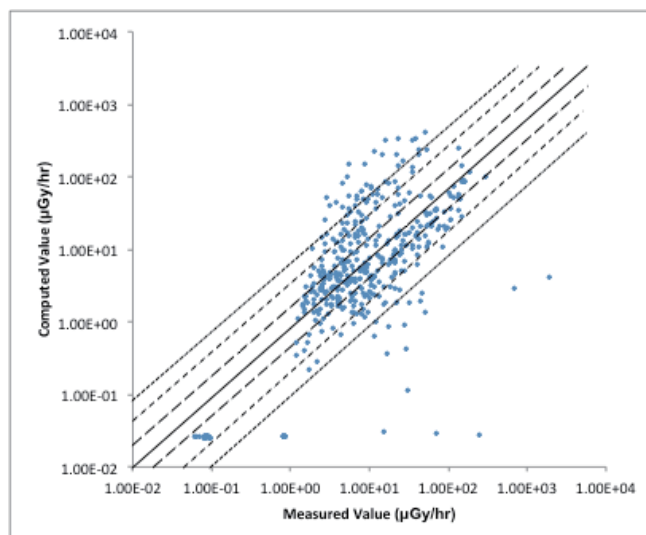
Figure 2. Scatter plot showing a comparison of the computed NARAC "baseline" case predicted values versus AMS data from March 18. The solid, long dash, short dash, and dotted lines delimit factors of 1, 2, 5, and 10 respectively.

3.2. "Baseline" Case Dose Estimates

The Total Effective Dose (TED) is the adult whole body dose resulting from inhalation, air immersion (during both initial plume passage and from resuspension), and ground-shine. Figure 3 shows both the predicted TED and the 50-year Committed Effective Dose (CED) from the "baseline" case. The CED is the adult combined internal dose from inhalation using a weighted sum of doses to various organs and is the internal dose component of the TED. The 50 mSv (5 rem) and 10 mSv (1 rem) levels shown in the plot as orange and yellow contours, respectively, are the early phase TED upper and lower U.S Protective Action Guide (PAG) dose levels for evacuation / sheltering. U.S. PAG levels are known to differ from those used in Japan.
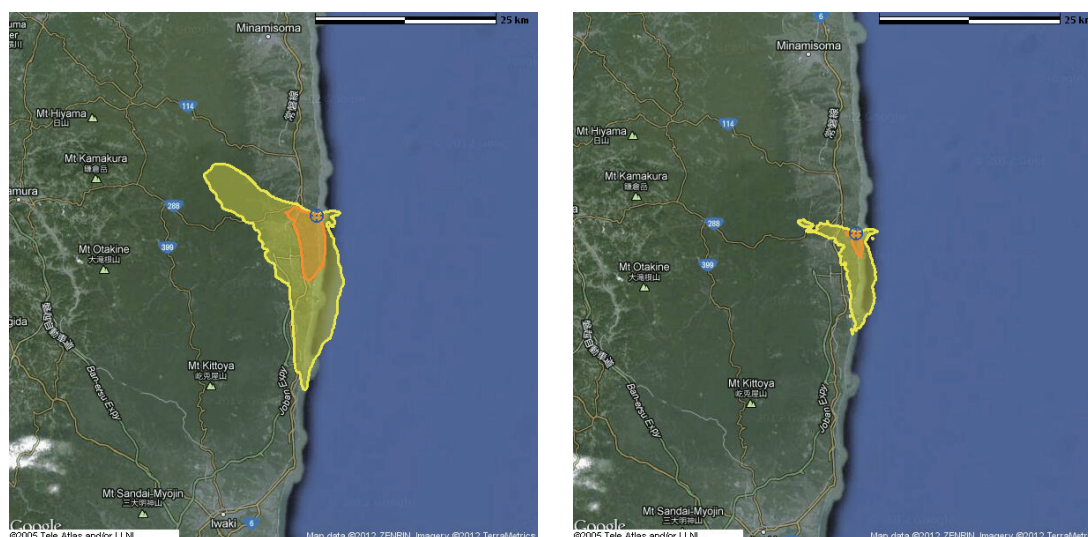
Figure 3. The Total Effective Dose (left panel) and the 50-year Committed Effective Dose (right panel) are shown for the "baseline" case. The contours delimit predicted areas exceeding 50 mSv / 5 rem (orange) and 10 mSv / 1 rem (yellow) for 4 days of exposure based on the "baseline" simulation for March 14-16 UTC. (Background map courtesy of Google)

164

3.3. Effects of Gas-Particle Partitioning on Thyroid Dose

The NARAC "baseline" case and other source term estimates conducted during the response modeled the emissions as respirable size particles, as little data were available on activity size distributions or the physical and chemical forms of the released material. Specifically, most NARAC analyses assumed a log-normal activity-size distribution with a median diameter of 1 μm, geometric standard deviation of 2, and minimum and maximum cut-offs at 0.1 μm and 10 μm respectively. However, U.S. Nuclear Regulatory Commission reactor analyses [10] have shown that iodine can be produced as both organically-bound and inorganic gases. In addition, LLNL laboratory analysis of combined paper and charcoal air filter samples at a few locations, including Yakota Air Base and the U.S. Embassy in Japan, are indicative of possible gas and particulate partitioning [8]. Cesium was observed almost exclusively on the paper filters that are expected to collect most of the particulate material. In contrast, only 30% of the ^{131}I was found on the paper filter and 70% passed through to the charcoal filter that is designed to collect gaseous iodine.

NARAC therefore performed a preliminary sensitivity study on the effects of different assumptions about the chemical/physical form of iodine on calculations of thyroid dose. Four different gas-particle phase partitioning assumptions were simulated:

- 100% respirable particles (the "baseline" case)
- 100% organically-bound gas (CH_3I)
- 100% inorganic gas (I_2)
- 25% particles, 30% inorganic gas, 45% organically-bound gas

The last mixture is a default partitioning used in NRC RASCAL modeling of nuclear reactor scenarios[10].

The same "baseline" case inputs described above were used in the thyroid dose simulations, apart from the use of different deposition and dose conversion factors. The former were derived from values found in the U.S. NRC's RASCAL 4.0 model documentation[10]. Gravitational settling was applied only to the particulate form. Reactive iodine was modeled using a dry deposition velocity value that was more than twice the value used for particulates (based on a typical RASCAL value for neutral stability and 3 m/s winds), while organically bound iodine gas were assumed to exhibit no dry deposition. Organically-bound iodine was modeled as not affected by wet deposition and the same conservative assumption was used for the reactive gas case. While the latter assumption may not be strictly true, wet deposition for reactive iodine gas is generally presumed to be much less than dry deposition, so this approximation may not have had a significant effect on the final results.

Thyroid dose was calculated from inhalation using dose conversion factors (DCFs) for 1-year old children and a breathing rate consistent with light physical activity levels. Dose conversion factors were derived from DCFPAK 1.8[11] (which in turn is based on ICRP Publications 56, 60, 66, 67, 69, 71, and 72). Specifically, NARAC used the DCFPAK I_2 "vapor" (V) and the CH_3I dose conversion factors for inorganic and organically-bound gases, respectively. Gas-phase DCFs are approximately twice the particle DCF, with the inorganic iodine DCF 20-30% higher than that for the organically-bound iodine. Since the ^{132}I DCF for 1-year old child thyroid exposures is two orders of magnitude less than for ^{131}I, ^{132}I (including ^{132}I activity produced from ^{132}Te) played a minor role in the dose estimates.

Both organically-bound and inorganic iodine gas simulations predicted a higher dose at any given distance than that resulting from particulate releases, or equivalently a greater downwind extent for any given dose level. This is apparent in Figure 4, which compares the results of the original "baseline" 100% respirable particle simulation with the calculation using a mixture of 25% particles, 30% inorganic gas, and 45% organically-bound gas. Both inorganic and organically-bound iodine gas

thyroid dose estimates were predicted to be similar in extent. It should be noted that these simulation represent the first steps of a sensitivity study only. The source term was not re-estimated based on the differences in predicted dose rates. Additional data is needed in order to develop more accurate estimates of the iodine gas-particle phase partitioning and thyroid dose exposures resulting from the Fukushima Daiichi releases.
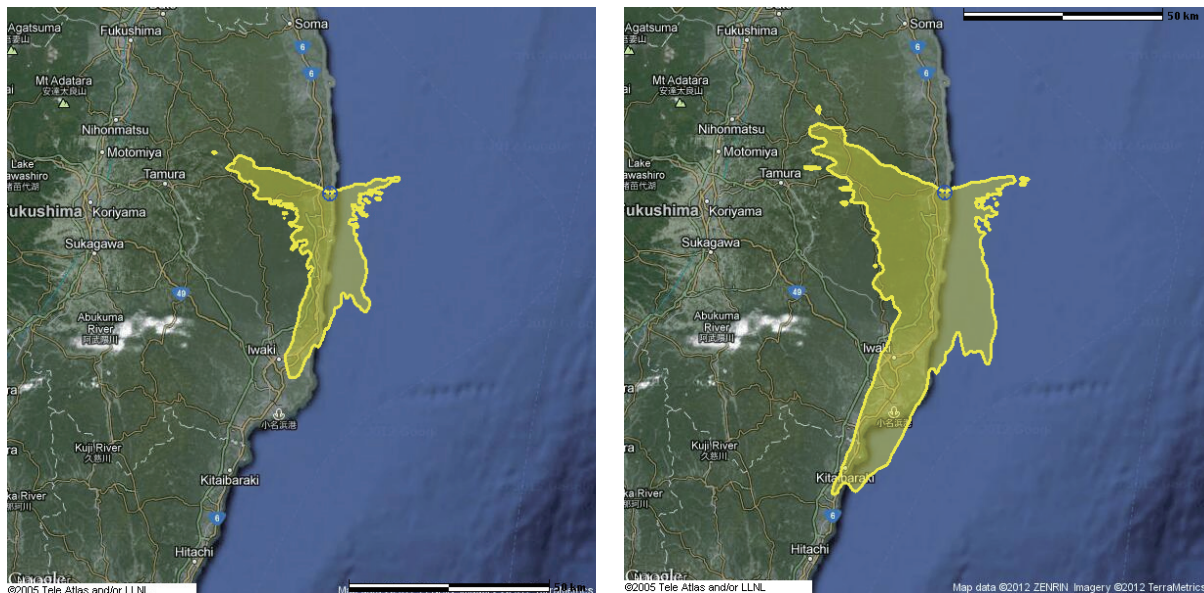
Figure 4. The two figures show the 70-year committed 1-year old child thyroid dose for iodine inhalation using the "baseline" source estimate over the March 14-16 UTC period for 100% particulate iodine (left panel) and a mixture of 25% particles, 30% inorganic gas, and 45% organically-bound gas (right panel). The yellow contour is the 50 mSv / 5 rem level that corresponds to the early phase U.S. Protection Action Guide level for KI administration to children. (Background map courtesy of Google)

4. Discussion

NARAC source reconstruction analyses resulted in a range of estimates for emission rates that were consistent with the available dose-rate data, within model and measurement uncertainties. Total release estimates for the two-day period of interest (March 14-16 UTC, 2011) varied within approximately a factor of three of the "baseline" case for the same radionuclide mix[2]. NARAC source estimates were found to be sensitive to a number of factors including:

- Source term assumptions (e.g., time-varying vs. constant emission rates, radionuclide mix and relative activity ratios, particle / activity size distributions, iodine gas / particle phase partitioning, height of release, reactor conditions)
- Meteorology (e.g., observational data, WRF analyses, WRF FDDA, or GFS global data)
- Model physics, including dry deposition, precipitation rates, type of precipitation (e.g., rain, snow), and precipitation scavenging parameters for both in-cloud and below cloud processes
- Selection of the radiological data to preferentially match in the source estimation process (e.g., MEXT data, AMS surveys)

Source term estimates are significantly more speculative during periods of off-shore wind flow, for which there is little to no regional radiological monitoring data.

NARAC source reconstruction estimates were also compared to other values published in the

literature that were documented in sufficient detail that comparisons could be made for the same March 14-16 UTC period (e.g., Chino et al. 2011[13]; GOJ 2011a[14], 2011b[15], and 2011c[16]; Stohl et al. 2011[17]). Despite the use of different radiological data (MEXT dose rate; MEXT dust data, Comprehensive Test Ban Treaty Organization [CTBTO] global monitoring data), meteorological models, source estimation methodologies, and assumptions regarding reactor conditions, these estimates agreed with a factor of approximately six[2].

4. Conclusion

The Fukushima Daiicihi accident generated a unique and voluminous data set, including both local and global radiological measurements from MEXT, TEPCO, CTBTO global monitoring data, U.S. DOE aerial and ground surveys, and U.S. EPA RadNet[12] monitors. To date, most atmospheric dispersion source estimation efforts have used only a fraction of these data. Model physics improvements are needed to more accurately simulate complex meteorological conditions and dispersion on both regional and global scales, including the use of data assimilation and ensemble techniques to develop probabilistic dose estimates. Atmospheric dispersion modeling could be significantly informed by incorporating on-going nuclear reactor modeling and analyses; the results of radiochemical and spectral analyses that provide insight into radionuclide mixes and gas-particle partitioning of iodine; and/or internal dose monitoring data. Integration of data from multiple sources may allow different release events to be distinguished and may better constrain possible release rates during off-shore flow periods. The combined use of modeling and monitoring data has the potential to fill in key gaps in source and exposure estimates. In addition, such efforts will lead to improved capabilities for responding to future events of a similar scale and complexity.

References

1) Blumenthal, D., D. Bowman, and A. Remick, Adapting the U.S. Domestic Radiological Emergency Response Process to an Overseas Incident: FRMAC Without the F, Health Physics, 102(5) [2012], 485-488, and references cited therein

2) Sugiyama, G., J. Nasstrom, B. Pobanz, K. Foster, M. Simpson, P. Vogt, F. Aluzzi, and S. Homann, Atmospheric Dispersion Modeling: Challenges of the Fukushima Dai-ichi Response, Health Physics, 102(5) [2012], 493-508

3) Skamarock WC, Klemp JB , Dudhia J, Gill DO, Barker DM, Duda MG, Huang X-Y., Wang W, Powers JG. A Description of the Advanced Research WRF Version 3. NCAR Technical Note, NCAR/TN–475+STR, National Center for Atmospheric Research, Boulder CO [2008]. Available at: http://www.mmm.ucar.edu/wrf/users/docs/arw_v3.pdf

4) Environmental Modeling Center. The GFS Atmospheric Model. NCEP Office Note 442, Global Climate and Weather Modeling Branch, EMC, Camp Springs, Maryland [2003]. Available at:

http://nws.noaa.gov/ost/climate/STIP/AGFS_DOC_1103.pdf

5) Stauffer DR, Seaman NL. On Multi-Scale Four-Dimensional Data Assimilation. J. Appl. Meteor. 33 [1994], 416-434

6) Liu Y, Bourgeois A, Warner T, Swerdlin S, Hacker J. An implementation of obs-nudging-based FDDA into WRF for supporting ATEC test operations. 2005 WRF user workshop paper 10.7 [2005]
Available at
http://www.rap.ucar.edu/projects/armyrange/references/publications/Liu_WRF-WK.2005.pdf

7) Government of Japan. Ministry of Education, Culture, Sports, Science & Technology in Japan (MEXT), Reading of environmental radioactivity level (English version).
http://www.mext.go.jp/english/incident/1303962.htm

8) S. Kreek and N. Wimer, LLNL, personal communication.

9) Foster KT, Sugiyama G, Nasstrom JS, Leone, Jr. JM, Chan ST, Bowen BM. The Use of an Operational Model Evaluation System for Model Intercomparison. Int. J. Environment and Pollution 14 [2000] 77-88

10) U.S. Nuclear Regulatory Commission, RASCAL 4: Description of Models and Methods, NUREG-1940 [2011]

11) Eckerman KF, Leggett RW. User Guide to DCFPAK 2.2. Oak Ridge National Laboratory, Oak Ridge, TN [2008]

12) Environmental Protection Agency (EPA), Japanese Nuclear Emergency: Radiation Monitoring [2011]. Available at http://www.epa.gov/japan011/rert/radnet-data.html

13) Chino M, Nakayama H, Nagai H, Terada H, Katata G, Yamazawa H, Preliminary Estimation of Release Amounts of I-131 and Cs-137 Accidentally Discharged from the Fukushima Daiichi Nuclear Power Plant into the Atmosphere. J. Nuc. Sci and Tech. 48 [2011], 1129-1134.

14) Government of Japan, Ministry of Economy Trade and Industry News Release, INES (the International Nuclear and Radiological Event Scale) Rating on the Events in the Fukushima Dai-ichi Nuclear Power Station by the Tohoku District – off the Pacific Ocean Earthquake [12 April, 2011]
Available at: http://www.nisa.meti.go.jp/english/files/en20110412-4.pdf

15) Government of Japan, Report of Japanese Government to IAEA Ministerial Conference on Nuclear Safety – The Accident at TEPCO's Fukushima Nuclear Power Stations. Transmitted by Permanent Mission of Japan to IAEA [7 June 2011]
Available at: http://www.iaea.org/newscenter/focus/fukushima/japan-report/

16) Government of Japan, Additional Report of the Japanese Government to the IAEA – Accident at TEPCO's Fukushima Nuclear Power Stations. Transmitted by Nuclear Emergency Response Headquarters, Government of Japan [15 September 2011].
Available at: http://www.iaea.org/newscenter/focus/fukushima/japan-report2/

17) Stohl A., Seibert P, Wotawa G, Arnold D, Burkhardt JF, Eckhardt S, Tapia C, Vargas A, Yasunari T, Xenon-133 and caesium-137 releases into the atmospheric from the Fukushima Dai-ichi nuclear power plant: determination of the source term, atmospheric dispersion, and deposition. Atmos. Chem. Phys. Discuss. 11 [2011] 28319–28394.
http://www.atmos-chem-phys-discuss.net/11/28319/2011/doi:10.5194/acpd-11-28319-2011

Summary of Session 3

J. NASSTROM

Chairperson Dr. Yamazawa introduced Session 3 by describing the role of atmospheric dispersion simulations in helping to understand potential source terms and dose to populations. He stated that the key points that needed to be considered in source term estimation are:

(1) The methodology for estimating the source term using plant conditions and/or environmental data
(2) The limited availability of data, including plant monitoring data
(3) The nuclides that need to be considered (e.g., I-131, Te-132, I-132, Cs-134, Cs-137 and possibly others)
(4) Discrepancies between different source estimations

Dr. Yamazawa summarized the status of dispersion simulations as follows:

1. Model frameworks have been established
2. Parameters for dry and wet deposition need to be refined
3. Data assimilation of meteorological data into model forecasts is needed

Dr. Chino presented an effort to estimate time-varying reactor source terms from radionuclide air concentrations measurements and dose rate measurements. Atmospheric dispersion simulations using a unit release were scaled using the ratio of measured values to predicted values. The resulting predicted values were generally within a factor of 10 of measured values, which is reasonable for atmospheric dispersion simulation in complex conditions.

- Dr. Sugiyama inquired if any further source estimation refinement was planned. Dr. Chino said that this would be difficult as data is limited over land, but for plumes over the ocean, global and marine measurements could potentially be used.
- Dr. Solomon asked why the recent TEPCO source term estimate was higher than other estimates. Dr. Chino replied that TEPCO used a few data points taken at or inside the plant site boundary (e.g., very close to the release point), which therefore were very sensitive to wind direction, making the source term estimation process more uncertain.
- Dr. Homma asked if the measured dose rate was assumed to be air gamma dose rate and/or ground exposure dose rate. Dr. Chino responded that only model predictions of ground exposure rate were compared to measured dose rate, because only particulate radionuclides, and not noble gases, were considered.

Dr. Nagai presented a WSPEEDI dispersion and deposition modeling study that examined the effects of different methods for simulating precipitation scavenging. Using the Chino et al. (2011) source term and refined source estimates based on additional data, predicted values were generally found to be within a factor of 10 of measured values of Cs-137 and I-131 air concentration. Measured deposition in different areas could be attributed to dry or wet deposition, with dry deposition dominating in some areas and wet deposition dominating in other areas. By making different assumptions for the scavenging effectiveness of in-cloud rainout, below-cloud washout, cloud ice, snow and fog, the predicted ground exposure dose rate could be improved in several geographical areas.

- Dr. Homma asked if different chemical forms for radionuclides were considered. Dr. Nagai said this had not yet been considered.
- Dr. Homma then asked if deposition and scavenging were taken to be the same for all radionuclides. Dr. Nagai replied that the dry deposition velocity for Cesium and Iodine were

different, but precipitation scavenging was the same.

- Dr. Suzuki asked if the scavenging coefficients were different for snow and rain. Dr. Nagai said he had performed model tests varying the scavenging of rain and snow.
- Dr. Suzuki also inquired if the model predictions of rain vs. snow had been confirmed by observations. Dr. Nagai said they had been somewhat confirmed based on air temperature.
- Dr. Solomon asked if gaseous Iodine was assumed to deposit. Dr. Nagai responded that his work assumed Iodine deposited, and had a higher dry deposition velocity that other radionuclides. Dr. Bouville then commented that different Iodine forms exhibit different reactivity and deposition, with elemental Iodine being reactive and depositing, organic Iodine being less reactive, and Iodine salt being in between.
- Dr. Kurhihara asked if the simulations predicted the variable behavior of I/Cs ratios. Dr. Nagai said they do not yet, and that improvements were needed to the modeling of deposition processes.

Dr. Ohara presented the results of atmospheric dispersion modeling using the CMAQ chemical transport model with various assumptions for source terms (amounts and time variation) and different wet deposition sub-models. Model results were shown to be sensitive to the different assumptions. Further work is needed to further verify models with observed data, compare models, and explore the use of multi-model ensemble predictions for model improvement.

- Dr. Yamazawa asked why deposition results of CMAQ and WSPEEDI differed. Dr. Ohara replied that CMAQ uses a more complex wet deposition but that CMAQ wet deposition did not vary with particle size.
- Dr. Kajimoto said that 2-3 micrometer particle diameters may be released, instead of the assumed 1 micrometer. Dr. Ohara said it was difficult to set particle size.

Dr. Sugiyama presented a summary of U.S. DOE NARAC dispersion modeling activities that included routine plume forecasting using unit release rates, hypothetical source term dose prediction, arrival time and dose prediction for US territories, and source term estimation and model refinements using dose rate measurements. The model refinements used MEXT station dose rate measurements (compared to model predicted ground shine plus air immersion dose rate) and DOE/MEXT Aerial Measuring Survey (AMS) ground shine dose rates. Unlike several other studies, the noble gas contribution to the air immersion dose rate was used when comparing to MEXT station dose rate data. Estimated release quantities for the critical March 14-16 time period were similar to other estimates, within the expected range of uncertainties. Dr. Sugiyama observed that similar predictions of ground deposition could be be obtained in different ways. For example, higher assumed precipitation scavenging or higher source release rates can both produce higher ground deposition. Finally, thyroid dose predictions for particulate Iodine were compared to dose from a mixture of particulate and gaseous Iodine. Including gaseous Iodine increased the predicted thyroid dose for the same assumed released activity of Iodine.

- Dr. Solomon asked why the dose is higher for gaseous versus particulate iodine. Dr. Sugiyama said that in the preliminary NARAC model calculations, gaseous iodine gives a higher thyroid dose because of higher dose conversion factors for gaseous iodine compared to particulate iodine.
- Dr. Solomon then inquired if models can be used to work backward to determine information on gaseous versus particulate Iodine. Dr. Sugiyama said that there may be a way to get some qualitative indication but it was unclear that quantitative values could be obtained, although sensitivity analyses can be used to determine the relative effect of gaseous versus particle iodine. Dr. Bouville commented that non-reactive gas does not deposit, and this can be significant.

- Dr. Suzuki asked about data on nuclide composition. Dr. Sugiyama responded that data from DOE laboratory and spectral analysis was used where available.

Session 3 Discussion

In introducing the discussion following the Session 3 simulation, Dr. Yamazawa commented that there was much uncertainty in dispersion modeling, in particular in deposition modeling, and this can affect source term estimates.
- Dr. Kajimoto commented on experimental data, non-reactive iodine, elemental iodine, organic Iodine, and a NUREG document that had some information on this.
- Dr. Yamazawa stated that models provide reasonable predictions of ground deposition, where there is much more data, and that reconstruction of air concentrations is needed. He later added that further model testing versus deposition data in needed.
- Dr. Solomon commented that models could be used to fill in for missing data (such as times with missing air sampling data) and to estimate dose (particularly inhalation dose).
- Dr. Bouville said that human thyroid measurements can also be used, and potentially can be used to calibrate models. He emphasized that human measurements need to be analyzed, and that consistency is important tin these measurements.
- Dr. Ohara said air concentration is important, but that, in a model, the budget (air versus deposition) is also important, and a land/ocean comprehensive analysis is important.
- Dr. Homma said model predictions have large uncertainties. Simple models can be used to relate air and ground concentrations of Cs-137 and I-131, while complex models can help with timing.
- Dr. Solomon re-iterated that models could provide the "glue" to bring together air, ground and human measurements, and that data sets should be used independently at first and then cross-checked for consistency (consistency can give confidence). Dr. Balonov suggested that models should be tested in conditions with measured human thyroid dose, and then extrapolated to other areas. Dr. Thiessen stated that since models can get the same answer in different ways, it is important to understand uncertainties. Dr. Nasstrom commented that any co-located air concentration, deposition and precipitation measurements can be used to test and calibrate models, and improve confidence in predictions for other areas.
- Dr. Suzuki asked how resuspension for Iodine is considered. Dr. Nagai said I-131 decay makes I-131 resuspension less. Dr. Sugiyama indicated that resuspension is included in NARAC models in a simple manner. Dr. Suzuki said post-plume resuspension should be considered to which Dr. Homma responded that resuspension rates are small.   Dr. Balanov agreed that resuspension was small for Chernobyl, and may be small for Fukushima, but should be considered.

Session 4

Dose Reconstruction in Past Nuclear Incidents

Chair   :   K. THIESSEN
Co-chair   :   O. KURIHARA
Rapporteur :   G. SUGIYAMA

Methodology and Results of Internal Dose Reconstruction in Russia after the Chernobyl Accident: Generic Approach and Thyroid Dose

Mikhail BALONOV, Irina ZVONOVA

Institute of Radiation Hygiene, Mira St 8, 197101 St. Petersburg, Russia

Abstract

Reconstruction of internal dose for various populations has been conducted in Russia following past major environmental radionuclide releases resulting from operation of and emergencies at Mayak PA facility in Urals in 1950s, nuclear weapons tests at Semipalatinsk test site since 1949, and the Chernobyl accident in 1986. The objectives of those activities usually were radiation risk assessment and/or support of radiation and social protection programs and of epidemiological studies. The Russian internal thyroid dose reconstruction program that is the closest to the Fukushima program under development was the Chernobyl study for populations of the more affected areas. Radiation monitoring conducted in the affected areas included measurements of both environmental and food samples and human thyroid. The dose reconstruction procedure for various areas was structured according to availability of monitoring data. The paper presents general methodology for reconstruction of the internal dose in groups of inhabitants of the Chernobyl accident area and practical techniques for reconstruction of the ^{131}I absorbed dose in thyroid. The techniques are based on the results of radiation monitoring performed in 1986 in the Bryansk, Tula, Orel and Kaluga regions of Russia. The ^{131}I measurements of the thyroid as the data most relevant to internal dose are of first priority for dose reconstruction. Radionuclide intake estimation with foods is considered as the second priority and application of radioecological models as the third priority when measurement data are lacking. The developed internal thyroid dose reconstruction algorithms were converted in the official national methodology that was used for large scale reconstruction of average internal thyroid dose in more than four thousand Russian settlements affected by the Chernobyl fallout. The results were used both for decision making regarding radiation and social protection of the public and as support for epidemiological studies.

1. Introduction

Reconstruction of internal dose for various populations has been conducted in Russia following past major environmental radionuclide releases resulting from operation of and emergencies at Mayak PA facility in Urals in 1950s [1], nuclear weapons tests at Semipalatinsk test site since 1949 [2], and the Chernobyl accident in 1986 [3-5]. The objectives of those activities usually were as follows:
- retrospective check for compliance with regulations (radiation protection),
- radiation risk assessment for public and authority information,
- support of radiation and social population protection programs,
- support for epidemiological studies, and
- model validation.

The Russian internal dose reconstruction program that is the closest to the Fukushima dose reconstruction program under development was the Chernobyl study for populations of the more affected areas.

The Chernobyl program was topical in Russia for several reasons. First of all, internal exposure of thyroid with radioiodine has resulted by now in several hundred thyroid cancer cases in the residents of more affected areas who were children or adolescents in 1986 [6, 7]. Therefore, thyroid dose

reconstruction was necessary for identification of more exposed population groups as a basis for medical follow-up and epidemiological studies. Secondly, contribution of internal dose caused by intake of caesium radionuclides in collective effective dose was more than one third over 25 years [7, 8], and dose estimates were useful for justification of protection and remediation actions.

The paper presents general methodology for reconstruction of the internal dose in groups of inhabitants of the Chernobyl accident area, practical techniques for reconstruction of the ^{131}I absorbed dose in thyroid in the early period and summary of its results [3-5, 7, 8]. The techniques are based on the results of radiation monitoring performed in 1986 in the Bryansk, Tula, Orel and Kaluga regions of Russia.

2. Generic approach

In the general form, the committed dose $^{\Theta}D\ (t_j,\ t_{j+1})$ (effective dose $^{\Theta}E\ (t_j,\ t_{j+1})$ or equivalent dose $^{\Theta}H_T\ (t_j,\ t_{j+1})$ in an organ or tissue T) of a person of the age Θ at the time of radionuclide intake, attributed to an intake $^{\theta}I\ (t_j,\ t_{j+1})$ of a radionuclide r during the time period between moments t_j and t_{j+1}, is determined according to the formula [2]:

$$^{\theta}D\ (t_j,\ t_{j+1}) = {}^{\theta}I_h\ (t_j,\ t_{j+1}) \cdot {}^{\theta}d_h\ + {}^{\theta}I_g\ (t_j,\ t_{j+1}) \cdot {}^{\theta}d_g \tag{1}$$

where: index h means inhalation and index g means ingestion pathway;

$^{\Theta}d$ is the appropriate dose coefficient for inhalation or ingestion at the age Θ [9, 10].

In their turn, intakes $^{\Theta}I\ (t_j,\ t_{j+1})$ are determined as integrals of the intake rates $^{\Theta}i\ (t)$ over time:

$$^{\Theta}I_h(t_j, t_{j+1}) = \int_{t_j}^{t_{j+1}} {}^{\Theta}i_h(\tau)d\tau = \int_{t_j}^{t_{j+1}} {}^{\Theta}V_h(\tau) \cdot C_{air}(\tau) \cdot d\tau \tag{2a}$$

$$^{\Theta}I_g(t_j, t_{j+1}) = \int_{t_j}^{t_{j+1}} {}^{\Theta}i_g(\tau)d\tau = {}^{\Theta}F \cdot \int_{t_j}^{t_{j+1}} \sum_{i}^{m} {}^{\Theta}V_{gi} \cdot C_i(\tau) \cdot d\tau \tag{2b}$$

where: $^{\Theta}V_h$ is the inhalation rate of a person at the age Θ [10];

$C_{air}\ (t)$ is the time-dependent air activity concentration of radionuclide r;

$^{\Theta}F$ is the correction factor that accounts for culinary losses of the radionuclide, inaccuracy of assessment of the food ration, and efficiency of countermeasures for persons of age Θ [4, 11];

$^{\Theta}V_{gi}$ is the daily consumption rate of the i-th group of food products or drinking water by persons of age Θ without consideration for countermeasures;

$C_i\ (t)$ is the time-dependent average concentration of radionuclide r in the i-th group of raw food products without consideration for agricultural countermeasures.

Radionuclide intake with intake rate as above results in activity $^{\theta}Q\ (t)$ of radionuclide r in a particular organ or tissue or in the whole body of a person at the age θ at the time moment t:

$$^{\Theta}Q(t) = \int_{0}^{t} [{}^{\Theta}i_h(\tau) \cdot {}^{\Theta}R_h\ (t - \tau) + {}^{\Theta}i_g(\tau) \cdot R_g(t - \tau)] \cdot d\tau \tag{3}$$

where $^{\theta}R\ (t)$ is the retention function of radionuclide r in the organ or tissue or in the whole body of a person at the age θ following inhalation or ingestion, respectively [9, 11].

The selection of internal dose reconstruction technologies of the public residing in the affected area strongly depends on the availability of relevant monitoring and/or modeling data. Generally, use of

---

[2] The calculation is given for only one radionuclide, therefore, the index r was omitted.

those data can be summarized as follows:

1. Human measurements (WBC, thyroid, etc) + intake rate & dose modeling
2. Food and air concentration measurements + intake & dose modeling
3. Environmental measurements + transfer & intake & dose modeling
4. Source term + dispersion & transfer & intake & dose modeling
5. Combinations of the above

When radiological data of different types that can be used for internal dose reconstruction are available, the hierarchy of their use should be based on the certainty of the final results, see Fig. 1 as example for ingestion pathway [4, 11]. The content of radionuclides in the human body (thyroid for radioiodine or whole body for radiocaesium) is most closely connected with the internal dose, and, therefore, it is taken into consideration in the dose reconstruction process *in the first instance* - priority I in Figure 1. *In the second instance*, the results of radionuclide measurements of local food products jointly with the data on food rations of population groups are considered - priority II in Figure1. Only *in the third instance* the results of radioecological modeling are taken into consideration - priority III in Figure 1.

Generic approach to the internal dose reconstruction including Russian post-Chernobyl experience was considered in detail in [4, 11].

3. Monitoring data

Radiation monitoring conducted in the Russian areas affected by the Chernobyl radioactive fallout included numerous measurements of both environmental and food samples and human thyroid (45 thousand) and whole body (about 100 thousand in 1986). The measurement data were supplemented with numerous interviews aimed at clarification of both internal and external exposure conditions. Most of the public polls of that kind were conducted within one year after the accident. The dose reconstruction procedure for various areas was structured according to availability of local monitoring data.
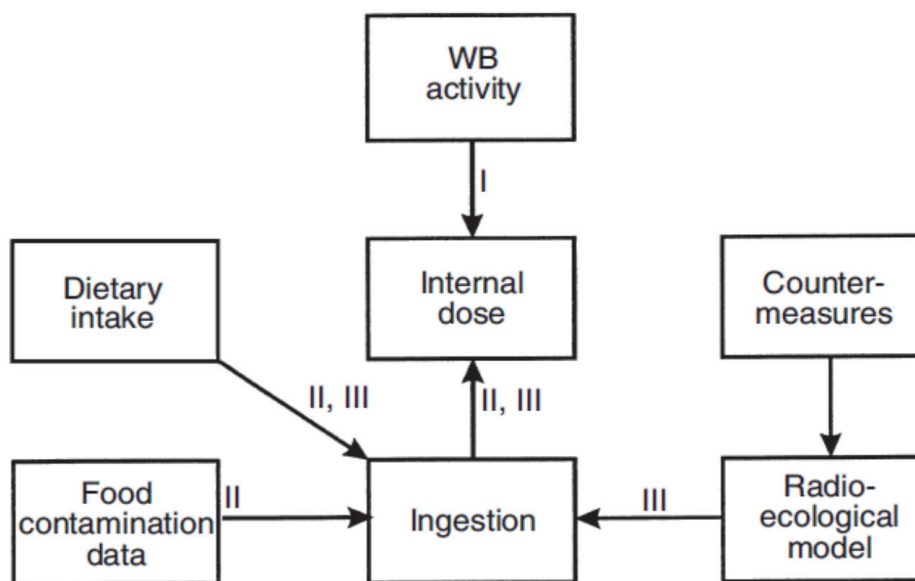
Figure 1. Priorities for selection of input data for internal dose reconstruction (ingestion)

For natural reasons, internal dose reconstruction process was focused on the areas with higher levels of radionuclide depositions. The three major ^{137}Cs spots formed by the Chernobyl fallout on the Russian territory can be seen on Figure 2 as yellow areas. They are located in the Bryansk, Kaluga, Tula and Orel regions. From the fallout meteorological conditions, it is well known that all the three spots were created on 28–30 April 1986 by rains during passage of the radioactive plume over those areas [4, 7].

The development of thyroid internal dose reconstruction methodology was based on some peculiarities of ^{131}I transfer in the ecological chain "air-pasture-cow-milk" with account for predominantly wet deposition conditions.

There are no time-trend data available for ^{131}I activity concentrations in milk in the first few days after the accident in the heavily affected areas of Russia. However, data are available for the period starting four days after the accident from the Bryansk region (total beta) and in two weeks from the Tula region (spectrometric measurements). The data in Fig. 3a show an exponential decline in ^{131}I activity concentration in milk normalized to ^{137}Cs deposition with an effective half-life of 4 to 5 days [4, 5, 7, 12] due to its short physical half-life and the reduction in iodine activity concentrations on plants because of weathering and plant growth. Leafy vegetables were also contaminated on their surfaces and also made a contribution to radiation dose to humans via the food chain.
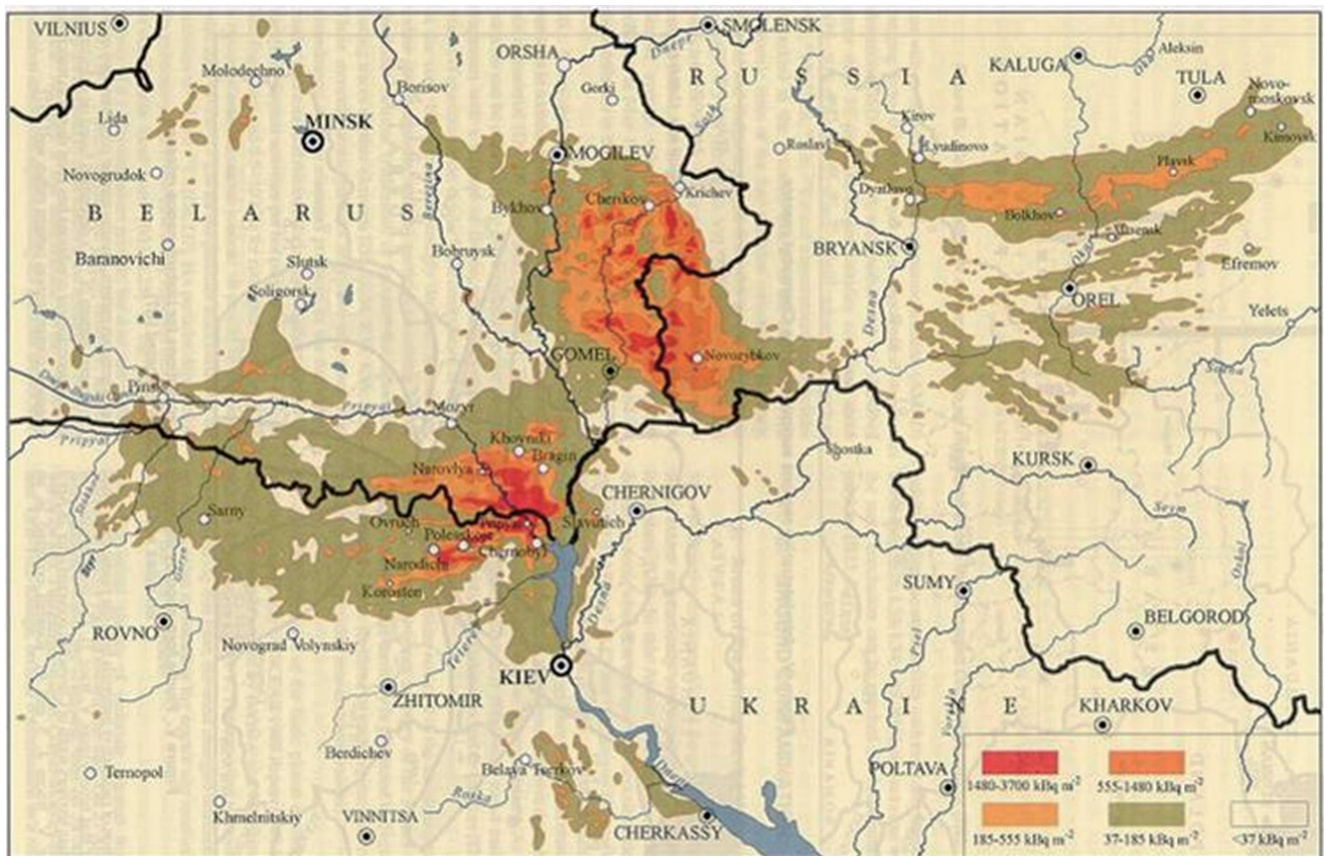
Figure 2. Post-Chernobyl ^{137}Cs spots in Belarus, Russia and Ukraine [7, 12]

The direct comparison of ^{131}I activity in milk in early May with ^{137}Cs soil deposition shows the contribution of dry deposition to ^{131}I in milk, because the linear relationship line shown does not go through the zero deposition point on Figure 3b. At ^{137}Cs soil deposition below about 30 kBq/m^2 (presumably dry fallout conditions) the ratio of ^{131}I in milk/^{137}Cs in soil is substantially larger than at higher soil deposition (presumably wet fallout).

4. ^{131}I intake model

From model assessment for conditions of predominantly wet deposition it was concluded that the proportion of radioiodine inhaled was small compared with that ingested over about one month, i.e. a few per cent. Furthermore, analysis has shown that ^{131}I was incorporated by the majority of inhabitants of the contaminated areas predominantly with milk and to a lesser extent with leafy vegetables. Based on monitoring and modeling results, the schematic intake function presented on Figure 4 was used for thyroid dose reconstruction. [3-5)]

a)
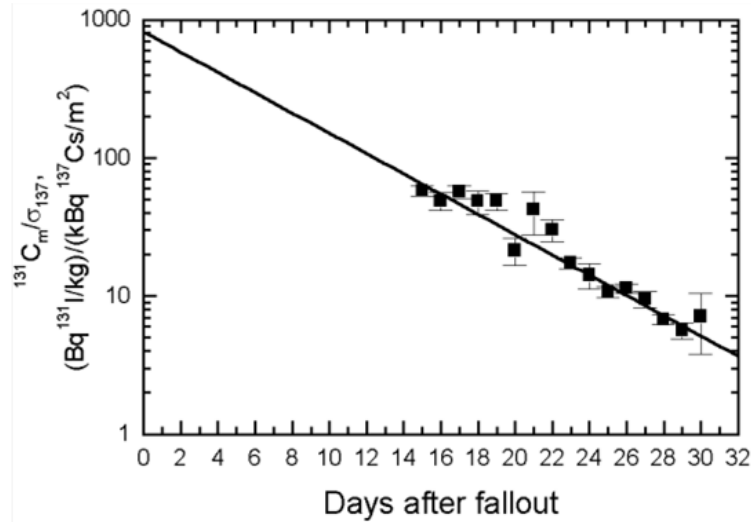
b)
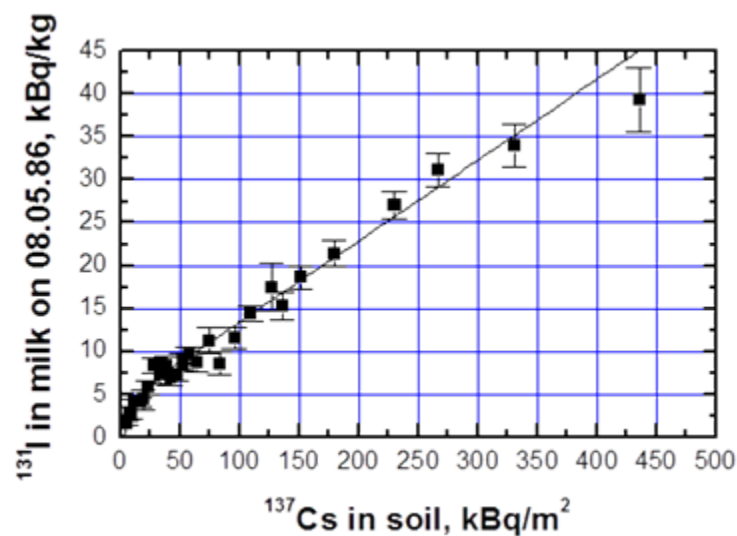
Figure 3. Variation of ^{131}I activity concentration in milk in the Tula region, Russia (a) with time after deposition, standardized by ^{137}Cs soil deposition and (b) with ^{137}Cs soil deposition (time corrected to 8 May 1986) [3, 4)]
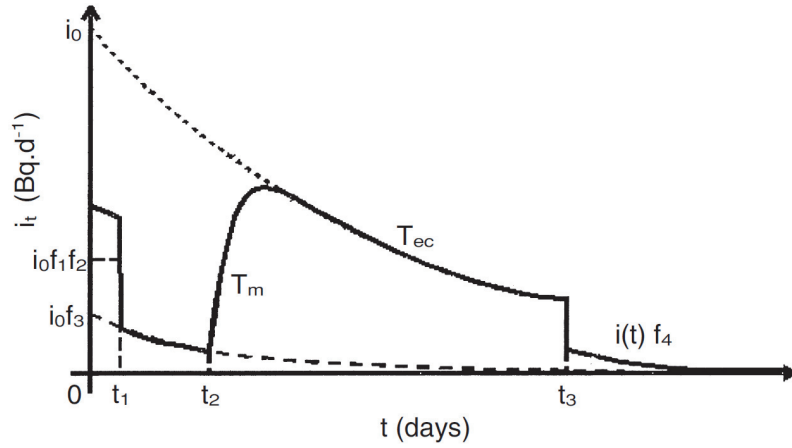
Figure 4. Schematic model of ^{131}I intake rate in human body after the Chernobyl accident, Russia [3-5)]

Figure 4 simulates ^{131}I generic intake rate (Bq/day) for inhabitants of age u with inhaled air i_{inh} and with food i_{ing}. Equations (4, 5) give its mathematical description:

$$i_{inh}(t, u, \sigma_{137}) = i_0 \cdot f_1(u) \cdot f_2(\sigma_{137}), \qquad 0 < t < t_1; \qquad (4)$$

$$i_{ing}(t) = \begin{cases} i_0 \cdot f_3 \cdot e^{-\ln 2 \cdot t / T_{ec}}, & 0 < t \leq t_2; \\ i_0 \cdot (f_3 \cdot e^{-\ln 2 \cdot t / T_{ec}} + (1 - f_3) \cdot (e^{-\ln 2 \cdot (t - t_2) / T_{tc}} - e^{-\ln 2 \cdot (t - t_2) / T_1})), & t_2 < t \leq t_3; \\ i_0 \cdot f_4 \cdot (f_3 \cdot e^{-\ln 2 \cdot t / T_{ec}} + (1 - f_3) \cdot (e^{-\ln 2 \cdot (t - t_2) / T_{ec}} - e^{-\ln 2 \cdot (t - t_2) / T_1})), & t_3 < t; \end{cases}$$

$$(5)$$

where: i_0 , kBq/day, is the parameter to be determined from monitoring data;

t , days, is time since the beginning of radioactive fallout in the region under consideration;

t_1 , days, is the period of inhalation from the plume assumed to be about 1 day;

t_2 , days, -is the time of beginning pasturing cattle from private farms in 1986;

$f_1(u)$, rel. un., is the ratio of the ^{131}I daily intake with milk and inhaled air by children and teenagers of age u to that of adults;

$f_2(\sigma_{137})$, dimensionless, is the ratio of ^{131}I inhalation to ^{131}I ingestion with milk depending on ^{137}Cs soil deposition, see [5] for technical details;

f_3 , dimensionless, is the ratio of ^{131}I intake with leafy vegetables and other surface contaminated food products to that with milk during the time of cattle stabling. For the Chernobyl fallout conditions in Russia, f_3 was assessed about 0.15 [5)].

f_4, dimensionless, is the factor of ^{131}I intake reduction due to food restrictions applied in May 1986. For persons who followed restrictions f_4 value was assessed to be about 0.15 and for the rest – 1.0.

T_1 = 1,5 days is the effective half-time for reduction of ^{131}I activity concentration in milk after single intake in a cow [13)];

T_{ec} , days, is the effective half-time for reduction of ^{131}I activity concentration in milk of cows pastured in the contaminated area. It was assessed to be 4.2 days based on the post-Chernobyl monitoring data in Russia [4)];

The dates of beginning of cattle pasturing were obtained through individual polls of inhabitants in 1987 and collection of official data from collective farms in 1995-1997.

180

5. Thyroid dose reconstruction methodology

In order to develop a thyroid dose reconstruction system we studied regularities of dose based on thyroid measurements on the radioiodine and radiocaesium soil deposition, ^{131}I activity concentration in milk and some other environmental radiation measurements. As in various affected settlements fallout conditions, countermeasures applied and age composition of monitored population groups were different, we standardized the assessed thyroid dose by those factors. To this effect, the standard dose was introduced as the arithmetic mean of all individual doses recalculated to one "reference" age 3 year, with the use of the dependencies of the average dose on age for urban and rural inhabitants, in the assumption that dairy cattle were pastured by the moment of radioactive depositions (t_2=0 on Figure 4), and that the countermeasures were not applied (t_3=∞)[3-5].

For the 'standard thyroid doses' in numerous settlements, a strong correlation of doses with ^{131}I activity concentration in milk time corrected to 8 May 1986 was observed – Figure 5. Similar correlation was observed between the standard dose and mean ^{137}Cs soil deposition in a settlement and its vicinity. Those regularities were used as an experimental basis for the methodology of the large scale thyroid dose reconstruction in Russia, see [5] for technical details.
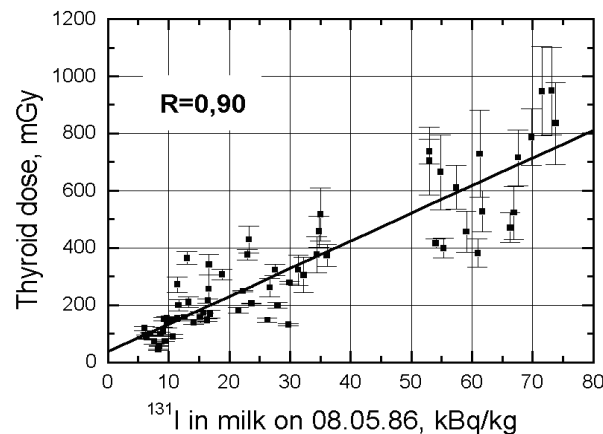
Figure 5. Dependence of the standard thyroid dose in rural settlements on the reference ^{131}I concentration in milk (as of 08.05.1986). Data from the Bryansk, Kalyga and Tula regions of Russia[4, 5].

According to the generic approach presented above, the methodology for the large scale reconstruction of settlement-average thyroid doses in six age groups was structured as follows.

a) In the settlements where in May-June 1986 at least ten measurements of ^{131}I activity in thyroid were conducted, the standard dose was assessed from those measurements using formula (3) and the mathematical description of Figure 4 in order to determine the unknown value of i_0, and then to calculate thyroid dose using formulae (2) and (1).

b) In the settlements where in May-June 1986 at least ten measurements of ^{131}I activity concentration in locally produced milk were conducted, a reference concentration was assessed as their mean value time corrected to 8 May 1986, and then the standard thyroid dose was assessed based on mathematical description of Figure 5.

c) In the other settlements with ^{137}Cs soil deposition above 30 kBq/m^2, first reference ^{131}I activity concentration in milk was assessed from ^{137}Cs soil deposition by means of mathematical description of Figure 3b and then standard thyroid dose was assessed based on mathematical description of Figure 5. For areas/settlements with low ^{137}Cs soil deposition (≤ 30 kBq/m^2) more sophisticated techniques were applied[5].

When settlement-specific standard thyroid doses were assessed by technique a) or b) or c) the mean doses in six age groups were calculated from the age dependence of internal thyroid dose, see e.g. [3] or Figure 5.13 in [12].

Based both on source term, foreign environmental measurements [7, 12] and our own early thyroid measurements in evacuees from the Pripyat city [13] we also considered contribution of shorter-lived iodine radionuclides (^{133}I and ^{132}I) to internal thyroid dose. It was concluded that for conditions of wet deposition and predominant food intake of radionuclides in Russia the contribution of shorter-lived radioiodines is negligible, However, it is not the case if radionuclides were deposited under dry weather conditions and if inhalation dominated as a radioiodine intake pathway [13].

6. Results of thyroid dose reconstruction in Russia

The developed internal thyroid dose reconstruction algorithms and supplementary data were converted in the official methodology approved by the Russian Ministry of Health [15]. This methodology has been used for large scale reconstruction of average internal thyroid dose in more than four thousand Russian settlements affected by the Chernobyl fallout [16].

Figure 6 presents the geographical distribution of the district-average thyroid doses of children and adolescents (<18 y in 1986) in the three countries more affected by the Chernobyl accident [7, 17]. In Russia, the highest doses were received by the residents of the west districts of the Bryansk region. The figure demonstrates good agreement of the data produced by the Belarusian, Russian and Ukrainian dose reconstruction experts.
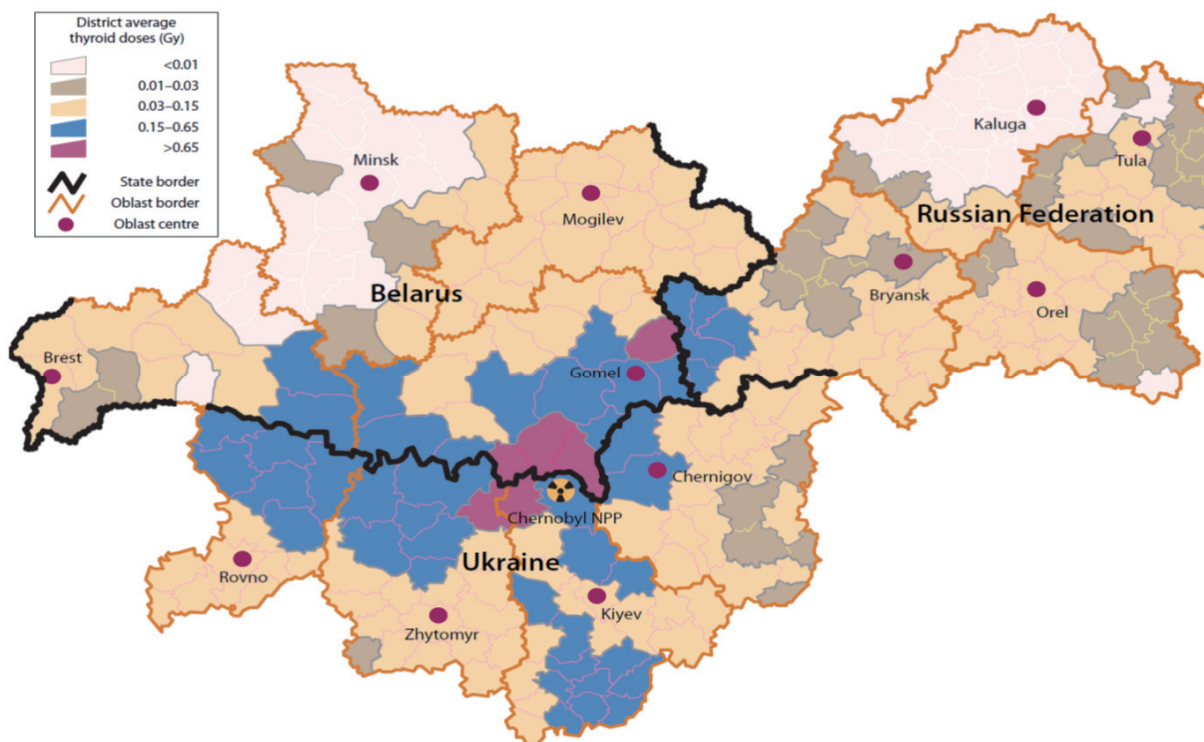
Figure 6. Average thyroid doses to children and adolescents who lived in 1986 in the most affected regions of Belarus, Russia and Ukraine [7, 17]

A summary of the results of internal thyroid dose reconstruction for Russia is presented in Table 1 [7]. Although region-average thyroid doses did not exceed 0.2 Gy even in pre-school children, in some more contaminated settlements it reached a few grays and in some individuals up to a few tens of grays. That high level of thyroid radiation exposure resulted in a few hundred radiation-induced thyroid cancers by 2005 in those who were children or adolescents in 1986 residing in the affected areas of Russia [7].

Table 1 Average and collective doses to the thyroid for the population of Russia [7]

Region	Average thyroid dose (mGy)					Popula-tion (ths. persons)	Collective dose (ths. man Gy)
	Pre-school children	School children	Adoles-cents	Adults	Total		
Bryansk	155	52	31	26	42	1 429	60.5
Tula	44	14	8	6	10	1 796	18.7
Orel	58	19	12	9	15	860	13.0
Kaluga	13	4	3	2	3	1 006	3.5
Other 15 'affected' regions[a]	10	3	2	2	3	32 134	94
Rounded total or average for entire 19 regions	18	6	4	3	5	37 225	190

[a] Belgorod, Kursk, Leningrad, Lipetsk, Nizhny Novgorod, Penza, Ryazan, Saratov, Smolensk, Tambov, Ulyanovsk and Voronezh oblasts, Chuvash, Mordoviya and Tatar autonomous republics.

Those data were used by national authorities for decision making regarding radiation and social protection of the public and by scientists as support for epidemiological studies.

7. Conclusions: application to consequences of the Fukushima-1 2011 accident

Russian experience of internal dose reconstruction following the Chernobyl accident and the other radiological events proved that this goal was achievable if relevant source term, environmental and human measurements were available and substantial research labor was invested.

From the Russian post-Chernobyl experience, mostly the generic approach can be used as applicable to the radiological consequences of the Fukushima-1 2011 accident. The reason why more specific Chernobyl algorithms are not directly applicable in Japan is that in the Russian areas affected a quarter of a century earlier by the Chernobyl fallout, the dominant thyroid exposure pathway was the ingestion of locally produced milk, dairy products and green vegetables contaminated with [131]I. In Fukushima prefecture, at the time of the accidental radionuclide release in the middle of March 2011, vegetation was not well developed for cattle grazing yet and, more generally, milk is a less important food component than it was in the Chernobyl-affected area in 1986. Therefore, intake functions and respective dose reconstruction schemes are rather different.

Thus, radioiodine intake (inhalation and ingestion) patterns in the Fukushima prefecture still have to be clarified with regard to specification of intake mechanisms and parameters and countermeasures applied. Appropriate data can be collected from the targeted local public polls. From the behavior and food/water consumption data combined with environmental and food measurements, the area-specific intake model should be constructed and applied for internal thyroid dose reconstruction as demonstrated in this paper.

Another important feature of the Fukushima case compared to the Chernobyl one is the shortage of human ^{131}I thyroid measurements, especially of spectrometric ones, conducted in March-April 2011. To the authors' knowledge, the total number of those measurements is less than 1500. That means that internal thyroid dose reconstruction cannot be directly based on that kind of data and the latter should be rather used for validation of model assessment. To this effect, the first-priority problem of identification and interviewing of all the persons, for whom thyroid measurements were conducted in March-April 2011, should be solved without delay. Another priority problem is the collection in one place of all the measurements conducted by various Japanese institutions and processing them in a unified manner using post-Chernobyl experience to the extent possible.

From the modeling of radioiodine intake following a major accidental release from a nuclear reactor it is known that the contribution of short-lived radioiodines to thyroid dose can be substantial in case of inhalation in dry weather conditions. As this was the case in some of the areas affected by the Fukushima accident, that contribution should be carefully assessed.

References

1) Degteva MO, Vorobiova MI, Tolstykh EI, Shagina NB, Shishkina EA, Anspaugh LR, Napier BA, Bougrov NG, Shved VA, Tokareva EE.   Development of an improved dose reconstruction system for the Techa River population affected by the operation of the Mayak Production Association. Radiat Res 166 (2006) 255–270.
2) Gordeev K, Shinkarev S, Ilyin L, Bouville A, Hoshi M, Luckyanov N, Simon SL Retrospective dose assessment for the population living in areas of local fallout from the Semipalatinsk nuclear test site. Part II: internal exposure to thyroid. J Radiat Res 47 (2006) A137–A141.
3) Zvonova I., Balonov M. and Bratilova A. Thyroid dose reconstruction for the population of Russia after the Chernobyl accident. Radiation Protection Dosimetry, 79 (1998) 175-178.
4) Balonov M, Bruk G, Zvonova I, et al Methodology of internal dose reconstruction for Russian population after the Chernobyl accident. Rad. Prot. Dos., 92 (2000) 247-253.
5) Zvonova I., Balonov M., Bratilova A., Vlasov A., Pitkevich V., Vlasov O., Shishkanov N. Methodology of Thyroid Dose Reconstruction for Population of Russia after the Chernobyl Accident. In: Harmonization of Radiation, Human Life and the Ecosystem, Proc. of 10th International Congress of the IRPA, International Conference Center Hiroshima, Hiroshima (2000) P-11-265.
6) Ivanov, V.K., A.I. Gorski, A.F. Tsyb et al. Radiation-epidemiological studies of thyroid cancer incidence among children and adolescents in the Bryansk oblast of Russia after the Chernobyl accident (1991–2001 follow-up period). Radiat. Environ. Biophys. 45 (2006) 9-16.
7) United Nations Scientific Committee on the Effects of Atomic Radiation. Sources and Effects of Ionizing Radiation (2008 Report to the General Assembly, with Annexes), Annex D. New York: United Nations; Volume II: 45–219 (2011).
8) M. I. Balonov, L. R. Anspaugh, A. Bouville and I. A. Likhtarev. Contribution of internal exposures to the radiological consequences of the Chernobyl accident. Rad. Prot. Dos., 127 (2007) 491–496.
9) ICRP Publication 67. Age-Dependent Doses to Members of the Public from Intake of Radionuclides: Part 2. Ingestion Dose Coefficients. Annals of the ICRP, v. 23, Nr.3/4 (1993)
10) ICRP Publication 71. Age-Dependent Doses to Members of the Public from Intake of

Radionuclides: Part 4. Inhalation Dose Coefficients. Annals of the ICRP, v. 25, Nr.3/4 (1995).

11) ICRU Report 68. Retrospective Assessment of Exposures to Ionising Radiation. J. of the ICRU, 2/2: 1-136 (2002).

12) International Atomic Energy Agency. Environmental consequences of the Chernobyl Accident and their remediation: Twenty years of experience. IAEA: Vienna (2006).

13) Balonov, M., Kaidanovsky, G., Zvonova, I., Kovtun, A., Bouville, A., Luckyanov, N. and Voillequer, P. Contributions of short-lived radioiodines to thyroid doses received by evacuees from the Chernobyl area estimated using early in-vivo activity measurements. Radiat. Prot. Dosim. 105 (2003) 593–600.

14) Korneev N.A., Sirotkin A.N. Radioecology Of Agricultural Animals. Energoatomizdat, Moscow, , 208 p (1987). (in Russian)

15) Reconstruction of thyroid doses caused by incorporation of radioiodine in inhabitants of localities of the Russian Federation subjected to radioactive contamination due to the accident at the Chernobyl NPP in 1986. Methodic Instruction of the Russian Ministry of Public Health Nr. MU - 2.6.1.1000-00 (2000) 79 p. (in Russian).

16) Mean Thyroid Doses for Inhabitants of Different Age Living in 1986 in Settlements of the Bryansk, Tula, Orel and Kaluga Regions Contaminated with Radionuclides due to the Chernobyl accident. Radiation and Risk, Special Issue, Ed. by M.I. Balonov and I.A. Zvonova, Obninsk-Moscow (2002) 1-94 (in Russian).

17) Russian Medical and Dosimetric Registry. District-average thyroid doses in children and adolescents in Belarus, Russia and Ukraine. Bulletin Radiation and Risk, 15 (2006), 86-87 (in Russian).

Dose Reconstruction Related to the Nuclear Weapons Tests Conducted by the U.S. in the Pacific in the 1950S

André BOUVILLE[1], Steven L. SIMON[2], Harold B.BECK[3]

[1]*U.S. National Cancer Institute (retired), Bethesda, MD USA 20892*
[2]*Division of Cancer Epidemiology and Genetics, National Cancer Institute, National Institutes of Health, 6120 Executive Blvd., Bethesda, MD USA 20892*
[3]*New York City, NY, USA*

Abstract

Nuclear weapons testing conducted at Bikini and Enewetak atolls during 1946-1958 resulted in exposures of the resident population of the present-day Republic of the Marshall Islands to radioactive fallout. This paper summarizes the results of a thorough and systematic reconstruction of radiation doses to that population, by year, age at exposure, and atoll of residence. The main results of this dose-reconstruction effort, which were presented in detail in a special issue of *Health Physics* (August 2010) are: (1) the determination that twenty of the 66 nuclear tests conducted in or near the Marshall Islands resulted in measurable fallout deposition on one or more of the inhabited atolls of the Marshall Islands; (2) the estimation of deposition densities (kBq m^{-2}) of all important dose-contributing radionuclides at each of the 32 atolls and separate reef islands of the Marshall Islands, following each of the twenty tests that are considered; (3) the estimation of age-dependent doses from external irradiation resulting from each test and aggregated on an annual basis; and (4) the estimation of age-dependent doses from internal irradiation to the red bone marrow, thyroid gland, stomach wall, and colon wall of representative individuals of the inhabited atolls and reef islands. The dose estimates are based on the available radiation measurement data (concentrations of ^{131}I in urine, whole-body measurements, concentrations of ^{137}Cs in soil, exposure rates, etc.) supplemented with a variety of models and assumptions. It was found that the total deposition of ^{137}Cs, external dose, and internal organ doses followed the same geographic pattern with the large population of the southern atolls receiving the lowest doses. Permanent residents of the southern atolls who were of adult age at the beginning of the testing period received external doses ranging from 5 to 12 mGy on average; the external doses to adults at the mid-latitude atolls ranged from 22 to 60 mGy on average, while the residents of the northern atolls received external doses in the hundreds to over 1000 mGy. Internal doses varied significantly by age at exposure, location, and organ; they are estimated to have been as high as about 20,000 mGy to the thyroid glands of young children exposed on Rongelap at the time of the Castle Bravo test of 1 March 1954.

Keywords: *Marshall Islands; radioactive fallout; radiation doses*

1. Introduction

From 1946 through 1958, 65 nuclear weapons tests, in seven series, were carried out by the United States at Bikini and Enewetak Atolls located at the northwestern end of the archipelago that makes up the Marshall Islands (Figure 1) and one additional test was carried out 100 km to the west of Bikini. The total explosive yield of the 66 tests was approximately 100 Mt (equivalent to 100 million tons of trinitrotoluene or TNT) [1-3], about 100 times the total yield of the atmospheric tests conducted at the Nevada Test Site. Radioactive debris from the detonations, dispersed in the atmosphere, was generally blown by the predominantly easterly winds towards the open ocean west of the Marshall Islands, though various historical reports (e.g. [4,5],) indicate that radioactive debris from a number of tests traveled in other directions. Of special significance was the largest test

conducted in the Marshall Islands, code-named Castle Bravo, a 15-Mt thermonuclear device tested on 1 March, 1954. As a result of unexpected wind shear conditions, heavy fallout of debris from Bravo on atolls east of the Bikini atoll test site resulted in high radiation doses to the populations of nearby atolls.

Figure 1. Atolls and reef islands of the Republic of the Marshall Islands, locations of nuclear test sites and of evacuated populations.

While the populations of Bikini and Enewetak were relocated before the testing began, other populations were evacuated following the Bravo test. Within about two days following the detonation of the Bravo test and the unexpected fallout on atolls to the east, the resident populations of Rongelap (including some Rongelap residents temporarily present on Ailinginae) and Utrik, as well as American military weather observers on Rongerik, were evacuated to avert continued exposure, to be decontaminated, and to receive immediate medical care for conditions of acute exposures[5].

In the month after the Bravo test, ^{131}I, an important radionuclide in fallout, was measured in urine collected about two weeks after the Bravo event from adults exposed on Rongelap, Ailinginae, and Rongerik[6]. Those measurement data have proven to be of significant value for reconstruction of internal dose for those groups. For example, Brookhaven National Laboratory used the activity measurements in urine as well as other data and assumptions to estimate internal thyroid dose for persons exposed on Rongelap, Ailinginae, and Utrik.[7] Internal doses from long-lived radionuclides on Rongelap and Utrik also were estimated[8] using whole-body and bioassay data collected years after the Bravo test.

Although numerous studies have been conducted over the past decades to monitor the Marshall Islands and people, to develop land remediation strategies, and to assess contemporary and possible future doses that might be received by inhabitants of certain atolls in the Marshall Islands, particular emphasis was often given to radiological monitoring or to the northern Marshall Islands. Many of those early studies were chronicled in a special issue of *Health Physics*[9].

This study, however, which was conducted between 2004 and 2010, is the first to estimate the deposition of all the radionuclides contributing to these doses at all atolls and to estimate doses to residents of all the atolls and islands from all nuclear tests conducted in the Marshall Islands. The overall purpose of the study was to derive an internally consistent set of radiation absorbed doses to

representative individuals of all Marshallese population groups alive during and after the years of nuclear testing in the Marshall Islands. The methods of dose reconstruction that were used in the study, as well as the estimated radiation doses, are summarized in this paper. Detailed information on the technical aspects and results of the study are presented in a special issue of *Health Physics* (August 2010), in which the articles related to dose reconstruction are:

- the estimation of the amounts of fallout that were deposited on the ground over each atoll and separate reef island of the Republic of the Marshall Islands[10];
- a model of atmospheric transport and deposition that was used to provide confirmation of the reliability of some of the estimated depositions[11].
- the estimation of doses from external irradiation[12];
- the estimation of the doses from internal irradiation[13];
- the analysis of bioassay data important to internal dose estimation[14];
- the interpretation of intake-related dosimetric factors[15]; and
- a recapitulation of the doses to all population groups of the Marshall Islands[16].

2. Summary of methods and findings

The following will be considered in turn:
(1) the deposition densities of ^{137}Cs and other radionuclides from each nuclear weapons test that resulted in measurable fallout over each atoll of the Marshall Islands,
(2) the exposure rates, normalized to H + 12 h, on each inhabited atoll after each test,
(3) external doses,
(4) internal dose, and
(5) a comparison of the doses from external and internal irradiation.

2.1. Fallout Activity Deposited on the Ground

As discussed elsewhere [10] a complete review of various historical and contemporary deposition- related data, some available only in gray literature, e.g., government laboratory reports and internal agency and laboratory memoranda, supplemented by meteorological analyses, was used to make judgments regarding which tests deposited fallout in the Marshall Islands and to estimate fallout deposition density and fallout transit times, known as times-of-arrival (TOA). In some instances, it was necessary to use the results of a well-established model of atmospheric transport and deposition [11] to corroborate or contradict our initial assumptions on the occurrence of fallout on particular atolls after certain tests. As a result of this analysis, we estimated that out of the 66 nuclear tests detonated in or near the Marshall Islands from 1946 through 1958, 20 tests, listed in Table 1, deposited measurable fallout in the Marshall Islands excluding the atolls on which the test sites were located. Each of these 20 tests was taken into account in the estimation of radiation doses.

The various types of data reviewed for estimating deposition included measurements of ^{137}Cs and other radionuclides in soil (both historical and contemporary), historical measurements of exposure rate following individual tests derived from aerial surveys, ground surveys and continuous-reading monitoring devices (strip-chart recorders), and historical measurements of beta activity collected on gummed film during the years of nuclear testing. The review of the various historical measurement data was used to make estimates of ^{137}Cs deposition density and fallout time-of-arrival (TOA) for each atoll and for each of 20 individual tests. The resultant total ^{137}Cs deposited by all tests from this analysis, after appropriate correction to account for radioactive decay and for the weathering effect of ^{137}Cs in the soils of the Marshall Islands, were then compared with the retrospective ^{137}Cs remaining in the soil as measured at various atolls by different investigators in 1978 and in 1991-93 [17,18]. This comparison

was used to demonstrate the validity and relative accuracy of our individual test ^{137}Cs deposition density estimates.

Table 1 Nuclear tests estimated to have deposited measurable fallout in the Marshall Islands [16]

Test name	Operation	Test site Atoll	Local date (dd/mm/yyyy)	Total yield (Mt)	Fusion yield[a] (Mt)
Yoke	Sandstone	Enewetak	01/05/1948	0.049	0
Dog	Greenhouse	Enewetak	08/04/1951	0.08	0
Item	Greenhouse	Enewetak	25/05/1951	0.05	0
Mike	Ivy	Enewetak	01/11/1952	10.4	4.7
King	Ivy	Enewetak	16/11/1952	0.5	0.25
Bravo	Castle	Bikini	01/03/1954	15	6
Romeo	Castle	Bikini	27/03/1954	11	3.7
Koon	Castle	Bikini	07/04/1954	0.11	0.04
Union	Castle	Bikini	26/04/1954	6.9	2.3
Yankee	Castle	Bikini	05/05/1954	13.5	4.5
Nectar	Castle	Enewetak	14/05/1954	1.7	0.85
Zuni	Redwing	Bikini	28/05/1956	3.5	2.25
Flathead	Redwing	Bikini	12/06/1956	0.37	0.18
Tewa	Redwing	Bikini	21/07/1956	5	2.7
Cactus	Hardtack I	Enewetak	06/05/1958	0.018	0
Fir	Hardtack I	Bikini	12/05/1958	1.4	0.7
Koa	Hardtack I	Enewetak	13/05/1958	1.4	0.7
Maple	Hardtack I	Bikini	11/06/1958	0.21	0.07
Redwood	Hardtack I	Bikini	28/06/1958	0.41	0.14
Cedar	Hardtack I	Bikini	03/07/1958	0.22	0.07

[a]Fusion yields as estimated by UNSCEAR (2000). Actual values are still classified.

Estimates for the ^{137}Cs deposition density and for the corresponding TOA at each atoll and for each of the 20 individual tests with measurable fallout are presented in tabular form in [10]. In this paper, only illustrative or summary results are provided. Our best estimates of the cumulative ^{137}Cs deposition density from all tests with 90% uncertainty ranges are shown in Table 2. The cumulative ^{137}Cs deposition densities are much greater on northern atolls (e.g., Rongelap and Rongerik) than on mid-latitude atolls (e.g., Kwajalein) or southern atolls (e.g., Majuro). Table 2, as can be noted, also provides estimates of deposition separately for southern and northern islands in Kwajalein atoll and in Rongelap atoll. The deposition densities differed by about 20% between south and north islands of Kwajalein but more than three times between islands of south and north Rongelap atoll (Table 2), reflecting differences in deposition due either to the large size of the atoll (Kwajalein), or in the case of Rongelap, to the position of the Bravo debris cloud trajectory relative to location of individual islands in the atoll. Throughout this section and elsewhere, we discuss findings relative to four groups of atolls or communities. Within each group, resident populations were exposed to similar levels of fallout as a consequence of the dispersion patterns of the nuclear debris clouds. The southern atoll group is well represented by Majuro, which is the national capital today and was home to about one-third of the population of the southern atolls in 1958, while the mid-latitude atolls are best represented by Kwajalein, which was home to about one-quarter of the total Marshall Islands population during the testing years. Our radiological findings for the southern atolls and mid-latitude atolls along with our radiological findings for the Utrik community and for the Rongelap Island community (both from the northern atolls) capture the range of exposures received by Marshallese at all atolls. In the case of Utrik and Rongelap, we define the "community" to be those exposed to fallout from the Bravo test on Utrik and Rongelap, respectively, and who were evacuated after the Bravo test. Our findings illustrate the geographic pattern as well as provide atoll- and atoll-group estimates of contamination, organ dose, and cancer risk as well as the dependence on age at exposure.

Table 2 Estimated total ^{137}Cs deposition grouped according to areas with relatively homogeneous deposition: mean values and 90% uncertainty range (5%-95%)

Atoll	Bq/m² (mean)	Bq/m² (GM[a])	5%	95%
Southern atolls:				
Ailinglaplap	1,500	1,300	690	2,600
Arno	2,200	2,000	1,100	3,600
Aur	2,000	1,900	1,200	3,000
Ebon	1,400	1,400	930	2,000
Erikub	2,400	2,300	1,600	3,300
Jabwot	1,700	1,500	770	2,900
Jaluit	1,500	1,400	7,760	2,400
Kili Island	1,500	1,400	860	2,300
Lae	2,000	1,700	690	4,000
Lib Island	2,400	2,000	890	4,500
Majuro	2,000	2,000	1,300	2,900
Maloelap	2,400	2,300	1,400	3,700
Mili	1,600	1,500	920	2,400
Namorik	1,300	1,200	720	2,000
Namu	2,000	1,700	750	3,800
Taongi	1,200	930	350	2,400
Ujae	1,600	1,200	470	3,300
Mid-lat. atolls				
Ailuk	7,500	6,800	3,600	13,000
Jemo Island	5,200	4,700	2,400	9,000
Kwajalein (south)	3,600	3,400	2,100	5,400
Kwajalein (north)	4,300	3,700	1,800	7,600
Likiep	5,500	4,800	2,400	9,900
Mejit	6,600	6,000	3,200	11,000
Ujelang	4,000	3,500	1,600	7,300
Wotho	4,000	3,800	2,300	6,200
Wotje	5,200	4,600	2,400	8,900
Utrik region:				
Taka	20,000	19,000	11,000	32,000
Utrik	29,000	26,000	14,000	48,000
Northern atolls:				
Alinginae	54,000	47,000	22,000	98,000
Bikar	68,000	56,000	24,000	130,000
Rongelap (north)	560,000	430,000	150,000	1,200,000
Rongelap Island	180,000	160,000	100,000	279,000
Rongerik	120,000	97,000	41,000	230,000

[a]GM stands for geometric mean

The test- and atoll-specific estimates of ^{137}Cs fallout were then used to estimate the deposition densities (kBq m^{-2}) of all other radionuclides considered in this study, taking into account the estimated fallout transit times. A nuclide mixture was assumed for all thermonuclear tests identical to that for the Castle Bravo nuclear test [19], adjusted for estimated fractionation effects, while a nuclide mixture of a typical plutonium-fueled fission device that was detonated at the Nevada Test Site was used for the non-thermonuclear tests [20]. For each atoll, fallout TOAs and the estimated fractionation of fallout were used to estimate deposition density for 63 activation and fission products (^{55}Fe, ^{64}Cu, ^{77}As, ^{83}Br, ^{88}Rb, ^{89}Sr, ^{90}Sr, ^{91}Sr, ^{92}Sr, ^{90}Y, ^{91m}Y, ^{92}Y, ^{93}Y, ^{95}Zr, ^{97}Zr, ^{95}Nb, ^{97m}Nb, ^{99}Mo, ^{99m}Tc, ^{103}Ru, ^{105}Ru, ^{106}Ru, ^{103m}Rh, ^{109}Pd, ^{112}Ag, ^{115}Cd, ^{117}Cd, ^{117m}In, ^{121}Sn, ^{127}Sn, ^{125}Sb, ^{127}Sb, ^{129}Te, ^{131m}Te, ^{132}Te, ^{133m}Te, ^{131}I, ^{132}I, ^{133}I, ^{135}I,

^{137}Cs, ^{139}Ba, ^{140}Ba, ^{140}La, ^{141}La, ^{142}La, ^{131}Ce, ^{134}Ce, ^{143}Pr, ^{144}Pr, ^{145}Pr, ^{147}Nd, ^{149}Nd, ^{149}Pm, ^{151}Pm, ^{153}Sm, ^{237}U, ^{240}U, ^{239}Np, ^{240m}Np) from each nuclear test, plus the cumulative deposition over all tests of $^{239+240}$Pu. Cumulative deposition densities in the four representative atolls are presented in Table 3 for 24 selected radionuclides.

The estimates of radionuclide deposition density, fractionation, and transit times reported in[10] allowed estimations of both external and internal dose to representative persons.

2.2. Radiation Doses

There are 30 atolls and four separate reef islands in the Marshall Islands. Ground deposition densities were estimated for 63 radionuclides plus ^{239,240}Pu for all the atolls and separate reef islands except the two atolls where the testing sites were located (Bikini and Enewetak). However, some of the atolls were not inhabited during all or part of the testing period either because they were historically used only for gathering food (Ailinginae, Bikar, Erikub, Jabat, Jemo Island, Knox, Taka, and Taongi) or because the residents were relocated for safety reasons (Bikini and Enewetak) or evacuated due to unexpected exposures (Ailinginae, Rongelap, Rongerik, Utrik). Thus, radiation doses were estimated for 26 population groups, including the residents of the 23 atolls and islands that were inhabited during the years of nuclear testing, and three other groups: persons from Rongelap who were on Ailinginae at the time of the Castle Bravo test, persons from Rongelap who were visiting the southern atolls at the time of the Castle Bravo test, and U.S. military weather observers on Rongerik. The dose assessment explicitly included members of the six Marshallese groups that were relocated or evacuated during the testing period: (i) 64 persons evacuated from Rongelap Atoll after the Bravo test, (ii) 18 persons from Rongelap evacuated from Ailinginae atoll after the Bravo test, (iii) 117 persons from Rongelap who were visiting the southern atolls at the time of the Bravo test, (iv) 157 persons from Utrik Atoll evacuated after the Bravo test, and the populations that normally resided on (v) Enewetak Atoll and (vi) Bikini Atoll but who had been relocated to Ujelang Atoll and Kili Island, respectively, before the testing program began. The Rongelap and Utrik populations, who were evacuated within about two days following the detonation of the Castle Bravo test on March 1, 1954, were returned to their home atolls in June 1957 and June 1954, respectively.

In addition to the whole-body doses from external irradiation, absorbed doses from internal irradiation to the thyroid, red bone marrow, stomach wall, and colon wall were estimated for members of the 25 Marshallese population groups by age group (children under 1 y, 1-2 y, 3-7 y, 8-12 y, 13-17 y, and adults) and for the U.S. military personnel on Rongerik. Those four specific organs and tissues were selected because they are expected to give rise to the largest number of cancers.
Estimated doses were derived for "representative" persons, that is, for persons that could be described to have habits, lifestyles, diet, and anthropometric characteristics typical of the Marshall Islands population for their age and gender (except in the case of military servicemen on Rongerik).

Doses were assessed on a yearly basis for exposures occurring from 1948, the year in which the first relevant test took place, to 1970, when the residual environmental contamination had reached negligible levels on most atolls.

The estimated total radiation absorbed doses include three components: (1) doses from external irradiation emitted by fallout deposited on the ground; (2) doses from internal irradiation from acute radionuclide intakes immediately or soon after fallout after each test; and (3) doses due to internal irradiation from chronic (i.e., protracted) intakes of radionuclides resulting from the continuous presence of long-lived radionuclides in the environment.

Table 3 Sum of radionuclide deposition densities (kBq m^{-2}) from all tests for 24 selected radionuclides at the four representative atolls

		REPRESENTATIVE ATOLL			
Nuclide	Half-life	Majuro	Kwajalein[a]	Utrik	Rongelap Island
^{55}Fe[b]	2.7 a	1.8×10^{-1}	3.1×10^{-1}	4.7×10^{0}	4.2×10^{1}
^{89}Sr	51 d	2.2×10^{2}	3.5×10^{2}	3.7×10^{3}	2.8×10^{4}
^{90}Sr	29 a	6.9×10^{-1}	1.2×10^{0}	1.1×10^{1}	7.5×10^{1}
^{92}Y	3.5 h	5.8×10^{0}	8.3×10^{2}	3.3×10^{4}	2.7×10^{6}
^{93}Y	10 h	2.1×10^{2}	2.7×10^{3}	8.1×10^{4}	2.1×10^{6}
^{95}Zr	64 d	1.5×10^{2}	2.5×10^{2}	4.2×10^{3}	3.9×10^{4}
^{99}Mo	66 h	1.6×10^{3}	4.0×10^{3}	7.3×10^{4}	7.6×10^{5}
^{103}Ru	39 d	1.8×10^{0}	2.0×10^{2}	3.0×10^{1}	1.8×10^{2}
^{106}Ru	370 d	4.0×10^{1}	7.0×10^{1}	6.1×10^{2}	4.3×10^{3}
^{131m}Te	30 h	2.4×10^{2}	9.4×10^{2}	1.1×10^{4}	1.1×10^{5}
^{131}I	8.0 d	1.3×10^{3}	2.5×10^{3}	2.3×10^{4}	1.7×10^{5}
^{132}Te	78 h	2.4×10^{3}	5.7×10^{3}	5.7×10^{4}	4.6×10^{5}
^{132}I	2.3 h	2.5×10^{3}	5.9×10^{3}	5.8×10^{4}	4.7×10^{5}
^{133}I	21 h	2.5×10^{3}	1.3×10^{4}	1.7×10^{5}	1.9×10^{6}
^{135}I	6.6 h	1.7×10^{2}	4.6×10^{3}	8.5×10^{4}	2.7×10^{6}
^{137}Cs	30 a	2.0×10^{0}	3.5×10^{0}	2.9×10^{1}	1.8×10^{2}
^{140}La	1.7 d	9.0×10^{2}	1.1×10^{3}	8.2×10^{3}	3.2×10^{4}
^{141}La	3.9 h	7.0×10^{0}	8.5×10^{2}	2.5×10^{4}	3.3×10^{6}
^{141}Ce	33 d	3.8×10^{2}	6.4×10^{2}	7.8×10^{3}	4.6×10^{4}
^{143}Ce	33 h	1.1×10^{3}	3.9×10^{3}	8.1×10^{4}	1.0×10^{6}
^{144}Ce	280 d	2.0×10^{1}	3.5×10^{1}	5.3×10^{2}	4.7×10^{3}
^{145}Pr	6.0 h	3.0×10^{1}	1.0×10^{3}	3.8×10^{4}	2.1×10^{6}
^{239}Np[b]	2.4 d	9.1×10^{3}	2.4×10^{4}	4.4×10^{5}	4.8×10^{6}
$^{239+240}$Pu	24000/6600a	7.2×10^{-2}	6.6×10^{-2}	3.5×10^{0}	1.6×10^{1}

[a]Deposition density in the southern part of the atoll, as the northern part was not inhabited.
[b]Activation product.

2.2.1. External doses

The doses from external irradiation arose from gamma rays emitted during radioactive decay of the fallout radionuclides during the passage of the radioactive cloud or after deposition on the ground. Doses received during the passage of the radioactive cloud are generally insignificant compared to those delivered after deposition of fallout on the ground. Exposure during the cloud passage was implicitly included by integration of the exposure rate from the initial time of fallout arrival rather than from the time when the exposure rate was at its peak.

The doses from external irradiation were estimated in three basic steps[12]:

1) estimation of the outdoor exposure rates at 12 h after each test and of the variation in the exposure rates with time at each atoll after each test;
2) estimation of the annual exposure from 1948 through 1970 and of the total exposure from TOA to infinity, obtained by integrating the estimated exposure rates over time, and,
3) estimation of the annual and cumulative absorbed doses to tissues and organs of the body by applying conversion factors from free-in-air (outdoor) exposure to tissue absorbed dose and by assuming continuous residence on the atoll (with corrections for temporarily resettled populations).

The outdoor exposure rates at each atoll were assessed in one of two ways depending on whether reliable measurements of exposure rates were available for a particular nuclear test and atoll

combination. If measurement data were available, they were assessed and a best estimate of the average exposure rate at 12 h post detonation (termed $\dot{E}12$) on the atoll or reef island was made. If no reliable exposure rate data were available to estimate $\dot{E}12$ directly, then the assessment of $\dot{E}12$ was derived from the estimates of ^{137}Cs deposition densities and TOA provided in[10] for each atoll and each test. The method relating the estimates of ^{137}Cs deposition densities and TOA to $\dot{E}12$ was developed by the Off-Site Radiation Exposure Review Project (ORERP) for estimating external whole-body dose from fallout originating at the Nevada Test Site [19].

The annual and cumulative exposures derived from the estimate of $\dot{E}12$ were estimated in[12] using the variation with time of the exposure rate calculated by [20,21], but modified to take fractionation into account, where necessary, as well as the "weathering effect" which reflects the gradual decrease of the exposure rate caused by the migration of the deposited activity into deeper layers of soil. The calculations were based on measurements carried out for six thermonuclear tests conducted in the Pacific (Mike, Bravo, Romeo, Yankee, Zuni, Tewa) and a non-thermonuclear test conducted at the Nevada Test Site (Tesla). The calculated variation with time of the exposure rates, normalized to a unit value at 12 h post detonation, for those seven tests is shown on Figure 2 for a typical fractionation level. It is clear that the exposure rates decrease very rapidly with time: most of the radiation exposure occurs within a few months following the nuclear test.

The conversion factors from free-in-air (outdoor) exposure to tissue absorbed dose depend on the energy distribution of the gamma-rays that are incident on the body and on the organ for which the dose is being estimated. However, for most of the fission and activation products that are created during a nuclear explosion, the gamma-ray energies resulting in external exposure are a few hundred keV or more and the variation in photon energy results in at most a few percent difference in dose per unit incident fluence for the various organs considered in this study [22]. Thus, energy and organ dependence in dose conversion factors were not taken into consideration; a single conversion factor, 6.6 x 10^{-3} mGy per mR, was used for adults for all organs. However, the conversion factor does depend on the age of the person, or, more precisely, her or his body size and shape. Thus, based on calculations using anthropomorphic phantoms that represented different ages [22], our calculated doses to adults from external irradiation were increased by 30% for children less than 3 years of age and by 20% for children 3 years of age through 14 years. While age and body size were important for the estimation of external dose to the organs considered, gender was not. Building shielding was estimated not to be important since houses at that time, made primarily out of palm fronds, did not provide any substantial reduction of gamma ray intensity.
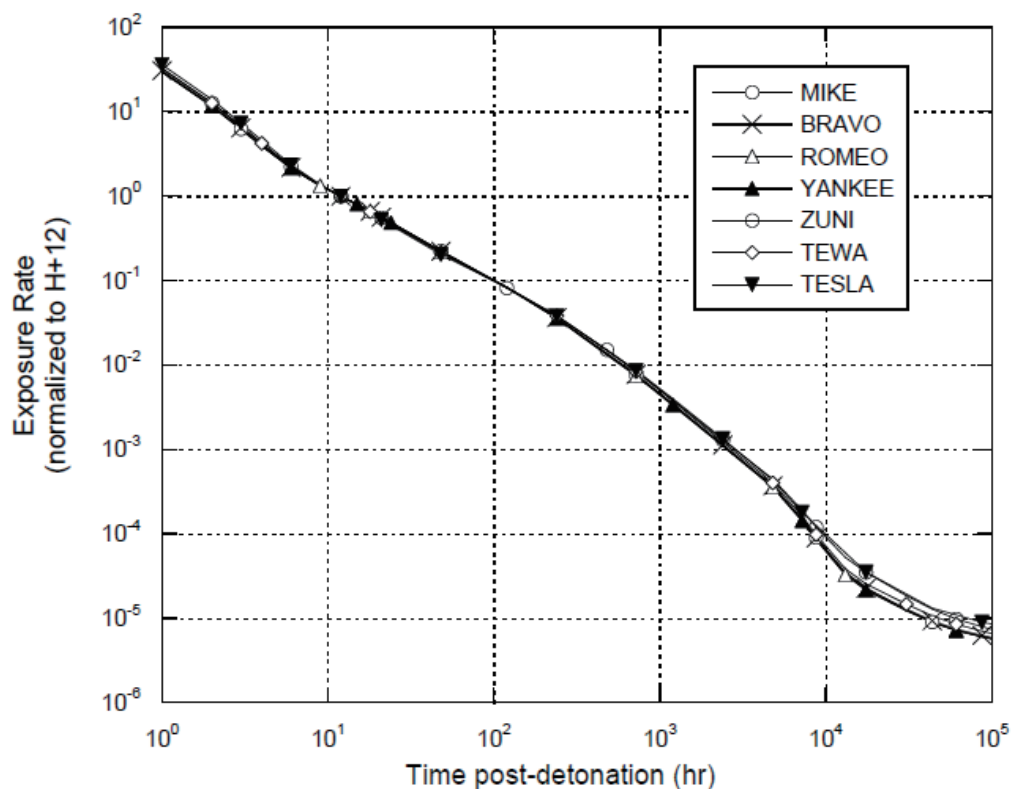
Figure 2. Variation with time of the normalized exposure rates for six thermonuclear tests and a non-thermonuclear test (Tesla) for a fractionation level, R/V, of 0.5 [20,21]

Annual absorbed doses from external irradiation from all important tests were estimated for the time period from 1948 through 1970; that is, until the annual doses had decreased to very low levels in comparison to the peak values observed in 1954. These annual doses were estimated for the relocated populations and for the populations continuously resident on all inhabited atolls of the Marshall Islands in three age categories (infants, children, and adults). The doses reported for the relocated populations include, where appropriate, contributions from exposures received before evacuation, during the period of resettlement, and following return to the atoll of origin. Annual doses to adults from external irradiation are presented in Figure 3; the doses were highest during the years of atmospheric testing in the Marshall Islands, after which they decreased to values that were, in 1970, less than 0.1% of the peak values observed in 1954. Our best estimates of the total external doses (mGy) from all tests and of the 90% uncertainty ranges are presented in Table 4 for representative adults of all 26 population groups, while the total external doses grouped in the 4 regions of the Marshall Islands are shown in Table 5. The geographic pattern of total external doses received is the same as for the deposition of ^{137}Cs and, as described, is much higher in the northern atolls than in the central and southern atolls.
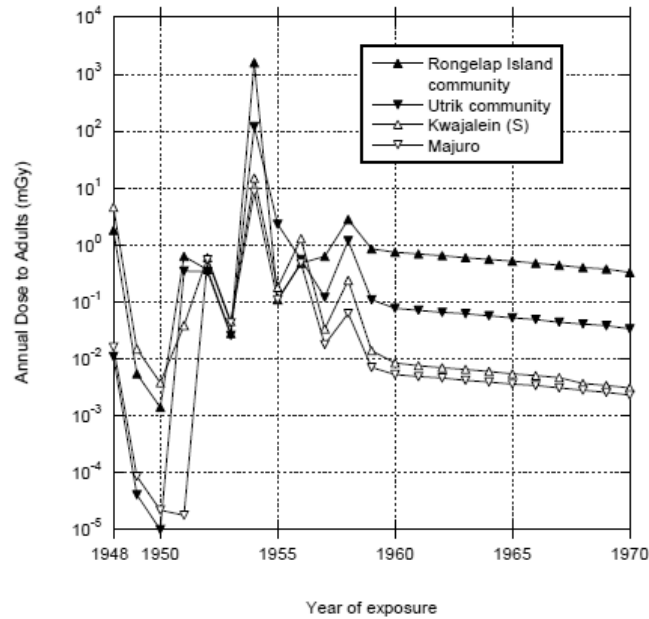
Figure 3. Estimated annual doses to adults, in mGy, for selected atolls

Table 4 Estimates of external doses (mGy) received by adults from the Bravo test, the entire Castle (1954) test series, and from all tests (dose estimates rounded to two significant digits)

Atoll or Population Group	Bravo	Castle Series	All tests
Ailinginae[a]	460	470	470
Ailinglaplap	0.37	5.3	6.9
Ailuk	37	57	59
Arno	2.3	9.3	10
Aur	3.4	7.7	10
Bikini community[a]	1.1	5.0	11
Ebon	0.70	4.8	5.3
Enewetak community (Ujelang)[a]	2.1	14	25
Jaluit	1.1	4.8	6.6
Kwajalein	1.0	15	22
Lae	1.6	7.8	10
Lib Island	0.7	11	12
Likiep	25	37	39
Majuro	2.3	8.7	9.8
Maloelap	5.2	11	12
Mejit Island	27	47	49
Mili	1.9	6.4	7.0
Namorik	0.9	4.4	5.5
Namu	0.7	9.0	11
Rongelap Island community[a]	1,600	1,600	1,600
Rongerik[b]	660	-	-
Ujae	1.0	6.4	8.6
Utrik community[a]	110	120	130
Wotho	4.3	13	23
Wotje	17	30	31

[a]Includesdose received while relocated.
[b]Dose to U.S. military personnel on Rongerik prior to evacuation.

196

Table 5. Four groups of atolls and islands based on similar total external dose (mGy) to adults from regional fallout. Atolls are listed alphabetically within each group.

Atoll or population group	Atolls	Average total whole-body dose from all tests through 1970 (mGy)	Range of average whole-body dose among atolls (mGy)
Southern atolls	Ailinglaplap, Arno, Aur, Ebon, Jaluit, Kili Island[a],Lae, Lib Island, **Majuro**, Maloelap, Mili, Namorik, Namu, Ujae.	9	5-12
Mid-latitude atolls	Ailuk, **Kwajalein**, Likiep, Mejit Island, Ujelang[b], Wotho, Wotje	35	22-59
Utrik community	**Utrik**[c]	130	-
Northern atolls	Ailinginae[c], **Rongelap Island**[c], Rongerik[d]	See Table 4 for values	470-1600

[a]Bikini community
[b]Enewetak community
[c]Includes doses received both when population was on home atoll as well as during relocations.
[d]American military weather observers exposed only to Bravo fallout.

2.2.2. Internal doses from acute intakes of radionuclides

The internal radiation doses resulting from acute intakes, defined as those that occurred during or soon after fallout deposition, were assumed to be primarily a consequence of ingesting radionuclides in, or on, debris particles that contaminated food surfaces, plates and eating utensils, the hands and face, and, to a lesser degree, drinking water [7,13]. Internal doses from other pathways of exposure, in particular, inhalation, were much lower than those due to ingestion and have not been explicitly estimated in this assessment. Fallout particles at northern atolls were typically large (tens to more than one hundred micrometers in diameter) resulting in generally low intakes by inhalation. Fallout deposited at southern atolls, even though generally composed of smaller sized particles, was often deposited with rainfall which significantly reduced the availability of the particles to be inhaled. Annual rainfall rates are three to four times greater in the southern atolls compared to the northern atolls [23].

The methods used in this study for estimating acute intakes of fallout radionuclides and resulting doses are based on: (1) the estimates of test-, atoll-, and radionuclide-specific deposition densities discussed above, (2) historical measurements of ^{131}I in pooled samples of urine collected from adults about two weeks after the Bravo test [6, 14]. As thyroid or whole-body measurements of ^{131}I were not conducted after the test, these measurements of ^{131}I in urine, performed on aliquots of complete 24-h samples, are crucial in the assessment of the intakes of radioactivity by the Marshallese[14]; and (3) assessment of appropriate values of gastrointestinal uptake for the radionuclides present in fallout particles [15]. These values are based on a review of the literature, taking into account the available urine bioassay data of the Marshallese population, specific circumstances of weapons test conditions (e.g., radionuclide fractionation and solubility), and specific conditions of population exposure (e.g., close-in vs. distant locations, and acute vs. chronic intakes) [15].

The assessment of internal doses was composed of the following six steps: (1) estimation of the intake of ^{131}I by populations on Rongelap, Ailinginae, and Rongerik, following the Bravo test using historical bioassay data, (2) estimation of the intake of ^{137}Cs at the same three atolls based on

the ratios of ^{137}Cs to ^{131}I calculated by[20,21] but corrected for fractionation, (3) estimation of the deposition density of ^{137}Cs following each of 20 tests on all inhabited atolls, (4) estimation of the intake of ^{137}Cs at all inhabited atolls assuming that the ratio of intake to deposition was the same at all atolls, (5) estimation of intakes of all radionuclides considered at all inhabited atolls following each nuclear test, and (6) estimation of annual and cumulative radiation absorbed doses to four organs (red bone marrow, thyroid, stomach, colon) of representative persons for all relevant birth years.

Detailed information on the acute intakes of the 24 most important radionuclides resulting from the Castle Bravo test, from all tests of the Castle series (see Table 1), and from all tests conducted at Bikini and Enewetak is presented in Table 6 for the populations of the 4 representative atolls. The intakes from the Castle Bravo test account for almost all of the intakes for the Rongelap and Utrik community members, while they only represent a small fraction of the total intakes for the Kwajalein and Majuro residents. With respect to the differences in intakes from all tests from one population to another, it is clearly shown in Table 6 that the acute intakes estimated for the population of the southern atolls are much smaller than those experienced by the more highly exposed Rongelap and Utrik populations. For example, adult Majuro residents had intakes of about 6% and 9% of the ^{131}I and ^{137}Cs (cumulated over all tests), respectively, of adult Utrik community members, and about 1%, and 2%, respectively, of the intakes of Rongelap community members exposed to Castle Bravo fallout on Rongelap Island.

Doses to the thyroid gland were much greater than those to the other organs and tissues, and were much greater for the Marshallese who resided on Rongelap and Utrik atolls at the time of the Castle Bravo test than for the residents of any other atoll (Table 7). The southern atolls, where about 73% of the population resided during the testing years, received the lowest organ doses. The population of mid-latitude atolls, home to about 23% of the total Marshall Islands population during the testing years, received organ doses that were about three times greater than at the southern atolls. The population of Utrik received doses intermediate in magnitude between the mid-latitude atolls and Rongelap, with thyroid doses about 35 times greater than the southern atolls. The Rongelap Island community received the highest doses with thyroid doses about 350- to 400-times greater than those received in the southern atolls. As presented in Table 8, the order of importance of the radionuclides that contributed most to the dose varied from one target tissue to another and, to a lower extent, from one representative atoll to another. In all atolls, ^{131}I and ^{133}I contributed most to the thyroid dose, while ^{132}Te and ^{239}Np were usually the most important contributors to the doses to other tissues.

Table 6 Estimated acute intakes (kBq) of 24 selected radionuclides by representative adults of four atoll populations from the Bravo test, the Castle (1954) series and over all tests (intakes account for relocations).

Radio-nuclide	Majuro Residents			Kwajalein Residents			Utrik Community			Rongelap Island Community		
	Bravo	Castle Series	Total	Bravo	Castle Series	Total	Bravo	Castle Series	Total	Bravo	Castle Series	Total
^{55}Fe*	1.0E-03	4.8E-03	5.6E-03	5.1E-04	6.5E-03	9.7E-03	1.3E-01	1.3E-01	1.3E-01	1.1E+00	1.1E+00	1.1E+00
^{89}Sr	1.2E+00	5.7E+00	6.6E+00	6.2E-01	7.9E+00	1.1E+01	7.5E+01	8.3E+01	8.4E+01	6.2E+02	6.2E+02	6.3E+02
^{90}Sr	3.9E-03	1.9E-02	2.2E-02	2.0E-03	2.5E-02	3.8E-02	2.5E-01	2.7E-01	2.8E-01	1.6E+00	1.6E+00	1.6E+00
^{92}Y	1.3E-03	1.5E-03	7.6E-03	6.1E-03	5.6E+00	5.9E+00	2.0E+02	2.1E+02	2.1E+02	6.9E+04	6.9E+04	6.9E+04
^{93}Y	8.5E-01	1.1E+00	1.8E+00	9.2E-01	3.3E+01	4.0E+01	1.3E+03	1.3E+03	1.3E+03	5.3E+04	5.3E+04	5.3E+04
^{95}Zr	8.6E-01	4.0E+00	4.7E+00	4.3E-01	5.5E+00	7.8E+00	1.1E+02	1.1E+02	1.1E+02	1.0E+03	1.0E+03	1.0E+03
^{99}Mo	1.0E+01	3.2E+01	3.8E+01	5.6E+00	7.2E+01	1.1E+02	1.8E+03	1.9E+03	1.9E+03	2.0E+04	2.0E+04	2.0E+04
^{103}Ru	2.6E-03	1.2E-02	5.5E-02	1.3E-03	1.7E-02	6.1E+00	1.7E-01	1.8E-01	8.8E-01	1.1E+00	1.1E+00	5.1E+00
^{106}Ru	2.3E-01	1.1E+00	1.3E+00	1.1E-01	1.5E+00	2.2E+00	1.4E+01	1.6E+01	1.6E+01	8.9E+01	9.0E+01	9.1E+01
^{131m}Te	1.5E+00	3.3E+00	4.2E+00	1.0E+00	1.5E+01	2.2E+01	2.3E+02	2.4E+02	2.5E+02	2.5E+03	2.5E+03	2.5E+03
^{131}I	7.6E+00	3.1E+01	3.7E+01	4.0E+00	5.0E+01	7.5E+01	5.4E+02	5.9E+02	5.9E+02	3.6E+03	3.6E+03	3.7E+03
^{132}Te	1.5E+01	4.9E+01	5.9E+01	8.2E+00	1.0E+02	1.6E+02	1.3E+03	1.4E+03	1.4E+03	9.9E+03	9.9E+03	9.9E+03
^{132}I	1.5E+01	5.1E+01	6.1E+01	8.4E+00	1.1E+02	1.6E+02	1.3E+03	1.4E+03	1.4E+03	1.0E+04	1.0E+04	1.0E+04
^{133}I	1.5E+01	2.6E+01	3.4E+01	1.1E+01	1.9E+02	2.7E+02	3.2E+03	3.4E+03	3.4E+03	4.4E+04	4.4E+04	4.4E+04
^{135}I	3.6E-01	4.1E-01	8.4E-01	5.7E-01	4.6E+01	5.2E+01	9.6E+02	1.0E+03	1.0E+03	6.1E+04	6.1E+04	6.1E+04
^{137}Cs	1.2E-02	5.4E-02	6.4E-02	5.8E-03	7.4E-02	1.1E-01	6.6E-01	7.3E-01	7.4E-01	3.1E+00	3.2E+00	3.2E+00
^{140}Ba	5.4E+00	2.3E+01	2.7E+01	2.8E+00	3.5E+01	5.2E+01	4.3E+02	4.6E+02	4.7E+02	3.2E+03	3.2E+03	3.2E+03
^{140}La	5.0E+00	2.7E+01	3.1E+01	2.3E+00	2.7E+01	4.0E+01	2.3E+02	2.6E+02	2.6E+02	5.7E+02	5.8E+02	5.9E+02
^{141}La	2.6E-03	2.8E-03	1.2E-02	9.4E-03	5.7E+00	6.1E+00	1.6E+02	1.6E+02	1.6E+02	6.7E+04	6.7E+04	6.7E+04
^{141}Ce	2.2E+00	9.8E+00	1.2E+01	1.1E+00	1.4E+01	2.0E+01	2.1E+02	2.2E+02	2.2E+02	1.2E+03	1.2E+03	1.2E+03
^{143}Ce	6.9E+00	1.6E+01	2.0E+01	4.4E+00	6.3E+01	9.1E+01	1.9E+03	1.9E+03	1.9E+03	2.7E+04	2.7E+04	2.7E+04
^{144}Ce	1.1E-01	5.3E-01	6.2E-01	5.6E-02	7.2E-01	1.1E+00	1.4E+01	1.5E+01	1.5E+01	1.2E+02	1.2E+02	1.2E+02
^{145}Pr	4.8E-02	5.5E-02	1.2E-01	8.8E-02	9.8E+00	1.1E+01	4.1E+02	4.2E+02	4.2E+02	4.8E+04	4.8E+04	4.8E+04
^{239}Np*	5.6E+01	1.7E+02	2.0E+02	3.2E+01	4.2E+02	6.2E+02	1.1E+04	1.1E+04	1.1E+04	1.3E+05	1.3E+05	1.3E+05

*Activation products

Table 7 Cumulative radiation absorbed doses (mGy) to four organs of representative persons by birth year (1930 to 1958) from acute intakes of fallout. Doses for Utrik and Rongelap communities account for relocations.

Birth Year	Majuro Residents				Kwajalein Residents				Utrik Community				Rongelap Island Community			
	RBM	Thy-roid	Stom-ach	Colon	RBM	Thy-roid	Stom-ach	Colon	RBM	Thyroid	Stom-ach	Colon	RBM	Thyroid	Stom-ach	Colon
<1931	1.2E-01	2.3E-01	3.3E-01	4.4E+00	2.8E-01	6.7E+01	1.1E+00	1.2E+01	2.3E+00	7.4E+02	1.6E+01	1.8E+02	2.5E+01	7.6E+03	5.3E+02	2.8E+03
1931	1.2E-01	2.3E-01	3.3E-01	4.4E+00	3.1E-01	7.1E+01	1.1E+00	1.2E+01	2.3E+00	7.4E+02	1.6E+01	1.8E+02	2.5E+01	7.6E+03	5.3E+02	2.8E+03
1932	1.2E-01	2.3E-01	3.3E-01	4.4E+00	3.1E-01	7.1E+01	1.1E+00	1.2E+01	2.3E+00	7.4E+02	1.6E+01	1.8E+02	2.5E+01	7.6E+03	5.3E+02	2.8E+03
1933	1.2E-01	2.3E-01	3.3E-01	4.4E+00	3.1E-01	7.1E+01	1.1E+00	1.2E+01	2.3E+00	7.4E+02	1.6E+01	1.8E+02	2.5E+01	7.6E+03	5.3E+02	2.8E+03
1934	1.2E-01	2.3E-01	3.3E-01	4.4E+00	3.1E-01	7.1E+01	1.1E+00	1.2E+01	2.3E+00	7.4E+02	1.6E+01	1.8E+02	2.5E+01	7.6E+03	5.3E+02	2.8E+03
1935	1.3E-01	2.3E-01	3.3E-01	4.4E+00	3.2E-01	7.2E+01	1.1E+00	1.2E+01	2.3E+00	7.4E+02	1.6E+01	1.8E+02	2.5E+01	7.6E+03	5.3E+02	2.8E+03
1936	1.3E-01	2.3E-01	3.3E-01	4.4E+00	3.2E-01	7.2E+01	1.1E+00	1.2E+01	2.3E+00	7.4E+02	1.6E+01	1.8E+02	2.5E+01	7.6E+03	5.3E+02	2.8E+03
1937	2.0E-01	2.9E-01	3.7E-01	4.7E+00	4.3E-01	8.6E+01	1.2E+00	1.4E+01	2.9E+00	8.7E+02	1.8E+01	2.0E+02	3.0E+01	9.7E+03	6.1E+02	3.1E+03
1938	2.0E-01	2.9E-01	3.7E-01	4.7E+00	4.3E-01	8.6E+01	1.2E+00	1.4E+01	2.9E+00	8.7E+02	1.8E+01	2.0E+02	3.0E+01	9.7E+03	6.1E+02	3.1E+03
1939	2.1E-01	2.9E+01	3.8E-01	4.8E+00	4.4E-01	8.7E+01	1.3E+00	1.4E+01	2.9E+00	8.7E+02	1.8E+01	2.0E+02	3.0E+01	9.7E+03	6.1E+02	3.1E+03
1940	2.1E-01	2.9E+01	3.8E-01	4.8E+00	4.4E-01	8.7E+01	1.3E+00	1.4E+01	2.9E+00	8.7E+02	1.8E+01	2.0E+02	3.0E+01	9.7E+03	6.1E+02	3.1E+03
1941	2.1E-01	2.9E+01	3.7E-01	4.8E+00	4.5E-01	8.7E+01	1.3E+00	1.4E+01	2.9E+00	8.8E+02	1.8E+01	2.0E+02	3.0E+01	9.8E+03	6.1E+02	3.1E+03
1942	2.1E-01	2.9E+01	3.7E-01	4.8E+00	4.1E-01	9.5E+01	1.3E+00	1.4E+01	2.9E+00	8.8E+02	1.8E+01	2.0E+02	3.0E+01	9.8E+03	6.1E+02	3.1E+03
1943	1.9E-01	3.0E+01	3.7E-01	5.5E+00	4.1E-01	9.7E+01	1.3E+00	1.6E+01	4.2E+00	9.1E+02	1.8E+01	2.3E+02	4.4E+01	1.0E+04	6.0E+02	3.7E+03
1944	1.9E-01	3.0E+01	3.7E-01	5.5E+00	4.1E-01	9.7E+01	1.3E+00	1.6E+01	4.2E+00	9.1E+02	1.8E+01	2.3E+02	4.4E+01	1.0E+04	6.0E+02	3.7E+03
1945	1.9E-01	3.0E+01	3.6E-01	5.6E+00	4.1E-01	9.7E+01	1.3E+00	1.6E+01	4.2E+00	9.1E+02	1.8E+01	2.3E+02	4.4E+01	1.0E+04	6.0E+02	3.7E+03
1946	1.9E-01	3.1E+01	3.7E-01	5.7E+00	4.0E-01	9.9E+01	1.3E+00	1.6E+01	4.2E+00	9.1E+02	1.8E+01	2.3E+02	4.4E+01	1.0E+04	6.0E+02	3.7E+03
1947	1.9E-01	3.1E+01	3.7E-01	5.7E+00	7.0E-01	1.1E+02	1.4E+00	1.8E+01	4.2E+00	9.1E+02	1.8E+01	2.3E+02	4.4E+01	1.0E+04	6.0E+02	3.7E+03
1948	1.3E-01	4.1E+01	4.1E-01	6.1E+00	3.1E-01	1.2E+02	1.3E+00	1.4E+01	2.4E+00	1.3E+03	2.1E+01	2.6E+02	2.5E+01	1.5E+04	6.9E+02	4.1E+03
1949	1.3E-01	4.1E+01	4.1E-01	6.1E+00	2.4E-01	9.8E+01	1.1E+00	1.3E+01	2.4E+00	1.3E+03	2.1E+01	2.6E+02	2.5E+01	1.5E+04	6.9E+02	4.1E+03
1950	1.3E-01	4.1E+01	4.1E-01	6.1E+00	2.4E-01	1.0E+02	1.1E+00	1.3E+01	2.4E+00	1.3E+03	2.1E+01	2.6E+02	2.5E+01	1.5E+04	6.9E+02	4.1E+03
1951	1.8E-01	4.3E+01	4.3E-01	6.3E+00	3.0E-01	1.0E+02	1.1E+00	1.4E+01	2.4E+00	1.3E+03	2.1E+01	2.6E+02	2.5E+01	1.5E+04	6.9E+02	4.1E+03
1952	1.5E-01	4.4E+01	4.3E-01	5.8E+00	2.5E-01	1.0E+02	1.1E+00	1.3E+01	2.4E+00	1.3E+03	2.1E+01	2.6E+02	2.5E+01	1.5E+04	6.9E+02	4.1E+03
1953	8.8E-01	4.9E+01	5.5E-01	8.1E+00	1.6E+00	1.3E+02	1.6E+00	1.8E+01	3.6E+01	1.8E+03	3.2E+01	3.8E+02	1.5E+03	2.1E+04	1.1E+03	6.1E+03
1954	1.2E-01	1.9E+01	1.6E-01	1.2E+00	2.3E-01	6.1E+01	6.0E-01	3.4E+00	1.8E+00	4.6E+02	5.7E+00	3.2E+01	1.6E+01	5.1E+03	1.5E+02	4.8E+02
1955	7.6E-02	4.3E+00	4.8E-02	7.4E-01	1.3E-01	9.9E+00	1.1E-01	1.6E+00	5.6E-02	6.5E+00	6.9E-02	1.0E+00	9.9E-02	1.3E+01	1.4E+00	1.9E+00
1956	1.9E-02	3.0E+00	2.5E-02	2.0E-01	3.5E-02	6.7E+00	5.9E-02	3.9E-01	2.2E-02	5.7E+00	5.7E-02	7.7E-01	4.2E-02	1.1E+01	1.2E+00	1.3E+00
1957	1.8E-02	6.9E-01	6.7E-03	1.1E-01	2.5E-02	9.2E-01	8.2E-03	1.3E-01	9.1E-02	6.2E+00	7.4E-02	1.1E+00	1.9E-01	1.2E+01	1.5E+00	2.0E+00
1958	3.0E-03	3.7E-01	2.5E-03	2.1E-02	4.2E-03	5.0E-01	3.1E-03	2.6E-02	1.9E-02	3.3E+00	2.9E-02	1.9E-01	3.9E-02	7.2E+00	6.7E-02	3.8E-01

200

Table 8 Radionuclides giving largest organ doses (mGy) from Bravo test to adults of four atolls (Majuro, Kwajalein, Utrik, and Rongelap) from acute intakes of fallout radionuclides. Utrik and Rongelap community doses account for relocations.

Organ and Rank[1]	Majuro Residents		Kwajalein Residents		Utrik Community		Rongelap Island Community	
	Nuclide	Dose	Nuclide	Dose	Nuclide	Dose	Nuclide	Dose
RBM								
1	Te-132	7.6E-03	Te-132	4.2E-03	Te-132	6.6E-01	Te-132	5.0E+00
2	Ba-140	6.7E-03	Ba-140	3.4E-03	Np-239	2.8E-01	Np-239	3.3E+00
3	Sr-89	3.9E-03	Sr-89	2.0E-03	Mo-99	2.8E-01	Mo-99	3.0E+00
4	Mo-99	1.5E-03	Mo-99	8.5E-04	Ba-140	1.9E-01	I-135	2.2E+00
5	Np-239	1.4E-03	Np-239	8.3E-04	I-133	1.5E-01	I-133	1.8E+00
Thyroid								
1	I-131	3.6E+00	I-131	1.9E+00	I-133	3.8E+02	I-133	4.2E+03
2	I-133	1.4E+00	I-133	1.0E+00	I-131	2.3E+02	I-131	1.7E+03
3	Te-132	4.0E-01	Te-132	2.2E-01	I-135	3.6E+01	I-135	1.3E+03
4	I-132	7.2E-02	I-132	4.0E-02	Te-132	3.5E+01	Te-132	2.6E+02
5	Te-131m	2.5E-02	Te-131m	1.7E-02	I-132	4.5E+00	I-132	4.7E+01
Stomach								
1	Np-239	1.9E-02	Np-239	1.1E-02	Np-239	3.8E+00	Y-92	9.6E+01
2	Te-132	1.1E-02	Te-132	6.2E-03	I-133	1.8E+00	Y-93	6.9E+01
3	I-132	9.7E-03	I-133	5.9E-03	Y-93	1.7E+00	La-141	6.3E+01
4	I-133	8.0E-03	I-132	5.3E-03	Ce-143	1.1E+00	Np-239	4.4E+01
5	Mo-99	5.5E-03	Mo-99	3.1E-03	Mo-99	1.0E+00	Pr-145	3.4E+01
Colon								
1	Np-239	3.4E-01	Np-239	1.9E-01	Np-239	6.6E+01	Np-239	7.6E+02
2	Te-132	2.0E-01	Te-132	1.1E-01	Te-132	1.7E+01	Y-93	4.4E+02
3	Ba-140	9.2E-02	Ba-140	4.7E-02	Ce-143	1.6E+01	Ce-143	2.2E+02
4	Mo-99	7.9E-02	Mo-99	4.4E-02	Mo-99	1.4E+01	Y-92	1.8E+02
5	La-140	6.3E-02	Ce-143	3.7E-02	Y-93	1.1E+01	Mo-99	1.6E+02

[1]Rank of 1 indicates radionuclide with highest organ dose; Rank of 5 indicates radionuclide with fifth highest organ dose.

2.2.3. Internal doses from chronic intakes of radionuclides

Following the deposition of radionuclides on the ground, chronic (i.e., protracted) intakes took place at rates much lower than those due to the acute intakes. While both acute and chronic intakes were primarily a result of ingestion, the environmental transport processes leading to chronic intakes were substantially different from those that gave rise to acute intakes. Chronic intakes were primarily a function of the consumption of seafood and of locally grown terrestrial foodstuffs internally contaminated with long-lived radionuclides via root uptake and, to a lesser degree, inadvertent consumption of soil [24]. A previous assessment [8] showed that five radionuclides account for essentially all the internal dose from chronic intake: ^{55}Fe, ^{60}Co, ^{65}Zn, ^{90}Sr, and ^{137}Cs.

The available historical whole-body counting and bioassay measurements were used as a basis to estimate the chronic intakes since a suitable dietary model covering the many years after the tests when lifestyles became more westernized, does not exist. Those whole-body and bioassay measurements were made on the Rongelap and Utrik evacuees for years after they returned to their respective home atolls [8]. During the first few weeks after their return and until the 1980s, a Brookhaven National Laboratory team regularly conducted measurements of whole-body activity of ^{137}Cs, ^{60}Co and ^{65}Zn, as well as urinary concentrations of ^{90}Sr. Measurements of ^{55}Fe in blood were

also performed, but only once [8].

The steps used to estimate the doses from chronic intakes of radionuclides were: (1) estimation of the chronic intakes by Rongelap and Utrik adult evacuees due to the Castle Bravo test, (2) estimation of the chronic intakes resulting from the Castle Bravo test by adults of all other atolls, based on the relative ^{137}Cs deposition, (3) estimation of the chronic intakes by adults resulting from tests other than Castle Bravo, again based on relative ^{137}Cs deposition, (4) estimation of the chronic intakes by children, and (5) estimation of the doses from chronic intakes from all tests and all population groups using ICRP recommended dose coefficients.

Detailed information on the estimation of chronic intakes and resulting doses is presented in [13]. Because of the absence of short-lived iodine isotopes which dominated the thyroid dose from the acute intakes, the thyroid doses from chronic intakes were not much greater than the doses to other organs and tissues (Table 9). Similar to the situation for acute intakes, only a few radionuclides contributed most of the organ absorbed dose. For all organs and for all four of the atolls and population groups discussed, ^{137}Cs was either the first or second most important contributor to internal dose from chronic intakes. For the evacuated Rongelap Island community, ^{137}Cs was the most important contributor to the chronic dose, whereas ^{65}Zn was the largest contributor to dose for the residents of all other atolls.

Table 9 Radionuclides giving cumulative highest organ doses (mGy) to adults of four atolls (Majuro, Kwajalein, Utrik, and Rongelap) from chronic intakes of long-lived radionuclides. Utrik and Rongelap community doses account for relocations.

Organ and Rank1		Majuro Residents		Kwajalein Residents		Utrik Community		Rongelap Island Community	
		Nuclide	Dose	Nuclide	Dose	Nuclide	Dose	Nuclide	Dose
RBM									
	1	Zn-65	7.1×10^{-1}	Zn-65	1.2×10^{0}	Zn-65	2.3×10^{1}	Cs-137	1.4×10^{1}
	2	Cs-137	2.4×10^{-1}	Cs-137	4.1×10^{-1}	Cs-137	7.7×10^{0}	Fe-55	2.6×10^{0}
	3	Fe-55	2.6×10^{-2}	Fe-55	4.5×10^{-2}	Fe-55	1.9×10^{0}	Zn-65	2.4×10^{0}
	4	Sr-90	1.4×10^{-2}	Sr-90	2.4×10^{-2}	Sr-90	2.0×10^{-1}	Sr-90	1.0×10^{0}
	5	Co-60	5.9×10^{-3}	Co-60	1.0×10^{-2}	Co-60	1.1×10^{-1}	Co-60	9.1×10^{-2}
Thyroid									
	1	Zn-65	5.2×10^{-1}	Zn-65	8.9×10^{-1}	Zn-65	1.8×10^{1}	Cs-137	1.4×10^{1}
	2	Cs-137	2.4×10^{-1}	Cs-137	4.1×10^{-1}	Cs-137	7.8×10^{0}	Zn-65	1.8×10^{0}
	3	Co-60	4.7×10^{-3}	Co-60	8.0×10^{-3}	Fe-55	1.5×10^{-1}	Fe-55	2.0×10^{-1}
	4	Fe-55	2.0×10^{-3}	Fe-55	3.4×10^{-3}	Co-60	8.6×10^{-2}	Co-60	7.2×10^{-2}
	5	Sr-90	5.2×10^{-5}	Sr-90	9.0×10^{-5}	Sr-90	7.6×10^{-4}	Sr-90	3.8×10^{-3}
Stomach									
	1	Zn-65	5.1×10^{-1}	Zn-65	8.7×10^{-1}	Zn-65	1.6×10^{1}	Cs-137	1.4×10^{1}
	2	Cs-137	2.5×10^{-1}	Cs-137	4.2×10^{-1}	Cs-137	7.6×10^{0}	Zn-65	1.7×10^{0}
	3	Co-60	7.1×10^{-3}	Co-60	1.2×10^{-2}	Fe-55	1.5×10^{-1}	Fe-55	2.2×10^{-1}
	4	Fe-55	2.1×10^{-3}	Fe-55	3.7×10^{-3}	Co-60	1.2×10^{-1}	Co-60	1.1×10^{-1}
	5	Sr-90	7.2×10^{-5}	Sr-90	1.2×10^{-4}	Sr-90	9.8×10^{-4}	Sr-90	5.2×10^{-3}
Colon									
	1	Zn-65	6.9×10^{-1}	Zn-65	1.2×10^{0}	Zn-65	2.2×10^{1}	Cs-137	1.6×10^{1}
	2	Cs-137	2.8×10^{-1}	Cs-137	4.8×10^{-1}	Cs-137	8.8×10^{0}	Zn-65	2.3×10^{0}
	3	Co-60	2.4×10^{-2}	Co-60	4.1×10^{-2}	Co-60	4.3×10^{-1}	Fe-55	6.0×10^{-1}
	4	Fe-55	5.9×10^{-3}	Fe-55	1.0×10^{-2}	Fe-55	4.3×10^{-1}	Co-60	3.7×10^{-1}
	5	Sr-90	1.0×10^{-3}	Sr-90	1.8×10^{-3}	Sr-90	1.4×10^{-2}	Sr-90	7.5×10^{-2}

[1]Rank of 1 indicates radionuclide with highest organ dose; Rank of 5 indicates radionuclide with fifth highest organ dose.

2.2.4. Comparison of doses by mode of exposure

The estimated cumulative internal doses to representative adults of four population groups are compared in Table 10 with the external doses for those same population groups.

With respect to the components of the internal dose, the dose from chronic intake exceeded the dose from acute intake for RBM and stomach wall, for all populations groups except the Rongelap Island community. For the Rongelap Island community, the acute doses for all organs exceeded the chronic doses. Because of the exposure to radioiodines in fallout, the absorbed dose to the thyroid gland from acute intakes exceeded the chronic dose to the thyroid, regardless of the population group. Acute doses to colon wall were also greater than the corresponding chronic doses for all four population groups.

With respect to the total internal dose relative to the external dose, external doses were much greater than the internal doses to RBM and stomach wall, regardless of the population group, but were comparable to the internal doses to the colon wall (greater by two-fold at the southern- and mid-latitude atolls, and about one-half for the Utrik and Rongelap Island communities). Internal doses to the thyroid were significantly greater than external doses, regardless of the population group. As was previously shown in Table 7, the internal doses from acute intakes varied substantially with year of birth, so that the relative importance of the three modes of exposure is different for children and for adults at the time of the tests.

Table 10 Comparison of estimates of acute internal and chronic internal doses (mGy) for four organs with external dose (at all organs) for adults at four representative atolls.

Organ / Mode of exposure	POPULATION			
	Majuro residents	Kwajalein residents	Utrik Community	Rongelap Community
Thyroid				
Acute	22	66	740	7,600
chronic	0.76	1.3	25	14
RBM				
Acute	0.11	0.25	2.3	25
chronic	0.98	1.7	33	17
Stomach wall				
Acute	0.32	1.1	16	530
chronic	0.75	1.3	24	14
Colon				
Acute	4.4	12	180	2,800
chronic	0.99	1.7	32	17
Whole-body external	9.8	22	130	1,600

2.2.5. Total doses

Total (external plus internal) organ absorbed doses can be presented in various ways to demonstrate the spatial and time-dependence of exposures received across the Marshall Islands and the dependence on age at exposure. Table 11 presents population-weighted total doses to adults within each of the four geographic areas. The estimated total doses are relatively comparable within each of the four population groups: residents of southern atolls, residents of mid-latitude atolls, the Utrik community, and the Rongelap Island community. Adults in mid-latitude atolls received cumulative organ doses approximately four times as great as adults in the most southern atolls.

Similarly, adults of the Utrik community received cumulative organ doses four to seven times as great as adults from the mid-latitude atolls. Adults among the Rongelap Island community received the largest cumulative doses, about ten times as great as adults from Utrik.

Recognizing that the doses within each of the four areas geographic areas with similar degrees of ^{137}Cs deposition can be represented by the doses to Majuro residents, Kwajalein residents, the Utrik community, and the Rongelap Island community, Table 12 provides cumulative radiation doses (external plus internal) at those atolls for all birth years from 1930 to 1958. Those born in or before 1930 would be of adult age at the time of the first tests and would have received approximately equal doses regardless of the birth year. Persons who were adults at the beginning of the testing period (born in 1930 or earlier) received relatively low thyroid doses from the large tests in 1954 compared to those who were very young at the time of those tests. Among the 4 representative population groups, cumulative thyroid doses ranged from 33 mGy for adults who lived on Majuro at the time of   testing to as high as 23,000 mGy for infants on Rongelap Island at the time of the Bravo test.

2.2.6. Uncertainties of estimated doses

Estimated doses and the uncertainties associated with those estimates varied by location, fallout event, calendar year, and age at time of exposure. The precision of our dose reconstruction is better for exposures received on Rongelap and Ailinginae than on Utrik, primarily because of the availability of historical urine bioassay data and large amounts of environmental monitoring data (both historical and contemporary), and both are more reliable than the estimated doses for persons exposed on the mid-latitude and southern atolls.

Of the exposure pathways examined, external irradiation was the most precise. An analysis was conducted to evaluate the uncertainty in the annual doses from external irradiation for each year of testing. Annual and cumulative exposures were often estimated from historical measurements or from relatively simple conversions from fallout deposition density. We found that the uncertainty of doses from external irradiation could be characterized by lognormal distributions with geometric standard deviations (GSD) of approximately 1.2 for exposure on Rongelap and Ailinginae, 1.5 for exposure on Utrik, and 1.8 for exposures on the other atolls [12]. The overall GSDs were smallest for the communities where the greatest doses were received from the 1954 tests. Conversely, the GSDs were largest for communities with the lowest doses from the 1954 tests.

In comparison to estimates of external dose, estimates of dose from internal irradiation are substantially more uncertain. Based on an analysis accounting for uncertainties in the most relevant and sensitive parameters involved in the internal dose assessment, we found that the uncertainty of doses from internal irradiation could be characterized by lognormal distributions with geometric standard deviations (GSD) of approximately 2.0 for exposure on Rongelap and Ailinginae, 2.5 for exposure on Utrik, and 3.0 for exposures on the other atolls [13]. Doses from chronic intake of radionuclides result from a more complex exposure situation and are more uncertain than the doses from acute intakes. However, doses from chronic intakes were small and refinements to the estimation of the uncertainty associated with them would contribute little to the overall dose uncertainty.

Table 11 Four groups of atolls and/or communities aggregated by total estimated organ dose (mGy) to adults from external irradiation and internal ingestion of radionuclides in regional fallout. Atolls are listed alphabetically within each group. Range is the doses from the atolls with minimum and maximum average value within each geographic group.

Population Group	Atolls of Exposure	Adult population average dose to RBM from all tests, mGy (min - max)[a]	Adult population average dose to thyroid from all tests, mGy (min - max)[a]	Adult population average dose to stomach wall of adults from all tests, mGy (min - max)[a]	Adult population average dose to colon wall from all tests, mGy (min - max)[a]
Rongelap Island community	Rongelap (and Ailinginae for Bravo test)	1,600	9,200	2,100	4,400
Utrik community	Utrik	160	890	170	340
Residents of mid-latitude atolls	Ailuk, Kwajalein, Likiep, Mejit Island, Ujelang[b], Wotho, Wotje	37 (24-65)	130 (89-220)	38 (24-66)	56 (36-100)
Residents of southern atolls	Ailinglaplap, Arno, Aur, Ebon, Jaluit, Kili[c], Lae, Lib Island, Majuro, Maloelap, Mili, Namorik, Namu, Ujae	10 (6.1-43)	30 (17-75)	10 (6.0-39)	14 (8.0-49)

[a]min to max range only applies to mid-latitude and southern atoll groups
[b]Enewetak community
[c]Bikini community

Table 12 Total radiation absorbed doses (mGy) to four organs of representative persons by birth year (<1931 through 1958): sum of external and internal irradiation (acute and chronic intakes of radionuclides); all values rounded to two significant digits. Doses for Utrik and Rongelap communities account for relocations.

Birth Year	Majuro Residents				Kwajalein Residents				Utrik Community				Rongelap Island Community			
	RBM	Thyroid	Stom-ach	Colon	RBM	Thyroid	Stom-ach	Colon	RBM	Thyroid	Stom-ach	Colon	RBM	Thyroid	Stom-ach	Colon
<1931	11	34	11	16	24	95	25	36	150	890	160	330	1,700	9200	2,200	4,400
1931	11	34	11	16	24	95	25	36	150	890	160	330	1,700	9200	2,200	4,400
1932	11	34	11	16	24	95	25	36	150	890	160	330	1,700	9200	2,200	4,400
1933	11	34	11	16	24	95	25	36	150	890	160	330	1,700	9200	2,200	4,400
1934	11	34	11	16	25	96	26	37	150	890	160	330	1,700	9200	2,200	4,400
1935	11	34	11	16	25	97	26	37	150	890	160	330	1,700	9200	2,200	4,400
1936	11	34	11	16	25	97	26	37	150	890	160	330	1,700	9200	2,200	4,400
1937	11	40	11	16	26	110	26	39	150	1,000	160	350	1,700	11,000	2,200	4,700
1938	11	40	11	16	26	110	26	39	150	1,000	160	350	1,700	11,000	2,200	4,700
1939	11	40	11	16	26	110	26	39	150	1,000	160	350	1,700	11,000	2,200	4,700
1940	14	42	13	18	29	120	29	42	170	1,000	180	370	2,000	12,000	2,500	5,000
1941	14	42	13	18	29	120	29	42	170	1,000	180	370	2,000	12,000	2,500	5,000
1942	14	42	13	18	29	120	29	42	180	1,000	190	370	2,000	12,000	2,500	5,000
1943	14	43	13	19	29	130	29	45	180	1,100	190	410	2,000	12,000	2,500	5,600
1944	14	43	14	19	29	130	29	45	180	1,100	190	410	2,000	12,000	2,500	5,600
1945	14	43	14	19	29	130	29	45	180	1,100	190	410	2,000	12,000	2,500	5,600
1946	14	44	14	19	29	130	29	45	180	1,100	190	410	2,000	12,000	2,500	5,600
1947	14	44	14	19	30	140	30	47	180	1,100	190	410	2,000	12,000	2,500	5,600
1948	14	54	14	20	26	150	27	40	180	1,500	190	440	2,000	17,000	2,600	6,000
1949	14	55	14	20	24	120	24	37	180	1,500	190	440	2,000	17,000	2,600	6,000
1950	14	55	14	20	24	120	24	37	180	1,500	190	440	2,000	17,000	2,600	6,000
1951	14	57	14	20	24	120	24	38	180	1,500	190	440	2,000	17,000	2,600	6,000
1952	14	57	14	20	24	120	24	37	180	1,500	190	440	2,000	17,000	2,600	6,000
1953	13	61	13	21	24	150	23	41	210	2,000	200	560	3,400	23,000	3,000	8,000
1954	5.7	25	5.5	6.9	11	72	11	15	73	530	71	100	520	5,600	650	980
1955	1.9	6.0	1.7	2.8	3.8	13	3.5	6.2	21	24	18	23	38	49	38	42
1956	1.1	4.0	1.0	1.42	2.2	8.7	2.1	3.3	11	15	9.2	13	31	40	31	33
1957	0.64	1.2	0.57	0.86	1.2	1.9	1.1	1.7	8.6	13	7.4	11	28	38	28	32
1958	0.47	0.76	0.42	0.60	0.80	1.2	0.73	1.2	6.5	8.4	5.5	7.8	23	29	24	25

3. Summary and concluding remarks

The most comprehensive retrospective evaluation of radiation exposure resulting from the atmospheric nuclear weapons tests conducted in the Pacific at Bikini and Enewetak atolls during 1946-1958 is summarized in this paper. Radiation doses were estimated for representative individuals of the entire population of the Marshall Islands that was alive at the time of the nuclear weapons tests. The calculated doses are based on the available radiation measurement data (concentrations of ^{131}I in urine, whole-body measurements, concentrations of ^{137}Cs in soil, exposure rates, etc.) supplemented with a variety of models and assumptions. The total deposition of ^{137}Cs, external dose, and internal organ doses were found to follow the same geographic pattern with the large population of the southern atolls receiving the lowest doses. Permanent residents of the southern atolls who were of adult age at the beginning of the testing period received external doses ranging from 5 to 12 mGy on average; the external doses to adults at the mid-latitude atolls ranged from 22 to 60 mGy on average, while the residents of the northern atolls received external doses in the hundreds to over 1000 mGy. Internal doses varied significantly by age at exposure, location, and organ; they are estimated to have been as high as about 23 Gy to the thyroid glands of young children exposed on Rongelap at the time of the Castle Bravo test of 1 March 1954.

The methods of dose reconstruction used in this paper may be useful in broader circumstances, such as nuclear reactor accidents. A number of important lessons can be derived from this analysis: (1) it is essential to use as many radiation measurements as possible, preferably on humans, in order to develop or calibrate models that can be applied to large population groups; (2) it is also important to collect as much information as possible to the lifestyle and dietary habits of the populations that may have been exposed; and (3) all of the collected information should be documented and archived in a single place, so that it could be accessed by generations of scientists who might be involved in dose reconstruction. Reconstruction of radiation doses many years after exposure can be an intensive effort and underscores the need for dependable data of various types. The amount of data necessary to make reliable estimates of radiation dose is significant and the collection of that information should not be overlooked following radiation accidents, but should be, in fact, a high priority.

References

1) DOE. United States Department of Energy, United States Nuclear Tests July 1945 through September 1992, DOE/NV-209-Rev. 15, U.S. Department of Energy, Nevada Operations Office, 15, 2000. Available from:
http://www.nv.doe.gov/library/publications/historical/DOENV_209_REV15.pdf
2) Simon SL, Robison WL. A compilation of nuclear weapons test detonation data for U.S. Pacific Ocean tests. Health Phys 73:258-264; 1997.

3) Breslin A, Cassidy M. Radioactive Debris from Operation Castle, Islands of the Mid-Pacific. United States Atomic Energy Commission, New York Operations Office, NYO-4623; 1955. Available at http://www.hss.energy.gov/HealthSafety/ IHS/marshall/env_docs.html

4) DNA. Compilation of Local Fallout Data from Test Detonations 1946-1962. Extracted from DASA 1251, Volume II-Oceanic U.S. Tests, DNA 1251-2-EX, 1 May 1979. Available at http://stinet.dtic.mil/.

5) Cronkite EP, Conard RA, Bond VP. Historical events associated with fallout from Bravo Shot – Operation Castle and 25 years of medical findings. Health Physics 73(1):176-186; 1997.

6   Harris PA. Summary of the results of urine analysis on Rongelap natives, Americans, and Japanese fishermen to date. Memo to Atomic Energy Commission. Los Alamos, NM: Los Alamos Scientific Laboratory; 1954.

7) Lessard ET, Miltenberger R, Conard R, Musolino S, Naidu J, Moorthy A, Schopfer C. Thyroid absorbed dose for people at Rongelap, Utrik and Sifo on March 1, 1954. Upton, NY: Brookhaven National Laboratory, Safety and Environmental Protection Division; BNL 51882; 1985.

8) Lessard ET, Miltenberger RP, Cohn SH, Musolino SV, Conard RA. Protracted exposure to fallout: the Rongelap and Utirik experience, Health Physics 46:511–527; 1984.

9) Simon SL; Vetter RJ. Consequences of Nuclear Testing in the Marshall Islands. Health Phys 73(1): 3-269 (entire issue); 1997.

10) Beck HL, Bouville A, Moroz BE, Simon SL. Fallout Deposition in the Marshall Islands from Bikini and Enewetak nuclear weapons tests. Health Phys. 99(2): 124-142; 2010.

11) Moroz BE, Beck HL, Bouville A, Simon SL. Predictions of radioactive fallout dispersion and deposition using the NOAA-HYSPLIT meteorological model. Health Phys. 99(2): 252-269; 2010.

12) Bouville A, Beck HL, Simon SL. Doses from external irradiation to Marshall Islanders from Bikini and Enewetak nuclear weapons tests. Health Phys. 99(2): 143-156; 2010.

13) Simon SL, Bouville A, Melo D; Beck HL. Acute and chronic intakes of fallout radionuclides by Marshallese from nuclear weapons testing at Bikini and Enewetak and related internal radiation doses. Health Phys. 99(2): 157-200; 2010a.

14) Harris PA, Simon SL, Ibrahim, SA. Urinary excretion of radionuclides from Marshall Islanders exposed to fallout from the Bravo nuclear test. Health Phys. 99(2): 217-232; 2010.

15) Ibrahim SA, Simon SL, Bouville A, Melo D, Beck HL. Transfer of fallout radionuclides through the human GI tract: Recommendations and justifications for f_1 values to be applied in the reconstruction of internal doses from regional nuclear tests. Health Phys. 99(2): 233-251; 2010.

16) Simon SL, Bouville A, Land C, Beck HL. Radiation doses and cancer risks in the Marshall Islands associated with exposure to radioactive fallout from Bikini and Enewetak nuclear weapons tests: summary. Health Phys 99(2): 105-123; 2010b.

17) Robison WL, Noshkin VE, Conrado CL, Eagle RJ, Brunk JL, Jokela TA, Mount ME, Phillips WA, Stoker AC, Stuart ML, Wong KM. The Northern Marshall Islands Radiological Survey: data and dose assessments. Health Phys 73(1):37-46; 1997.

18) Simon SL, Graham JC. Findings of the first comprehensive radiological monitoring program of the Republic of the Marshall Islands. Health Phys 73:66-85, 1997.

19) Hicks HG. Calculation of the concentration of any radionuclide deposited on the ground by offsite fallout from a nuclear detonation. Health Phys 42:585-600; 1982.

20) Hicks HG. Rates from Fallout and the Related Radionuclide Composition Livermore, CA: Lawrence Livermore National Laboratory, Report UCRL-53152, Parts 1–7; 1981.

21) Hicks HG. Rates from Local Fallout and the Related Radionuclide Composition, Results of Calculations of External Radiation Exposure of Selected U.S. Pacific Events. Livermore, CA: Lawrence Livermore National Laboratory, report UCRL-53505; 1984.

22) Jacob P, Rosenbaum H, Petoussi N, Zankl M. Calculation of Organ Doses from Environmental Gamma Rays Using Human Phantoms and Monte-Carlo Methods. Part II: Radionuclides Distributed in the Air or Deposited on the Ground. GSF-Bericht 12/90. GSF-Institut für Strahlenschutz. Neuherberg; 1990.

23) Arnow T. The Hydrology of the Northern Marshall Islands, Atoll Research Bulletin No. 30, Washington, D. C: National Academy of Sciences-National Research Council, May 31, 1954.

24) Simon SL. Soil ingestion by humans: a review of data, history, and etiology with application to risk assessment of radioactively contaminated soil. Health Physics 74(6):647-672; 1998.

Summary of Session 4

G. SUGIYAMA

Presentation 1: Methodology and Results of Internal Dose Reconstruction in Russia after the Chernobyl Accident (Mikhail BALANOV, IRH, Russia)

Dr. Mikhail Balanov described internal dose reconstruction conducted after Chernobyl. His talk described how generic dose reconstruction techniques provided in ICRU Report 68 could be applied. Chernobyl dose estimation was based on data from I-131 in the thyroid and milk and Cs-137 from soil, food, and human body measurements, along with personal interviews. For Chernobyl, cesium internal dose from intake of dairy products was a major dose contributor, while inhalation dose was negligible relative to ingestion. Dr. Balanov concluded his talk with recommendations for performing large-scale Fukushima internal dose reconstruction for the public, using the same general methods applied after Chernobyl. He also emphasized the importance of assessing the contribution of short-lived isotopes as part of this process.

- In response to a question, Dr. Balanov stated that during Chernobyl cows were in pasture in the USSR, but not in northern Europe. A member of the audience observed that milk measurements in Fukushima in March 2011 showed I-131. This milk contamination might be due to inhalation or soil ingestion since cows were not on pasture.
- Dr. Homma inquired whether whole body counting cesium dose increased for the first year and then decreased. Dr. Balanov replied that large-scale whole body counting in Russia did not show increasing dose.
- In wrapping up the question period for the presentation, there appeared to be general agreement that due to the different environmental conditions in Japan in March 2011 from those during Chernobyl, Fukushima dose assessment likely will be focused on other (non-ingestion) dose pathways.

Presentation 2: Dose Reconstruction Related to the Nuclear Weapons Tests Conducted by the U.S. in the Pacific in the 1950s (Andre Bouville, NIH, U.S.)

Dr. Andre Bouville summarized U.S. nuclear weapons tests in the Pacific and discussed the NCR assessment of cancer risks to Marshall Island populations published in Health Physics 99(2) August 2010. Dose estimation was conducted for Cs-137 and 62 other radionuclides for each test and atoll. A relationship was established between exposure rate and Cs-137 fallout. Internal dose consisted of both acute internal dose and chronic dose resulting from ingestion of food. Acute dose was determined from I-131 concentrations in urine and a new biokinetic model relating iodine intake to urine excretion that was substituted for conventional pathway models (applicable to Nevada tests) and thyroid counts (used in Chernobyl). Chronic intake dose was estimated using bioassays of various radionuclides in the human body, urine and blood. Dr. Bouville concluded by showing comparisons of acute and chronic dose in adults, child thyroid dose by birth year, and the six nuclear tests (Bravo and the Castle series) that were the highest contributors to Marshall Island population dose.

General Discussion

Chair   :   T. HOMMA
Co-chair   :   K. THIESSEN
Rapporteur   :   G. SUGIYAMA

Summary of General Discussion

G. SUGIYAMA

Dr. Homma began the closing discussion by re-iterating that the goal of Fukushima dose reconstruction is estimation of dose and health risks to inform the scientific and medical community, as well as the public. Various dose estimate methodologies are available including internal dose estimation, simulation, and calibration of modeling using available data. Dr. Homma then summarized some of the important scientific topics raised in the symposium presentation including:

- Radionuclide mix
- Chemical forms and partitioning of radioiodine
- Deposition processes
- Effectiveness of protective actions
- Population and individual behavior

He also outlined key aspects of uncertainty such as determining:

- How to reduce uncertainties by obtaining additional information
- What sources of uncertainty are most important
- Limitations of data
- Limitations of simulation
- How to communicate uncertainty and risk estimates to the public

A discussion followed on the difficulties of communicating dose risks to the public, including possible use of medical risk approaches and comparisons to natural (background) sources.

- Dr. Balanov recommended avoiding calculations of cancer counts, casualties, or collective dose at least for low doses.
- Dr. Momose suggested expressing results in terms of percentile values.
- Dr. Bouville indicated a preference for reporting in terms of confidence intervals.
- Drs. Ban, Homma, and Tolmachev discussed the need to determine uncertainties in average values separately from uncertainties due to variation between individuals.

A second discussion covered aspects of dose estimation methodology. Gaps in data were proposed as a possible focus for a second symposium.

- Dr. Balanov stated that reconstruction should be done by age groups and locations and recommended setting up working group to discuss dose rate reconstruction methods and standardize approaches.
- Drs. Yamazawa and Suzuki discussed the usefulness of establishing relationships between cesium deposition and thyroid dose, but were unsure whether sufficient data is available to determine this relationship given the high variability in Cs/I ratios, and whether simulation could be used to fill in the gaps.
- Dr. Balanov pointed out the relationship developed between cesium contamination and thyroid dose for Chernobyl. However, he also noted that this may not work for Fukushima because Cs/I ratios vary significantly.
- Dr Suzuki remarked on the large uncertainties in iodine uptake and the need to validate human measurements.
- Dr. Homma stated that several methodologies for iodine dose could be used to confirm inhalation dose (air concentrations, modeling, etc.).
- Dr. Balanov recommended interviewing people for whom thyroid measurement have been taken to determine the individuals location as a function of time, food ingestion, etc.
- Dr. Bouville emphasized the importance of collecting and analyzing all available data.

A third topic of discussion focused on tracking of personal behavior.

- Dr. Ohtsuru described an on-going detailed survey of personal behavior (movement, ingestion of milk, etc.) for 450,000 potentially exposed individuals, including information on hour-by-hour movement and indoor/outdoor location for the period of March 11-April 1.
- Dr. Momose suggested that it may be possible and would be important to establish correlations between external radioiodine and cesium exposures depending on personal behaviors.
- Drs. Ban and Bouville commented on the need to combine survey results with other data such as WBC, thyroid measurements, and external dose measurements. Dr. Ban asked if interviews after WBC scans are available. Dr. Momose said questions were asked on how people evacuated and food eaten, but the results have not been put in a database.

A fourth discussion focused on thyroid dose estimation.

- Dr. Suzuki commented that the Hosada method used for thyroid dose measurements in adults has much uncertainty when used to predict child thyroid dose. Dr. Balanov then noted that using an adult as a detector was not a valid approach.
- Dr. Bouville stated that all data needs to be collated and validated as a necessary first step before determine how to estimate thyroid dose.

The 1st NIRS Symposium on Reconstruction of Early Internal Dose
in the TEPCO Fukushima Daiichi Nuclear Power Station Accident